STUDIES ON MACROCYCLIC PEPTIDES: CONTROLLING CHEMOSELECTIVITY IN EFFORTS TOWARD THE TOTAL SYNTHESIS OF RUBIYUNNANIN A

A Dissertation

Presented to the Faculty of the Graduate School

of Cornell University

in Partial Fulfillment of Requirements for the Degree of

Doctor of Philosophy

by

Anthony Frederick Tierno

August 2016

© 2016 Anthony Frederick Tierno

STUDIES ON MACROCYCLIC PEPTIDES: CONTROLLING CHEMOSELECTIVITY IN EFFORTS TOWARD THE TOTAL SYNTHESIS OF RUBIYUNNANIN A

Anthony Frederick Tierno, Ph.D.

Cornell University 2016

Chemoselectivity remains a significant challenge in synthetic chemistry; in fact, one could make the argument that it's one of the greatest unmet challenges facing complex molecule synthesis. Collections of catalysts that afford such selectivity do not exist, nor do the methods to build such a collection. The focal point of my doctoral studies encompassed the synthesis of macrocyclic ligands capable of delivering control in chemoselectivity. Work focused on two areas: (1) the synthesis of macrocyclic peptide and cyclophane based ligands capable of inducing specific metal-catalyzed, site-selective epoxidations and hydrogenations, and (2) the application of these catalysts toward total synthesis of complex molecules; specifically in this case to the synthesis of rubiyunnanin A. Methods were developed for on-resin (solid phase peptide synthesis) macrocyclizations to stream line collections of macrocyclic ligands. Rubiyunnanin A is a bicyclic, iso-dityrosine belonging to the RA family of natural products. It contains a unique skeletal structure in that the adjacent tyrosine residues form (1) a *trans*-amide and (2) an unprecedented carbon-carbon bond. An effort toward the total synthesis of rubiyunnanin A led to the development of a one-pot/tandem palladium allylation/Heck reaction, and an unprecedented chemoselective carboxylic acid reduction. This chemoselective protocol progressed to the discovery of a site-selective, tandem amide coupling/reduction sequence.

BIOGRAPHICAL SKETCH

Anthony Tierno was born in Allentown, Pennsylvania in 1986. He graduated from Northampton Area High School in 2005. Tony continued his academic pursuits at the Pennsylvania State University, where he obtained his B.Sc. in Life Science as a member of the Schreyer Honors College (SHC) in May of 2009. Soon after, he began his graduate studies at Cornell University in the Chemistry and Chemical Biology department. In July of 2010, Tony began his work in the laboratory of Professor Chad Lewis, where he worked on the synthesis of macrocyclic peptide ligands designed to control chemoselectivity in polyene epoxidations and hydrogenations, and the total synthesis of rubiyunnanin A. Tony was a Bayer Teaching Excellence Award winner in 2011 and a Proctor & Gamble Award winner in 2016.

ACKNOWLEDGEMENTS

I would like to thank all of those who have helped me and inspired me during my studies at Cornell University. First and foremost, I would like to thank Dr. Chad Lewis for his advice and instruction. I could never have predicted how much I would learn from working in his lab. Chad led his group into ambitious and creative projects, and I am a far better chemist for having faced the challenges that ensued. I would also like to thank the Department of Chemistry who funded my entire time in graduate school and for the invaluable advice of my committee members, Drs. Bruce Ganem and Frank Schroeder.

I am very thankful for my opportunity to grow as a teacher while working with the undergraduates here at Cornell. I want to specifically thank Drs. Tom Ruttledge and Bruce Ganem for the teaching assistantships they afforded me. It was my pleasure to work with two individuals who are passionate about teaching and allowed me to grow in my love for it as well.

I want to thank all of my lab mates I've worked with over the years; Meagan Hinze, Matt Moschitto, David Vaccarello, Anirudra Paul, and Jessica Daughtry. I want to specifically thank Matt. He's an amazing chemist and I will miss our conversations. I want to also thank the Brett Fors group who adopted both Matt and me toward the end of our graduate careers.

Finally, I would like to recognize my parents, Jane and Fred, for their steadfast love and support through all my life endeavors. My girlfriend, Elizabeth, has supported me and made sacrifices for me that I can never repay. There's nothing like getting a warm hug from her at the end of a tough day. Last but definitely not least, I would like to thank my brother Ryne. He is my best friend and hero. He taught me what it means to never give up. I would never have accomplished any of my goals without him, let alone be the person I am today.

TABLE OF CONTENTS

LIST OF FIGURES, SCHEMES AND TABLES

LIST OF ABBREVIATIONS

Ac: acetyl
AcOH: acetic acid
APCI: atomic pressure chemical ionization
AORR: allylic oxide regio resolution
Ar: aromatic, argon
Bn: benzyl
Boc: *tert*-butyloxycarbonyl
Bu: butyl
CAN: ceric ammonium nitrate
Cbz: carboxybenzyl
COSY: correleated spectroscopy
CSA: camphorsulfonic acid
DART: direct analysis in real time
dba: dibenzylideneacetone
DBU: 1,8-diazabicyclo[5.4.0]undec-7-ene
DCC: dicyclohexyl carbodiimide
DCM: dichloromethane
DIAD: diisopropyl azodicarboxylate
DIBAL-H: diisopropylaluminum hydride
DIEA: diisopropylethylamine
DMAP: 4-dimethylaminopyridine
DMF: dimethylformamide
DMP: Dess-Martin periodinane
DMSO: dimethylsulfoxide
dppa: diphenylphosphoryl azide
dppe: 1,2-bis(diphenylphosphino)ethane
dppf: bis(diphenylphosphino)ferrocene
dr.: diastereomeric ratio
EDC: 1-ethyl-3-(3-dimethylaminopropyl)carbodiimide
ee: enantiomeric excess
EOM: ethyloxymethyl
er: enantiomeric ratio
ESI: electrospray ionization
EtOAc: ethyl acetate
Et_2O: diethyl ether
HATU: (1-[Bis(dimethylamino)methylene]-1H-1,2,3-triazolo[4,5-b]pyridinium 3-oxid hexafluorophosphate)
HMBC: heteronuclear multiple bond correlation
HOAt: 1-Hydroxy-7-azabenzotriazole
HPLC: high-pressure liquid chromatography
HSQC: heteronuclear single quantum coherence
Hz: hertz
IC_{50}: half maximal inhibitory concentration
iPr: isopropyl

IR: infrared spectroscopy
LC/MS: liquid chromatography mass spectrometry
MALDI: matrix-assisted laser desorption/ionization
Mes: mesityl
mCPBA: *meta*-chloroperoxybenzoic acid
Me: methyl
MeCN: acetonitrile
MeOH: methanol
MOM: methoxymethyl
M.P.: melting point
NADH: nicotinamide adenosine dinucleotide
NMM: N-methylmorpholine
NBS: N-bromo succinimide
NMP: N-methyl-2-pyrrolidone
NMR: nuclear magnetic resonance
nOe: nuclear Overhauser effect
NOESY: nuclear Overhauser effect spectroscopy
Ph: phenyl
pin: pinacol
ppm: parts per million
pTsOH: *para*-toluenesulfonic acid
py: pyridine
Ra-Ni: Raney®-nickel
Red-Al: sodium bis(2-methoxyethoxy)aluminumhydride
R_f: retention factor
ROESY: rotating frame nuclear Overhauser effect spectroscopy
RT: retention time
SAR: structure activity relationship
SPPS: solid phase peptide synthesis
TBS: *tert*-butyldimethylsilyl
TEA: triethylamine
Tf: trifluoromethylsulfonyl
TFA: trifluoroacetic acid
THF: tetrahydrofuran
TLC: thin layer chromatography
TMS: trimethylsilyl
Ts: tosyl
XPhos: 2-dicyclohexylphosphino-2′,4′,6′-triisopropylbiphenyl

Chapter 1: Review of the Synthetic Advances in Macrocyclic Peptide Natural Products

1.1 Overview of macrocyclic peptide natural products

Macrocyclic peptides comprise a diverse and growing family of natural products that have presented unique biosynthesis, biofunctions, bioactivities and synthetic challenges for the organic chemistry community. These molecules range in size from dipeptides and oligopeptides to polypeptides containing hundreds of amino acid residues. They include proteinogenic amino acids (precursors to proteins and co-translationally included) and non-proteinogenic amino acids (post-transitionally modified or non-ribosomal peptide synthetase-derived (NRPS) including N-formylmethionine, selenocysteine and pyrrolysine). There are two classifications of naturally occurring cyclic peptides: homodetic and heterodetic. Homodetic cyclic peptides contain amino acids connected solely by amide bonds. Heterodetic cyclic peptides contain amino acids that connect through at least one non-amide bond.[1] Examples of such non-amide bonds usually consist of ester and disulfide bonds; however, there is a distinct subclass of these natural products containing cyclophane moieties.[1b,2] Given the breadth of examples in this subclass and the ensuing reviews present in the literature, this introduction to cyclic peptides will specifically focus on the phenyl glycine derived (e.g. complestatin **1.1**), iso-dityrosine (e.g. piperazinomycin

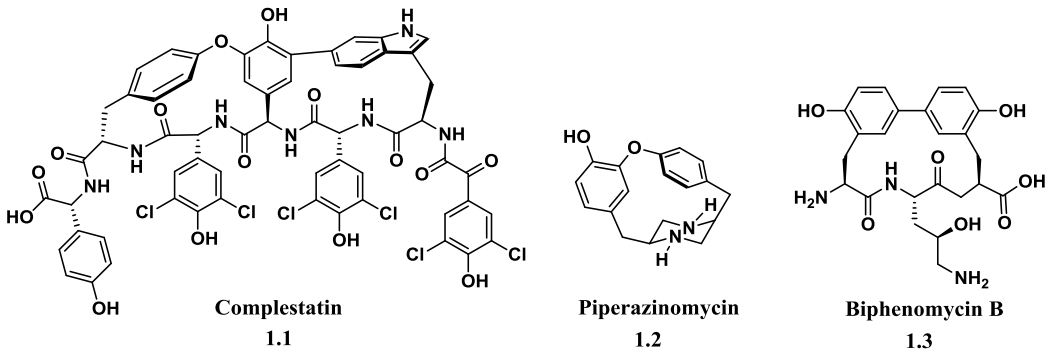

Figure 1.1. Examples of cyclophane based natural products.

1.2) and other tyrosine/tryptophan derived (e.g. biphenomycin **1.3**) natural products associated with aryl oxidative coupling. It is not uncommon to observe cross-links between electron rich amino acid side chains. Their fascinating biological activities and properties warrant study as they comprise a relatively potent class of natural products offering several advantages as potential drug candidates. These advantages are not necessarily widespread among all macrocyclic peptide natural products, but usually include the following properties: 1) their cyclic structures reduce zwitterionic interactions and hydrogen bonding motifs found in linear peptides, and enable more cell permeable and lipophilic capabilities; 2) they are absorbed more rapidly in the digestive track, thus making them less susceptible to enzyme degradation; and 3) their more rigidified structures show improved pharmacological properties, attributed to their higher binding affinities and/or selectivities.[3] Such medicinal properties and unique oxidatively coupled/modified skeletal frameworks have garnered a great deal of attention from the organic synthetic community, resulting in many total synthesis endeavors providing some new and creative methodologies. For the purposes of this synthetic review, phenyl glycine derived natural products will be omitted due to the vast studies and reviews already reported on this important class.[1b,2,4] The focus will be directed toward iso-dityrosine and other tyrosine/tryptophan related peptide natural products as they directly relate to the synthetic efforts our group has pursued toward rubiyunnanin A, B and C.

1.2 Total synthesis advances in oxidatively coupled tyrosine/tryptophan natural products

As a vast and steadily growing class of natural products, cyclic peptides present themselves in all types of organisms, which have evolved a multitude of biosynthetic strategies for their construction. Typical N-C terminal cyclizations to form amide bonds dominate the known cyclic

peptide natural products and this biosynthesis has been well documented.[5] However, unique and unprecedented cyclic peptides are constantly being isolated, for example recently in 2015 isolated streptide from a pathogenic model of *Streptococcus thermophilus.*[6] This cyclopeptide alkaloid has a unique tryptophan-to-lysine cross-linking, whose structure/biosynthesis has no precedent to date. Cyclopeptide alkaloids and other hybrid oxidatively coupled tyrosine/tryptophan based cyclic peptides continue to be isolated, and have continued to attract attention from the synthetic community over the last decade. Herein are reported recent advances in the synthesis of some of these natural products.

Biphenomycin B is an antibiotic produced by a strain of *Streptomyces* displaying potent antibacterial activity towards Gram-positive bacteria.[7] Consequently, it has become a lead structure in pharmaceuticals derived from natural sources. As part of a research and development program, Bayer Pharmaceuticals developed a kilogram-scale synthesis of desoxy-biphenomycin B **1.13** that has close connections to the first total synthesis of biphenomycin B reported by Schmidt and co-workers.[8] This synthesis takes advantage of two keys steps; 1) a Suzuki cross coupling to install the biaryl linkage and 2) a late stage double asymmetric hydrogenation (Scheme 1.1).[9] The synthesis of dehydroamino acid **1.5** was accomplished by benzyl protection of aldehyde **1.4** followed by a tetramethylguanidine mediated Horner-Wadsworth-Emmons reaction with phosphonate **1.11**. The synthesis of boronic acid **1.7** was accomplished by converting aldehyde **1.6** to a cyclic acetal by means of catalytic sulfuric acid. This acetal was subjected to a bromo-lithium halogen exchange pathway that furnished the desired aldehyde **1.7** following a global hydrolysis. Suzuki cross coupling of aryl bromide **1.5**

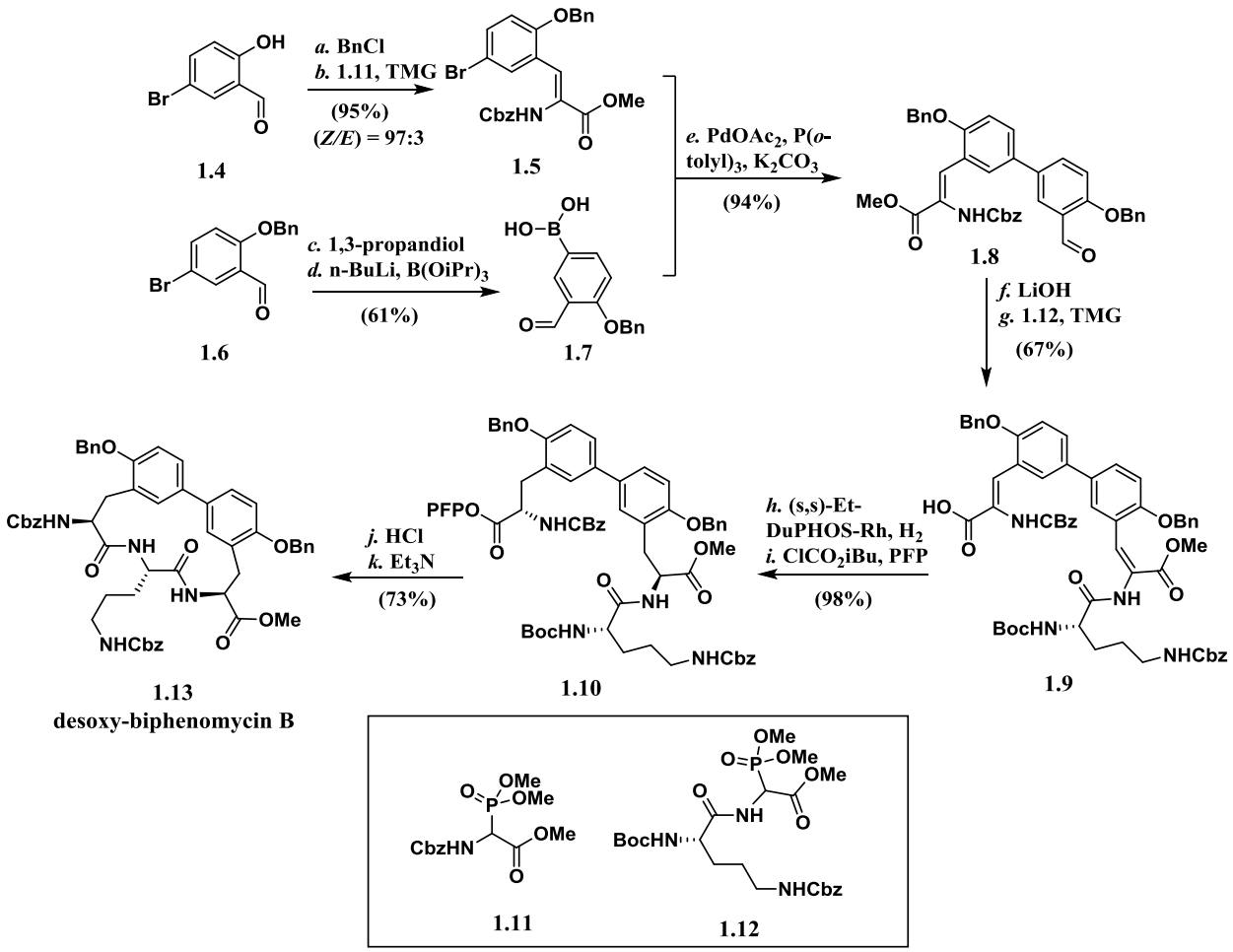

Scheme 1.1. Biphenomycin core synthesis by double asymmetric hydrogenation.

and aryl boronate **1.7** formed biphenyl **1.8**, which underwent hydrolysis of the dehydroamino acid portion of the molecule to yield an unsaturated lithium carboxylate that was used directly in the next reaction. Another tetramethylguanidine mediated Horner-Wadsworth-Emmons reaction with phosphonate **1.12**, gave the tripeptide **1.9**. Almost none of the (*E*)-isomer was observed in the Horner-Wadsworth-Emmons reactions, providing a greater than 97:3 ratio of the (*Z*):(*E*) olefin isomers. This tripeptide underwent double asymmetric hydrogenation with great success in 98% yield with 99% diastereomeric excess to furnish the fully saturated tripeptide **1.10**. The C-terminus was then converted to an active pentafluorophenyl ester. Following N-Boc

deprotection, the macrocyclization was induced by *in-situ* free-basing with triethylamine under dilute conditions to furnish desoxy-biphenomycin B **1.13**. This sequence could be conducted on a 700 g scale in an efficient synthesis where the longest linear sequence produced an overall 19.5% yield.

TMC-95A and TMC-95B (Figure 1.2) are two proteasome inhibitors isolated as fermentation products of *Aposispora montagnei*. They represent a unique class of cyclic peptide natural products containing a biaryl linkage between a tyrosine residue and a highly oxidized tryptophan residue. Each natural product also features an unprecedented acylated (*Z*)-propenylamine substructure. Biological studies have shown that TMC-95A and TMC-95B inhibit chymotrypsin-like, trypsin-like and post-glutamyl peptide hydrolytic activities of the proteasome with IC_{50} values of 5.4 nM, 200 nM and 60 nM, respectively. TMC-95A has also shown some cytotoxicity against human cancer cell lines of HCT-116 and HL-60 with IC_{50} values of 4.4 uM and 9.8 mM, respectively.[13] Their novel structures and noteworthy biological activities have unsurprisingly made TMC-95A and TMC-95B interesting targets for total synthesis.[14]

Danishefsky reported the total synthesis of TMC-95A and TMC-95B through a key

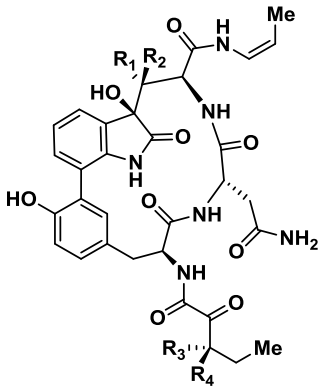

TMC-95	R_1	R_2	R_3	R_4
A	H	OH	Me	H
B	H	OH	H	Me
C	OH	H	Me	H
D	OH	H	H	Me

Figure 1.2. Structural features of TMC-95 A-D.

Suzuki cross coupling and a thermal rearrangement of a silylallyl amide to form the propenylamide moiety (Scheme 1.2).[14a] Oxindole **1.14** underwent an aldol condensation with the Garner aldehyde[15] resulting in a 1:1.3 mixture of (*Z*):(*E*) isomers of oxazolidine **1.15**. Although the isomers were separable by means of chromatography, the (*Z*)-isomer could be converted to the desired (*E*)-isomer by an iodine mediated isomerization. This isomerization presumably occurs via thermolysis in dimethoxyethane (DME) with catalytic iodine. The Garner aldehyde

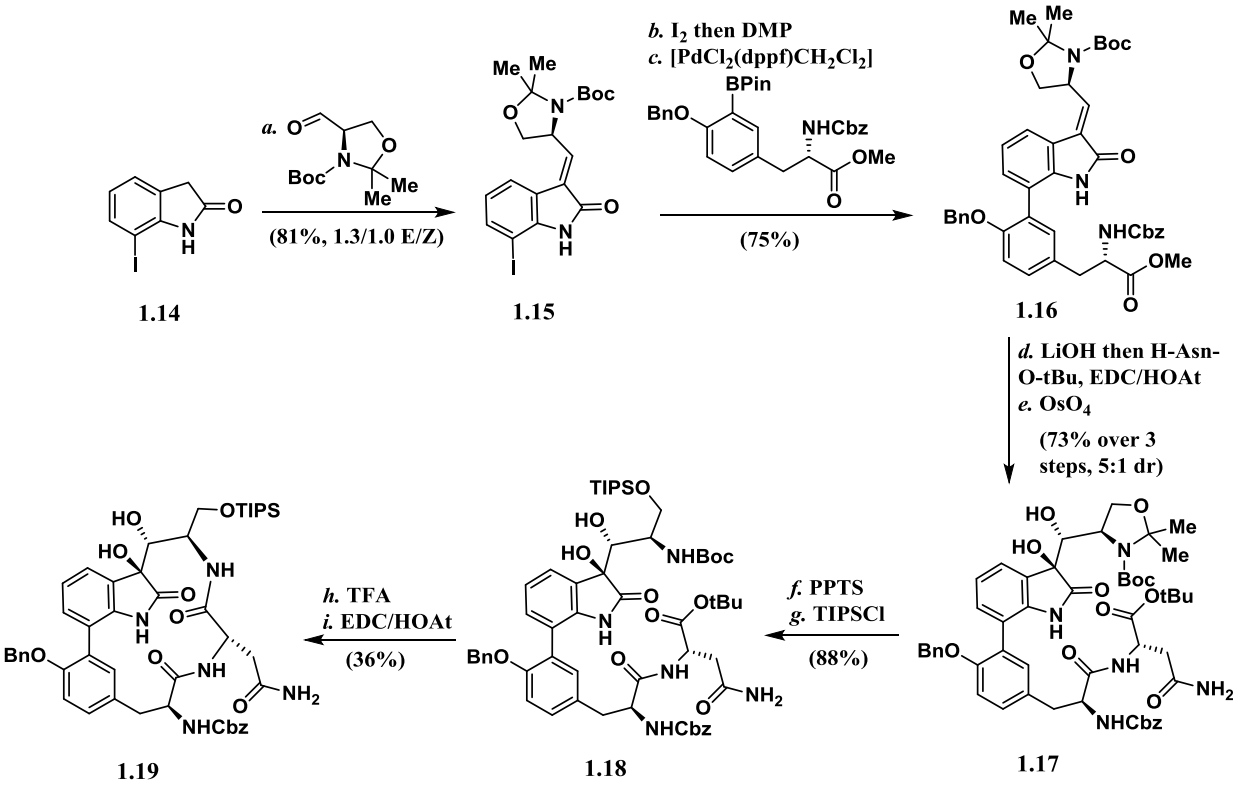

Scheme 1.2. Route to the biphenyl linkage and macrocyclization for TMC-95A and B.

was chosen over other tested aldehydes because it had provided the highest stereoselectivity in the subsequent asymmetric dihydroxylation reaction. Such an oxazolidine has shown to serve as a directing group for stereoselective reactions at the proximal sites of unsaturation. With oxazolidine **1.15** in hand, a Suzuki cross coupling with previously prepared tyrosine borate

furnished the biaryl domain **1.16** of TMC-95A and TMC-95B. Basic hydrolysis and EDC mediated coupling to H-Asn-OtBu, set the stage for the OsO_4-mediated dihydroxylation to the *Re* face of the olefin resulting in a 5:1 product ratio in favor of the desired diastereomer **1.17**. Acid treatment to cleave the N,O-acetonide and subsequent TIPS protection resulted in dipeptide **1.18**, which after N-Boc deprotection was macrocyclized with HATU activation under 2 mM concentration to afford macrocycle **1.19** in a 36% yield. For some insight into the properties of these late stage molecules, the authors found it interesting that the (*R*)-diastereomer of the diol did not participate in the cyclization. In general, the macrocyclization was a challenging, sensitive step noted by the authors because of the cycles' complexity and rigidity (optimized yield of 36%). The total synthesis was completed by TIPS deprotection of the cyclic peptide **1.20** followed by a tetra-TES protection to give fully protected cyclic peptide **1.21** (Scheme 1.3). The selective oxidation of the primary alcohol by use of a Jones oxidation followed an EDC mediated coupling of the silylallyl amine to give silylallyl amide **1.22**. A key sequence successfully accomplished the synthesis of the TMC-95A and TMC-95B mixture by thermal rearrangement of the silylallyl amide to cleanly yield the desired (*Z*)-propenylamide with subsequent global deprotection. Although not completely known, the mechanism of the rearrangement is suggested to proceed by 1,4-silyl and 1,4-hydride shifts.

There have been other contributions made to the syntheses of TMC-95A and TMC-95B including that of Williams and co-workers who finished a formal synthesis that converges into the previously discussed Danishefsky total synthesis.[14b] Inoue and co-workers, also utilized a Suzuki cross coupling tactic, however, their synthetic contribution to the (*Z*)-propenylamide was made by way of a decarboxylative anti-elimination.[14c] More recently in 2014, Coste and

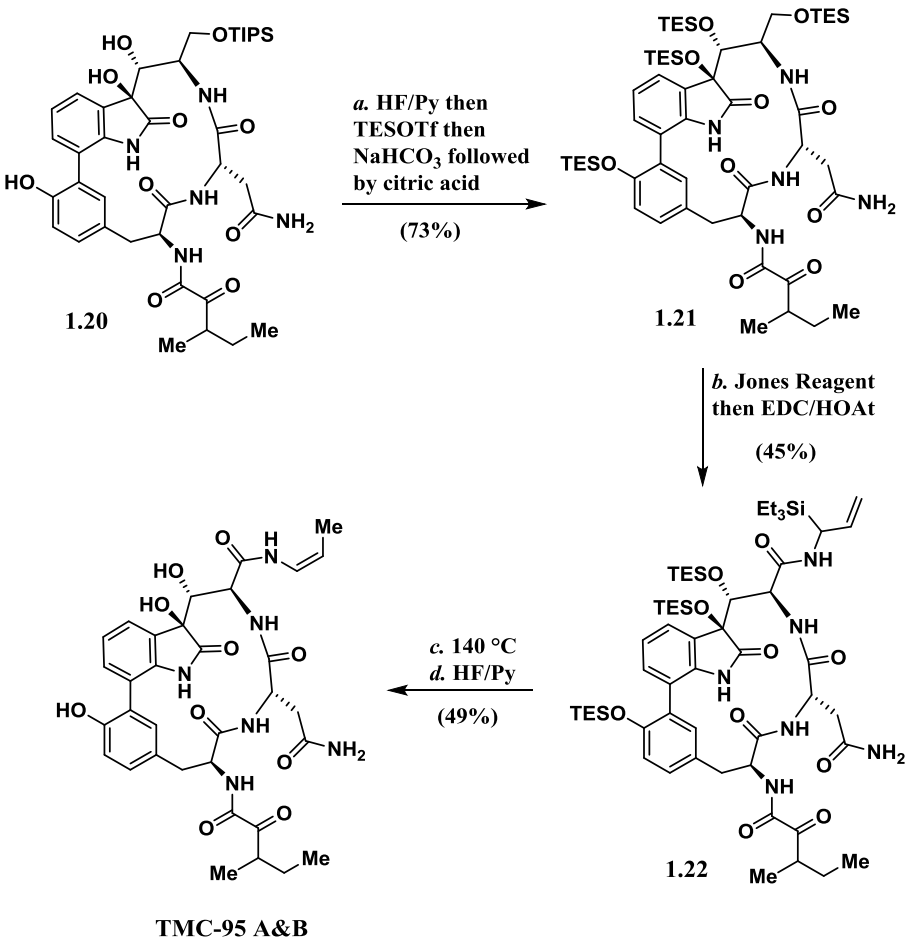

Scheme 1.3. Formation of (*Z*)-propenylamide to synthesize TMC-95A&B.

co-workers devised another synthesis for TMC-95A (Figure 1.3).[16] Using an asymmetric, organocatalytic aldol reaction between oxindole **1.23** and ketone **1.24** afforded oxindole **1.25**. Over twelve linear steps, oxindole **1.25** was transformed into tripeptide **1.26**, which when treated with $PdCl_2$(dppf) undergoes an intramolecular Suzuki-Miyaura reaction to close the macrocycle in a 50% yield under dilute conditions of 1 mM. The synthesis marks an efficient route to the core of TMC-95A **1.27** utilizing a macrocyclic cross coupling reaction, a strategy that is prevalent in the synthesis of iso-dityrosine based cyclic peptide natural products.

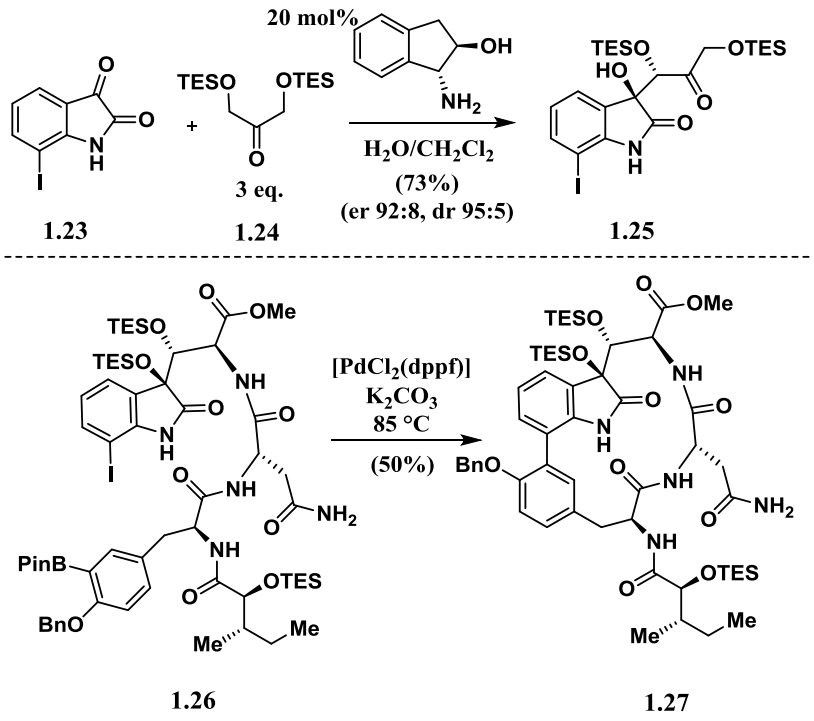

Figure 1.3. Key transformations towards the Coste core synthesis of TMC95-A.

The study of the fungal genus *Aspergillus* has produced a diverse array of cyclic peptide natural products, of which azonazine is one example isolated from a Hawaiian marine sediment-derived fungus.[10] The core of azonazine consists of a cyclic diketopiperazine unit that is very similar to that of the piperazinomycin, and also contains oxidatively coupled tyrosine and tryptophan residues. This core presents a unique skeletal challenge due to its rigid nature and has become an interesting target for total synthesis.[11] The first total synthesis and subsequent revised structure of ent-(-)-azonazine (from (+)-azonazine) was first reported in 2013 by Yao and co-workers (Scheme 1.4).[12] The Yao synthesis would achieve the construction of the core through a self-proclaimed biomimetic oxidative cyclization. BEP coupling of tyrosine derivative **1.28** to commercially available N-Boc-D-Trp-OH afforded dipeptide **1.29**. Diketopiperazine formation was mediated by N-Boc deprotection and subsequent basic treatment with an aqueous solution of sodium bicarbonate. O-Demethylation with BBr_3 furnished diketopiperazine **1.30** with the

tyrosine and tryptophan residues unprotected. This molecule sets up the crucial oxidative cyclization to complete the core synthesis. Through an extensive screen of iodine(III) reagents and $Fe(acac)_3$, it was ultimately found that two equivalents of $PhI(OAc)_2$ (PIDA) in TFE gave the best conversion, or combined yields of the desired isomers **1.31** and **1.32**. Most conditions

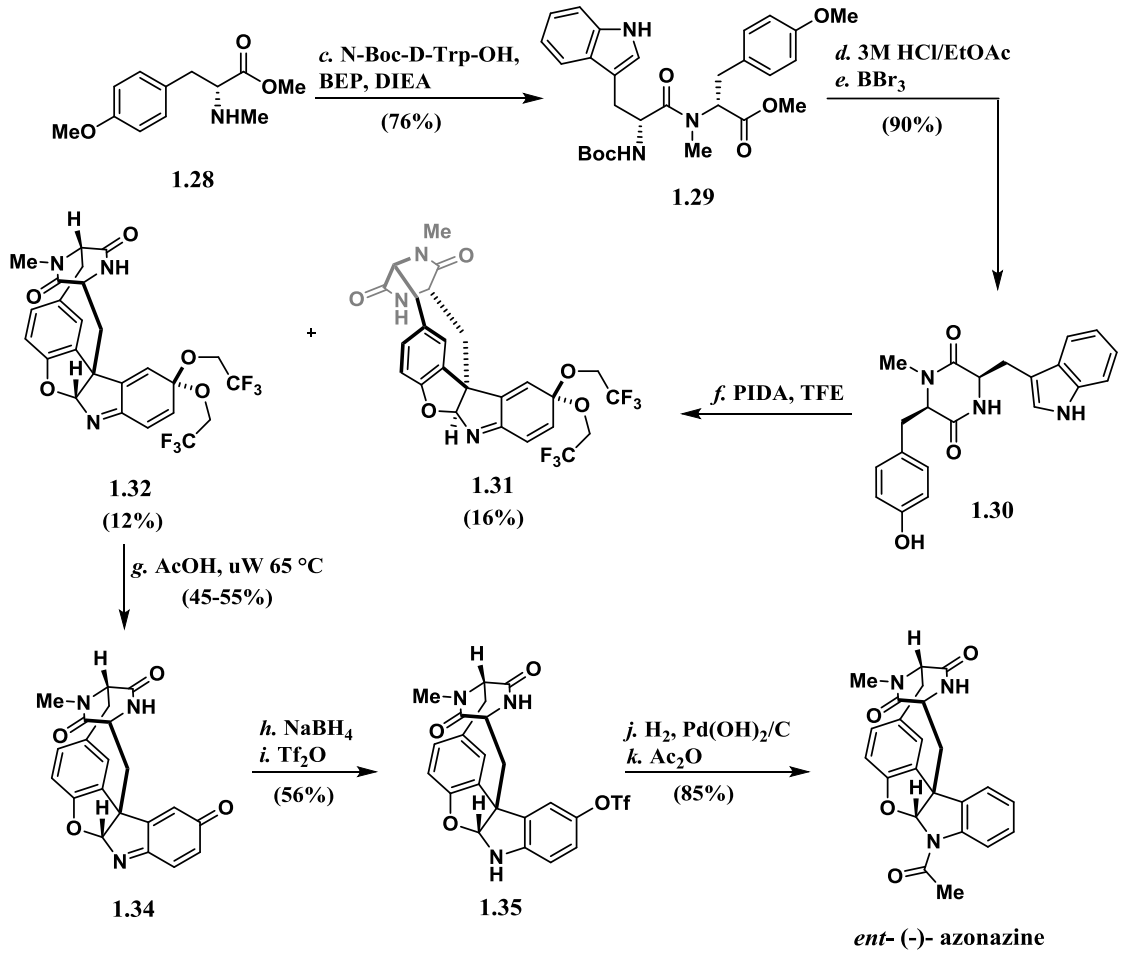

Scheme 1.4. Total synthesis and structural revision of ent-(-)-azonazine.

led to recovered starting materials or complex mixtures. The benzofuranoindole isomer **1.31** was then taken to the natural product (+)-azonazine over five steps where it was discovered the originally proposed structure was assigned incorrectly. The benzofuranoindole isomer **1.32**, upon treatment with AcOH with microwave assistance, furnished deprotected quinone **1.34**, and

immediate reduction followed by triflation gave the stable, protected phenol **1.35**. A hydrogenolysis of the triflate and subsequent N-acetylation of the indole afforded the desired ent-(-)-azonazine. The hypervalent iodine oxidative cyclization was accomplished in moderate yields at best, but nevertheless provided an expedient synthesis to the core of azonazine borrowing from some lessons learned in efforts toward the syntheses of diazonamide A.

Diazonamide A (Figure 1.4) arguably represents one of the most complex cross-linked, oxidatively coupled side chains in cyclic peptide natural products. Diazonamide A was isolated from the colonial ascidian *Diazona angulate*, collected from ceilings in caves from the Philippine islands.[17] It exhibits biological activities in the range of antimicrobial, antiviral and cytoxicity. More specifically, diazonamide A has shown IC_{50} values less than 15 ng/mL for some tumor cells.[17] Its high potency, unique skeletal structure and rarity from natural sources generated high interest among synthetic chemists.[18] In 2001, Harran completed the first total synthesis of the originally proposed structure of diazonamide A.[18b,c] However, differences in qualitative observations (stability and chromatographic properties) of their synthesized materials compared

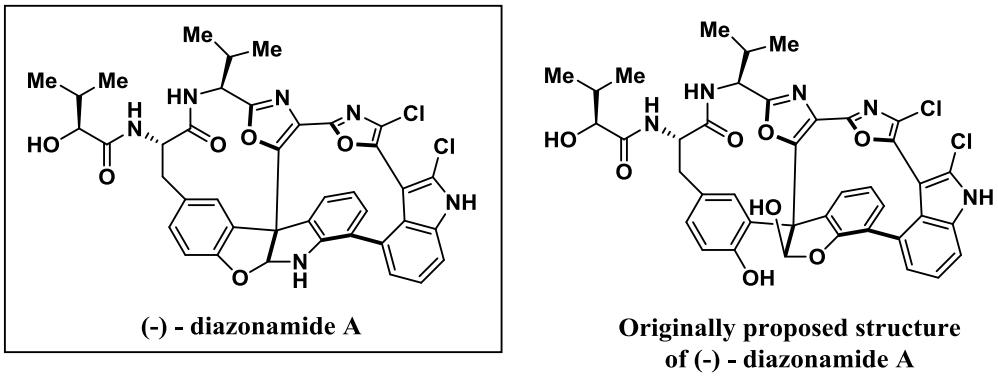

Figure 1.4. (-) – diazonamide A and the originally proposed structure.

to that of natural samples led the Harran group to revise the structure of diazonamide A.

In 2002, Nicolaou and co-workers finished the first total synthesis of the revised structure of diazonamide A.[18a] In the first total synthesis,[19] Nicolaou utilized an electrophilic aromatic substitution and an intramolecular Witkop-photocyclization.[20] This particular derivation of the Witkop-photocyclization was first used in work done by Harran and co-workers (Scheme 1.5).[21] The oxindole precursor **1.38** to the key electrophilic aromatic substitution was synthesized over a three step sequence starting from oxazole **1.36**. This was accomplished by a methyl ester reduction and subsequent benzyl protection of the allylic alcohol to give oxazole **1.37**. Deprotonation using n-BuLi and carbanion quench with a previously prepared isatin afforded the aforementioned electrophile **1.38**. p-TsOH mediated electrophilic aromatic substitution with a tyrosine residue and subsequent N-Boc protection yielded a mixture of two oxindole epimers **1.39** and **1.40**. As the authors note, at the time of the purification of these epimers, it was not known which was correct. Both were taken through the synthesis separately to which epimer **1.40** was eventually diagnosed as the correct isomer. After macrocyclization of the left-hand ring system, the free phenol of cyclic peptide **1.41** was O-Boc protected. The remaining unprotected alcohol underwent a dual oxidation sequence using IBX:$NaOCl_2$ to give carboxylic acid **1.42**. This set up a key sequence in their synthesis; from indole **1.43**, an oxazole forming $POCl_3$ mediated cyclodehydration followed by a Witkop-photocyclization (moderated by LiOAc, a 450 W lamp and epichlorohydrin as a scavenger) furnished the indole cross-linked, bicycle **1.44**. This sequence of transformations occurred in an incredibly efficient fashion netting yields of 53% and 33% yields, respectively. It should be noted, as already mentioned, this photocyclization had been previously well studied in Harran's first total synthesis of diazonamide A. Over a five step sequence, cyclic peptide **1.44** could be converted to the final structure through a chlorination procedure using NCS and a DIBAL-H reduction of the oxindole

forming the benzofuranoindole via an iminium intermediate. The total synthesis was accomplished with 24 steps overall.

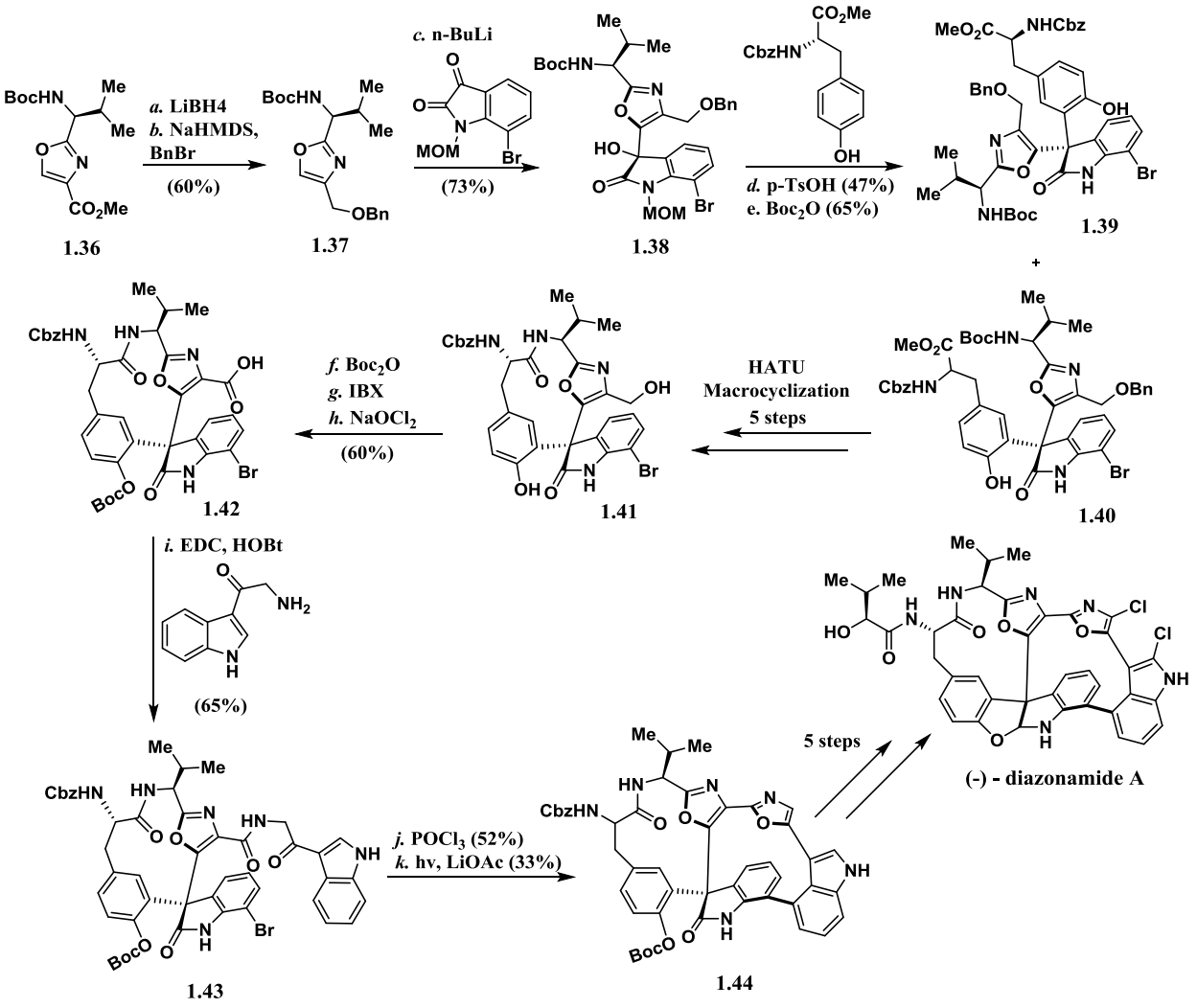

Scheme 1.5. First total synthesis of diazonamide A by Nicolaou and co-workers.

Nicolaou and co-workers had developed a second generation total synthesis of diazonamide A in which the retrosynthesis was distinct from the first.[22] The synthesis was constructed in the opposite manner in that the macrocyclization of the right-half of the molecule was completed before that of the left-half (Scheme 1.6 and Scheme 1.7). The key steps to the synthesis

included the cross-linking of indoles, previously achieved by the Witkop-photocyclization, through an intermolecular Suzuki cross coupling, and a powerful heteropinacol cascade mediated by SmI_2. Suzuki cross coupling of aryl bromide **1.45** with borate **1.46** gave biaryl indole **1.47** with consistently good yields. Biaryl indole **1.47** was expediently converted to aldoxime **1.48** by desilylation, subsequent oxidation and condensation with O-methyl hydroxylamine. In a powerful transformation, SmI_2 mediated an intramolecular heteropinacol reaction to form the right-half ring of diazonamide A. In one pot, the resulting free amine underwent an EDC mediated amide coupling to furnish alcohol **1.49.** Oxidation of the secondary alcohol to the ketone and cyclodehydration mediated by $POCl_3$ gave the cross-linked oxazoles **1.50**. As in the initial Nicolaou synthesis, the left-half cycle was formed by a HATU driven macrolactamisation of carboxylic acid **1.51**. The cyclization proved to be difficult even under

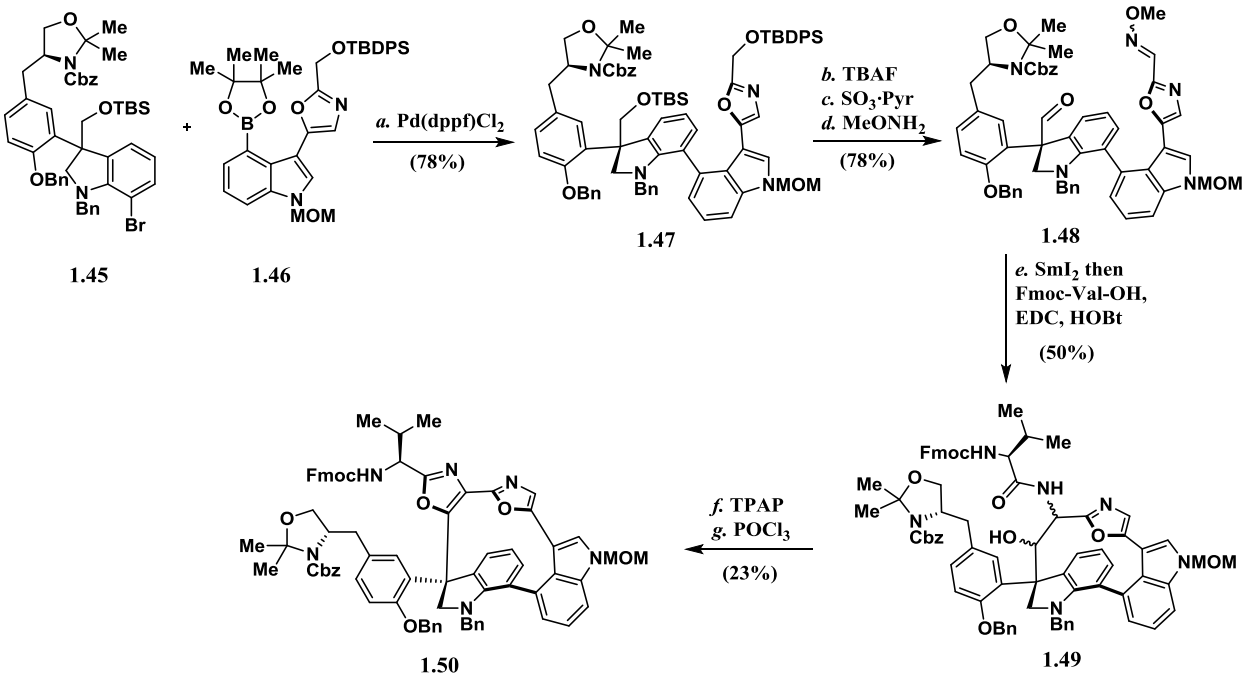

Scheme 1.5. Intramolecular heteropinacol cascade in the 2nd generation synthesis.

extreme dilution (uM concentrations), yet it was found that HATU/collidine facilitated the cyclization at 0.1 mM using a CH_2Cl_2/DMF mixture. A fortuitous effect of this cyclization is that it also mediated a resolution of the C10 epimers. Only the cyclic peptide with the stereochemical disposition of **1.52** was isolated. The opposite C10 epimer did not participate in the macrocyclization presumably due to high levels of strain in the amide formation. With cyclic peptide **1.52** in hand, it was found that hydrogenation conditions using $Pd(OH)_2$ not only facilitated a protecting group change to O-Cbz, it also allowed the oxidation of the indole into oxindole **1.53** in unprecedented fashion. From this point, the total synthesis of diazonamide A could be finished in the same manner as the first total synthesis the authors reported. The 2nd generation synthesis totaled an overall 31 steps, but contained powerful and unique transformations.

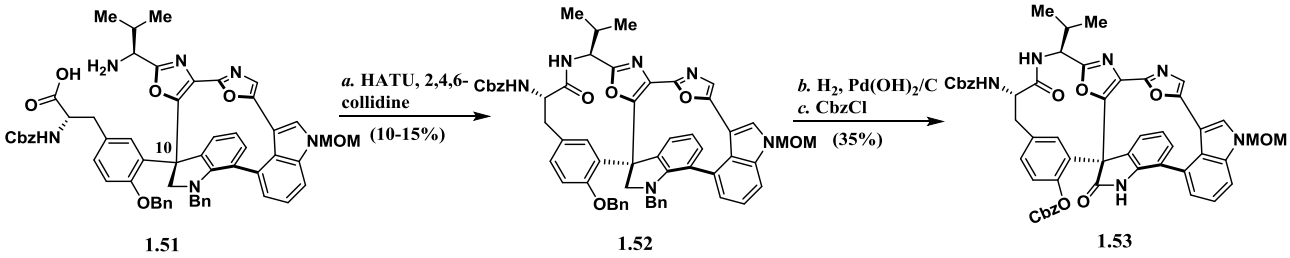

Scheme 1.6. Intramolecular macrolactamisation cascade in the 2nd generation synthesis.

In 2011, MacMillan and co-workers contributed to the story of diazonamide A with a total synthesis effort that sought outright control of the stereocenter formation of the previously labeled C10 site.[23] Both previous syntheses by Nicolaou relied on resolutions/purifications of the epimers. This distinct synthesis would rely on three key transformations; 1) an asymmetric addition of an indole to an unsaturated aldehyde, 2) a macroaldolization and 3) a Stille-Kelly type protocol[24] that would mediate the macrocyclization of the right-half of diazonamide A

(Scheme 1.8). Biaryl linkage **1.54** was produced by a Suzuki cross coupling between a 2-iodo tyrosine residue and a borylated indole. Subjection of the biaryl linkage **1.54** to an excess of propynal using an imidazolidinone catalyst gave the benzofuranoindole **1.55** in great yield with a greater than 20:1 diastereomeric ratio. Upon deprotection and reprotection of the indole as the trifluoroacetamide, ozonolysis furnished saturated aldehyde **1.56**. With this aldehyde in hand, the macroaldolization reaction was screened. The authors proposed an unconventional 13-membered macrocyclization technique that would be more efficient than the 12-membered ring macrolactamisation that proved problematic in the Nicolaou syntheses. Indeed, they discovered that the $MgBr_2$ mediated aldol reaction gave cyclic peptide **1.57** in efficient yields. After multiple cyclodehydration reactions to give the cross-linked oxazoles, the remaining O-benzyl protected phenol was deprotected and reprotected as the triflate **1.58**. Under a microwave assisted Stille-Kelly protocol, the triflate was converted to the aryl borate which underwent the intramolecular cross coupling in a tandem sequence to furnish the cross-linked cyclic peptide **1.60**. This intermediate could be advanced to diazonamide A over three steps through a halogenation sequence (that included bromination, selective chlorination and then Pd catalyzed debromination) and global deprotection. This afforded an overall 20 step total synthesis of diazonamide A that presented a stereospecific synthesis of the benzofuranoindole moiety and presented interesting alternatives to the synthesis of the strained macrocycles in the molecule's framework.

In 2015, Harran and co-workers made an outstanding contribution to the total synthesis of diazonamide A and to diazonamide based-drugs. In the Harran original synthesis (2003),[25]

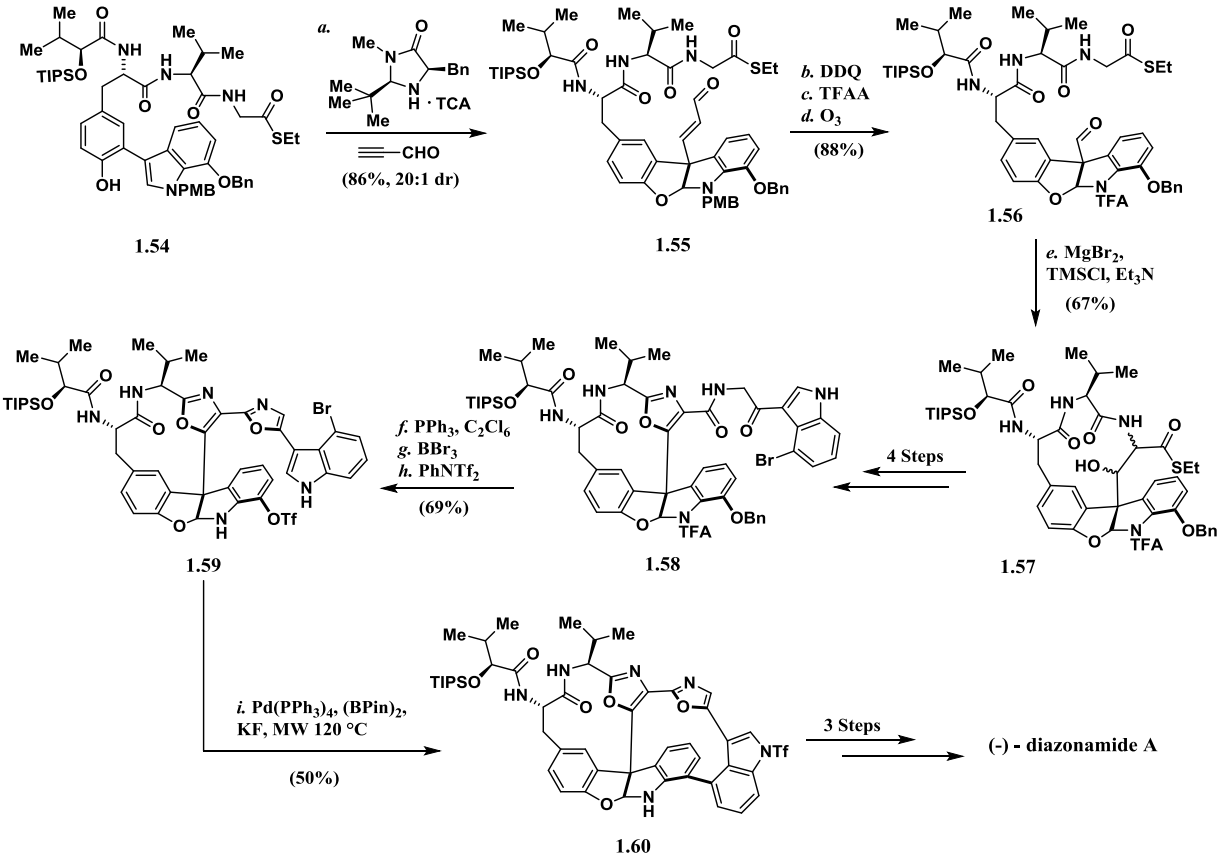

Scheme 1.8. Total synthesis of diazonamide A performed by MacMillan and co-workers.

the left-hand macrocycle and the benzofuranoindole of diazonamide A was prepared in one step by what could be considered a parallel biosynthesis mediated by an $PhI(OAc)_2$ (PIDA) oxidative cyclization (Figure 1.5). However, this transformation produced a somewhat complicated impurity profile and the low yields diminished its applicability to drug production. In an alternative method, electrolysis gave an anodic oxidation in a 3:1 product ratio using a controlled potential of +1.6 V in wet DMF open to air. This procedure provided a major advance to that of the oxidative cyclization using $PhI(OAc)_2$. Harran and co-workers turned their attention to the synthesis of DZ-2384 **1.66**, a simplified developmental candidate for diazonamide A (Scheme 1.9). DZ-2384 **1.66** showed a 10 to 50-fold higher efficacy than diazonamide A as a cancer therapeutic.[26] The synthesis begins with a kilogram scale preparation of dipeptide **1.62**

by reaction of serine residue **1.61** with 5-fluoroindole in the presence of acetic anhydride. The mechanism of reaction is not completely understood, the authors propose it to proceed through an oxazolone intermediate. After coupling of acid **1.62** to L-Ser-OMe and incremental oxidation

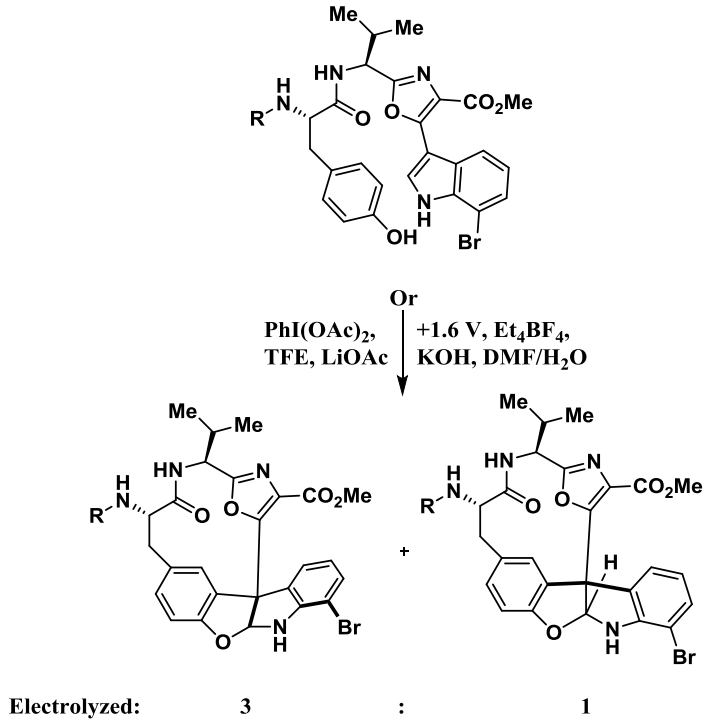

Figure 1.5. Two-fold approach to parallel biosynthesis of diazonamide A core.

by DDQ, oxazole **1.63** was isolated as a single isomer. Subjection to Deoxo-fluor and subsequent oxidation via $BrCCl_3$ with DBU afforded bisoxazole **1.64**. A sequence of deprotection and couplings to a tyrosine and (S)-2-hydroxyisovaleric acid residue, respectively, afforded unprotected tripeptide **1.65**. The previously discussed electrolytic macrocyclization afforded DZ-2348 **1.66** directly in a 48% yield with a diastereomeric ratio favoring the desired 2.3:1. This established the synthesis of DZ-2384 in 13 total steps with an overall 5.7% yield from L-tert-leucine.

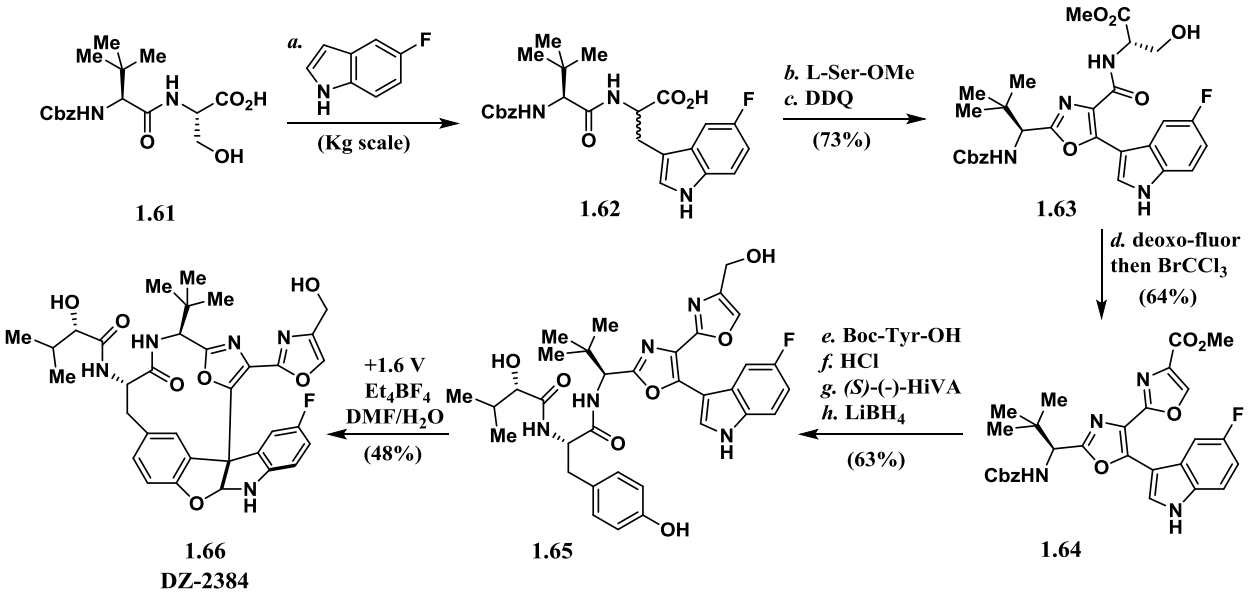

Scheme 1.9. Synthesis of DZ-2384 **1.66** by means of electrolytic macrocyclization.

Over the years there have been various other unique macrocyclization events that have been documented in efforts toward the total synthesis of diazonamide A. In particular, there have been two interesting examples of macrocyclizations to synthesize the benzofuranoindole and left-hand macrocycle of diazonamide A by Sammakia[27] and Magnus (Figure 1.6).[28] Sammakia and co-workers provided the cyclization by forming a hindered quaternary center by nucleophilic addition of an oxindole into a bromo-cyano oxazole electrophile. Magnus and co-workers provided their cyclization by first applying a TBAF induced S_N2/S_N1 macrocyclization. Refluxing the O-aryl ethers in chloroform then induced a rearrangement to the corresponding C-aryl cross-linking to furnish the desired epimer in a favorable 7:3 product ratio.

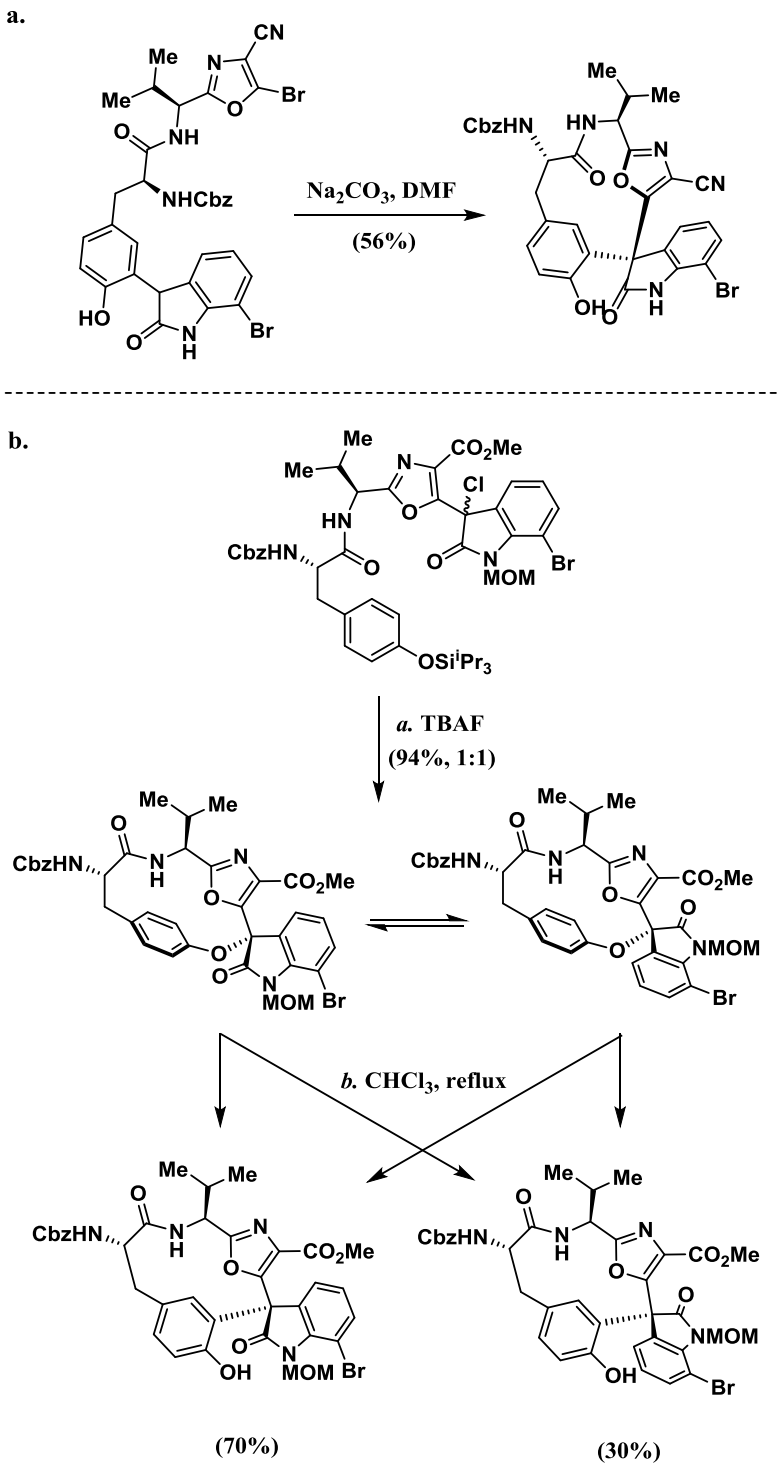

Figure 1.6. Developed macrocyclization techniques in the synthesis of diazonamide A by (a) Sammakia and (b) Magnus.

1.3 Total synthesis advances in oxidatively coupled iso-dityrosine peptide natural products

The bastadin family of natural products are isolated from several marine sponges (*Ianthella basta*, *Ianthella quadrangulata* or *Dendrilla cactos*) and provide a class of very potent anti-cancer substances.[29] The key skeletal features of the bastadins consist of two aryl ether linkages based upon dopamine and highly brominated tyrosines. Bastadines are split into two sub-

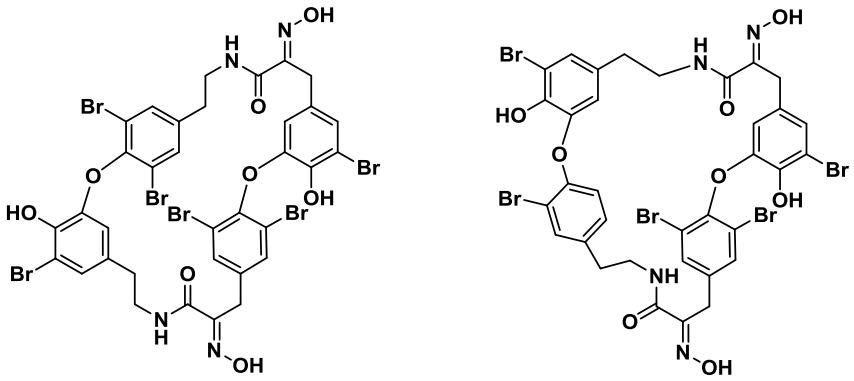

Figure 1.7. Bastadin sub-families of bastaranes and isobastaranes.

families; bastaranes (e.g. bastadin bs6) where the left-hand aryl linkage is *meta-para* and isobastaranes (e.g. bastadin bs19) where the left hand aryl linkage is *para-meta* (Figure 1.7). Bastadin bs6 shows promise in the area of anti-cancer research with sub-nanomolar ranges of potency. Bastadin bs6 has also been shown to have anti-angiogenic activity by the induction of selective apoptosis in endothelial cells, both *in vitro* and *in vivo*.[30] Naturally, its potent bioactivities made it an interesting target for natural product synthesis. A total synthesis of bastadin 6 was accomplished by Kobayashi and co-workers in 2005 by development of a novel Ce(IV) mediated coupling of dibrominated tyrosine (Scheme 1.10).[31] Dibrominated

tyrosine derivative **1.67** underwent an oxidative radical homo-coupling by treatment with CAN to provide diaryl ether **1.68**. Reduction of the cyclic carbamate **1.68** with $Na_2S_2O_4$ gave primary amine **1.69.** EDC and HOBt mediated amide coupling of primary amine **1.69** with

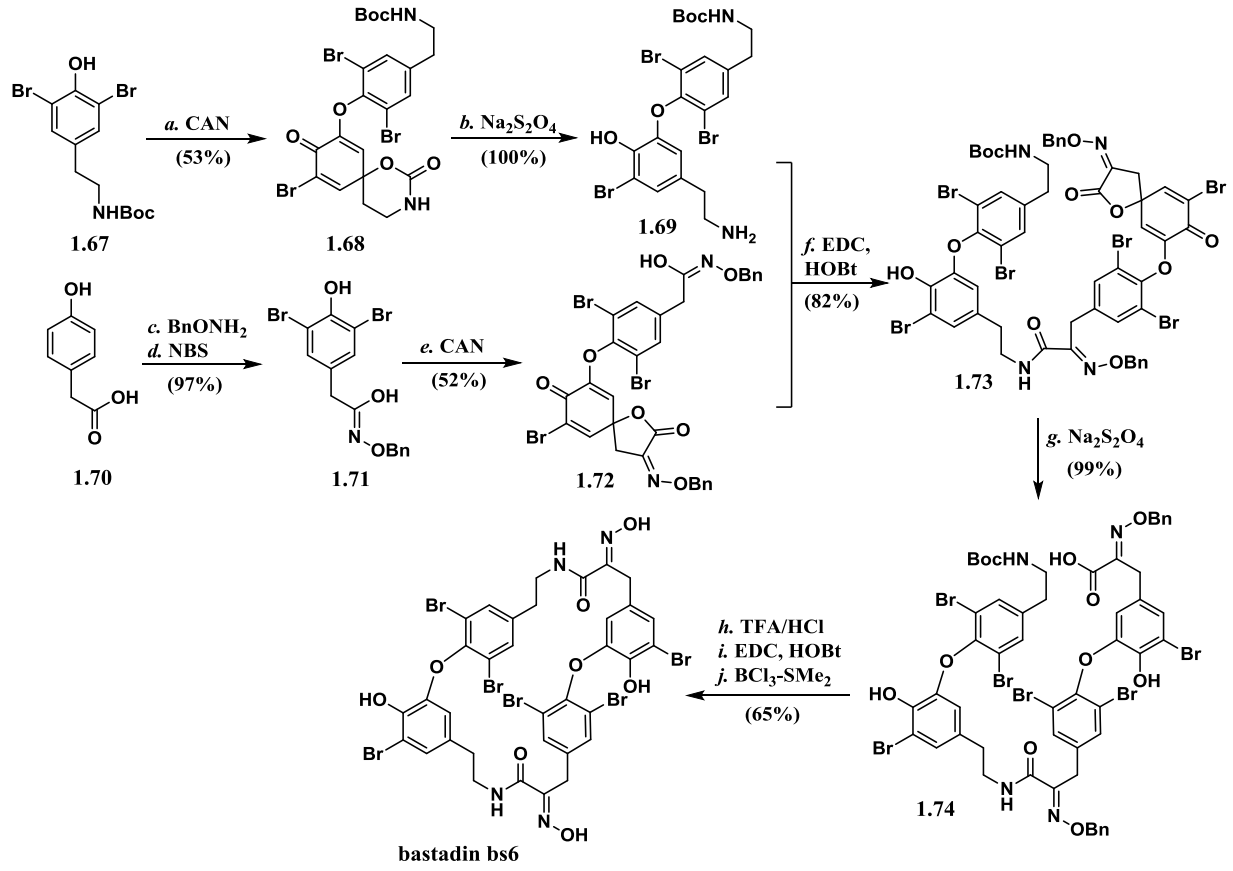

Scheme 1.10. Total synthesis of bastadin 6 using CAN-mediated oxidative coupling.

acid oxime **1.72** provided diaryl ether **1.73**. The acid oxime **1.72** could be synthesized over 3 steps starting with 4-hydroxyphenyl pyruvic acid **1.70**. Condensation with benzyl hydroxylamine and subsequent bromination with NBS gave dibrominated tyrosine **1.71**. Acid oxime **1.72** could then be accessed by the aforementioned oxidative radical homo-coupling using CAN. Diaryl ether **1.73** could be reduced to oxime **1.74** by use of $Na_2S_2O_4$. Deprotection of the N-Boc group using TFA/HCl and macrocyclization mediated by EDC and HOBt could be

followed by benzyl deprotection of the oximes using BCl_3-SMe_2 to give bastadin 6. The overall yield of the convergent synthesis was 26% with a 9 step, longest linear sequence. It was an efficient synthesis of a potential drug candidate that contained a unique and novel Ce(IV)-mediated oxidation of highly brominated tyrosine residues.

Piperazinomycin is a macrocyclic piperazine that was isolated as a minor metabolite of *Streptoverticillium olivoreticuli* subsp. *neoenacticus* that has been shown to have some inhibitory activities against fungi and yeast.[32] Piperazinomycin, structurally, contains the simplest diaryl ether of iso-dityrosine natural products (Scheme 1.11). There have been various total syntheses

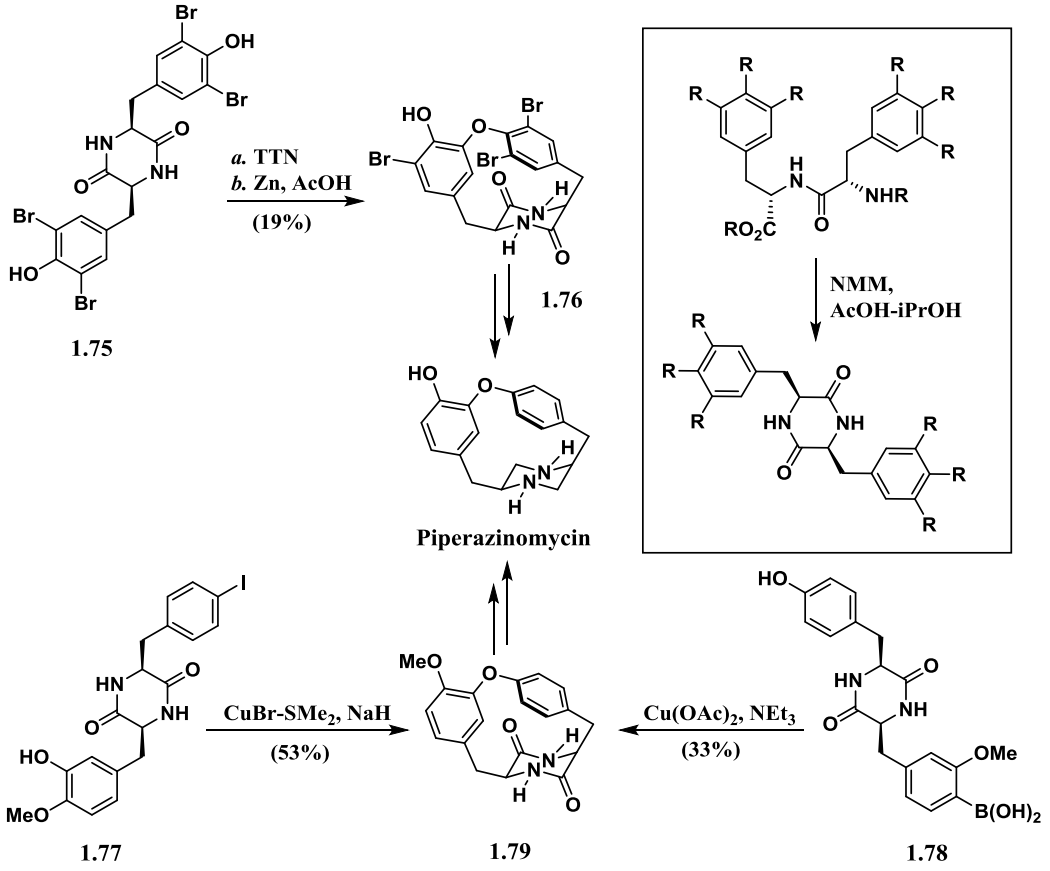

Scheme 1.11. Various total synthesis routes to the construction of piperazinomycin.

of piperazinomycin, the first of which was completed in 1986 by Yamamura and co-workers.[33] They took advantage of a thallium(III) nitrate (TTN) induced intramolecular oxidative coupling of highly brominated tyrosine derivative **1.75**. The conditions of this oxidative coupling resulted in over oxidation of the phenol. The reaction required a reduction with zinc powder to trigger a reductive rearomatization of macrocyclic piperazine **1.76**. Further transformations of dehalogenation and reductions of the amides furnished piperazinomycin. Boger and co-workers took a different approach to the total synthesis by utilizing an Ullmann type oxidative cross coupling.[34] From the mixed dopamine, iodophenylalanine piperazine **1.77**, subjection to sodium hydride and CuBr-SMe_2 in refluxing DMF afforded macrocyclic piperazine **1.79**, which could easily be transformed to piperazinomycin via borane reduction and demethylation by HBr. More recently in 2009, Ghosh and co-workers utilized a Chan-Lam type cross coupling to build the macrocyclic piperazine core.[35] Chan-Lam procedure[36] using $Cu(OAc)_2$ and triethylamine at room temperature gave macrocyclic piperazine **1.79** from boronic acid **1.78** in a modest yield. It should be noted that all three groups arrived at the piperazine species in the same manner. Respective dipeptides could undergo diketopiperazine formation by dilute treatment with NMM in an acetic acid/isopropanol mixture. Although Yamamura's method of using the oxidative coupling conditions with TNN was least efficient of the three presented methods at synthesizing the core of piperazinomycin, this tandem oxidation/reductive rearomatization method was chosen to be used again in other syntheses of iso-dityrosine natural products such as the deoxybouvardins, RA-VII, K-13, OF4949-III and the eurypamides.[1b,2]

Another class of interesting iso-dityrosine natural products is Janetka's HIV-protease inhibitors

K-13 and OF4949-IV (Scheme 1.13). They are both tripeptide β-strand mimics resulting from their strained macrocyclic structures.[37] K-13 is a natural inhibitor of the angiotensin converting enzyme (ACE) and OF4949-IV is a competitive inhibitor of aminopeptidase B. Although they are both metalloprotease inhibitors, their bioactivities are very specific. K-13 does not inhibit aminopeptidase B and OF4949-IV shows no activity against ACE.[38] This is mostly likely due to the fact that although both K-13 and OF4949-IV contain the similar substructure of a biaryl ether iso-dityrosine moiety, K-13 maintains a *para-meta* fusion whereas OF4949-IV maintains a *meta-para* fusion that has a significant topological effect on the molecules' interactions. It should be noted the macrocyclic nature is key to the β-strand like properties and removal of the cycle completely shuts down all bioactivities for both K-13 and OF4949-IV.[39] Jackson and co-workers have developed a divergent synthesis of both K-13 and OF4949-III by utilizing an intramolecular and an intermolecular Negishi cross coupling followed by a macrolactamisation, respectively.[40]

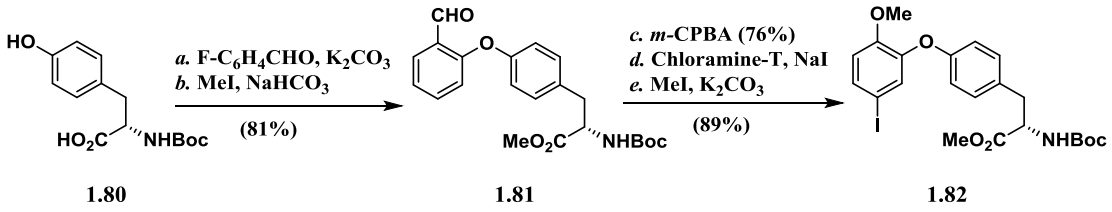

1.80 **1.81** **1.82**

Scheme 1.12. Synthesis of iodinated aryl ether intermediate **1.82**.

The common intermediate to this divergent synthesis was iodinated aryl ether **1.82** (Scheme 1.12). Using N-Boc tyrosine **1.80** as a nucleophile in an SNAr with 2-fluorobenzaldehyde followed by methyl ester formation with MeI gave benzaldehyde aryl ether **1.81**. *m*-CPBA mediated Baeyer-Villiger reaction converted the benzaldehyde to a phenol, and following chloramine-T iodination and methylation of the phenol, benzaldehyde aryl ether **1.81** was converted to the iodinated aryl ether **1.82**. Iodinated aryl ether **1.82** could be used directly to

synthesize both K-13 and OF4949-III (Scheme 1.13). N-Boc deprotection of iodinated aryl ether **1.82** followed by coupling to N-Boc-Asn-ONp gave dipeptide **1.83**. Intermolecular Negishi cross coupling of a zincate serine derivative with dipeptide **1.83** using Pd_2dba_3 and $P(o\text{-}tol)_3$

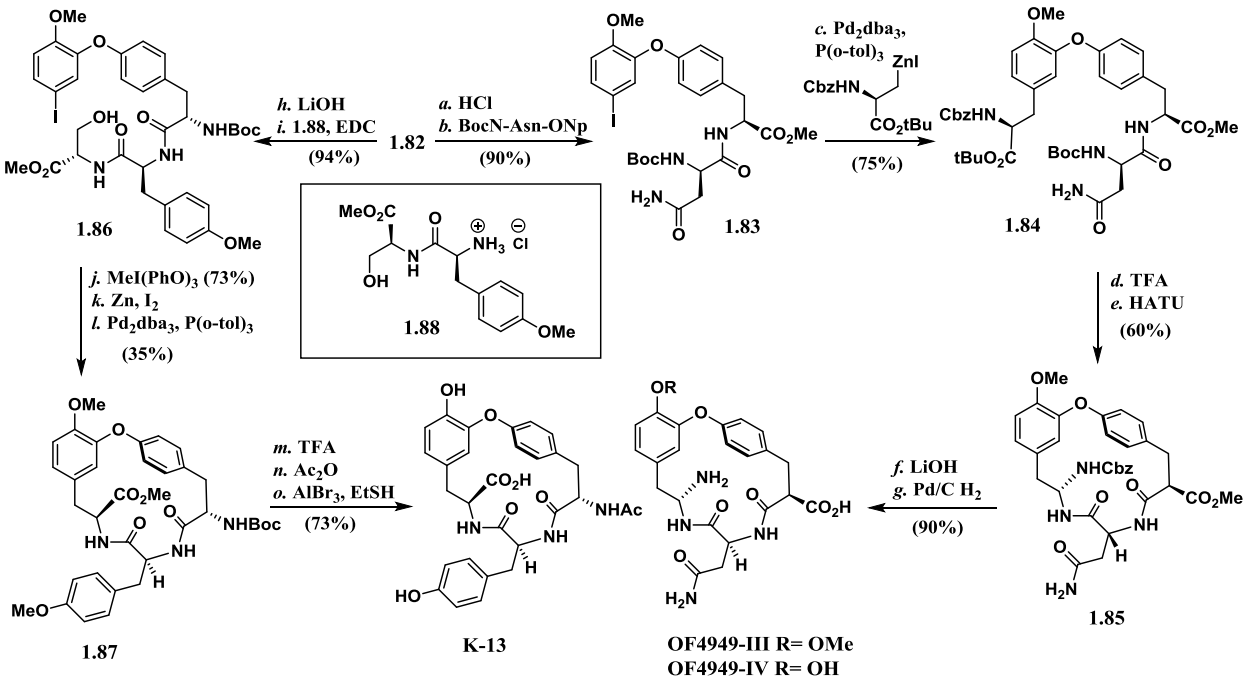

furnished tripeptide **1.84**. Global TFA deprotection and treatment with HATU induced the

Scheme 1.13. Total syntheses of K-13 and OF4949-III.

macrolactamisation to afford cyclic peptide **1.85**. Although an envisioned macrolactamisation is an obvious retrosynthetic disconnection, this synthesis is one of the few examples of an iso-dityrosine natural product synthesis containing a macrolactamisation reaction. It should be noted that K-13 and OF4949-IV contain a unique structural feature of being tripeptides as compared to most other members of this class of natural products being dipeptides. The reduction of strain may allow for an easier amide formation to occur (17-membered ring vs 14-memebered ring). Methyl ester hydrolysis with LiOH and N-Cbz deprotection by hydrogenolysis with Pd/C afforded OF4949-III. Considering the total synthesis of K-13, methyl ester hydrolysis of

iodinated aryl ether **1.82** using LiOH followed by EDC mediated coupling with dipeptide **1.88** gave tripeptide **1.86**. Iodination-Mitsunobu of the serine residue on tripeptide **1.86** followed by activation of the resulting alkyl iodide with zinc powder set up a novel intramolecular Negishi cross coupling (using Pd_2dba_3 and $P(o\text{-}tol)_3$) furnishing macrocyclic tripeptide **1.87**. Protecting groups swap driven by treatment with TFA and subsequent acylation with acetic anhydride, preceded a global demethylation with ethyl thiol and $AlBr_3$, affording K-13. This intramolecular Negishi cross coupling was a route that was also envisioned for the total synthesis of OF4949-III, however, the intermolecular Negishi cross coupling was necessary due to the instability of the alkyl zincate derivatives of serine located on the N-terminus of a peptide or amino acid.

Boger and co-workers synthesized K-13 and OF4949-III using a similar macrolactamisation used by Jackson in Scheme 1.13.[41] This macrocyclization was mediated by a diphenylphosphoryl azide (dppa). The aryl ether linkage was produced earlier utilizing a similar Ullmann type cross coupling in their synthesis of piperazinomycin. Janetka and co-workers had one of the initial total syntheses of K-13 and OF4949-III;[42] however, they chose to not take advantage of a macrolactamisation of these less strained tripeptide macrocycles, but instead utilized an intramolecular SNAr reaction with $RuCp^+$ complexed arenes (Scheme 1.14). $RuCp^+$ complexed tyrosine **1.89** could be coupled to tyrosine based dipeptide **1.90** to forge $RuCp^+$ complexed tripeptide **1.91**. Intramolecular SNAr macrocyclization using 2,6-ditert-butyl-sodium phenoxide as base gave $RuCp^+$ complexed macrocyclic tripeptide **1.92**. Decomplexation by irradiation with a 350 nm light source followed by global demethylation using ethyl thiol and $AlBr_3$ yielded K-13. Although not shown, the synthesis of OF4949-III proceeded with the same forward synthesis as K-13.

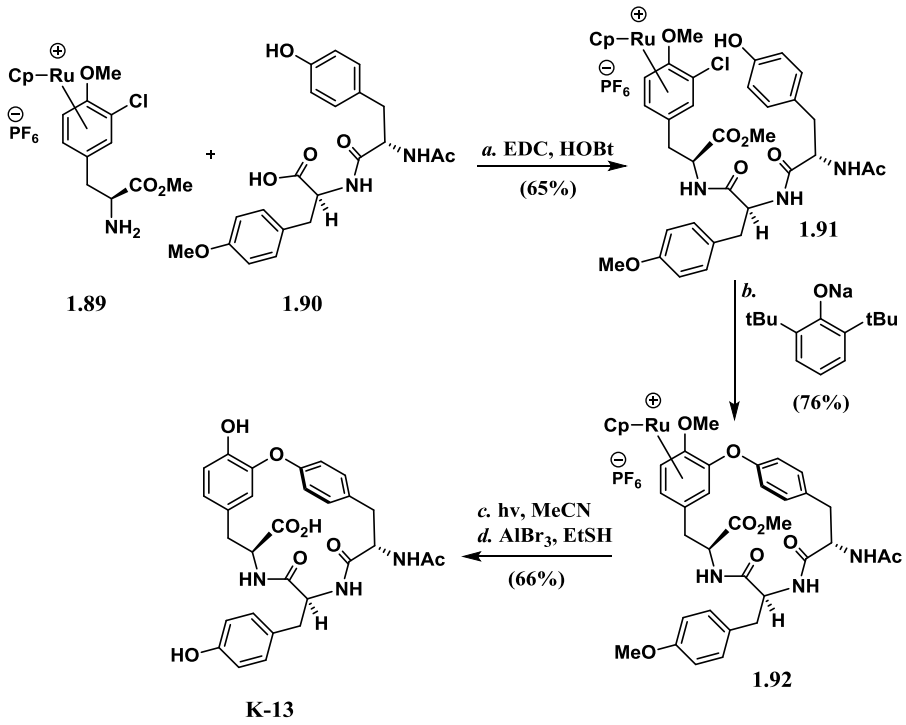

Scheme 1.14. Total synthesis of K-13 by a $RuCp^+$ complexed SNAr.

RP 66453 presents a unique configuration in the iso-dityrosine class of peptide natural products. Similar to phenyl glycine based peptides, both C-C biaryl linkages and C-O biaryl ether linkages are present. RP 66453 is a secondary metabolite isolated from an *Actinomycetes* strain and is considered a neurotensin antagonist.[43] Structural modifications of RP 66453 have led to the discovery of potent neurotensin antagonists claimed to have possible treatment properties for psychosis, Parkinson's and Alzheimer's diseases.[44] Efforts have been made toward the total synthesis of RP 66453. The only synthesis known is that of an atropisomer (*aS(P),S,S,S,S,S*), compared to that of the correct diastereomer (*aR(M),S,S,S,S,S*).[45] In 2003, Zhu and co-workers completed the synthesis of the incorrect diastereomer with two key steps; 1) formation of the C-O aryl ether linkage completed by an intramolecular SNAr, (similar to that of the work done on deoxybouvardin and phenyl glycine related natural products such as vancomycin),[4] and 2)

formation of the C-C aryl fusion by an intramolecular Suzuki cross coupling (Scheme 1.15). With subjection to CsF under dilute conditions, tripeptide **1.93** was converted to biaryl ether **1.94**

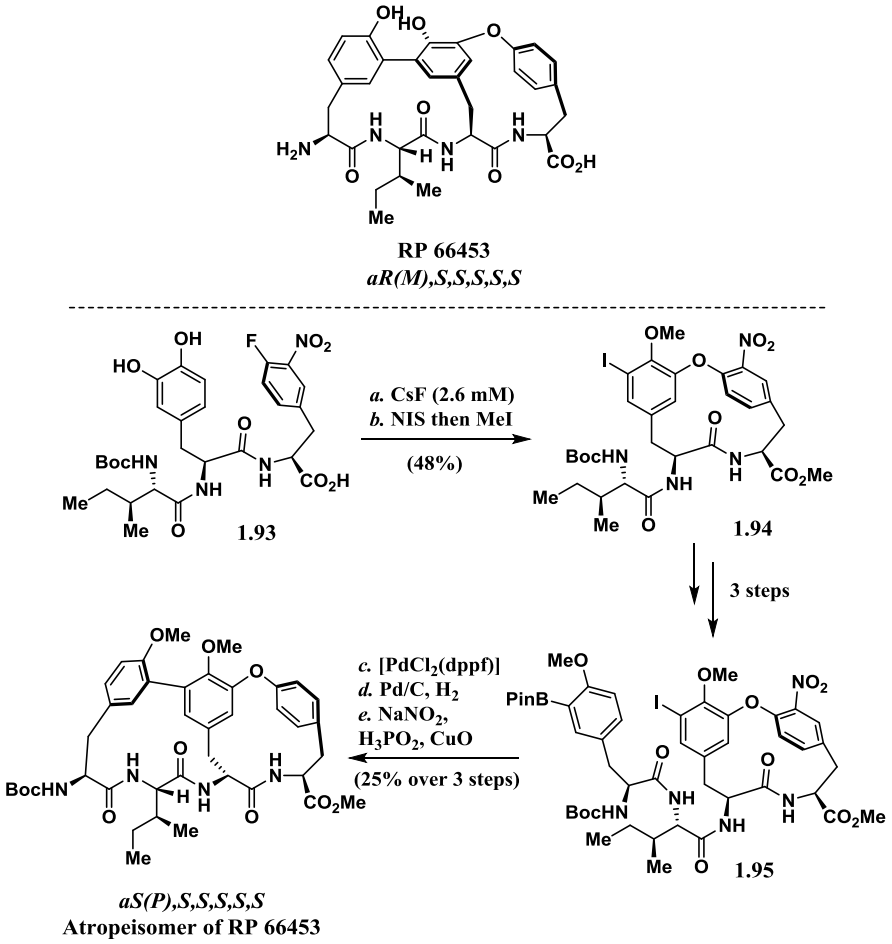

Scheme 1.15. Total synthesis of atropisomer (diastereomer) of RP 66453.

after iodination with NIS and phenol O-methylation with MeI. Aryl ether **1.95** underwent macrocyclization by intramolecular Suzuki cross coupling mediated by [$PdCl_2$(dppf)] and this intermediate proceeding through a deprotection/denitration sequence, could be converted to the *aS(P),S,S,S,S,S*) atropisomer of RP 66453. Albeit the incorrect diastereomer, the total synthesis is expedient and efficient in a way that combines multiple methodologies discovered by the synthetic community in the synthesis of iso-dityrosine peptide natural products. Through

thermal studies done on natural sources, it was discovered that the synthesized atropisomer was indeed the more thermodynamically stable diastereomer of the natural product, leading to the interesting notion that nature does in fact biosynthesize the less thermodynamically stable isomer. The harsh conditions needed to accomplish an intramolecular Suzuki cross coupling would impede access to the correct isomer of RP 66453.

Another important class of natural products are the Rubiaceae-type macrocyclic peptides of which the first to be isolated were the antitumor molecules bouvardin and deoxybouvardin in 1977 (isolated from flowers of *Bouvardia ternifolia* (Rubiaceae)) followed by their closely related analogs belonging to the RA family of antibiotics (Figure 1.8).[1a,46] Up through 2013, there have been 44 Rubiaceae cyclic peptides isolated from higher plants (vascular). These molecules have garnered much attention, comparatively to other iso-dityrosine natural products, because of their potential as chemotherapeutics. Rubiaceae-type cyclic peptides have shown potent antitumor activities *in vitro* and *in vivo*.[46] In fact, bouvardin has been investigated as an antitumor drug candidate by the U.S. National Cancer Institute (through to clinical development) and RA-VII had been reported to be in phase I clinical trials at the Japan National Cancer Institute in the 1990's.[47] RA-VII's therapeutic ratio (index) had been reported to be 400 and its chemosensitivity was reported to be not that dissimilar from that of standard antitumor drugs adriamycin, mitomycin C, cisplatin, vinbrastine, and 5-FU. However, attention the Rubiaceae-type cyclic peptides have received is a function of their unique bicyclic skeletal structure

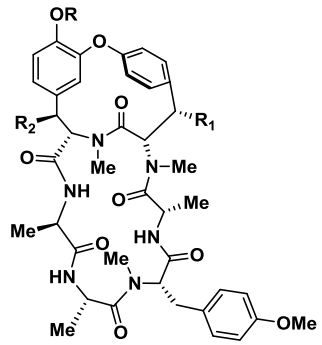

bouvardin - R, R_2=H, R_1=OH
deoxybouvardin (RA-V) - R, R_1, R_2=H
RA-IV - R=Me, R_1=H, R_2=OH
RA-VII - R=Me, R_1, R_2=H

RA-XII - R=β D-glucose, R_1, R_2=H
RA-XVI - R=β D-glucose, R_1=H, R_2=OAc

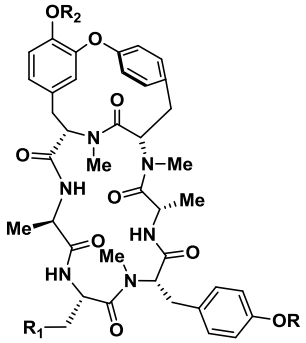

RA-I - R=Me, R_1=OH, R_2=H
RA-II - R, R_1=H, R_2=Me
RA-III - R=Me, R_1=OH, R_2=Me
RAI-III - Conformational isomer of RA-III
RA-VI - R=Me, R_1=OH, R_2=Me, *D-tyr
RAI-VI - Conformational isomer of RA-VI
RA-VIII - R=Me, R_1=OH/CH_3, R_2=Me
RA-X - R=Me, R_1=CH_2CO_2H, R_2=Me
RA-XI - R=Me, R_1=CH_2CO_2H, R_2=H
RA-XIII - R=Me, R_1=CH_2CO_2H, R_2=β D-glucose
RA-XV - R=Me, R_1=H, R_2=β 6-OAc-D-glucose
RA-XIX - R=Me, R_1=$CH(CH_3)_2$, R_2=Me
RA-XX - R, R_1, R_2=Me
RA-XXI - R, R_1=Me, R_2=H
RA-XXII - R=Me, R_1=OH/CH_3, R_2=H
RA-XXIII - R=Me, R_1=CH_2CONH_2, R_2=Me
RA-XXIV - R=Me, R_1=CH_2CONH_2, R_2=H

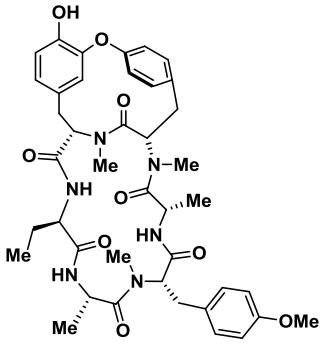

RA-XVII

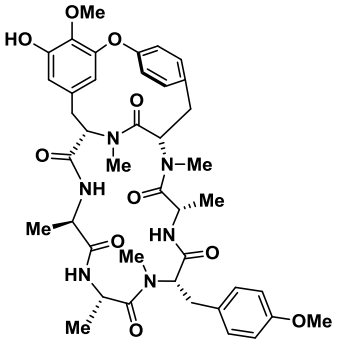

RA-XVIII

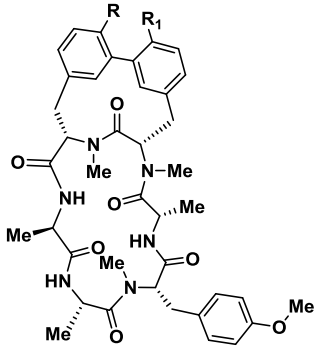

rubiyunnanin B - R=β D-glucose, R_1=OH
neo-RA-V - R, R_1=OH
allo-RA-V - R=H, R_1=OH

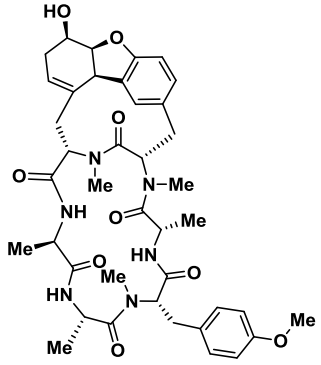

rubiyunnanin A

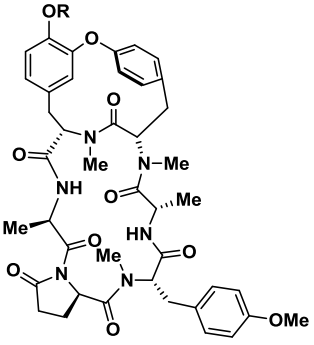

RA-IX - R=Me
RA-XIV - R=β D-glucose

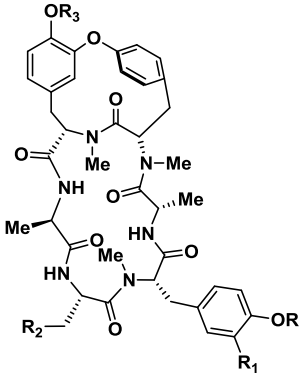

rubiyunnanin C - R=Me, R_1, R_3=H, R_2=CH_2CONH_2
rubiyunnanin D - R, R_1, R_3=H, R_2=CH_2CO_2H
rubiyunnanin E - R=Me, R_1=OH, R_2=CH_2CO_2H, R_3=H
rubiyunnanin F - R=Me, R_1=H, R_2=CH_2CONH_2, R_3=β D-glucose
rubiyunnanin G - R, R_1, R_2=H, R_3=β D-glucose
rubiyunnanin H - R=Me, R_1, R_2=H, R_3=β D-glucose

Figure 1.8. Representations of bouvardin, deoxybouvardin, the associated analogs of the RA family and the associated rubiyunnanin family of natural products.

as much as it's about their bioactivities. To the synthetic community, these molecules pose an unprecedented challenge due to their highly strained conformations. This comment is specifically in reference to the very rigid L,L-cyclodityrosine cycle associated with the pharmacophore of this class of molecules.[1b] There are two key distinguishing attributes to the pharmacophore; 1) the 14-memebered ring formation by the oxidative coupling of two adjacent tyrosines, and 2) the resulting *cis* peptide bond caused in part by the oxidative coupling of the phenols. This has fueled studies into new macrocyclization methodologies considering, as mentioned in the discussion of the K-13 and OF4949-III synthetic endeavors (17-membered rings), there are no examples of macrolactamisation as a way to form the iso-dityrosine dipeptide cycles (14-memeberd ring) due to the severe ring strain. Boger and co-workers reported the first total synthesis of bouvardin using the same Ullmann type cross coupling their group had utilized to synthesize piperazinomycin, K-13 and OF-4949-III (Scheme 1.16).[48] The synthesis of the β-OH tyrosine moiety started with the DIBAL-H reduction of unsaturated methyl ester **1.96**. The resulting allylic alcohol could be used for a Sharpless asymmetric epoxidation to give enantiopure epoxide **1.97**. After PDC oxidation of the primary alcohol to a carboxylic acid, the epoxide was opened with methylamine and the resulting methylated amine was N-Boc protected to give benzylic alcohol **1.98**. The benzylic alcohol **1.98** could be protected with treatment of TBDMS-Cl and the resulting silanol ester could be deprotected with K_2CO_3 to yield β-OH tyrosine derivative **1.99**. EDC mediated coupling to pentafluorophenol set up a Yamaguchi esterification type amide bond formation with methylated L-DOPA **1.100** to give dipeptide **1.01**. In the key transformation, Ullmann coupling with CuBr-SMe_2 mediated the macrocyclization to give dipeptide aryl ether **1.102**. N-Boc deprotection followed by coupling to linear peptide

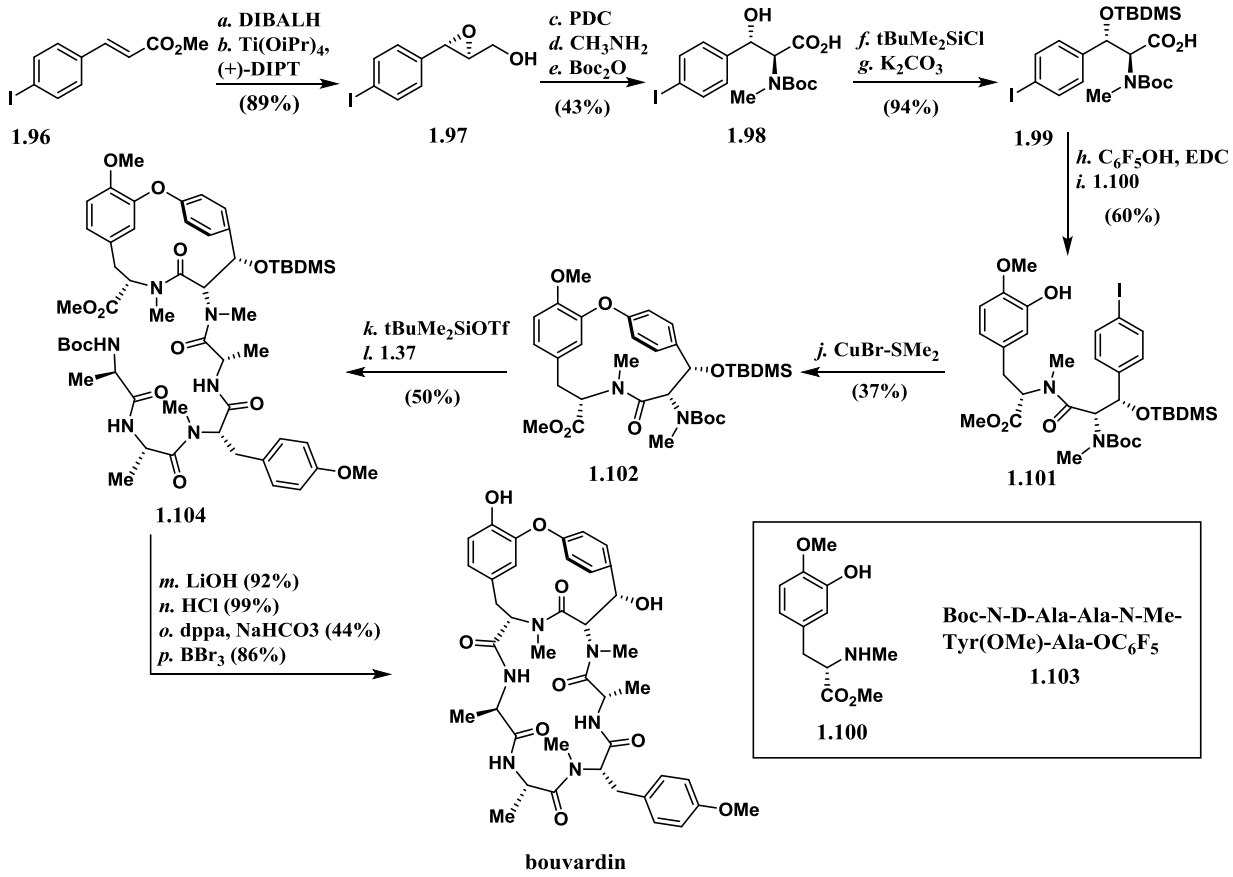

Scheme 1.16. Total synthesis of bouvardin.

1.103 furnished linear hexa-peptide **1.104**. Methyl ester hydrolysis and N-Boc deprotection with LiOH and HCl, respectively, set up the diphenylphosphoryl azide (dppa) mediated macrocyclization event. Selective demethylation of the biaryl ether system by BBr_3 afforded bouvardin in an 86% yield. Despite the potential sensitivity to BBr_3, regioselective demethylation presumably occurred through some proximal bidentate complexation to the ether.

Despite the various methods mentioned above for the syntheses of iso-dityrosine based natural products, Zhu and co-workers developed and applied their own intramolecular SNAr macrocyclization. They utilized an electron-rich phenol addition to an electron-deficient nitro-

fluoro aryl moiety in the total synthesis of deoxybouvardin.[4a,49] After the pharmacophore of deoxybouvardin and multiple analogs had been synthesized in this manner by both Zhu and Boger,[50] Zhu reported an updated, more efficient 2nd generation total synthesis using their method (Scheme 1.18).[51] This synthesis first requires the ability to make nitro-fluoro phenylalanine enantioselectivly (Scheme 1.17).[52] This could be achieved by alkylation of benzyl

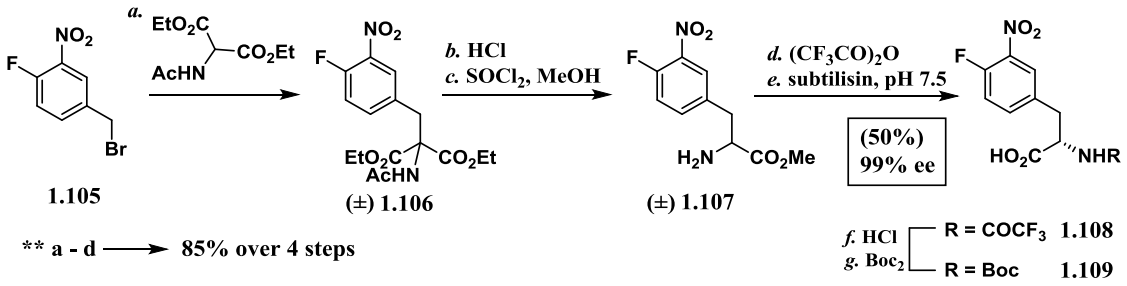

Scheme 1.17. Enzymatic synthesis of enantiopure nitro-fluoro phenylalanine analogs.

bromide **1.105** with an N-Acyl amino malonate to afford racemic malonate **1.106**. Reflux under heavily acidic conditions followed by thionyl chloride mediated methyl esterification afforded racemic nitro-fluoro phenyl alanine **1.107**. The free amine could be protected with a trifluoroacyl group and an enzyme mediated kinetic resolution using subtilisin yielded the free acid of one enantiomer **1.108** and the methyl ester of the other respective enantiomer of the trifluoroacyl protected nitro-fluoro phenylalanine. It should be noted that the protected amino acid **1.108** needed to undergo a deprotection/protection sequence to change the protecting group to an N-Boc for the synthesis. The enzymatic procedure was attempted on both N-Boc and N-Cbz protected racemates with low conversions and low enantiomeric excess. So the trifluoroacyl protecting group was settled upon for the resolution procedure. Since this reported resolution, new methodologies were developed for the synthesis of these nitro-fluoro amino acids mainly utilizing Schoellkopf auxiliary chemistry.[53] With nitro-fluoro phenylalanine **1.109** in hand, an expedient total synthesis of deoxybouvardin analog RA-VII was carried out. Nitro-fluoro

phenylalanine **1.109** was coupled to protected L-DOPA **1.110** using EDC/HOBt to give dipeptide **1.111** to which both protected phenols underwent an *in-situ* desilylation.

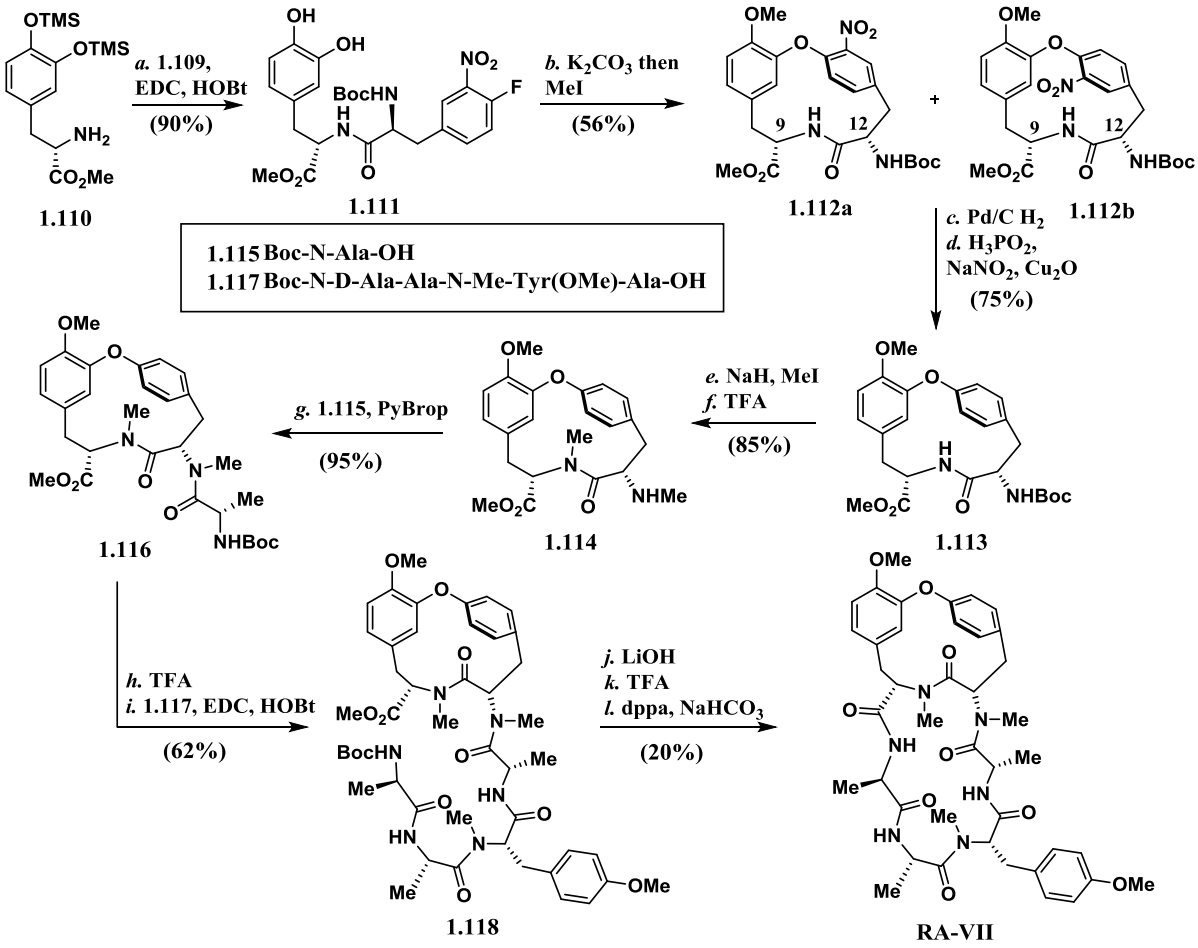

Scheme 1.18. Second generation total synthesis of deoxybouvardin RA-VII.

Dipeptide **1.111** underwent an intramolecular SNAr to forge the cyclic aryl ether bond. This was followed by *in-situ* methylation of the remaining unprotected phenol to give atropodiastereomers of dipeptide aryl ethers **1.112a** and **1.112b**. An important property of this 2nd generation synthesis was that the stereo integrity of C9 was not problematic. In the aforementioned first syntheses of the deoxybouvardin pharmacophore, C9 was extremely sensitive to epimerization

from (9S,12S)-**1.119** to the more thermodynamically stable (9R,12S)-**1.120** when considering the intramolecular SNAr from dipeptide **1.121** (Figure 1.9). Using NaH, the desired diastereomer could be isolated. The atropdiastereomers **1.112a** and **1.112b** could undergo a two-step reduction sequence to diverge both isomers to the single isomer aryl ether **1.113**. Methylation of

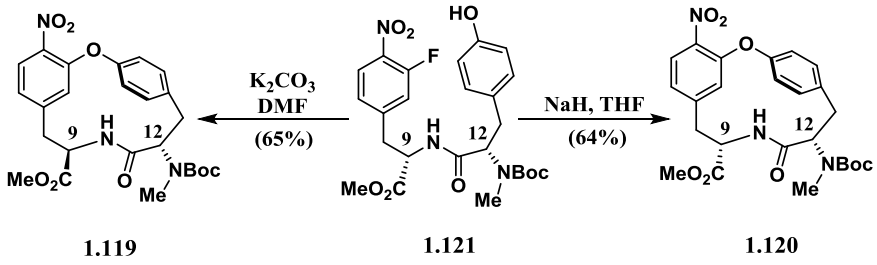

1.119 **1.121** **1.120**

Figure 1.9. Epimerization of C9 in first generation syntheses of deoxybouvardin analogs like RA-VII.

the internal *cis* amide followed by N-Boc deprotection using TFA afforded free methylated amine **1.114**. This free amine was coupled to alanine residue **1.115** using PyBrop to give tripeptide **1.116**. N-Boc deprotection with TFA and subsequent EDC/HOBt mediated coupling to peptide **1.117** furnished hexa-peptide **1.118**. Following deprotection of the methyl ester and N-Boc with LiOH and TFA, respectively, the peptide was cyclized using diphenylphosphoryl azide (dppa), albeit in poor conversion, to yield RA-VII. Both the Boger and Zhu methods have been the focal points in the synthesis of many RA analogs. Through extensive structure-activity relationship studies by Boger and Itokawa,[54] it was proven that the cyclic iso-dityrosine moiety was indeed the pharmacophore of this class of natural products. In depth studies by Boger[54a-d] have indicated some trends in the structure-activity relationship; 1) N-methylation is not key to observed bioactivity but demethylated versions are less potent (but still active), 2) though functionalization of the phenolic hydroxyl is not key to the observation of bioactivity, the

potency is greatly affected by the manner in which it is functionalized, and 3) the rigid, cyclic nature is essential for bioactivity.

The rubiyunnanin natural products have been isolated much more recently than that of bouvardin, deoxybouvardin and RA analogs.[46] Most of the rubiyunnanin family had not been isolated prior to 2010. Rubiyunnanin A and rubiyunnanin B are two members of this family that have intriguing skeletal structures (Figure 1.8). Rubiyunnanin A maintains the typical 18-membered cyclic peptide found in iso-dityrosine natural products and is most likely a product of an oxidative coupling between two tyrosine residues in the same fashion as most other iso-dityrosines. However, there are three key characteristics that make rubiyunnanin A distinct from the rest of the family; 1) the amide forming the bicycle is proposed to be a *trans* amide unlike the commonly seen *cis* amide, 2) the two tyrosine residues form an unprecedented carbon-carbon bond, and 3) as a function of this carbon-carbon bond, one of the tyrosine residues is partially reduced. Rubiyunnanin B is unique to the rest of the family in one aspect that the oxidative coupling of the two tyrosine residues does not result in a carbon-oxygen bond but only a carbon-carbon bond, which has previously only been seen in RP 66435. This carbon-carbon fusion of the phenols creates an unparalleled strained bicycle, maintaining a higher level of rigidity compared to that of its family members. Biosynthetic mechanisms for the synthesis of plant cyclopeptides have not been well established, but there has been a proposed biosynthetic pathway for the formation of rubiyunnanin A and B; specifically originating from a non-ribosomal type mechanism (Figure 1.10).[46c,d] It is well established that these types of couplings could occur through free radical meditated carbon-carbon couplings and it is established that the free hydroxyl of the phenol and the *ortho*-carbon can generate free radicals. The RA natural

products would then arise from a radical coupling of the hydroxyl of one tyrosine with the *ortho*-carbon of the other tyrosine. Rubiyunnanin B could arise from a diradical coupling of two

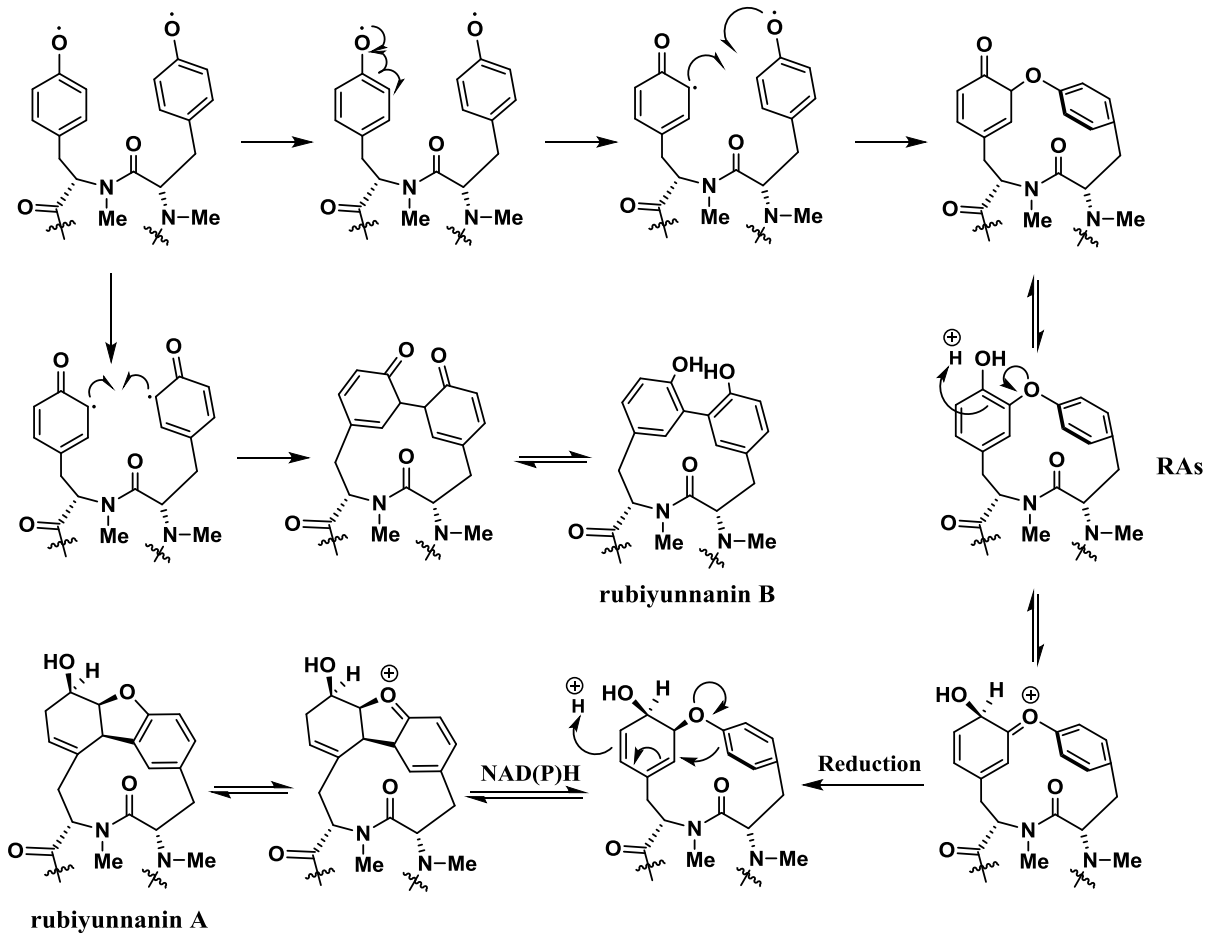

Figure 1.10. Possible biosynthetic pathways for the synthesis of rubiyunnanin B, and rubiyunnanin A through the RA pathway.

ortho-carbon free radicals followed by a glycosyl-transfer. One possibility for the biosynthesis of rubiyunnanin A could arise from an electrophilic aromatic substitution reaction catalyzed by NAD(P)H with subsequent rearomatization of the tyrosine residue. Rubiyunnanin A has never been synthesized and only analogs of rubiyunnanin B have been achieved.[55] Most notably among the attempts was recent work by Takeya and co-workers in 2012, who synthesized allo-RA-V and neo-RA-V.[56] Their synthesis began with the preparation of boronic acid **1.123** by

benzyl protection of phenol **1.122** under Mitsunobu conditions followed by palladium catalyzed borylation and subsequent hydrolysis (Scheme 1.19). Iodo-tyrosine **1.125** could be synthesized from benzylated tyrosine **1.124** with N-methylation by use of tetra-butylammonium bromide as a phase transfer catalyst for NaOH and N-Boc deprotection by treatment with TFA. Amine **1.125** was directly taken into an EDC/HOAt mediated coupling with aforementioned boronic acid **1.123** to afford dipeptide **1.126**. The key step to the synthesis was an intramolecular Suzuki-Miyaura cross coupling to give cyclic iso-dityrosine **1.127** and **1.127'** in modest yields as a

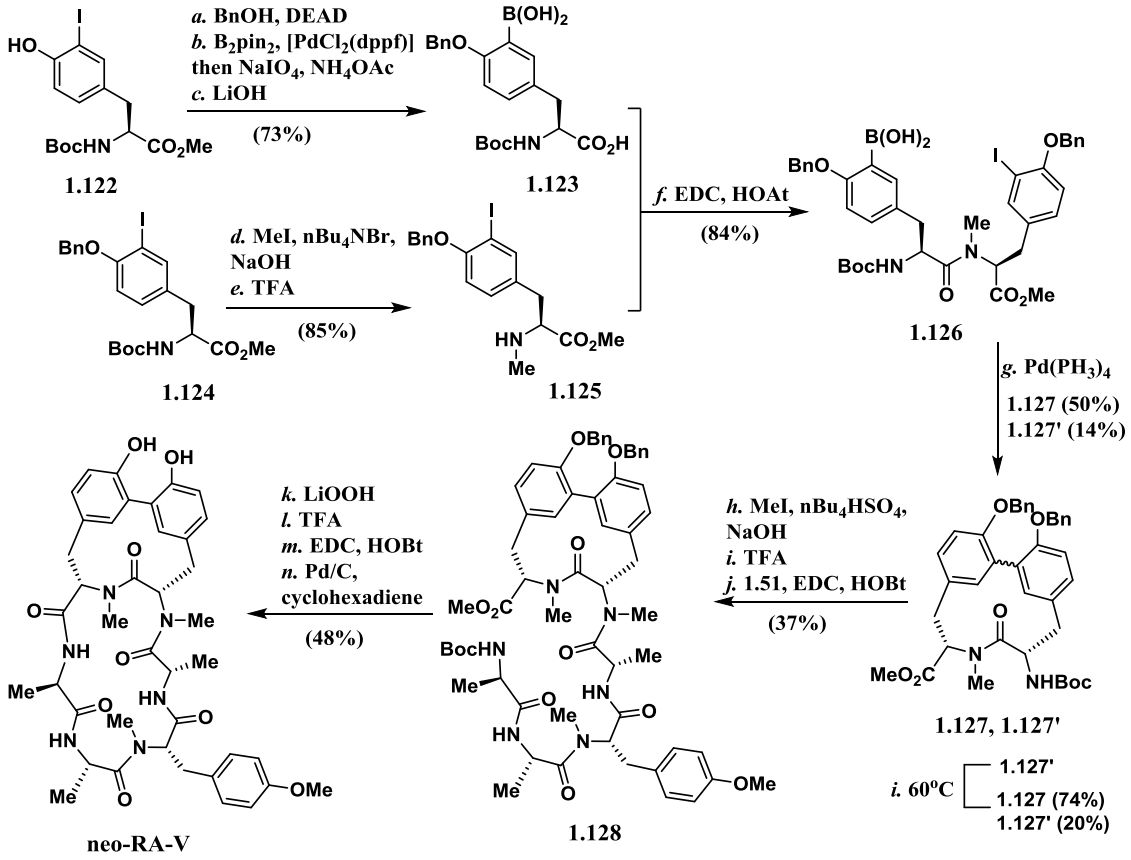

Scheme 1.19. Total synthesis of neo-RA-V.

mixture of atropdiastereomers (3.5:1 respectively). The two atropisomers had different properties and were separable by chromatography. Subjection of atropisomer **1.127'** to heat in

toluene did lead to a 74% conversion to atropisomer **1.127** (20% recovery of **1.127'**). Although spectral experiments could not identify the exact identities of the two atropisomers, it was clear that **1.127** was the more thermodynamically stable atropisomer and so was presumptuously the species carried forward in the synthesis. Cyclic iso-dityrosine **1.127** could be N-methylated using phase transfer catalysis and N-Boc deprotected with TFA to set up an EDC/HOBt mediated coupling with peptide **1.117** to give hexa-peptide **1.128**. N-Boc and methyl ester hydrolysis with TFA and LiOOH, respectively, followed by macrocyclization and debenzylation furnished neo-RA-V. The aforementioned analog studies of rubiyunnanin B also took advantage of a similar intramolecular Suzuki-Miyaura cross coupling to provide multiple phenol O-methyl analogs (analogs varied by identity of the amino acids in the peptide backbone).

The structure-activity relationship studies that have been explored on the pharmacophore of bouvardin, deoxybouvardin, the corresponding RA analogs and the rubiyunnanin family of natural products, have led to findings of interesting trends in the bioactivities of all these molecules (Figure 1.11).[46,54] In considering natural products deoxybouvardin, RA-VII and RA-XII, it can be seen that although methylated analog RA-VII is more potent than free hydroxyl deoxybouvardin, the β-glycosylated RA-XII loses much of its potency in a few direct comparative cancer cell lines. However, in complete contradiction of this trend, rubiyunnanin B completely loses its bioactivity upon deglycosylation yielding analog neo-RA-V. It should be noted that although this is the case, rubiyunnanin B is not as potent as the aforementioned deoxybouvardin and RA analogs. IC_{50} values of taxol and CPT were included as reference points wherein deoxybouvardin and RA-VII are the only natural products with relatively similar

potencies. Not shown in this Figure are the activities for rubiyunnanin C-H, which not surprisingly, show a similar trend to that of RA-VII versus RA-XII. Rubiyunnanin C is the most biologically active of the rubiyunnanin family but upon studying the glycosylated member's rubiyunnanin F, G and H, a trending loss of bioactivity will be noticed just as with the case for deoxybouvardin. Our group became very interested in rubiyunnanin A and B for their unique skeletal structures and bioactivities. Without a known synthesis of rubiyunnanin A and a lack of

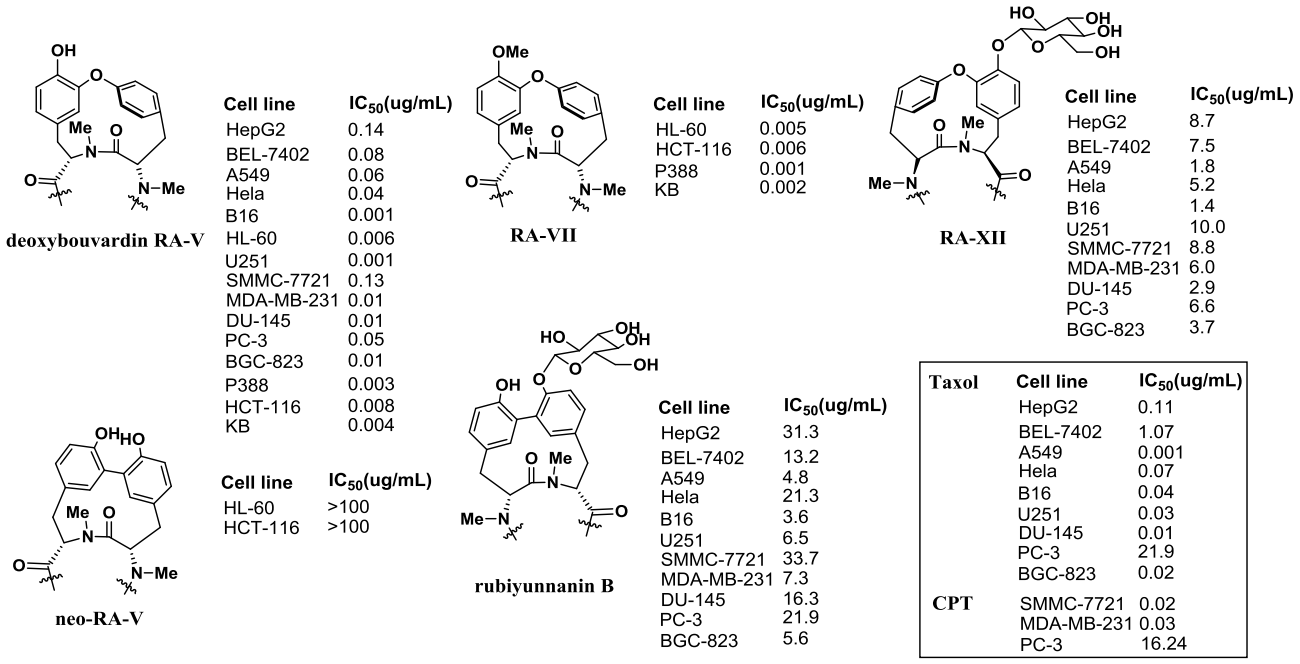

Figure 1.11. Representative IC_{50} values for deoxybouvardin, RAs and rubiyunnanins.

studies done for its potential biological activities, the first total synthesis was sought after. Our group had previously developed a carbasugar synthesis methodology that could be applied to the total synthesis of rubiyunnanin B. Stability studies of phenols, glycosylated versus carbasugar substituted, could provide valuable structure-activity-relationships.[57] This study/synthesis could help us better understand why glycosylation of rubiyunnanin B is imperative for its biological

activity and in turn, possibly help us develop an analog of the family pharmacophore that is potent in its antitumor activity.

REFERENCES

[1] (a) Tan, N. H.; Zhou, J. *Chem. Rev.* **2006**, *106*, 840-895. (b) Gulder, T.; Baran, P. S. *J. Nat. Prod.* **2012**, *29*, 899-934.

[2] Feliu, L.; Planas, M. *International Journal of Peptide Research and Therapeutics.* **2005**, *11*, 53-97.

[3] (a) Swift, R. V.; Amaro, R. E. *Chem. Biol. Drug Des*. **2013**, *81*, 61. (b) Hess, S.; Ovadia, O.; Shalev, D. E.; Senderovich, H.; Qadri, B.; Yehezkel, T.; Salitra, Y.; Sheynis, T.; Jelinek, R.; Gilon, C.; Hoffman, A. *J. Med. Chem.* **2007**, *50*, 6201-6211. (c) Hewitt, W. M.; Leung, S. S.; Pye, C. R.; Ponkey, A. R.; Bednarek, M.; Jacobson, M. P.; Lokey, R. S. *J. Am. Chem. Soc.* **2015**, *137*, 715-721.

[4] (a) Rao, A. V. R.; Gurjar, M. K.; Reddy, K. L.; Rao, A. S. *Chem. Rev.* **1995**, *95*, 2135-2167. (b) Okano, A.; Nakayama, A.; Schammel, A. W.; Boger, D. L. *J. Am. Chem. Soc.* **2014**, *136*, 13522-13525. (c) Aldemir, H.; Richarz, R.; Gulder, T. A. *Angew. Chem. Int. Ed.* **2014**, *53*, 8286-8293. (d) Nicolaou, K. C.; Mitchell, H. J.; Jain, N. F.; Winssinger, N.; Hughes, R.; Bando, T. *Angew. Chem. Int. Ed.* **1999**, *38*, 240-244. (e) Nicolaou, K. C.; Li, H.; Boddy, C. N. C.; Ramanjulu, J. M.; Yue, T.-Y.; Natarajan, S.; Chu, X.-J.; Bräse, S.; Rübsam, F. *Chem. Eur. J.* **1999**, *5*, 2584-2601. (f) Evans, D. A.; Wood, M. R.; Trotter, B. W.; Richardson, T. I.; Barrow, J. C.; Katz, J. L. *Angew. Chem. Int. Ed.* **1998**, *37*, 2700-2704. (g) Zhang, A. J.; Burgess, K. *Angew. Chem. Int. Ed.* **1999**, *38*, 634-636. (h) Boger, D. L.; Miyazaki, S.; Kim, S. H.; Wu, J. H.; Loiseleur, O.; Castle, S. L. *J. Am. Chem. Soc.* **1999**, *121*, 3226-3227. (i) Kahne, D.; Leimkuhler, C.; Lu, W.; Walsh, C. *Chem. Rev.* **2005**, *105*, 425-448.

[5] Trauger, J. W.; Kohli, R. M.; Mootz, H. D.; Marahiel, M. A.; Walsh, C. T. *Nature* **2000**, *407*, 215–218.

[6] Schramma, K. R.; Bushin, L. B.; Seyedsayamdost, M. R. *Nature Chemistry* **2015**, *7*, 431-437.

[7] Uchida, I.; Shigematsu, N.; Ezaki, M.; Hashimoto, M.; Aoki, H.; Imanaka, H. *J. Antibiot.* **1985**, *38*, 1462-1468.

[8] Schmidt, U.; Meyer, R.; Leitenberger, V.; Griesser, H.; Lieberknecht, A. *Synthesis.* **1992**, *1992*, 1025-1030.

[9] Berwe, M.; Jöntgen, W.; Krüger, J.; Cancho-Grande, Y.; Lampe, T.; Michels, M.; Paulsen, H.; Raddatz, S.; Weigand, S. *Org. Process Res. Dev.* **2011**, *15*, 1348-1357.

[10] Wu, Q. X.; Crews, M. S.; Draskovic, M.; Sohn, J.; Johnson, T. A.; Tenney, K.; Valeriote, F. A.; Yao, X. J.; Bjeldanes, L. F.; Crews, P. *Org. Lett.* **2010**, *12*, 4458-4461.

[11] Ghosh, S.; Kinthada, L. K.; Bhunia, S.; Bisai, A. *Chem. Commun.* **2012**, *48*, 10132-10134.

[12] Zhao, J. C.; Yu, S. M.; Liu, Y.; Yao, Z. J. *Org. Lett.* **2013**, *15*, 4300-4303.

[13] Koguchi, Y.; Kohno, J. U. N.; Nishio, M.; Takahashi, K.; Okuda, T.; Ohnuki, T.; Komatsubara, S. *J. Antibiot.* **2000**, *53*, 105-109.

[14] (a) Lin, S.; Yang, Z. Q.; Kwok, B. H.; Koldobskiy, M.; Crews, C. M.; Danishefsky, S. J. *J. Am. Chem. Soc.* **2004**, *126*, 6347-6355. (b) Albrecht, B. K.; Williams, R. M. *Org. Lett.* **2003**, *5*, 197-200. (c) Inoue, M.; Sakazaki, H.; Furuyama, H.; Hirama, M. *Angew. Chem. Int. Ed.* **2003**, *42*, 2654-2657.

[15] Garner, P.; Park, J. M. *J. Org. Chem.* **1987**, *52*, 2361-2364.

[16] Coste, A.; Bayle, A.; Marrot, J.; Evano, G. *Org. Lett.* **2014**, *16*, 1306-1309.

[17] Lindquist, N.; Fenical, W.; Van Duyne, G. D.; Clardy, J. *J. Am. Chem. Soc.* **1991**, *113*, 2303-2304.

[18] (a) Nicolaou, K. C.; Bella, M.; Chen, D. Y. K.; Huang, X.; Ling, T.; Snyder, S. A. *Angew. Chem. Int. Ed.* **2002**, *41*, 3495-3499. (b) Li, J.; Jeong, S.; Esser, L.; Harran, P. G. *Angew. Chem.*

Int. Ed. **2001**, *40*, 4765-4769. (c) Li, J.; Burgett, A. W. G.; Esser, L.; Amezcua, C.; Harran, P. G. *Angew. Chem. Int. Ed.* **2001**, *40*, 4770-4773.

[19] Nicolaou, K. C.; Chen, D. Y.; Huang, X.; Ling, T.; Bella, M.; Snyder, S. A. *J. Am. Chem. Soc.* **2004**, *126*, 12888-12896.

[20] Yonemitsu, O.; Cerutti, P.; Witkop, B. *J. Am. Chem. Soc.* **1966**, *88*, 3941-3945.

[21] Burgett, A. W.; Li, Q.; Wei, Q.; Harran, P. G. *Angew. Chem. Int. Ed.* **2003**, *42*, 4961-4966.

[22] Nicolaou, K. C.; Bheema Rao, P.; Hao, J.; Reddy, M. V.; Rassias, G.; Huang, X.; Chen, D. Y.; Snyder, S. A. *Angew. Chem. Int. Ed.* **2003**, *42*, 1753-1758.

[23] Knowles, R. R.; Carpenter, J.; Blakey, S. B.; Kayano, A.; Mangion, I. K.; Sinz, C. J.; MacMillan, D. W. *Chem. Sci.* **2011**, *2011*, 308-311.

[24] Kelly, T. R.; Li, Q.; Bhushan, V. *Tetrahedron Lett.* **1990**, *31*, 161-164.

[25] Ding, H.; DeRoy, P. L.; Perreault, C.; Larivee, A.; Siddiqui, A.; Caldwell, C. G.; Harran, S.; Harran, P. G. *Angew. Chem. Int. Ed.* **2015**, *54*, 4818-4822.

[26] (a) Caldwell, C.; Hanson, G.; Harran, S.; Harran, P. G.; Wei, Q.; Zhou, M. US Patent #7,851,620 B2 Issued December 14, **2010**. (b) Wei, Q.; Zhou, M.; Xu, X.; Caldwell, C.; Harran, S.; Wang, L. US Patent #8,592,469 B2 Issued November 26, **2013**.

[27] Mai, C. K.; Sammons, M. F.; Sammakia, T. *Angew. Chem. Int. Ed.* **2010**, *49*, 2397-2400.

[28] Cheung, C. M.; Goldberg, F. W.; Magnus, P.; Russell, C. J.; Turnbull, R.; Lynch, V. *J. Am. Chem. Soc.* **2007**, *129*, 12320-12327.

[29] Bedos-Belval, F.; Rouch, A.; Vanucci-Bacqué, C.; Baltas, M. *Med. Chem. Commun.* **2012**, *3*, 1356-1372.

[30] Aoki, S.; Cho, S.-h.; Ono, M.; Kuwano, T.; Nakao, S.; Kuwano, M.; Nakagawa, S.; Gao, J.-Q.; Mayumi, T.; Shibuya, M.; Kobayashi, M. *Anti-Cancer Drugs* **2006**, *17*, 269-278.

[31] Kotoku, N.; Tsujita, H.; Hiramatsu, A.; Mori, C.; Koizumi, N.; Kobayashi, M. *Tetrahedron* **2005**, *61*, 7211-7218.

[32] Tamai, S.; Kaneda, M.; Nakamura, S. *J. Antibiot.* **1982**, *35*, 1130-1136.

[33] Nishiyama, S.; Nakamura, K.; Suzuki, Y.; Yamamura, S. *Tetrahedron Lett.* **1986**, *27*, 4481-4484.

[34] Boger, D. L.; Zhou, J. *J. Am. Chem. Soc.* **1993**, *115*, 11426-11433.

[35] Ghosh, S.; Kumar, A. S.; Mehta, G. N.; Soundararajan, R.; Sen, S. *Arkivoc* **2009**, 72-78.

[36] (a) Chan, D. M. T.; Monaco, K. L.; Wang, R.-P.; Winters, M.P. *Tetrahedron Lett.* **1998**, *39*, 2933-2936. (b) Evans, D. A.; Katz, J. L.; West, T. R. *Tetrahedron Lett.* **1998**, *39*, 2937-2940. (c) Lam, P. Y. S.; Clark, C. G.; Saubern, S.; Adams, J.; Winters, M. P.; Chan, D. M. T.; Combs, A. *Tetrahedron Lett.* **1998**, *39*, 2941-2944.

[37] Janetka, J. W.; Raman, P.; Satyshur, K.; Flentke, G. R.; Rich, D. H. *J. Am. Chem. Soc.* **1997**, *119*, 441-442.

[38] (a) Sano, S.; Ikai, K.; Kuroda, H.; Nakamura, T.; Obayashi, A.; Ezure, Y.; Enomoto, H. *J. Antibiot.* **1986**, *39*, 1674-1684. (b) Sano, S.; Ikai, K.; Katayama, K.; Takesako, K.; Nakamura, T.; Obayashi, A.; Ezure, Y.; Enomoto, H. *J. Antibiot.* **1986**, *39*, 1685-1696.

[39] Boger, D. L.; Yohannes, D. Biomed. *Chem. Lett.* **1993**, *3*, 245-250.

[40] Nolasco, L.; Perez Gonzalez, M.; Caggiano, L.; Jackson, R. F. *J. Org. Chem.* **2009**, *74*, 8280-8289.

[41] Boger, D. L.; Yohannes, D. *J. Org. Chem.* **1990**, *55*, 6000-6017.

[42] Janetka, J. W.; Rich, D. H. *J. Am. Chem. Soc.* **1997**, *119*, 6488-6495.

[43] Helynck, G.; Dubertret, C.; Frechet, D.; Leboul, J. *J. Antibiot.* **1998**, *51*, 512-514.

[44] Clerc, F. F.; Dubroeucq, M. C.; Helynck, G.; Leboul, J.; Martin, J. P. FR 2720066 (WO 9532218), **1995** [Chem. Abstr. **1996**, *124*, 233154x and *124*, 233155y].

[45] (a) Bois-Choussy, M.; Cristau, P.; Zhu, J. *Angew. Chem. Int. Ed.* **2003**, *42*, 4238-4241. (b) Krenitsky, P. J.; Boger, D. L. *Tetrahedron Lett.* **2003**, *44*, 4019-4022.

[46] (a) Xu, K.; Wang, P.; Yuan, B.; Cheng, Y.; Li, Q.; Lei, H. *Chemistry. Central Journal* **2013**, *7*, 81. (b) Fan, J. T.; Su, J.; Peng, Y. M.; Li, Y.; Li, J.; Zhou, Y. B.; Zeng, G. Z.; Yan, H.; Tan, N. H. *Bioorg. Med. Chem.* **2010**, *18*, 8226-8234. (c) Fan, J.-T.; Chen, Y.-S.; Xu, W.-Y.; Du, L.; Zeng, G.-Z.; Zhang, Y.-M.; Su, J.; Li, Y.; Tan, N.-H. *Tetrahedron Lett.* **2010**, *51*, 6810-6813. (d) Huang, M.-B.; Zhao, S.-M.; Zeng, G.-Z.; Kuang, B.; Chen, X.-Q.; Tan, N.-H. *Tetrahedron* **2014**, *70*, 7627-7631.

[47] Chemistry and Pharmacology (The Alkaloids); Cordell, G. A., Eds.; Academic Press: San Diego, 1997; Vol. 49, pp 315-336.

[48] (a) Boger, D. L.; Patane, M. A.; Zhou, J. *J. Am. Chem. Soc.* **1994**, *116*, 8544-8556. (b) Boger, D. L.; Yohannes, D. *J. Org. Chem.* **1988**, *53*, 487-499.

[49] (a) Burgess, K.; Lim, D.; Martinez, C. I. *Angew. Chem. Int. Ed.* **1996**, *35*, 1077-1078. (b) Zhu, J. *Synlett* **1997**, *1997*, 133-144.

[50] (a) Beugelmans, R.; Bigot, A.; Bois-Choussy, M.; Zhu, J. *J. Org. Chem.* **1996**, *61*, 771-774. (b) Bigot, A.; Beugelmans, R.; Zhu, J. P. *Tetrahedron* **1997**, *53*, 10753-10764. (c) Boger, D. L.; Borzilleri, R. M. *Bioorg. Med. Chem. Lett.* **1995**, *5*, 1187-1190.

[51] Bigot, A.; Tran Huu Dau, M. E.; Zhu, J. *J. Org. Chem.* **1999**, *64*, 6283-6296.

[52] Vergne, C.; BoisChoussy, M.; Ouazzani, J.; Beugelmans, R.; Zhu, J. P. *Tetrahedron: Asymmetry* **1997**, *8*, 391-398.

[53] Schöllkopf, U.; Groth, U.; Deng, C. *Angew. Chem. Int. Ed.* **1981**, *20*, 798-799.

[54] (a) Boger, D. L.; Patane, M. A.; Jin, Q.; Kitos, P. A. *Bioorg. Med. Chem.* **1994**, *2*, 85-100. (b) Boger, D. L.; Zhou, J. *Bioorg. Med. Chem.* **1996**, *4*, 1597-1603. (c) Boger, D. L.; Zhou, J. *J. Am. Chem. Soc.* **1995**, *117*, 7364-7378. (d) Boger, D. L.; Zhou, J.; Winter, B.; Kitos, P. A. *Bioorg. Med. Chem.* **1995**, *3*, 1579-1593. (e) Hitotsuyanagi, Y.; Anazawa, Y.; Yamagishi, T.; Samata, K.; Ichihara, T.; Nanaumi, K.; Okado, N.; Nakaike, S.; Mizumura, M.; Takeya, K.; Itokawa, H. *Bioorg. Med. Chem. Lett.* **1997**, *7*, 3125-3128. (f) Hitotsuyanagi, Y.; Matsumoto, Y.; Sasaki, S.-i.; Suzuki, J.; Takeya, K.; Yamaguchi, K.; Itokawa, H. *J. Chem. Soc., Perkin Trans. 1* **1996**, 1749-1755. (g) Hitotsuyanagi, Y.; Kondo, K.; Takeya, K.; Itokawa, H. *Tetrahedron Lett.* **1994**, *35*, 2191-2194.

[55] Liu, N. N.; Zhao, S. M.; Zhao, J. F.; Zeng, G. Z.; Tan, N. H.; Liu, J. P. *Tetrahedron* **2014**, *70*, 6630-6640.

[56] Hitotsuyanagi, Y.; Odagiri, M.; Kato, S.; Kusano, J.; Hasuda, T.; Fukaya, H.; Takeya, K. *Chem. Eur. J.* **2012**, *18*, 2839-2846.

[57] Moschitto, M. J.; Vaccarello, D. N.; Lewis, C. A. *Angew. Chem. Int. Ed.* **2015**, *54*, 2142-2145.

Chapter 2: Synthetic Effort Overview of Macrocyclic Peptide and Cyclophane Ligands

2.1 Introduction to chemoselective challenges in synthetic chemistry

Chemoselectivity remains a daunting challenge for synthetic chemists. Development of chemoselective protocols arguably pales in comparison to advancements made in stereoselective reactions.[1] Relatively and generally speaking, nature has had millions of years to perfect this practice compared to mankind, especially when considering the total synthesis of complex natural products. Our group aimed to develop new types of ligands, both peptide and cyclophane based, that could expand the toolbox of chemoselective reactions in the synthetic field. There are many examples of chemoselective transformations found in nature; one contribution to our motivation was the ability of bleomycin A_2 **2.1** (Figure 2.1) to selectively cleave DNA.

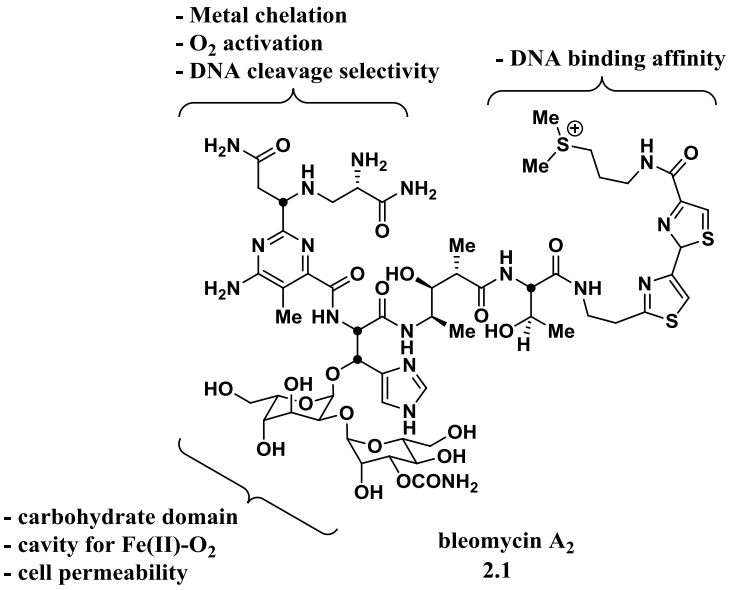

Figure 2.1. Bleomycin A_2 (**2.1**) with functional roles of subunits.

Bleomycin's mode of action is thought to occur through DNA binding with a subsequent degradation that is both metal (Fe^{2+} or Cu^{1+}) and oxygen dependent.[2] The cationic C-terminus acts as the binding agent to the DNA strand while the N-terminus pyrimidine serves as the active

Fe^{II}-O_2 site. The carbohydrate domain acts not only to aid cell permeability but also as the cavity for the Fe^{II}-O_2 active site. It has also been known to cleave RNA but for this specific discussion it cleaves double stranded DNA at the 5'-GC and 5'-GT sites chemoselectivity.[3] In a representative mechanism (Scheme 2.1), a C4'-H atom abstraction event takes place revealing

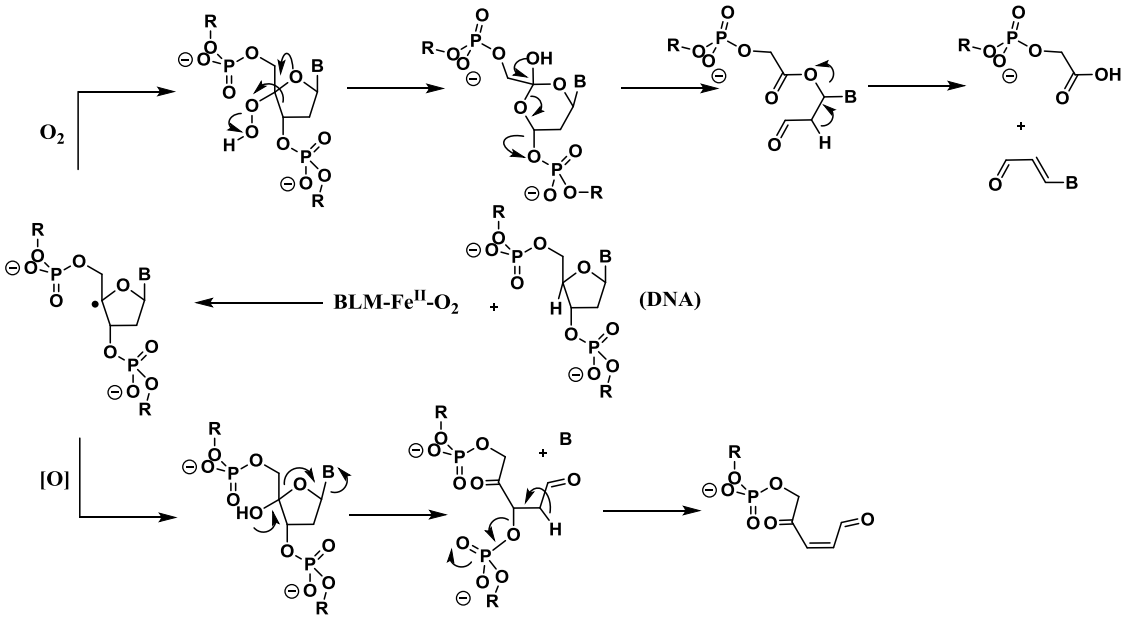

Scheme 2.1. Primary mechanisms of DNA cleavage induced by bleomycin A_2.

two possible cleavage sites.[4] Both degradations of the deoxyribose backbone proceed through oxidations to form orthoester intermediates, which cause ring opening and subsequent cleavage of the furan ring systems. While extensive studies of the biophysical, chemical and biological properties have revealed fascinating information about bleomycin A_2, it was the structural properties that facilitated our motivation. An X-ray structure disclosed by Umezawa in 1978 of P-3A (**2.2**) (Figure 2.2) is taken to represent the Fe and Cu square-planar metal complexes with the presumed trans-axial oxygen activation.[5] It should be noted that there are studies that implicate a complexation of the disaccharide carbamoyl group to the metal center by

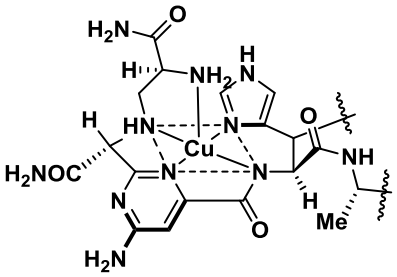

2.2

Cu^{II} P-3A

Figure 2.2. Cu^{II} complex of (+)-P-3A

displacement of the axial amine that would then facilitate the formation of the aforementioned cavity created by the carbohydrate domain.[6]

Bleomycin A_2 inspired the design and synthesis of a class of macrocyclic peptide ligands (Scheme 2.2) that could incorporate an active metal center encapsulated within a cavity that would allow for preferential reactivity to be transmitted to specific substrates. The premise would be such that individually customized amino acids, such as the natural ones (example aspartic acid) or the unnatural ones (example triazole), would undergo iterative peptide couplings

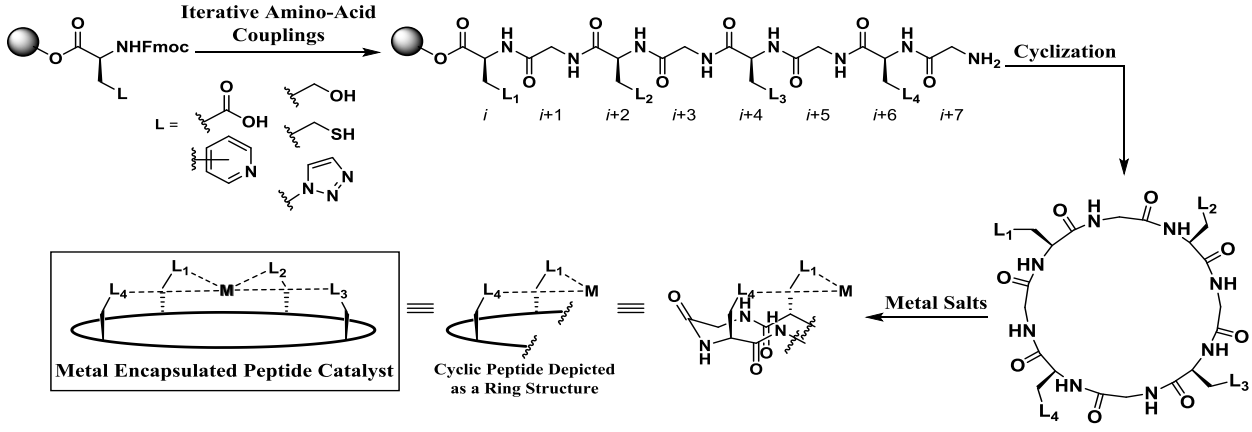

Scheme 2.2. General model for the synthesis of macrocyclic ligands.

followed by a macrocyclization event. The cyclic, tetra-dentate ligands could then encapsulate a metal creating a cavity for an active catalytic site. This would result in a situation where the

reaction upon a specific substrate could occur chemoselectively by the orientation at which the substrate interacted with the active site inside of the catalyst cavity. Take notice of the example using the epoxidation of (+)-limonene (Figure 2.3). Most common epoxidation reagents will selectivity epoxidize the endocyclic olefin (Figure 2.3 (a)),[7] whereas upon creating a cavity, size-

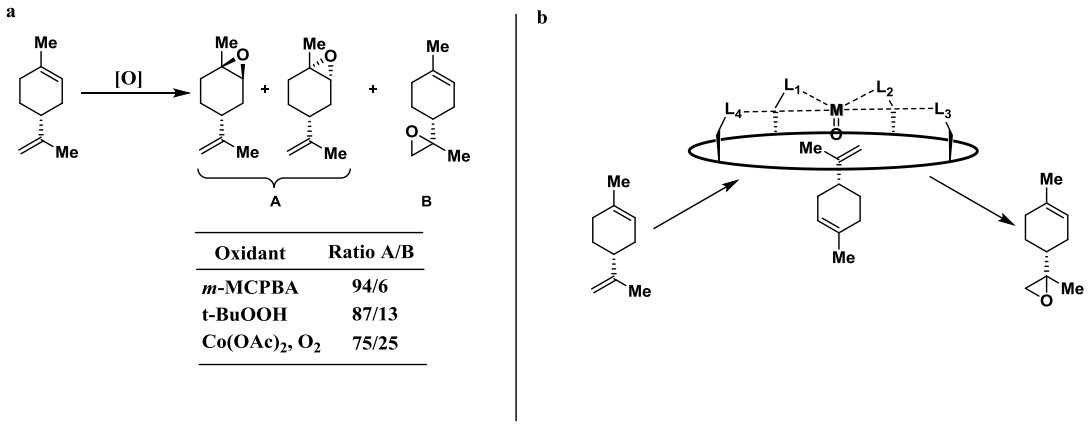

Oxidant	Ratio A/B
m-MCPBA	94/6
t-BuOOH	87/13
$Co(OAc)_2$, O_2	75/25

Figure 2.3. (a) representative selectivity using common epoxidation reagents and (b) cartoon illustration of how selectivity may be manipulated.

exclusion principles may dictate a reversal of chemoselectivity. This is in fact a solution to chemoselective challenges for which there is some literature precedence.[8] In 1987 Suslick reported a bulky Mn^{III} porphyrin catalyst that showed success, albeit limited, at reversing selectivity when studying diene epoxidation.[9] The premise being that a bulky porphyrin catalyst could prevent the epoxidation of more electron rich olefins (more alkyl substitution) compared to less electron rich olefins if those respective olefins were more accessible to the catalyst. Considering Table 2.1, diene entries 3 and 6 show very little change; however, entries (1-2), and (4-5) show a significant manipulation (1:1 regio-isomers product profile) when using the bulky Mn(TTPPP)(OAc) catalyst. Remarkably, entries (7-8) show almost complete reversal of the chemoselectivity trend seen in the epoxidation of these diene substrates. Although with limited

scope and results, this study was a positive indication that the aforementioned size-exclusion of substrates within a catalyst cavity was achievable.

	Diene	A	B	Oxidant	Ratio A:B
1			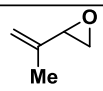	mCPBA Mn(TTPPP)	85:15 67:33
2	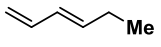	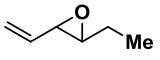	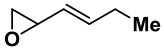	mCPBA Mn(TTPPP)	88:11 55:45
3	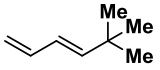	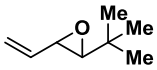	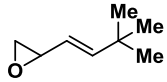	mCPBA Mn(TTPPP)	25:75 11:89
4	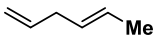	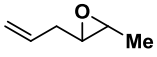	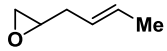	mCPBA Mn(TTPPP)	98:02 63:37
5	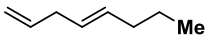	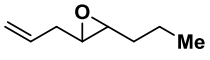	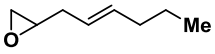	mCPBA Mn(TTPPP)	97:03 48:52
6	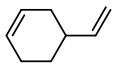	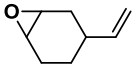	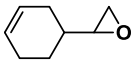	mCPBA Mn(TTPPP)	97:03 80:20
7	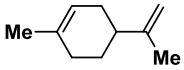	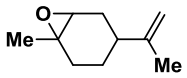	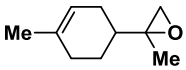	mCPBA Mn(TTPPP)	90:10 36:64
8	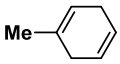	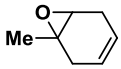	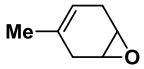	mCPBA Mn(TTPPP)	91:09 04:96

Table 2.1. Epoxidation of diene substrates: 0.5 umol cat., 10 umol of 4'-(imidazoyl-1-yl)acetophenone, 1mmol substrate, 0.07 mmol NaOCl in 0.5 mL CH_2Cl_2.

Peptide based catalysis in its own right is a growing field and has shown to be relevant in the challenges considering chemoselective chemistry. More specifically, the Miller group has arguably been the biggest contributor to advances in the chemoselective toolbox by utilizing small-molecule peptide catalysts.[10] Regarding polyenes, Miller has made the argument that selective functionalization of similarly reactive olefins has really only been observed in the context of enzymes to this point in time and small-molecule catalysts have only been shown to work in limited fashion. The challenge is that there are no set criteria for what is needed to manipulate such selectivity let alone the existence of any protocols on how to discover those criteria. In 2012, Miller developed a class of small-molecule peptides, through vast screening,

that were able to catalyze in highly-selectively the epoxidation of the polyene farnesol (Figure 2.4). mCPBA epoxidized farnesol almost equally at all three olefinic sites, however, peptide catalysts **2.3** and **2.4** were far more selective. More importantly, they induced different

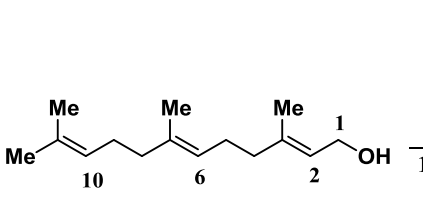

10 mol% peptide cat.
10 mol% HOBt
10 mol% DMAP
1.1 eq DIC, 1.5 eq H_2O_2
$CHCl_3$

Catalyst or Oxidant	Selectivity (-2,3	-6,7	-10,11)
m-MCPBA	1.0	2.2	2.7
2.3	>100	1.0	1.0
2.4	1.0	8.2	1.2

* Ratios determined by GC integration

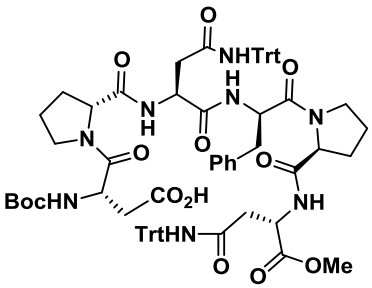

2.3

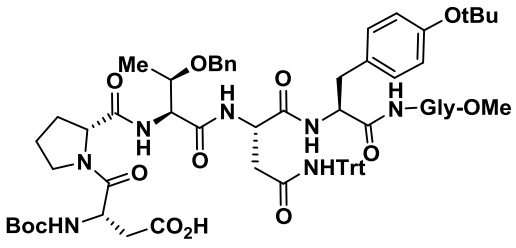

2.4

Figure 2.4. Chemoselective epoxidation of farnesol using two peptide catalysts.

selectivity. Catalyst **2.3** was able to almost exclusively catalyze the epoxidation of the -2,3 olefin whereas, albeit in a lesser relative selectivity, catalyst **2.4** was able to selectively catalyze the epoxidation of the -6,7 olefin. Although the mechanism of the reaction and its subsequent selectivity is not quite known, this is a superb example of using peptide catalysis to induce chemoselective epoxidations of a polyene. Using inspiration from Nature, and the work done by both the Suslick and Miller groups, our group undertook the challenge of synthesizing macrocyclic peptide catalysts capable of delivering chemoselective transformations.

2.2 Synthesis of the triazole based macrocyclic peptide ligands

The first generations of macrocyclic peptide catalysts were designed to be triazole amino acid derivatives of alanine and homoalanine. Histidine residues have proven to be adequate ligands but suffer from the fact that imidazole is oxidatively sensitive.[11] Triazoles do not suffer the same drawbacks. These unnatural amino acids would then undergo iterative peptide couplings followed by a macrocyclization just as discussed in Scheme 2.2. It was thought these triazole residues could be accessed by the use of an N-protected serine β-lactone derivative. Vederas and co-workers took advantage of nucleophilic β-additions to afford the free carboxylic acid of newly synthesized serine derivatives.[12] This was accomplished by the addition of Grignards with

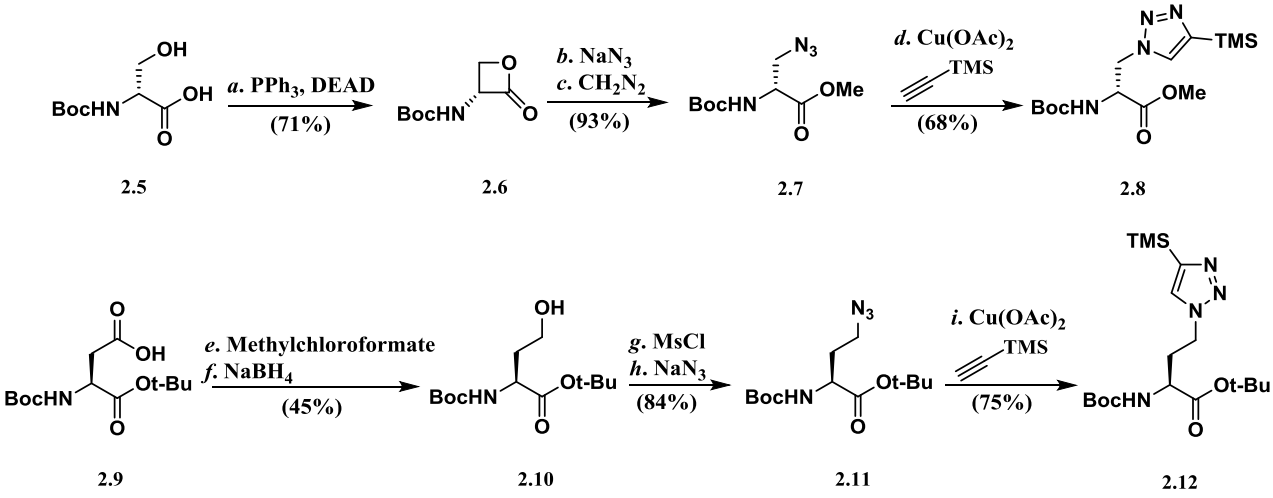

Reagents: a) PPh_3, DEAD, THF, -78 ^oC-23 ^oC; b) NaN_3, DMF; c) CH_2N_2, C_6H_6, MeOH; d) $Cu(OAc)_2$, TMS-acetylene:THF (1:1)(v:v), 60 ^oC; e) Methylchloroformate, NMM, THF, 0 ^oC; f) $NaBH_4$, THF, MeOH, 0 ^oC; g) MsCl, Et_3N, CH_2Cl_2, 0 ^oC; h) NaN_3, DMF; i) $Cu(OAc)_2$, TMS-actelylene:THF (1:1)(v:v), 60 ^oC.

Scheme 2.3. Synthesis of triazole based alanine and homoalanine.

CuCN activation. We took advantage of the fact that sodium azide could be used to synthesize azido alanine derivatives (Scheme 2.3). Boc-D-serine **2.5** underwent lactonization using Mitsunobu conditions with PPh_3 and DEAD to yield β-lactone **2.6**. It is of importance to note that other commercial azodicarboxylate reagents such as DIAD were not as fruitful. Followed

by treatment with NaN_3 and diazomethane, the β-lactone **2.6** could be opened to afford Boc-N-methyl azido alanine methyl ester **2.7**. Amino acid **2.7** could be transformed via a [3+2] cycloaddition to the desired triazole substituted alanine **2.8**. Conditions using sodium ascorbate with a mixture of *tert*-butanol and water did not yield the desired product, only insoluble brown oil. The reaction only proceeded smoothly in THF without the presence of the sodium ascorbate reducing agent. The reasons for the success of this abnormal procedure are unknown. The homoalanine derivative of the triazole amino acid could be synthesized in a similar manner starting with the Boc-L-aspartate *tert*-butyl ester **2.9**. Formation of the mixed anhydride with methylchloroformate followed by in-situ reduction with $NaBH_4$ gave the desired hydroxy homoalanine **2.10**. MsCl protection and subsequent displacement with sodium azide gave azido homoalanine **2.11** with some challenge. Under the basic conditions, side products including lactonization and intramolecular displacement of the mesylate by the N-Boc protecting group, became problematic producing inseparable mixtures of a high impurity product profile. Therefore, the protection and substitution with sodium azide had to be monitored scrupulously. Subjecting azido homoalanine **2.11** to the [3+2] conditions used in the alanine triazole synthesis afforded the triazole substituted homoalanine **2.12**. The triazole based amino acids had sparing solubility in organic solvents, and without the vinyl TMS protection; they became unusable for solution phase synthesis. Considering Scheme 2.2, there are two ways to proceed with the amino acids synthesized: 1) both alanine and homoalanine substituted triazole amino acids could be taken into the iterative peptide couplings and subsequent macrocyclization; 2) both alanine and homoalanine substituted azide amino acids could be taken into the iterative peptide couplings and subsequent macrocyclization, proceeded by a global, tetra-cycloaddition reaction. Both routes to the desired macrocycles were attempted and the general scheme can be found in

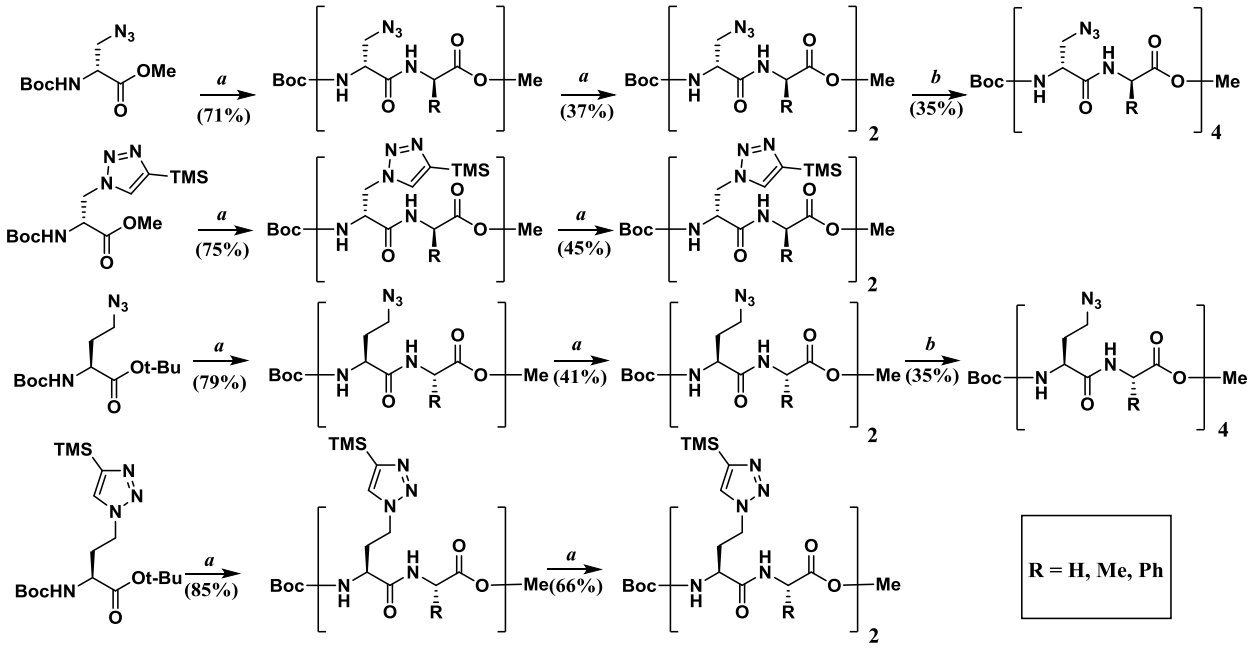

Reagents: a) LiOH, THF, MeOH, 0 °C, then TFA, CH_2Cl_2, then EDC, HOBt, DIPEA, DMF or THF; b) LiOH, THF, MeOH, 0 °C, then TFA, CH_2Cl_2, then HATU, HOAt, DIPEA, DMF.

Scheme 2.4. Solution phase synthesis of azide and triazole derived alanine and homoalanine.

Scheme 2.4. However, it became quickly apparent that solution phase synthesis of the macrocyclic peptides would not be viable. The linear tetra- and octa- peptides of both triazole and azide derived amino acids, respectively, were insoluble in organic solvents and became extremely challenging to purify. The yields represented in Scheme 2.4 are indicative of this problem as they were isolated by filtration from the crude reaction mixtures. The solution to the issue of insolubility was alleviated by the use of solid phase peptide synthesis (SPPS). Azido alanine **2.7** and azido homoalanine **2.11** could, in facile fashion, be converted to the Fmoc protected amino acids by subjection to TFA in CH_2Cl_2 to deprotect the N-Boc groups followed by protection with Fmoc-OSU. The resulting Fmoc protected amino acids of **2.7** and **2.11** could then undergo iterative peptide couplings (Scheme 2.5). The alternating linear sequences of azido D-alanine and L-phenylalanine could be cleaved off SPPS Wang resin by TFA/Et_2O washes, and macrocyclized under dilute conditions with PyBOP to afford macrocycle **2.13**. Although

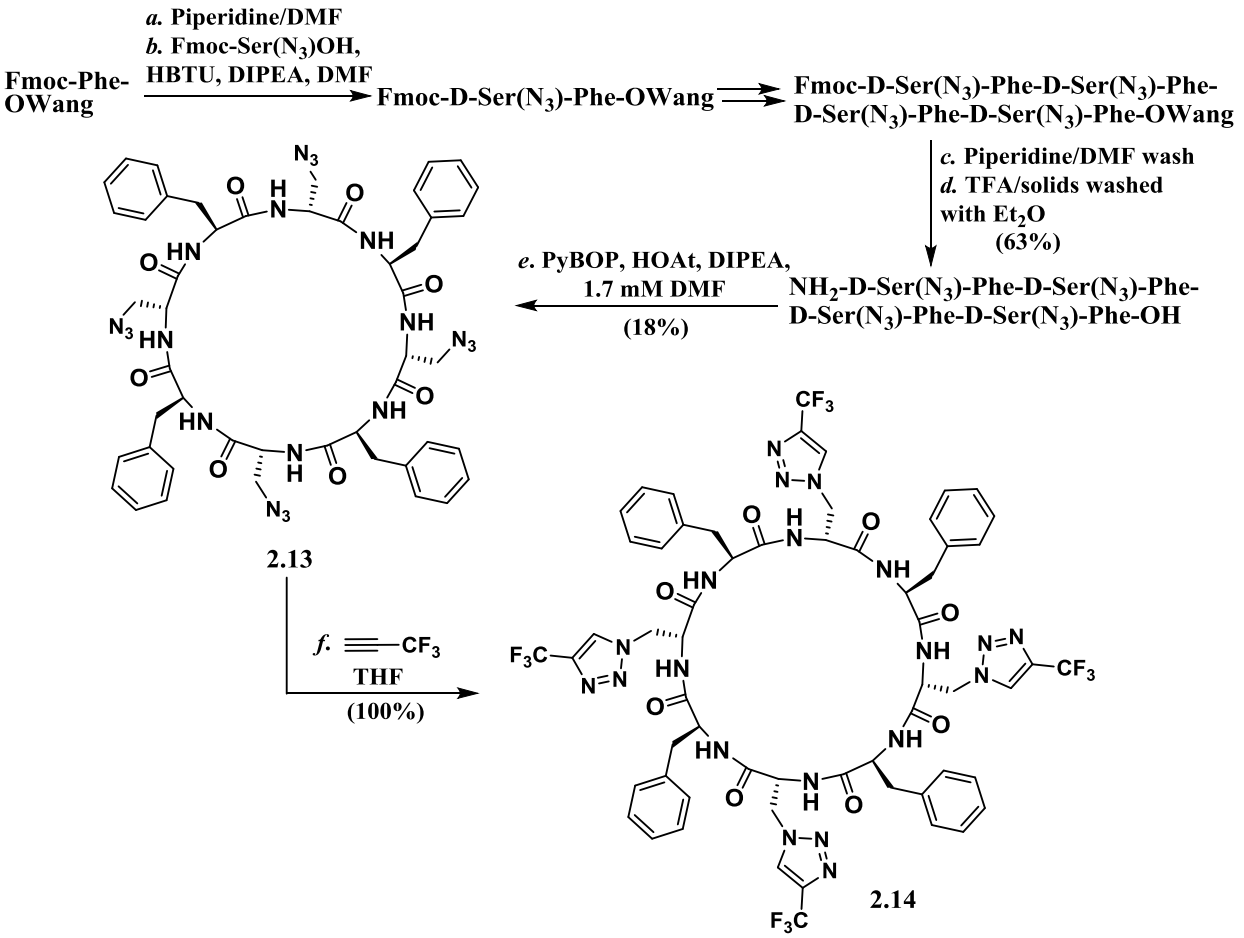

Scheme 2.5. SPPS of azido D-alanine and L-phenylalanine macrocyclic peptide

the conditions for macrocyclization were screened, the highest conversion to the isolated desired product was in the use of PyBOP. L-phenylalanine was originally chosen to aid solubility of the desired octa-peptide but also to provide a UV-active marker to make isolation and analytical analysis easier. Both L-alanine and glycine were used in place of L-phenylalanine with unfruitful attempts at any desired macrocyclization. Fmoc derivatives of the triazole based amino acids **2.8** and **2.12** could be synthesized by the aforementioned method used with azido based amino acids **2.7** and **2.11**; however, the N-Fmoc triazole based protected amino acids were not stable to SPPS coupling conditions. Treatment of macrocycle **2.13** with TMS-acetylene as in Scheme 2.3, failed to produce the desired tetra-triazole macrocycle. Eventually it was

discovered that upon using super stoichiometric Cu salts, the desired [3+2] cycloadditions were not occurring. Applying a co-mix of 1,2,3-trifluoroacetylene and THF in an absence of Cu salts afforded the desired tetra-triazole macrocycle **2.14** after heating to reflux for six days in a sealed vessel. TMS-acetylene did not undergo the [3+2] cycloadditions without Cu-mediated most likely due to a mismatch in electronics without the use of a catalyst. Macrocycle **2.14** was easily purified as it precipitated from the reaction solution. Unfortunately, the tetra-triazole macrocycle **2.14** was extremely difficult to work with in regards to solubility. This model of macrocyclic peptide was abandoned; SPPS is not atom efficient providing a disadvantage in the need of the synthesis for the N-Fmoc protected unnatural amino acids, the poor macrocyclization conversion, limitations to volatile and electron deficient alkynes and the solubility issues, all propagated the need for a more soluble macrocyclic peptide with a less laborious synthesis.

2.3 Synthesis of aspartic acid based macrocyclic peptide ligands

With limited success in synthesizing macrocyclic peptide ligands containing triazole residues as substitutes for more oxidation prone histidine residues, my efforts were refocused on using aspartic acid residues as the active ligand in the macrocyclic peptides. Partially this change in direction was motivated by recent success of the Ball group in developing methods to synthesize and test vast libraries of aspartate containing linear peptides as ligands for Rh^{II} catalysis.[13] An interesting example of this methodology was the formation of a dirhodium complex by the bridging of two nona-peptides, self-proclaimed metallopeptides, for the activation of diazo esters (Figure 2.5).[14] The linear sequences were simply made through SPPS and could be metalated in solution or on resins. Upon metalation, two isomers were formed one in which the two sequences ran parallel with one another (coined “isomer a”) and a second where the sequences

ran anti-parallel with one another (coined "isomer b"). The two isomers could be separated by HPLC. For hydrosilation specifically, Ball was able to make 22 sequences, each providing two

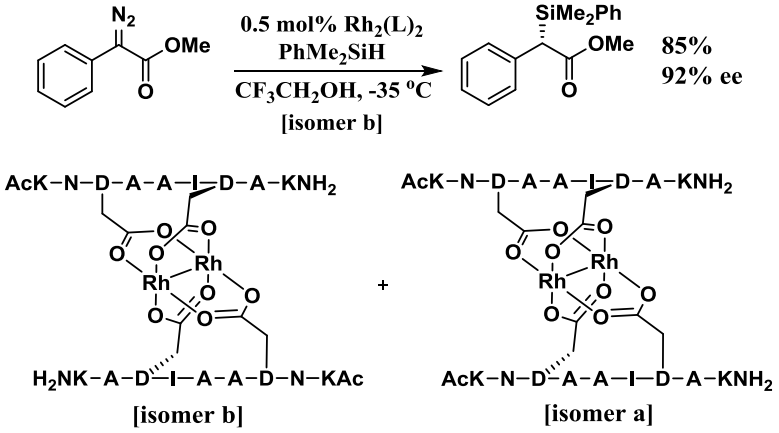

Figure 2.5. Si-H carbenoid insertion with peptide dirhodium complexes.

isomers, and these catalysts were screened in the enantioselective, carbenoid Si-H bond insertion with great success.

The change in direction towards aspartate based macrocyclic peptide ligands was also partially inspired by a specific example of a calix[4]arene based dirhodium complex synthesized by the Du Bois group (Figure 2.6).[15] The structural design was what made it interesting to our endeavors as the calix[4]arene bowl had created a cavity sitting below an active catalytic site.

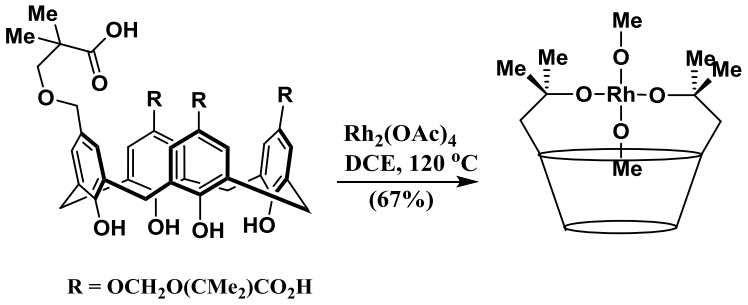

Figure 2.6. Calix[4]arene based dirhodium complex.

This design is similar in theory to the model used to construct the tetra-triazole type macrocyclic peptide ligands. Unfortunately, in the metalation of the calix[4]arene, only two of the four acetates were substituted resulting in a dirhodium complex where one of the acetate ligands was encapsulated by the calix[4]arene. The complex however was still catalytically active.

With the Ball and Du Bois literature as precedence, SPPS was used (Scheme 2.6) to synthesize a small collection of tetra- and bis-carboxylate macrocyclic peptides by utilizing on-resin

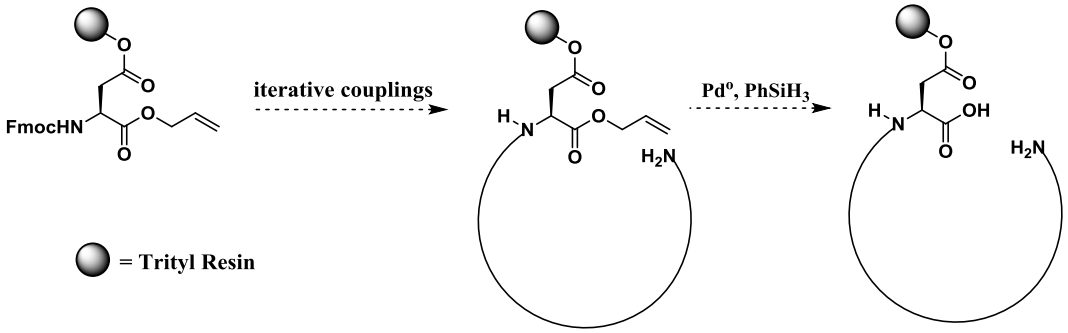

Scheme 2.6. Diagram of SPPS on-resin cyclization synthesis

cyclization technology.[16] Allylated aspartic acid residues that were bound to trityl resin through the side chain functionality could be deallylated and cyclized while still bound to the trityl resin. This is advantageous compared to that of solution phase macrocyclization because it not only eliminates oligomerization due to concentration effects but also allows easier screening of the reaction conditions. In a situation where all amino acids used in SPPS are commercially available, access to the macrocyclization event on-resin is extremely facile. In this design, it would be easy to screen different peptide sequences to achieve maximum efficiency in the macrocyclization event. This was not the case in the lengthy and challenging synthesis of the tetra-triazole based macrocyclic peptides. In the context of macrocyclization in peptide synthesis there are two key factors to consider: 1) alternating D- and L- amino acids will allow side chain

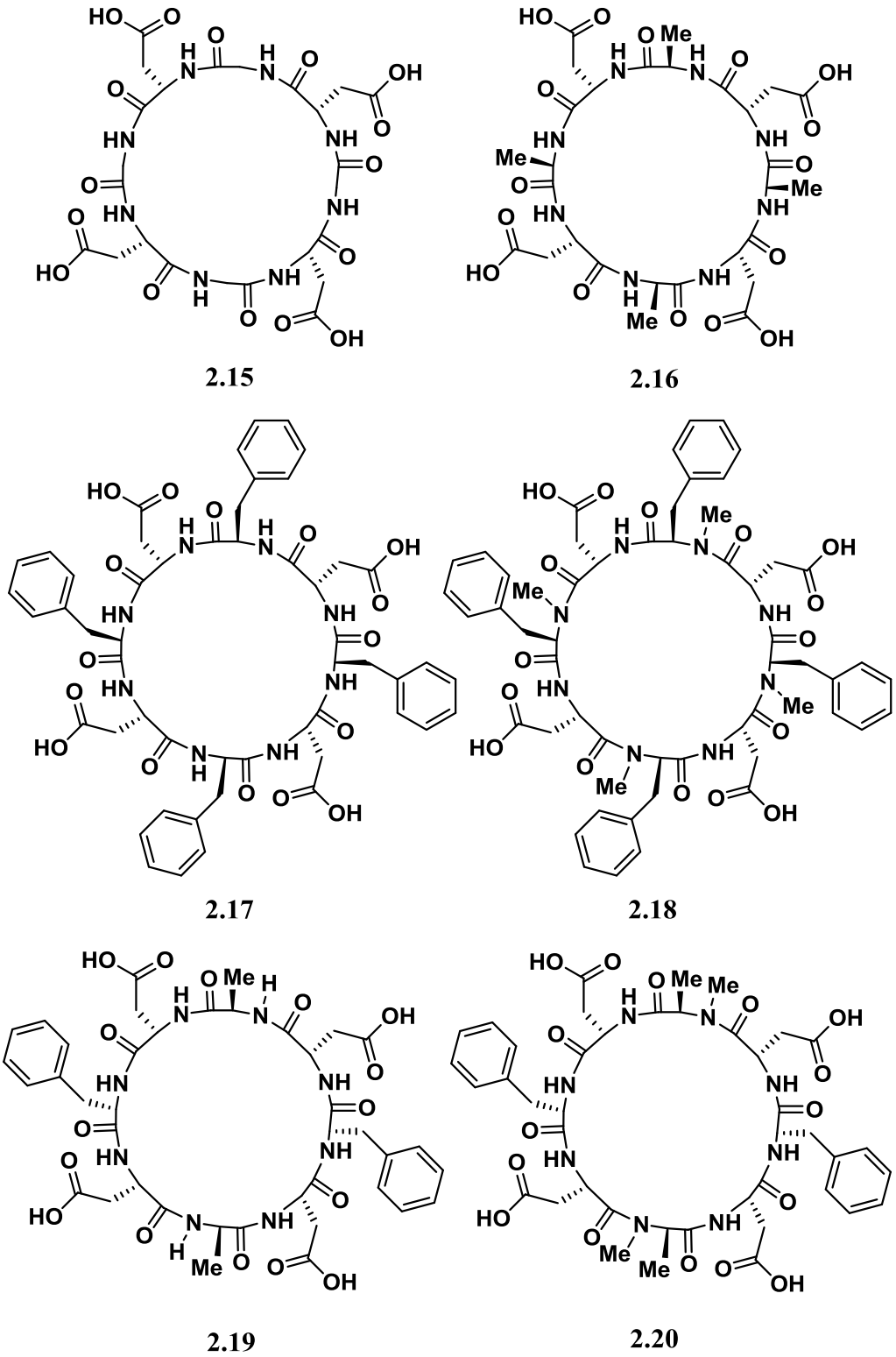

Figure 2.7. Examples of successfully synthesized tetracarboxylate peptides

functionality to align in such a way that would facilitate the cyclization event and 2) N-methylation of amides facilitate β-turns through avoidance of $A_{1,3}$ strain in peptide backbones allowing for facilitation of the cyclization event.[17] With these criteria in mind, a small collection of tetra carboxylate peptides (Figure 2.7) were synthesized including glycine derived **2.15**, D-alanine derived **2.16**, D-phenylalanine derived **2.17**, N-methylated D-phenylalanine derived **2.18**, mixed species of D-alanine and L-phenylalanine derived **2.19**, and mixed species N-methylated D-alanine and L-phenylalanine **2.20**. For example, the linear sequence of mixed species **2.19**,

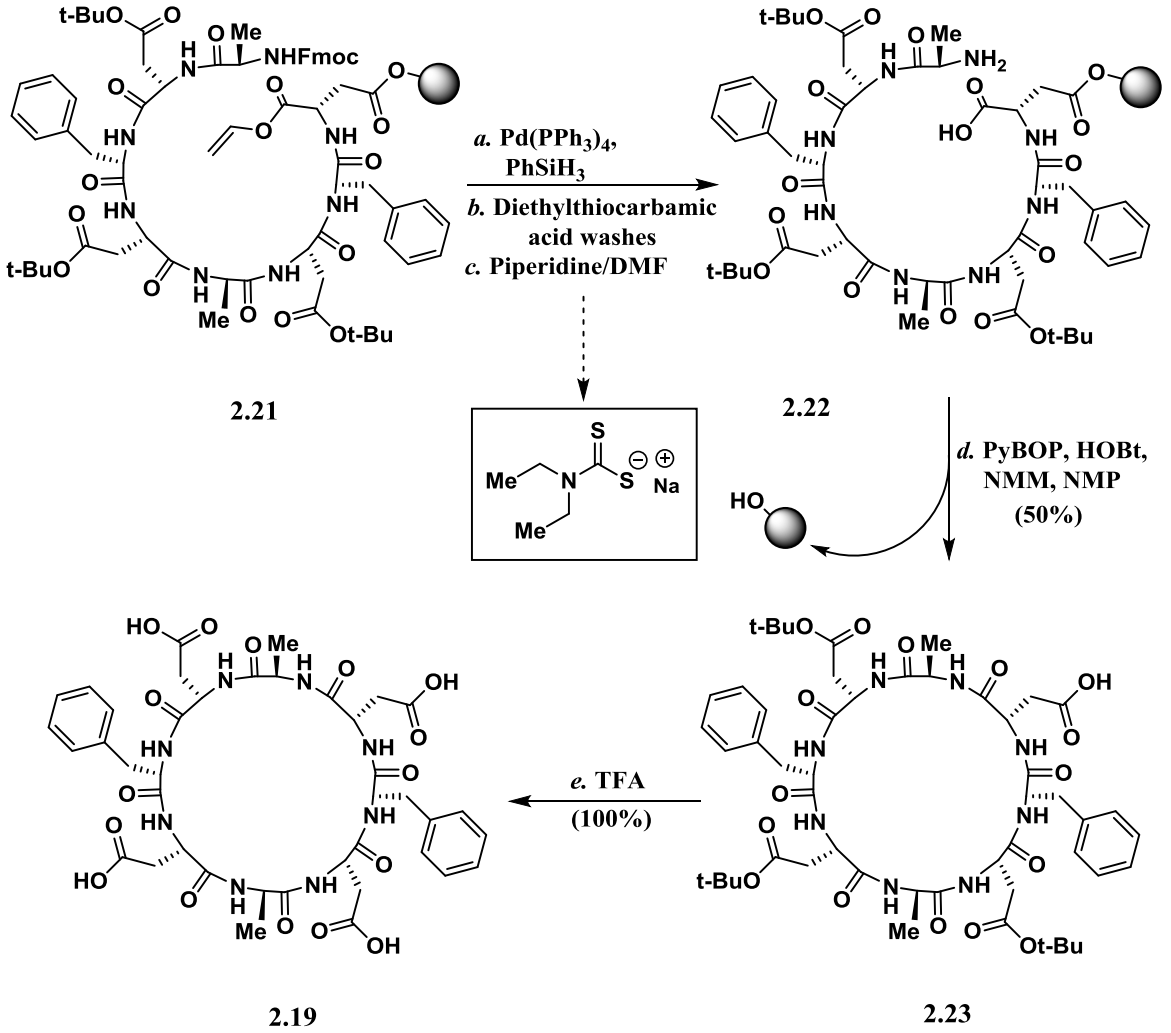

Scheme 2.7. On-resin synthesis of macrocyclic peptide **2.19**.

could be synthesized through iterative SPPS (Scheme 2.7). The respective on-resin linear sequence **2.21** could be deallylated by treatment with $Pd(PPh_3)_4$ and triphenylsilane. Washing the resin with diethylthiocarbamic acid eliminated any excess Pd encapsulated by the trityl resin. With subjection of the resin to a piperdine/DMF mixture, the N-terminus could be deprotected resulting in the free N- and C- termini of the linear peptide **2.22**. Identical to typical SPPS coupling conditions, the deprotected peptide chain could undergo macrocyclization with the treatment of peptide coupling agents, a base and a solvent that is typically known to swell solid phase resins. The resulting macrocyclic peptide was released from the resin upon the treatment of TFA. However, this typical chain of events resulted in low yields of desired macrocycles along with a high impurity profile. It was discovered that upon treatment of linear peptide **2.22** with coupling agents, the macrocyclization event had occurred proceeded by a facile cleavage of the cycle from the resin without acidic treatments. Therefore, upon treatment with PyBOP, HOBt, and NMM in NMP (DMF could also be used with slightly lower yields and longer reaction times), macrocyclic peptide **2.19** could be isolated in a modest yield by HPLC purification away from any byproducts including 1,1,1-phosphoryltripyrrolidine. It should be noted that cleavage of the peptide during coupling conditions never reached full conversion. Subjecting the resin to TFA also produced some quantities of the desired product **2.19**, directly, albeit mixed with other carboxylate peptide fragments that made for a more difficult purification. Upon treatment of TFA, tetracarboxylate **2.19** was isolated. Not surprisingly, the tetracarboxylate macrocyclic peptides suffered from poor solubility in organic solvents. Metalation attempts for macrocyclic peptides **2.17** and **2.19** were the most promising. Insolubility made monitoring the metalations with rhodium sources a challenge. However, metalation with peptides **2.17** and **2.19** using $Rh_2(OAc)_4$ with Hunig's base in 2,2,2-

trifluoroethanol furnished blue-green powders upon HPLC purification. Unfortunately, we were unable to obtain any crystal structures or spectral data that conclusively identified the synthesized dirhodium complex **2.24**. There was mass spectrum support (MALDI) that seemed to indicate a possible bis-substituted metalation event (Figure 2.8) not unlike what Du Bois and

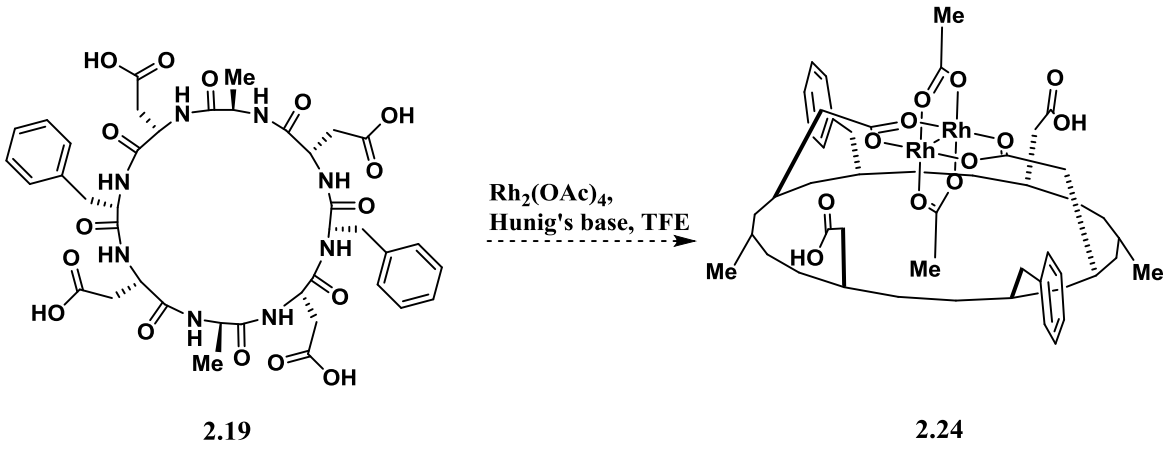

2.19 **2.24**

Figure 2.8. Possible outcome for the metalation of peptide **2.19**.

co-workers witness when synthesizing calix[4]arene dirhodium complexes. However, even this data is highly inconclusive. It should be noted that *trans*-metalation is highly unrepresented and the calix[4]arene work by Du Bois is the only example. Metalation of tetra-carboxylate **2.19** could have also occurred in a typical *cis*-metalation similar to that of $Rh_2(esp)_2$.

With difficulties in determining the outcome of the metalations using the tetra-carboxylate macrocyclic peptides, our focus was turned toward using bis-carboxylate macrocyclic peptides. Bis-carboxylate macrocyclic peptide **2.28** was synthesized by a similar method as that shown in Scheme 2.7. The linear D-alanine, L-phenylalanine and glycine mixed species **2.25** was subjected to the same deallylation and Fmoc deprotection, however, the on-resin macrocyclization of deprotected peptide **2.26** with PyBOP, HOBt, and Hunig's base in DMF

behaved in typical fashion without the release of the macrocyclic peptide (Scheme 2.8). On-resin macrocyclic peptide **2.26** could then be released from trityl resin as well as undergo global

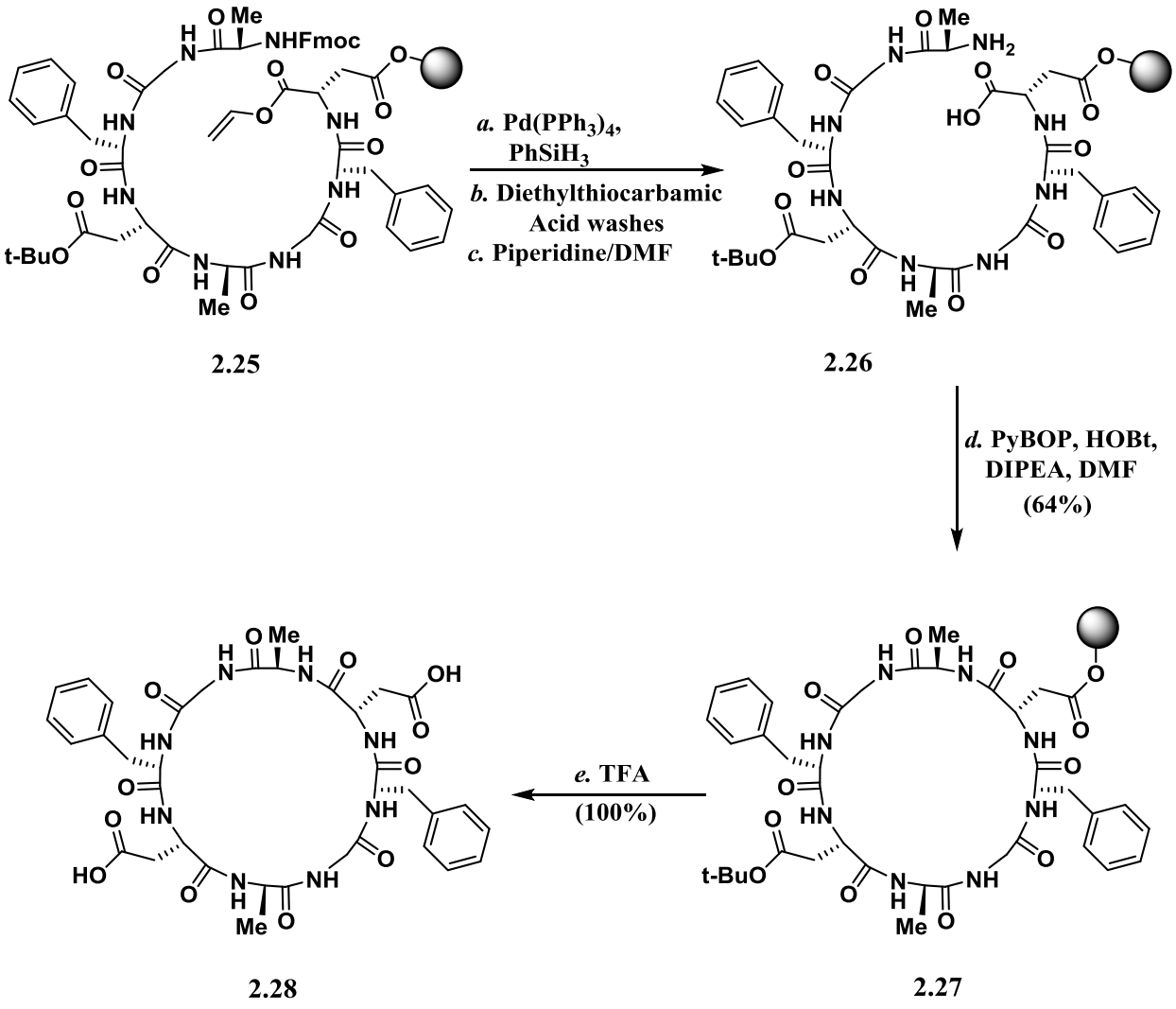

Scheme 2.8. On-resin synthesis of macrocyclic peptide **2.28**.

carboxylate deprotection with treatment of TFA. Metalation of macrocyclic peptide **2.27** with $Rh_2(OTFA)_4$ using Hunig's base in 2,2,2-trifluoroethanol resulted in a blue-green powder upon HPLC purification (Figure 2.9). Once again, due to solubility issues, no crystal structure or spectral data was collected that could identify dirhodium complex **2.29**. ^{19}F NMR studies

indicated the consumption of $Rh_2(OTFA)_4$ and there was mass spectrum support (MALDI) that indicated the existence of dirhodium complex **2.29**; however, the dimeric macrocyclic peptide

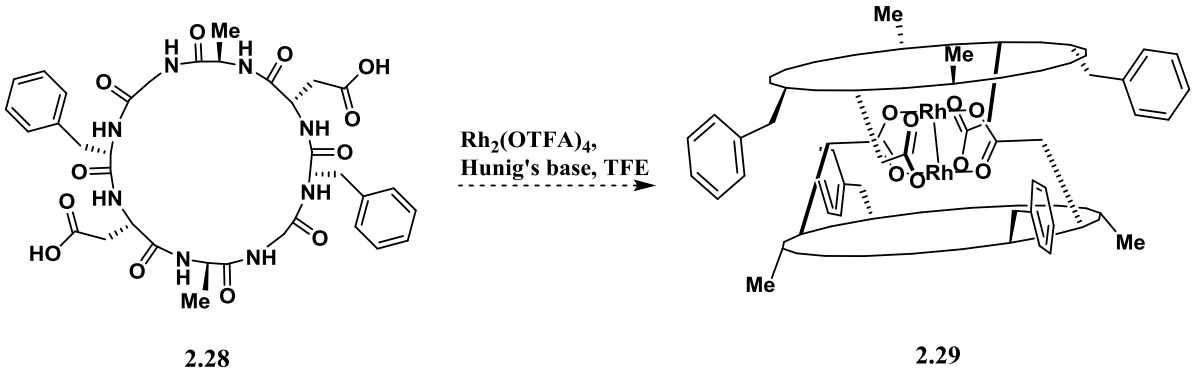

2.28 **2.29**

Figure 2.9. Possible outcome for the metalation of peptide **2.28**.

structure was not unambiguously proven. Even though exact identity of dirhodium complexes tetra-carboxylate **2.24** and bis-carboxylate **2.29** was unknown, the catalytic activity of both were probed. This was done by screening the reactions of both potential catalysts, in a stoichiometric manner, with styrene and ethyl diazo acetate. Regardless of stoichiometry of reagents and solvent, there was no cyclopropanation detected. The same reaction using $Rh_2(OAc)_4$ as the catalyst was however successful. Doping in amounts of $Rh_2(OAc)_4$ into the test reactions containing catalysts **2.24** and **2.29** started to indicate conversion to the desired cyclopropanation product, further suggesting that potential catalysts **2.24** and **2.29** were catalytically inactive.

2.4 Overview of inherent challenges in macrocyclic peptide ligand syntheses

In general, there are multiple challenges that exist in the syntheses of macrocyclic peptide ligands. Regardless of using none-functional amino acids as solubilizing groups, the use of N-methylated amides or the use of bulky solubilizing groups such as trimethylsilanes, the macrocyclic peptides all suffered from extremely poor solvent solubility. Aside from the polar

nature of some of the discussed macrocyclic peptides, symmetric peptides of this nature have been shown to form "peptidic tubes" by stacking in solutions.[18] It is unclear as to whether or not the solubility of these molecules is caused by solution stacking of the peptides but it is quite certainly a possibility. Nevertheless, to this extent without the ability to obtain crystal structure data or definitive spectral proof, it is difficult to identify the exact makeup of the isolated dirhodium complexes, and then in turn, be able to diagnose whether or not the complex is catalytically active. There has been some discussion in the literature about certain criteria needed for the construction of dirhodium complexes. In considering these discussions, there are two points of contention that may have also contributed to some of the aforementioned challenges;[19,15] 1) α-dimethyl substitution to the carboxylate seems to be a key factor and 2) the presence of secondary and tertiary amines, and carboxamide ligation competition with aspartate residues, may be detrimental to the formation of dirhodium complexes . Considering all of these challenges, we decided that a different, non-peptidic based approach needed to be taken in order to build the desired catalysts.

2.5 Synthesis of cyclophane based macrocyclic ligands

Over the past three decades there have been significant advances in the synthesis of macrocyclic cyclophanes in an attempt to advance the organic chemistry field beyond the dominance of

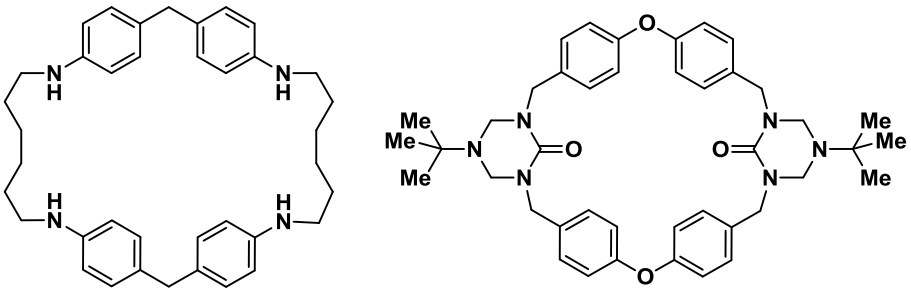

2.30 2.31

Figure 2.10. Literature examples of synthetic macrocyclic cyclophanes.

cyclodextrins, calix[*n*]arenes, crown-ethers and cucurbiturils. Among the advances made, cyclophanes have been synthesized for host-guest interactions (e.g. cyclophane **2.30**), self-assembled nanotubes (e.g. cyclophane **2.31**), chiral shift reagents, general synthetic methodologies, etc. (Figure 2.10).[20] Adapting our group's previous models for macrocyclic peptide ligands to these classes of macrocyclic cyclophanes, an amino acid cyclophane hybrid molecule **2.36** was synthesized (Scheme 2.9). Under a modified Friedel-Crafts type reaction,

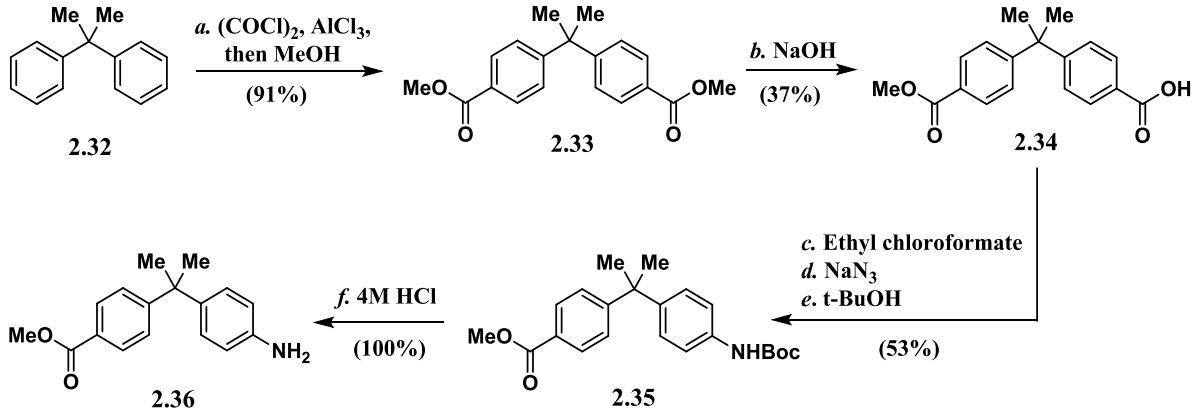

Reagents: a) $AlCl_3$, $(COCl)_2$, CH_2Cl_2, 0 °C then MeOH, 23 °C; b) NaOH, THF:MeOH (3:1)(v:v); c) Ethyl chloroformate, NEt_3, 0 °C, then NaN_3, H_2O, 0 °C, then PhMe:t-BuOH (1:1)(v:v), 90 °C; d) 4M HCl, CH_2Cl_2.

Scheme 2.9. Synthesis of hybrid amino acid **2.36**.

commercially available 2,2-diphenylpropane **2.32** could be converted to the bis methyl ester **2.33** by $AlCl_3$ activation of oxalyl chloride and upon treatment with 1.0 equivalent of NaOH, a mono hydrolysis afforded acid **2.34**. A one-pot Curtius rearrangement transformed acid **2.34** into N-Boc protected aniline **2.35** in a modest yield and the deprotection upon treatment of 4M hydrochloric acid gave the hybrid amino acid **2.36**. The newly synthesized hybrid could be coupled to *tert*-Butyl protected L-serine to give dipeptide **2.37** shown in Scheme 2.10. The

material could be split for hydrolysis or N-Boc deprotection, and taken into iterative amide couplings to form the macrocycle represented in Scheme 2.10. Upon acquiring the macrocycle, the side chains of the serine residues could be deprotected and functionalized. However, through detailed screening this macrocyclization was never successfully achieved, mainly dimers of the represented pieces were isolated. With the difficulties experienced in synthesizing this

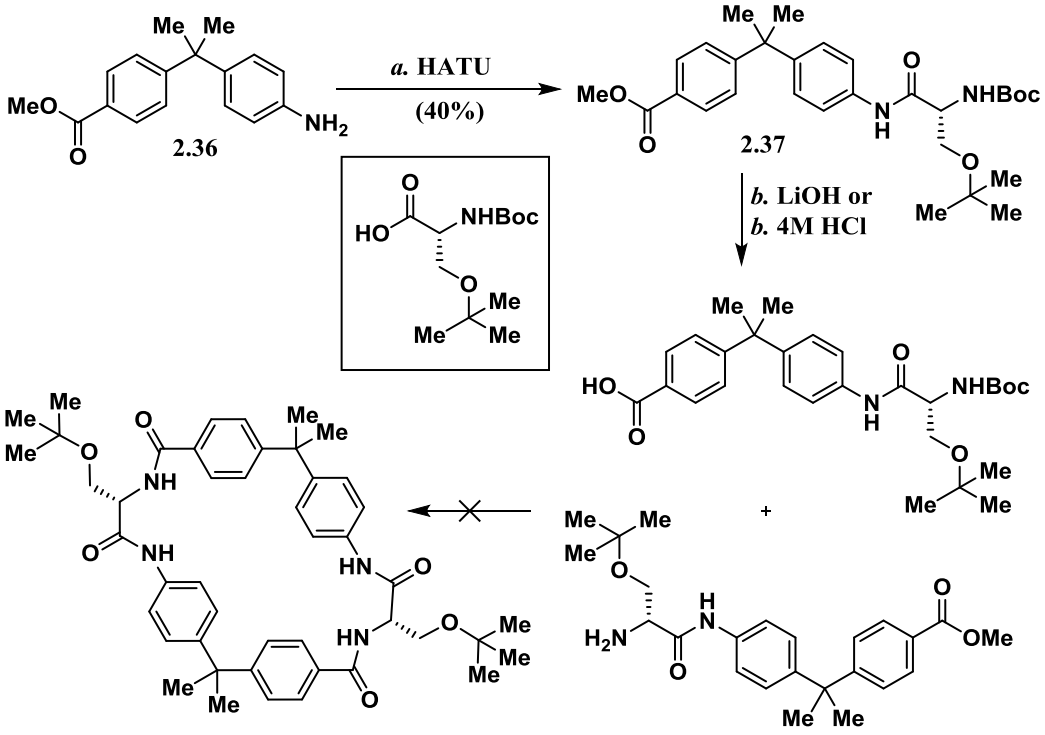

Scheme 2.10. Attempted synthesis of macrocycles using hybrid amino acid **2.36**.

peptidic/cyclophane hybrid macrocycle, our group completely abandoned the use of amino acids as the functional source for installing the ligands on the macrocycle platform. A small collection of cyclophane macrocycles/macrocyclic ligands were synthesized (Figure 2.11).

The cyclophane macrocycles synthesized fit into two different categories; 1) bis-carboxylate macrocycles **2.38**, **2.39** and **2.40** that were intended to be used for dirhodium complex ligands;

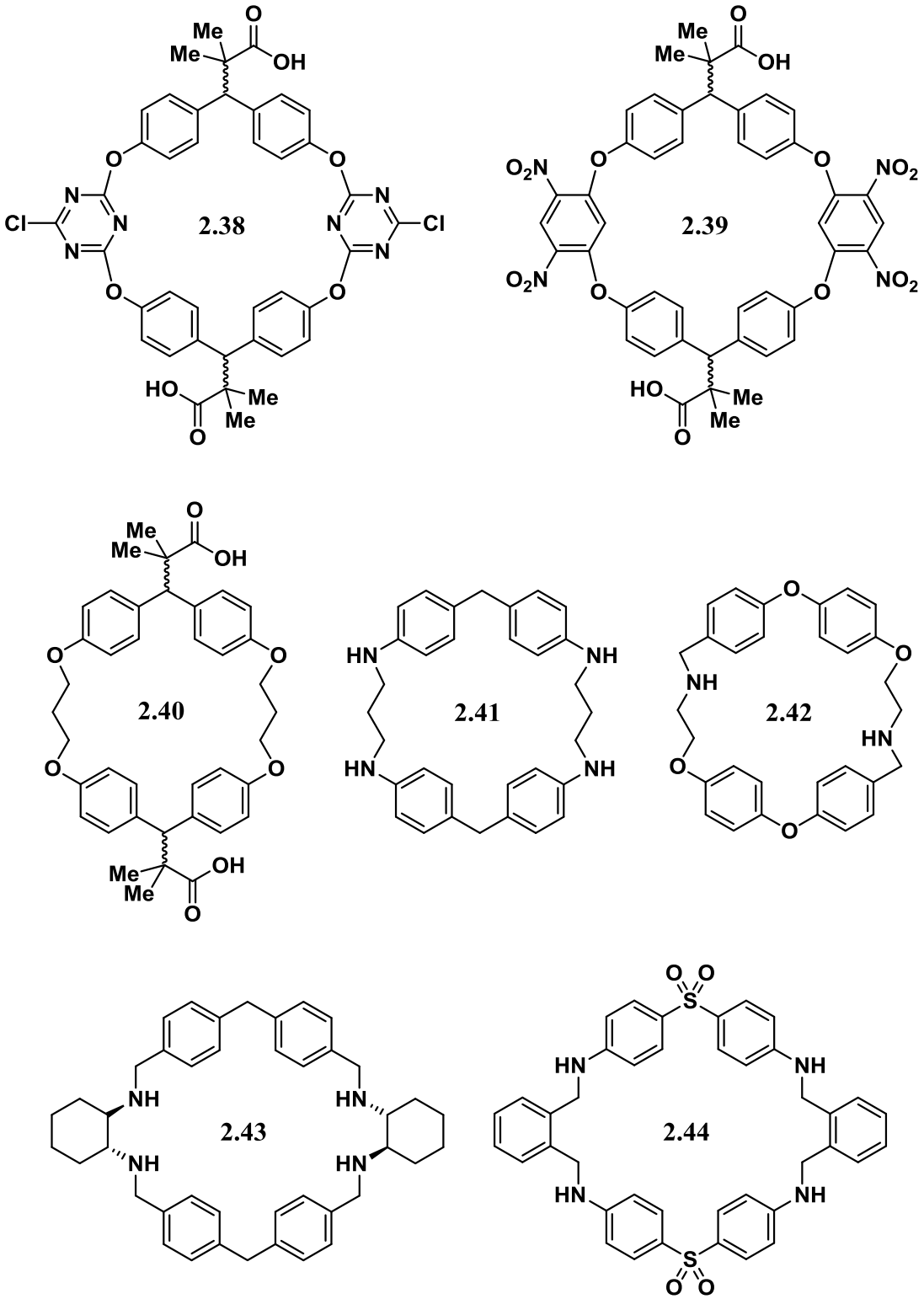

Figure 2.11. Synthesized cyclophane based macrocycles.

and 2) secondary amine based macrocycles that were intended to be further functionalized to build the desired ligands. Key to the first class of cyclophane macrocycles was the synthesis of the carboxylate functionalized cyclophane linker **2.47** (Scheme 2.11). This was accomplished by

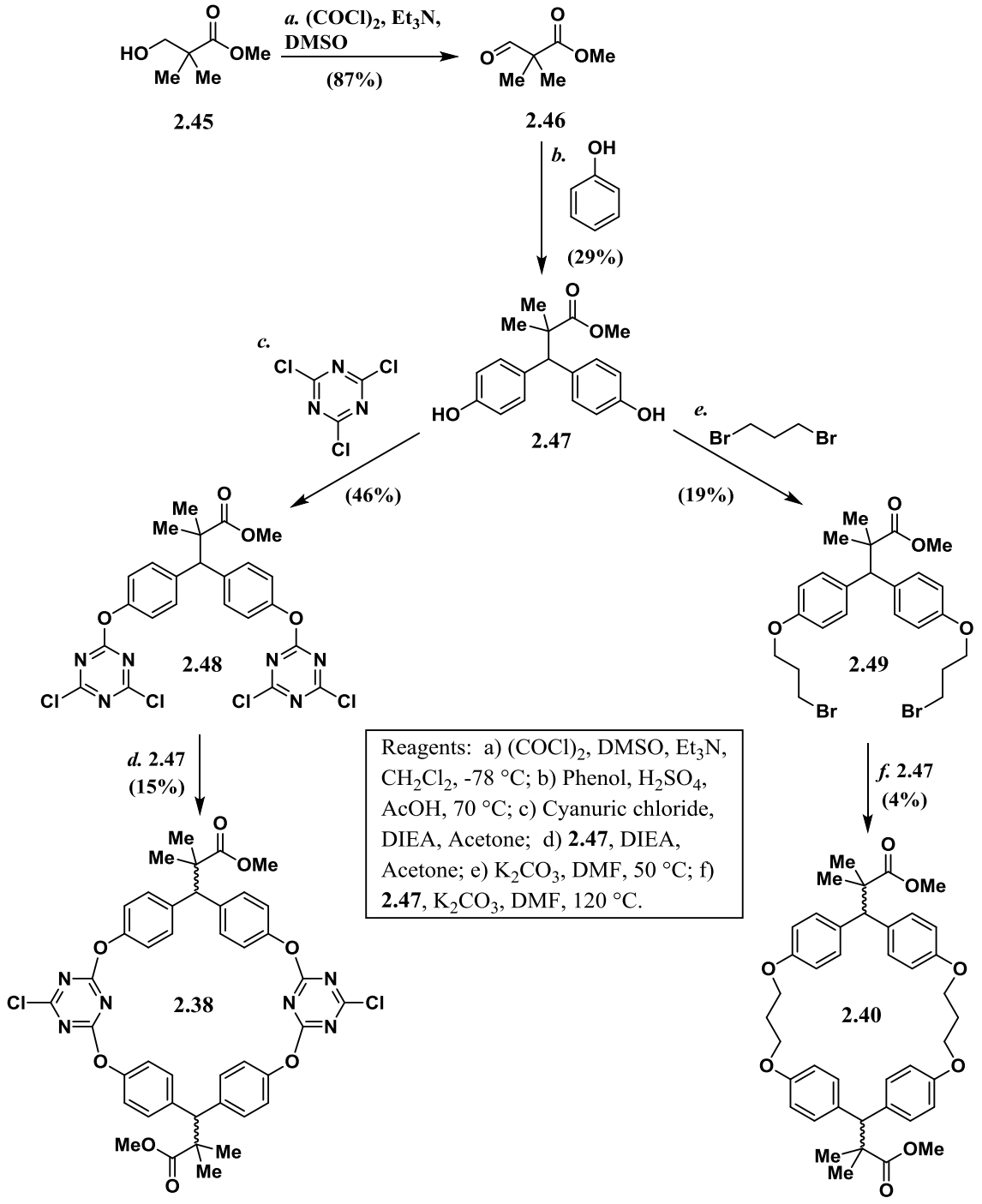

Scheme 2.11. The synthesis of biscarboxylate macrocycles **2.38** and **2.40**.

a Swern oxidation of commercially available alcohol **2.45** to give aldehyde **2.46**. Treating aldehyde **2.46** with an excess of phenol in a mixture of sulfuric/acetic acid produced the cyclophane linker **2.47**. With this molecule in hand, a double SNAr reaction with cyanuric chloride yielded aryl ether **2.48** and treatment with another equivalent of cyclophane linker **2.47** with Hunig's base in acetone under dilute conditions of 0.025 M gave macrocycle **2.38**. It soon became apparent that finding the correct macrocyclization partner for the cyclophane linker **2.47** was crucial, not necessarily from a synthetic throughput standpoint but for the stability of the macrocycles themselves. Upon methyl ester hydrolysis of macrocycle **2.38**, the resulting bis acid macrocycle was extremely unstable with a life time of only a few minutes even at 0 °C. Although not all decomposition pathways are known for this instability, the molecule was moisture sensitive lending to a deconstructing of the macrocycle framework though SNAr reactions with water. Cyanuric acid was detected in the material as it decomposed. Double alkylation of cyclophane linker **2.47** with dibromopropane produced dibromide **2.49** and treatment with another equivalent of cyclophane linker **2.47** with K_2CO_3 in DMF under dilute conditions of 0.020 M at 120 °C for two days gave macrocycle **2.40** albeit in low yields. Surprisingly, upon hydrolysis of macrocycle **2.40** to the bis acid, this macrocycle suffered from solubility issues. Unexpectedly, macrocycle **2.40** was less soluble, generally, in organic solvents than that of the respectively heteroatom populated macrocycle **2.38**. The reasons for this are unclear except, in speculation, some of the alkyl chain/aryl ether based macrocycles are known to encapsulate solvent molecules resulting in a lessening of their solubility.[21] Through some unsuccessful screenings of other macrocyclization partners for the cyclophane linker **2.47**, it was eventually found that a difluorodinitrobenzene partner fit our needs in stability and solubility adequately (Scheme 2.12). Through some protecting group adjustments, cyclophane linker **2.47**

could be converted to carboxylic acid **2.50** by hydrolysis with NaOH followed by acetate protecting by treatment with Ac_2O in pyridine. Acid **2.50** was then converted to bisphenol **2.51** first by EOM-Cl protection of the acid and deprotection of the phenols with a basic methanol solution. In a one-pot procedure, bisphenol **2.51** and 1,3-difluoronitrobenzene were mixed in equimolar amounts dilute in DMSO with K_2CO_3 to provide macrocycle **2.52** in a modest yield.

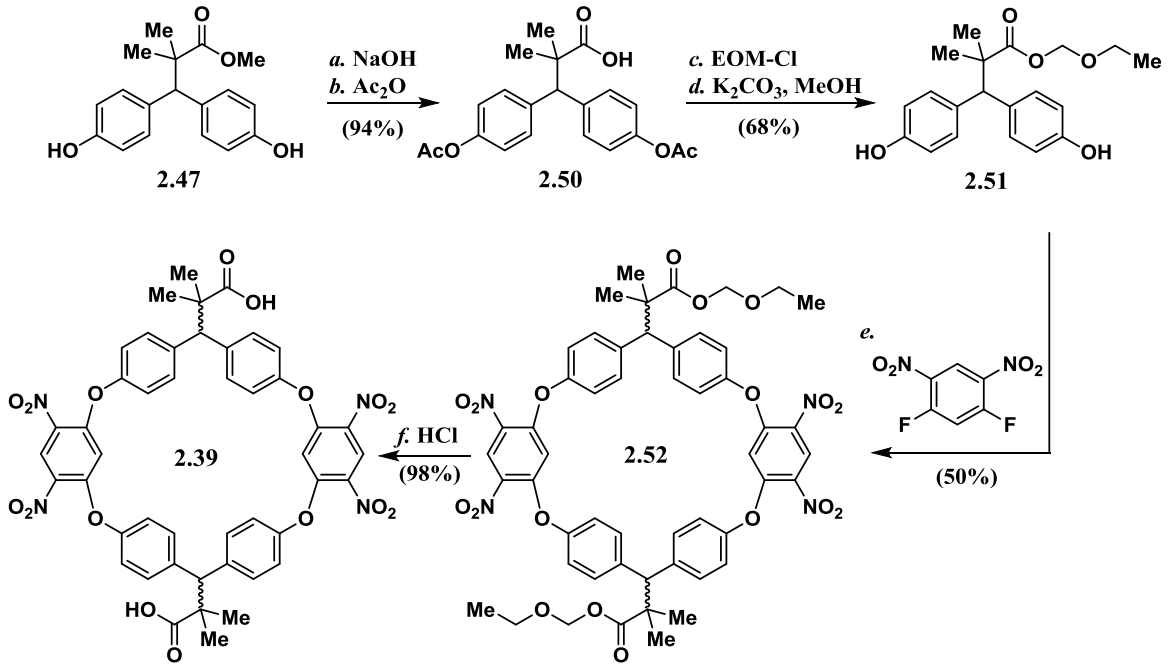

Reagents: a) NaOH, MeOH, H_2O; b) Ac_2O, pyridine; c) EOM-Cl, K_2CO_3, DMF; d) K_2CO_3, THF:MeOH:H_2O (3:1:1)(v:v:v); e) 1,3-difluorodinitrobenzene, K_2CO_3, 0.05 M DMSO; f) 3 M HCl, THF.

Scheme 2.12. The synthesis of biscarboxylate macrocycle **2.39**.

1,3-difluorodinitrobenzene could easily be synthesized by nitration of commercial 1,3-difluorobenzene in sulfuric acid/nitric acid. Macrocycle **2.52** was then subjected to 3 M HCl(aq) to produce the desired biscarboxylate macrocycle **2.39**. Unlike the previous successfully made macrocycles presented in Scheme 2.11, macrocycle **2.39** had a life time of a few months stored at 0 °C and there were no solubility issues in commonly used organic solvents. The synthesis of

this macrocycle produces two isomers in reference to the plane of the macrocycle; one where the carboxylic acids are *syn* in relation and one where the carboxylic acids are *anti* in. Only the *syn* relationship will be amenable to the formation of any dirhodium complex. Unfortunately, the two isomers were not separable by chromatography means and crystallization/resolution attempts were non-fruitful. This complicates any metalation process. A comprehensive screening was undertaken to form the dirhodium complex using rhodium sources $Rh_2(OAc)_4$, $Rh_2(OTFA)_4$ and synthetically prepared $Rh_2(CO_3)_4Na_4$ from refluxing $Rh(OAc)_4$ in Na_2CO_3(aq). Under no circumstances, were any species isolated that incorporated the encapsulation of rhodium within macrocycle **2.39** by ^{1}H NMR analysis or by any mass spectrometry support. However, MALDI analysis of some isolated species (all green powders) indicated the oligomerization of macrocycle **2.39** by intermolecular metalation. Although this observation is expected for the *anti* isomer of macrocycle **2.39**, it is not expected for the relative *syn* isomer even if they exist as a mixture. The reasons for the failure for the *syn* isomer metalation are unclear and largely unproven, speculation would seem to indicate that against our best efforts to model such a system it's possible that upon substitution of one carboxylate, a second intramolecular substitution is not possible. With the failures met for this class of bis-carboxylate cyclophane macrocycles, more emphasis was put on the aforementioned second class of cyclophane macrocycles.

The second class of secondary amine based macrocycles our group was targeting were all synthesized by combined methods of alkylation and reductive aminations. Tetraaniline macrocycle **2.41** was synthesized from commercially available dianiline **2.53** in three steps (Scheme 2.13) by first tosylating both anilines to give tosylamide **2.54**. Macrocyclization with

dibromopropane occurred cleanly to produce macrocycle **2.55** in low yields but without oligomer byproducts due to the deactivation by the tosyl protecting groups. The tetratosylate **2.55** could be deprotected completely by an aqueous HBr catalyzed phenol tosyl transfer to give macrocycle **2.41**. Macrocycles **2.43** and **2.44** were synthesized in a very facile fashion from two very cheap

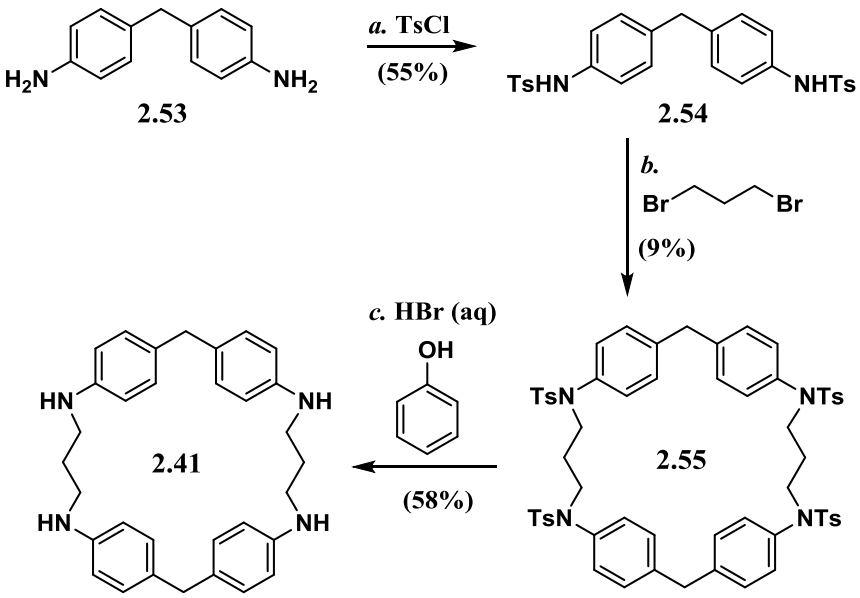

Reagents: a) TsCl, pyridine, CH_2Cl_2; b) dibromopropane, K_2CO_3, 50 mM, DMF, 130 °C; c) HBr(aq), phenol, 100 °C.

Scheme 2.13. The synthesis of tetraaniline macrocycle **2.41**.

commercial sources of BPA and dapsone, respectively (Scheme 2.14). Macrocycle **2.44** was synthesized in one step by combining an equimolar amount of dapsone and commercially available phthaldialdehyde under reductive amination conditions using $NaBH_3CN$ and acetic acid. The reaction was performed dilute in 0.05 M MeOH. The desired product could be filtered from the reaction solution directly and dried. Macrocycle **2.43** could be synthesized from commercially available BPA in a few steps. Through a literature procedure involving a Pd catalyzed cyanation, BPA could be converted to aryl cyanide **2.56**.[22] Subsequent

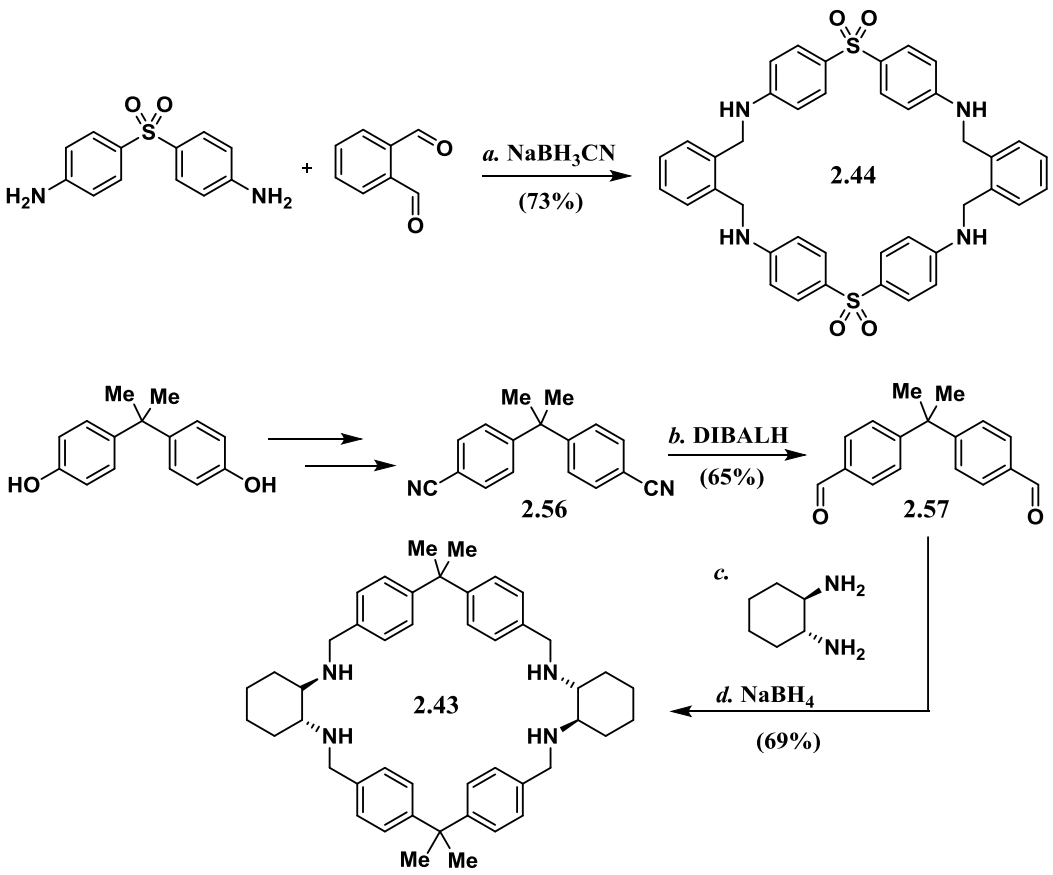

Reagents: a) $NaBH_3CN$, AcOH, 0.05 M MeOH; b) DIBALH, toluene; c) cyclohexyldiamine, 0.035 M C_6H_6, then $NaBH_4$, THF, MeOH.

Scheme 2.14. The synthesis of tetraaniline macrocycle **2.44** and tetraamine macrocycle **2.43**.

treatment with DIBALH gave dialdehyde **2.57**. It should be noted that this reduction was carried out with toluene as any other typical solvents used for this reaction such as THF or CH_2Cl_2, resulted in complete recovery of the starting material. A one-pot procedure cyclizing dialdehyde **2.57** with enantiopure cylcohexyldiamine followed by in-situ reduction of the tetraimine with $NaBH_4$ produced macrocycle **2.43**. The tetraimine intermediate would not form at concentrations higher than 0.035 M in benzene leading to oligomeric byproducts. Macrocycle **2.42** could be synthesized beginning with a mono-substitution SNAr reaction with hydroquinone and p-fluorobenzaldehyde to form phenol **2.58** (Scheme 2.15). Phenol **2.58** could be

transformed into bromide **2.59** by alkylation with dibromoethane using NaOH in ethanol. Treatment with NaN_3 in DMF gave alkyl azide **2.60**. Treatment of the alkyl azide with trimethylphosphine produced a phosphazide which undergoes loss of N_2 to form an

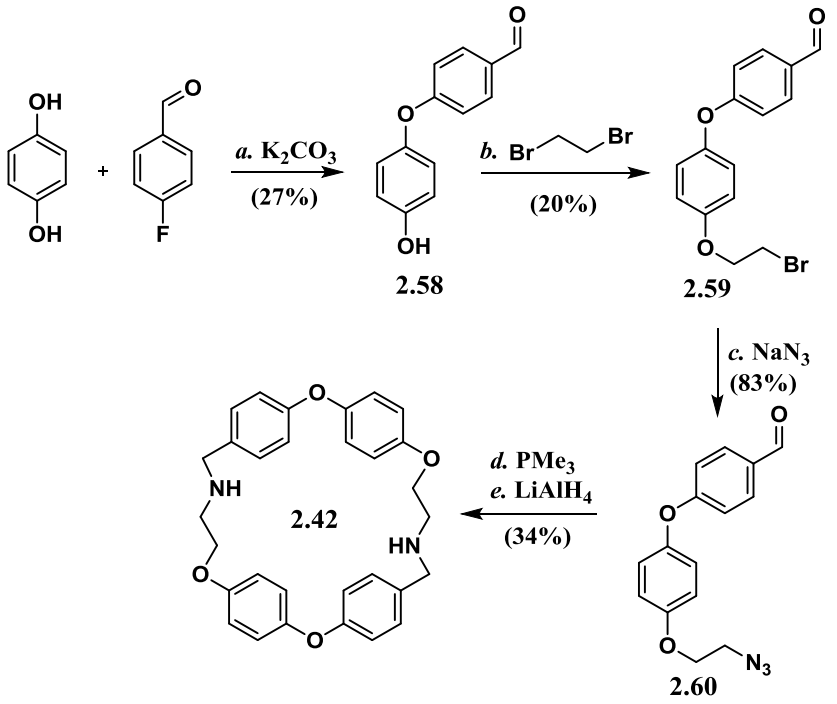

Reagents: a) K_2CO_3, DMA; b) Dibromoethane, NaOH, EtOH; c) NaN_3, DMF; d) PMe_3, 0.09 M CH_2Cl_2 then $LiAlH_4$, THF.

Scheme 2.15. Synthesis of macrocycle **2.42** by Staudinger reduction/dimerization.

iminophosphorane under Staudinger reduction conditions. The iminophosphorane under the dilute conditions of 0.09 M in CH_2Cl_2 allows for the dimerization/macrocyclization event to take place to give the bisimine derivative of macrocycle **2.42**. In a one pot procedure, the solvent was concentrated, and the crude material was dissolved in THF and reduced with $LiAlH_4$ to give macrocycle **2.42**. The dimerization event to form the bisimine occurs in almost quantitative yield, however, the reduction with $LiAlH_4$ is the source of the low yield. Macrocycle **2.42** was recovered as a mixture with trimethylphosphine oxide. Attempts at purification were met with

significant challenges and so the macrocycle was carried as a mixture into further functionalization reactions. This was mainly done as trimethylphosphine oxide should be a benign presence in any functionalization reaction of the secondary amines making losses of material in attempted purifications expendable.

With macrocycles **2.41**, **2.42**, **2.43** and **2.44** in hand, screening for functionalization of the secondary amines began in order to transform the macrocycles into macrocyclic ligands. Functionalization for these macrocycles refers to specifically two sets of reactions; 1) the alkylation of an alkyl bromide such as commercially available bromoacetonitrile or 3-

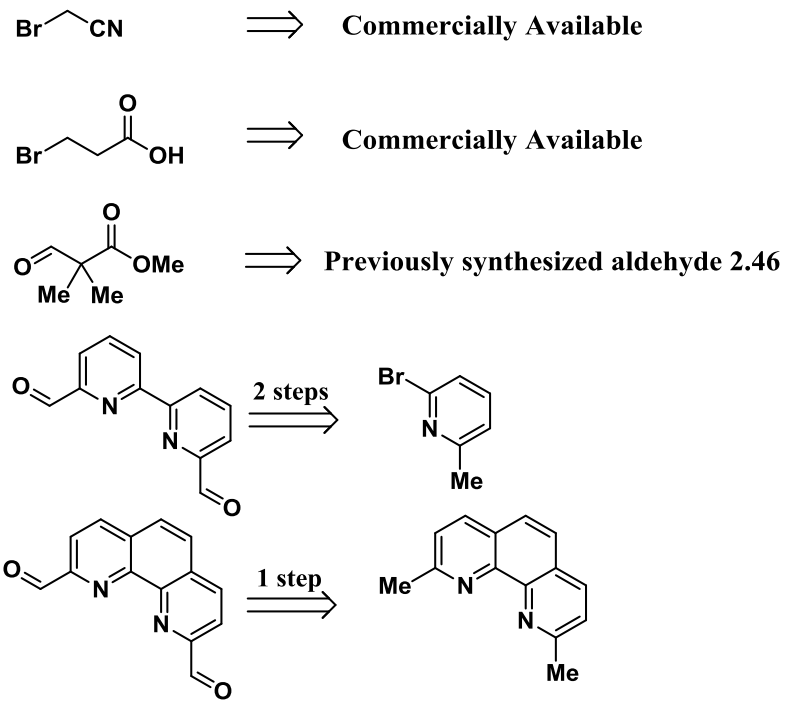

Figure 2.12. Functionalization agents for synthesized macrocycles.

bromopropionic acid, and 2) dehydration to form stable, cyclic aminals with dialdehydes (Figure 2.12). Considering dialdehydes in conjunction with modeling of the aforementioned

macrocycles, we sought after bipyridinyl dialdehyde, available in two steps from 2-bromo-6-methylpyridine by a Ni mediated homo-coupling and subsequent selenium dioxide oxidation,[23] and phenanthroline dialdehyde, available in one step by selenium dioxide oxidation of commercially available neocuprione.[24] Previously synthesized aldehyde **2.46** could also be used for these functionalization purposes. Although macrocycle **2.44** was the easiest and most high yielding to synthesize, attributing to its single step synthesis, it became quickly apparent that the withdrawn nature of the anilines due to the sulfone-mediated deactivation became problematic for functionalization. Attempts were made to reduce the sulfone to a sulfide aryl ether with $LiAlH_4$ and Zn mediated reductions; however, these attempts were unsuccessful and led to decomposition of the macrocycle framework itself. Functionalization was far more fruitful with macrocycle **2.41** as seen in Scheme 2.16. Using 20.0 equivalents of bromoacetonitrile in DMF, macrocycle **2.41** could be tetra alkylated followed by a global hydrolysis to the tetra acid **2.61** using NaOH (aq) in a modest yield over two steps. Unfortunately, any attempts at metalation to form a dirhodium complex were unsuccessful. Subjecting macrocycle **2.41** to $POCl_3$ provided stable macrocycle **2.62** where the final P-Cl bond of the phosphoramide could be used to functionalize the macrocycle. Unfortunately, that bond could not be functionalized. The substitution of the anilines made the phosphorous relatively too electron rich for further substitution. Even under harsh basic conditions (KOH and heat), a simple substrate such as methanol could not be substituted. Over extended periods (multiple days), aqueous hydroxide would slowly hydrolyze the macrocycle to the corresponding phosphoric acid. However, the formation of cyclic aminals by dehydration of aldehydes by macrocycle **2.41** showed promise. This dehydration event was shown to be highly electronic and sterically limited. Condensation with benzaldehyde resulted in complete recovery of the starting material macrocycle **2.41**,

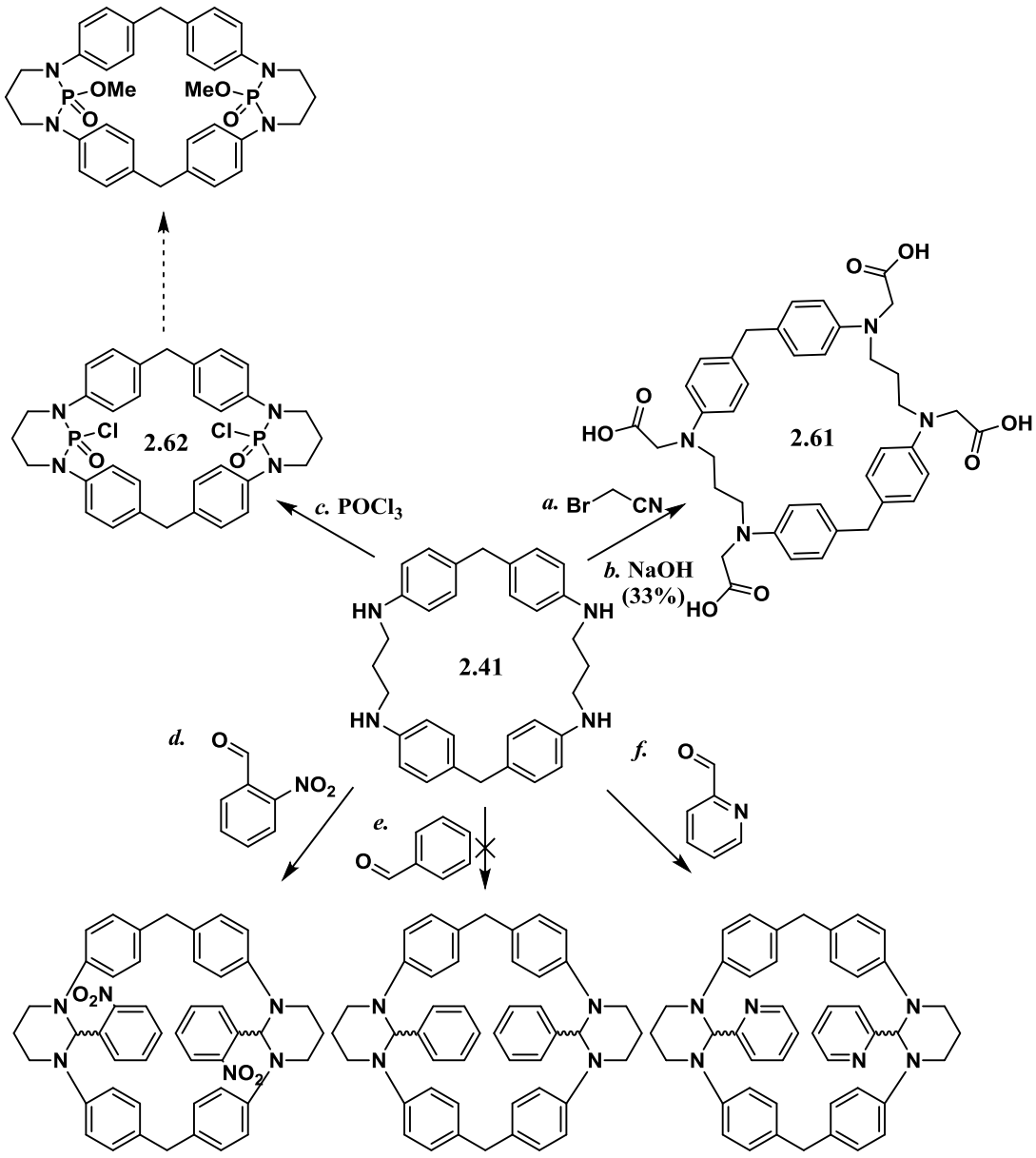

Reagents: a) bromoacetonitrile, K_2CO_3, DMF, 90 °C; b) NaOH, H_2O; c) $POCl_3$, Et_3N, CH_2Cl_2; d) 2-nitrobenzaldehyde, 1,3-difluorobenzene, 100 °C; e) benzaldehyde, 1,3-difluorobenzene, 100 °C; f) 2-pyridinyl carboxaldehyde, 1,3-difluorobenzene, 100 °C.

Scheme 2.16. General results for the functionalization of macrocycle **2.41** by use of alkylations, phosphorylation and condensation to form aminals.

whereas condensation with 2-nitrobenzaldeyhde gave complete conversion to the bis-aminal macrocycle. It should be noted that solvent played a largely important role in the success of these condensations. Through extensive screening, the reactions only worked with fluorinated solvents specifically 1,3-difluorobenzene. The only non-fluorinated solvent to show any condensation was THF but the conversions were limited to less than 15% in most cases. A potential explanation for this phenomenon could be the propensity for these cyclophane macrocycles toward π-stacking interactive properties in solution or even a related hydrogen bonding mediated stacking. A fluorinated solvation could disrupt these interactions making functionalization more facile. It should be noted that electron rich benzaldehydes, such as anisaldehyde, do not participate in the condensations nor do hindered ester derivatives of 2-formylbenzoic. Alkyl aldehydes such as the previously synthesized aldehyde **2.46**, do not participate in the aminal formation either. However, 2-pyridinyl carboxyaldehyde did participate in the condensation reaction. This was a positive result concerning the possibility of using bipyridinyl dialdehyde and phenanthroline dialdehyde as functionalization agents. The condensation product with 2-pyridinyl carboxyaldehyde could not be used as a ligand however; the reaction formed two inseparable isomers. As with macrocycle **2.39**, the isomers are thought to be the *syn*- and *anti*- relationship of the pyridines in relation to the plane of the macrocycle. Depending on the batch, the isomeric ratio would shift but to never more diverse than a 3:2 ratio in either population; regardless, it is unclear as to the identities of each isomer from a spectral sense. Macrocycle **2.41** was heated in 1,3-difluorobenzene in an equimolar amount of bipyridinyl dialdehyde (Figure 2.13), however, the desired encapsulation to give the bipyridinyl macromolecule was never detected. The product profile of the reaction contained three major species. One of which is the oxidized bipyridinyl dialdehyde to the bipyridinyl dicarboxylate

presumably occurring in the presence of any oxygen. Under inert conditions using degassed 1,3-difluorobenzene, this oxidation was significantly slowed but would occur in prolonged reaction times reaching 24 hours or longer. As anticipated, the presence of this byproduct is directly proportional to the amount of recovered starting material macrocycle **2.41**. The other two species isolated are the mono-condensation product and the resulting oxidation of that mono-condensation product to the carboxylic acid just as seen with the starting material bipyridinyl

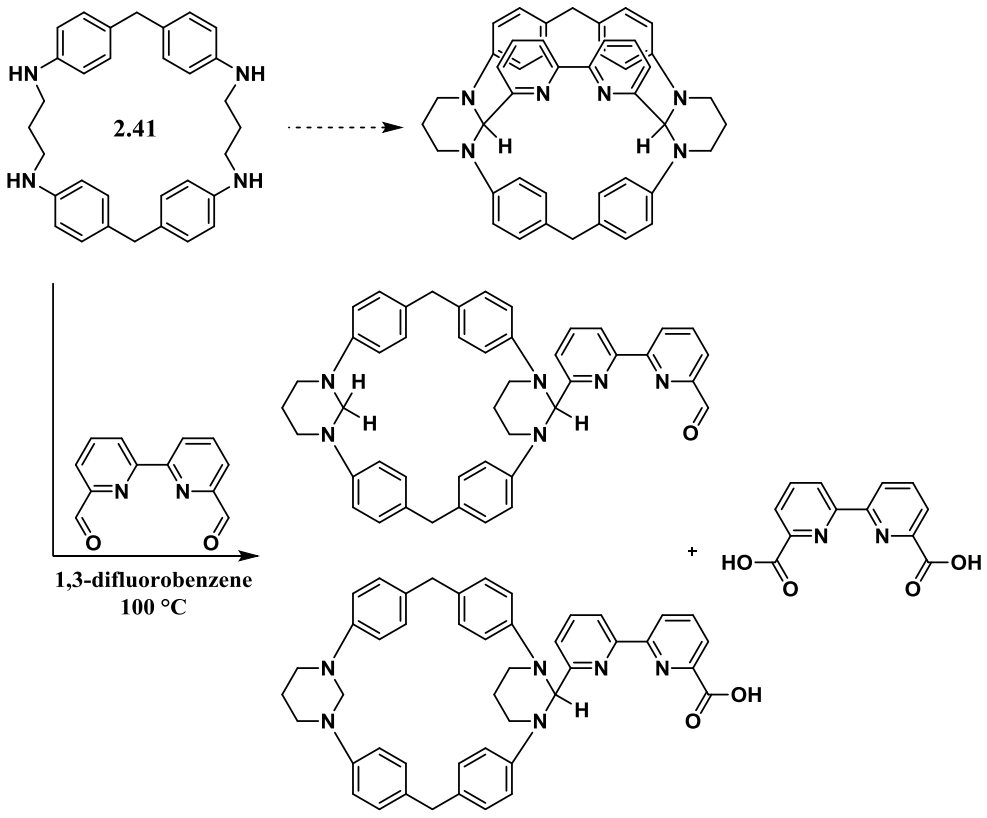

Figure 2.13. Product profile for encapsulation of bipyridinyl dialdehyde by macrocycle **2.41**.

dialdehyde. Under inert, prolonged reaction times greater than 24 hours, the mono-condensed species is more likely to undergo the terminating oxidation step than to undergo the second, intramolecular condensation event. Attempting this transformation in a glovebox eliminates any

oxidation pathways, however, the desired bipyridinyl macromolecule was never isolated, only the aforementioned mono-condensed product could be detected with minute amounts of what appeared to be the intermolecular linking of two macrocycles **2.41** by one molecule of bipyridinyl dialdehyde. This macromolecular linkage was not isolated but was detected by mass spectrometry support. Similar reactions could be repeated with the phenanthroline dialdehyde with similar results. Macrocycle **2.43** afforded an added opportunity to synthesize a ligand that could impart chirality on a potential substrate. However, macrocycle **2.43** suffered from the worst solubility of the synthesized macrocycles leading to problematic functionalization reactions. Unlike macrocycle **2.41**, complete alkylation with any of the aforementioned alkyl bromide sources was difficult and the solubility of the resulting mixtures made purification problematic. Macrocycle **2.43** did not participate in aldehyde condensation reactions. Macrocycle **2.43** did however cleanly produce the corresponding phosphoramide when subjected to $POCl_3$ in the same fashion as with macrocycle **2.41**. Considering that macrocycle **2.43** consists of non-aniline secondary amines, the phosphorous center was even more electron rich making the P-Cl bond more unreactive than that of macrocycle **2.62**. The difficulties we had faced with these tetra-secondary amine macrocycles, warranted investigations into the functionalization of bis-secondary amine macrocycle **2.42**. Reductive amination with bipyridinyl dialdehyde faced the same challenge that macrocycle **2.41** faced with aminal formation in that the desired double reductive amination reaction never took place and instead the only isolable/detected product was the mono-condensed product with corresponding reduction of the remaining unreactive pyridinyl aldehyde (Figure 2.14).

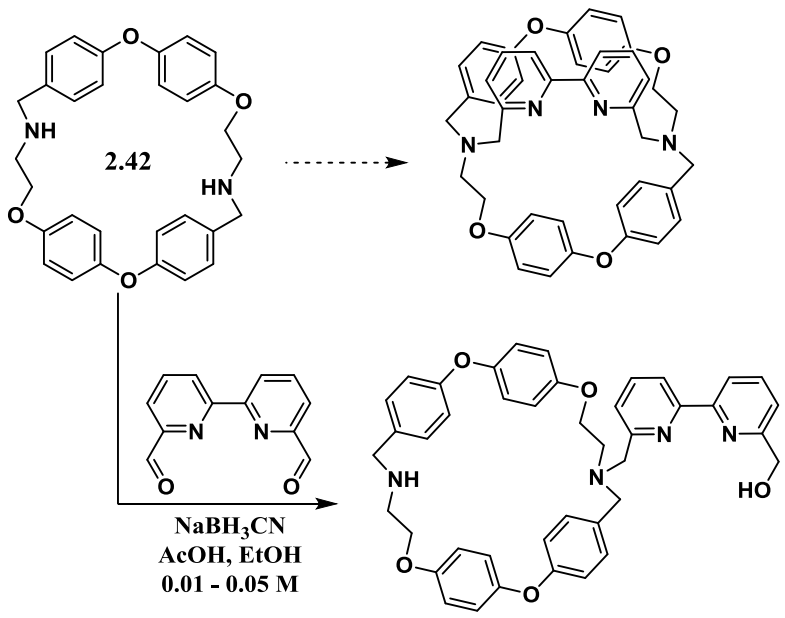

Figure 2.14. Product profile for encapsulation of bipyridinyl dialdehyde by macrocycle **2.42**.

2.6 Overview of inherent challenges in cyclophane macrocyclic ligand syntheses

Our group's efforts towards making cyclophane macrocyclic ligands were unsuccessful as with the efforts towards synthesizing macrocyclic peptide ligands. As predicted cyclophane macrocycles were far more usable considering their solubility and purification as compared to that of the macrocyclic peptides. Unfortunately, we were unable to successfully functionalize the macrocycles. Metalation of the carboxylate functionalized macrocycles resulted in non-isolable mixtures that seemed, by mass spectrometry analysis, to indicate intermolecular metalation of rhodium sources instead of the desired intramolecular metalation. Synthesis of pyridinyl macromolecular ligands were also unsuccessful as, in general, an intermolecular functionalization was achievable, however, in no instances was the second, intramolecular functionalization to form the macromolecular ligand detected or isolated. It should be noted that other cyclophane macrocycle ligand syntheses were attempted using the knowledge gained in these studies by other graduate students from our group, but were unfortunately met with the same success documented within this overview chapter.

REFERENCES

[1] Shenvi, R. A.; O'Malley, D. P.; Baran, P. S. *Acc. Chem. Res.* **2009**, *42*, 530-541.

[2] Hecht, S. M. *J. Nat. Prod.* **2000**, *63*, 158-168.

[3] Boger, D. L.; Cai, H. *Angew. Chem. Int. Ed.* **1999**, *38*, 448-476.

[4] (a) Burger, R. M.; Drlica, K.; Birdsall, B. *J. Biol. Chem.* **1994**, *269*, 25978-25985. (b) Westre, T. E.; Loeb, K. E.; Zaleski, J. M.; Hedman, B.; Hodgson, K. O.; Solomon, E. I. *J. Am. Chem. Soc.* **1995**, *117*, 1309-1313. (c) Sam, J. W.; Tang, X.-J.; Peisach, J. *J. Am. Chem. Soc.* **1994**, *116*, 5250-5256.

[5] (a) Iitaka, Y.; Nakamura, H.; Nakatani, T.; Muraoka, Y.; Fujii, A.; Takita, T.; Umezawa, H. *J. Antibiot.* **1978**, *31*, 1070-1072. (b) Takita, T.; Muraoka, Y.; Nakatani, T.; Fujii, A.; Iitaka, Y.; Umezawa, H. *J. Antibiot.* **1978**, *31*, 1073-1077.

[6] Akkerman, M. A. J.; Neijman, E. W. J. F.; Wijmenga, S. S.; Hilbers, C. W.; Bermel, W. *J. Am. Chem. Soc.* **1990**, *112*, 7462-7474.

[7] Sheng, M. N.; Zajacek, J. G. *J. Org. Chem.* **1970**, *35*, 1839-1843.

[8] (a) Sen, A.; Suslick, K. S. *J. Am. Chem. Soc.* **2000**, *122*, 11565-11566. (b) Liu, H.-Y.; Yam, F.; Xie, Y.-T.; Li, X.-Y.; Chang, C. K. *J. Am. Chem. Soc.* **2009**, *131*, 12890-12891.

[9] Suslick, K. S.; Cook, B. R. *J. Chem. Soc., Chem. Commun.* **1987**, 200-202.

[10] (a) Lichtor, P. A.; Miller, S. J. *Nature Chemistry.* **2012**, *4*, 990-995. (b) Tadross, P. M.; Jacobsen, E. N. *Nature Chemistry* **2012**, *4*, 963-965.

[11] (a) Schöneich, C. *J. Pharm. Biomed. Anal.* **2000**, *21*, 1093-1097. (b) Uchida, K.; Kawakishi, S. *Arch. Biochem. Biophys.* **1990**, *283*, 20-26. (c) Uchida, K.; Kawakishi, S. *J. Agric. Food. Chem.* **1990**, *38*, 1896-1899.

[12] (a) Arnold, L. D.; Drover, J. C. G.; Vederas, J. C. *J. Am. Chem. Soc.* **1987**, *109*, 4649-4659. (b) Arnold, L. D.; Kalantar, T. H.; Vederas, J. C. *J. Am. Chem. Soc.* **1985**, *107*, 7105-7109.

[13] (a) Sambasivan, R.; Zheng, W.; Burya, S. J.; Popp, B. V.; Turro, C.; Clementi, C.; Ball, Z. T. *Chem. Sci.* **2014**, *5*, 1401. (b) Sambasivan, R.; Ball, Z. T. *Angew. Chem. Int. Ed.* **2012**, *51*, 8568-8572. (c) Popp, B. V.; Ball, Z. T. *J. Am. Chem. Soc.* **2010**, *132*, 6660-6662. (d) Zaykov, A. N.; MacKenzie, K. R.; Ball, Z. T. *Chem. Eur. J.* **2009**, *15*, 8961-8965.

[14] Sambasivan, R.; Ball, Z. T. *J. Am. Chem. Soc.* **2010**, *132*, 9289-9291.

[15] Brodsky, B. H.; Du Bois, J. *Chem. Commun.* **2006**, 4715-4717.

[16] Fletcher, J. T.; Finlay, J. A.; Callow, M. E.; Callow, J. A.; Ghadiri, M. R. *Chem. Eur. J.* **2007**, *13*, 4008-4013.

[17] White, C. J.; Yudin, A. K. *Nature Chemistry* **2011**, *3*, 509-524.

[18] (a) Horne, W. S.; Stout, C. D.; Ghadiri, M. R. *J. Am. Chem. Soc.* **2003**, *125*, 9372-9376. (b) Ball, Z. T. *Acc. Chem. Res.* **2013**, *46*, 560-570.

[19] Zalatan, D. N.; Du Bois, J. *J. Am. Chem. Soc.* **2008**, *130*, 9220-9221.

[20] (a) Nour, H. F.; Hourani, N.; Kuhnert, N. *Org. Biomol. Chem.* **2012**, *10*, 4381-4389. (b)Tanaka, K.; Nakai, Y.; Takahashi, H. *Tetrahedron: Asymmetry* **2011**, *22*, 178-184. (c) Shimizu, L. S.; Hughes, A. D.; Smith, M. D.; Davis, M. J.; Zhang, B. P.; Zur Loye, H. C.; Shimizu, K. D. *J. Am. Chem. Soc.* **2003**, *125*, 14972-14973.

[21] Odashima, K.; Itai, A.; Iitaka, Y.; Koga, K. *J. Org. Chem.* **1985**, *50*, 4478-4484.

[22] Inouye, M.; Miyake, T.; Furusyo, M.; Nakazumi, H. *J. Am. Chem. Soc.* **1995**, *117*, 12416-12425.

[23] (a) Newkome, G. R.; Lee, H. W. *J. Am. Chem. Soc.* **1983**, *105*, 5956-5957. (b) Beynek, N.; Uluçam, G.; Benkli, K.; Koparal, A. e. T. *Helv. Chim. Acta* **2008**, *91*, 2089-2096.

[24] Adam, R.; Ballesteros-Garrido, R.; Vallcorba, O.; Abarca, B.; Ballesteros, R.; Leroux, F. R.; Colobert, F.; Amigó, J. M.; Rius, J. *Tetrahedron Lett.* **2013**, *54*, 4316-4319.

Chapter 3: Efforts toward the Total Synthesis of Rubiyunnanin A

3.1 Original regio-divergent synthetic efforts towards rubiyunnanin A and B

The original synthesis of rubiyunnanin A was planned utilizing a regio-divergent opening of a racemic allylic oxide that would also provide access to a pathway for the synthesis of rubiyunnanin B. This was based upon a strategy of allylic oxide regio-resolution (AORR), a strategy that our group has previously published to gain access to carbasugar natural products.[1] An example of this strategy can been seen in Figure 3.1, where 4-methylphenol undergoes

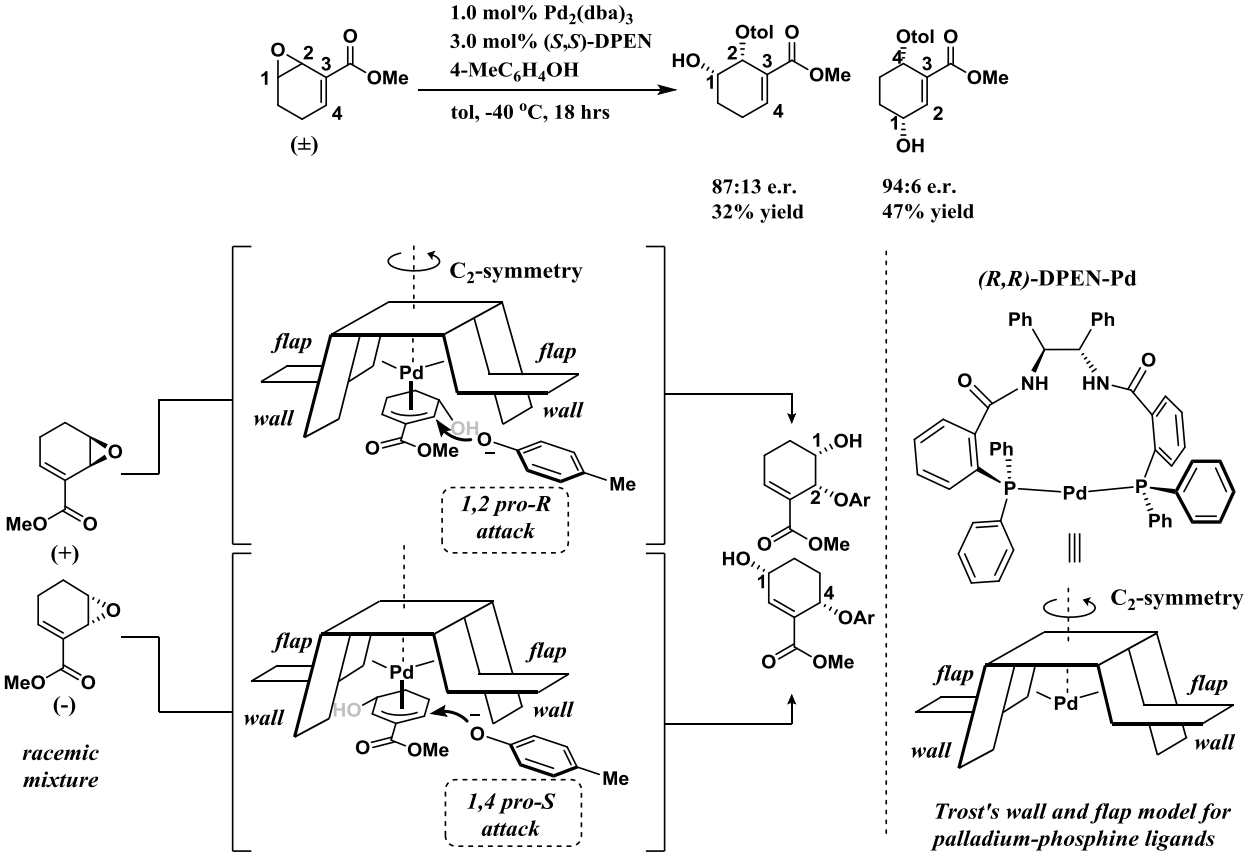

Figure 3.1. Example and mechanistic explanation for the AORR strategy developed by the Lewis group to establish access to carbasugar natural products.

a regio-divergent addition to a Pd π-allyl species mediated by the (*R*,*R*)-DPEN ligand. The Trost wall and flap model[2] predicts that one enantiomer of the allylic oxide will participate in a 1,2 pro-(*R*) attack resulting in enantioenriched *syn*-(1,2) addition to the activated Pd π-allyl species,

whereas the other enantiomer of the allylic oxide will participate in a 1,4 pro-(*S*) attack resulted in enantioenriched *syn*-(1,4) addition to the activated Pd π-allyl species. As indicated in Figure 3.1, *syn*-(1,2) and *syn*-(1,4) were produced in a 32% yield (87:13 e.r.) and a 47% yield (94:6 e.r.), respectively. We envisioned that we could use the same AORR strategy to synthesize the cores of rubiyunnanin A and B (Scheme 3.1). Regio-resolution of racemic epoxide **3.1** using tyrosine **3.2** might produce enantioenriched *syn*-(1,2) addition **3.3** and *syn*-(1,4) addition **3.4**. Product dipeptide **3.3** might be further advanced by an intramolecular Heck, subsequent deprotection, and macrolactamization to provide access to the core benzofuran **3.5** of rubiyunnanin A. A (3,3)-sigmatropic rearrangement of diol **3.4** (reminiscent of a Claisen type rearrangement) would

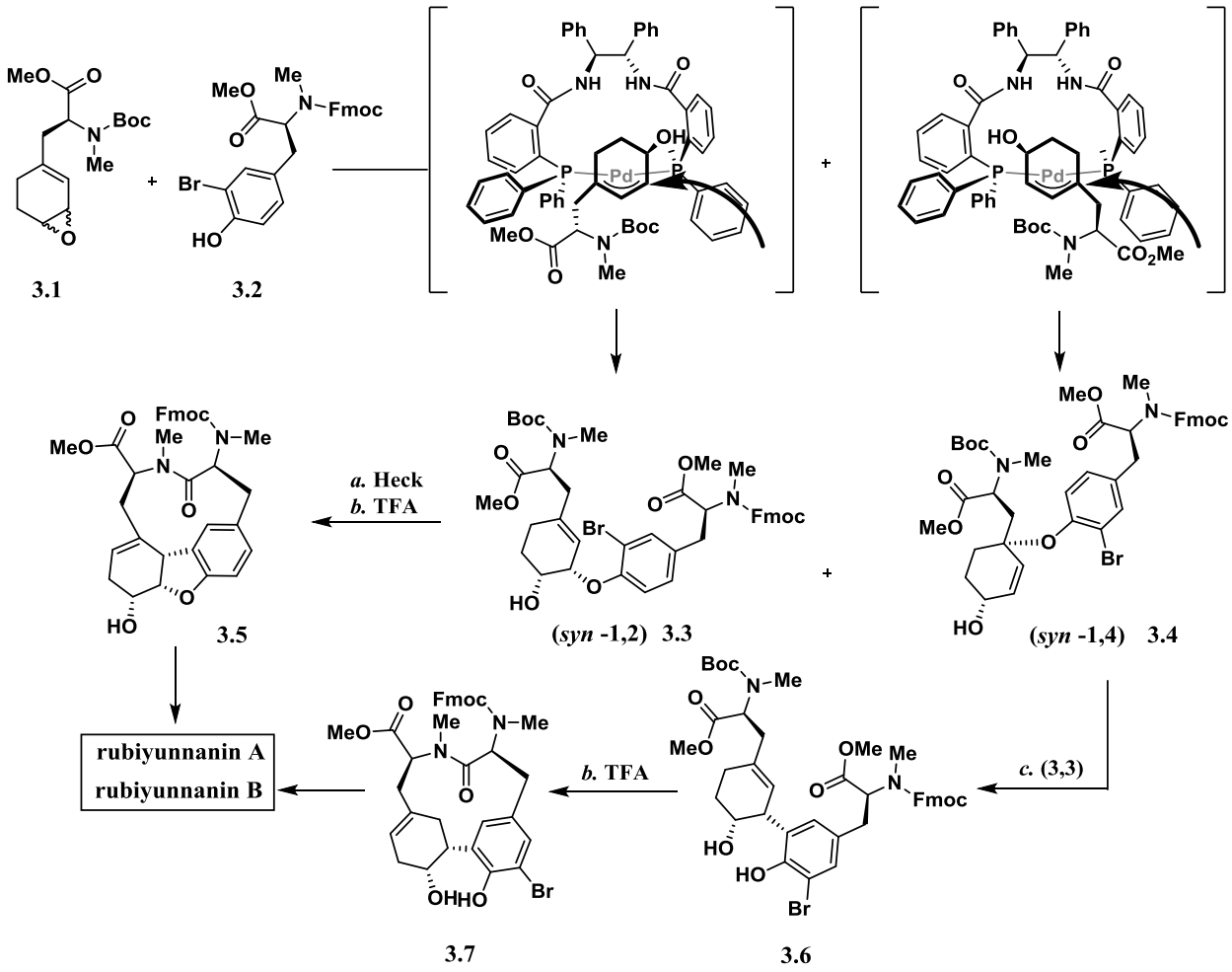

Scheme 3.1. Forward synthetic plan for the total synthesis of rubiyunnanin A and B.

give diol **3.6** and subsequent macrolactamization would provide a precursor (**3.7**) to the core of rubiyunnanin B. This intermediate would require an aromatization (oxidation) to provide the C-C biaryl linkage of rubiyunnanin B. This aromatization presumably could be executed by a dehydrative process involving strong acids such as phosphoric acid, or it could be achieved through possible dehydrogenation techniques through Pd, Pt, Ru, Rh, or Ir embedded SiO_2 or Al_2O_3 catalyts.[3]

To study this key regio-resolution for the total synthesis of rubiyunnanin A and B, we needed to prepare 5,6-dihydro-L-phenylalanine **3.13**. While (1,4) and (2,5)-dihydrophenylalanine residues are known,[4] 5,6-dihydro-L-phenylalanine **3.13** has not been reported in the literature. An initial route to the molecule was devised employing a Negishi cross coupling of 1-bromo-1,3-cyclohexadiene **3.11**, which was prepared as in Scheme 3.2. Mono-oxidation of 1,4-

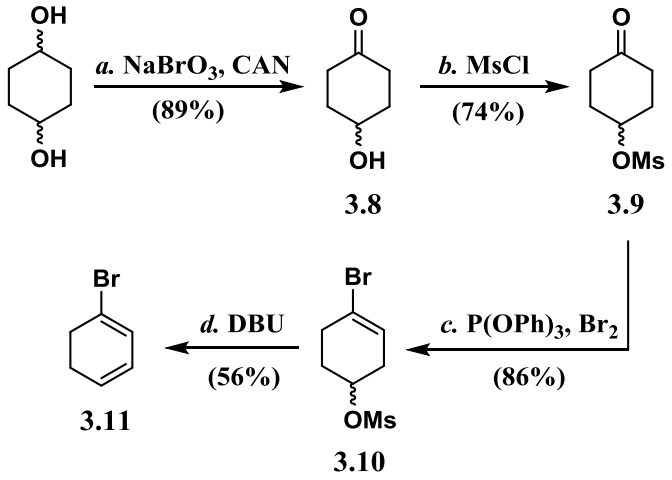

Reagents: (a) $NaBrO_3$, CAN, MeCN:H_2O; (b) MsCl, pyridine;
(c) $P(OPh)_3$, Br_2, NEt_3, CH_2Cl_2, -78 - 23 °C; (d) DBU, 50 °C.

Scheme 3.2. Synthesis of 1-bromo-1,3-cyclohexadiene.

cyclohexadiol using $NaBrO_3$ and ceric ammonium nitrate (CAN) afforded ketone **3.8**, which underwent mesylation to form ketone **3.9**. Although the full mechanism is not known, the mono-

selectively could be an effect caused by intramolecular chelation of the diol to the cerium(IV) salts. Cyclohexanone **3.9** could be converted to the vinyl bromide **3.10** in consistently high yields with $P(OPh)_3$ and Br_2.[5] The proposed mechanism for this transformation includes three key steps; 1) facile formation of an oxophosphonium bromide species upon the reaction of the ketone with the activated phosphonium bromide, 2) evolution of the oxophosphonium bromide species into a *gem*-dihalide by loss of triphenyl phosphate, and 3) dehydrohalogenation to provide the vinyl bromide. Proof of this mechanism can found in the GC detection of the aforementioned *gem*-dihalide species. Finally the 1-bromo-1,3-cyclohexadien **3.11** could be

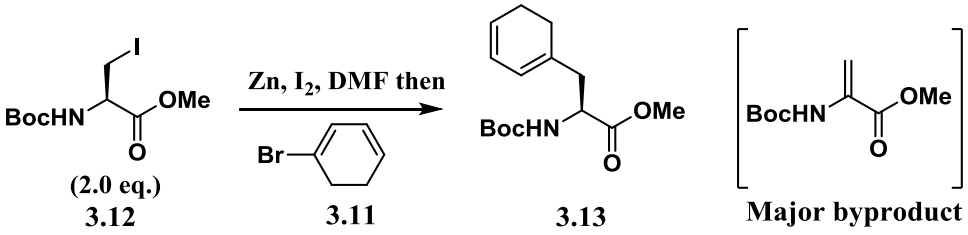

(2.0 eq.) **3.12** **3.11** **3.13** **Major byproduct**

Entry	Zn Source	Catalyst	Additive	Yield %[a]
1	Zn dust	$Pd(Ph_3)_4$	-	21
2	Zn dust	$PdCl_2(PPh_3)_2$	-	27
3	Zn dust	$Pd(OAc)_2$, TBAB	-	n.d.[b]
4	Zn dust	Pd_2dba_3, $P(o\text{-tol})_3$	-	44
5	Zn dust	Pd_2dba_3, $P(2\text{-furyl})_3$	-	15
6	Zn dust	Pd_2dba_3, X-phos	-	35
7	Zn dust	$NiCl_2(PPh_3)_2$	-	20
8	$ZnCl_2$	Pd_2dba_3, $P(o\text{-tol})_3$	-	n.d.[c]
9	Zn/Cu	Pd_2dba_3, $P(o\text{-tol})_3$	-	53
10	Zn dust	Pd_2dba_3, $P(o\text{-tol})_3$	TMEDA	44
11	$ZnCl_2$	Pd_2dba_3, $P(o\text{-tol})_3$	TMEDA	n.d.[c]
12	Zn/Cu	Pd_2dba_3, $P(o\text{-tol})_3$	TMEDA	52

[a] Yields were calculated by column chromatography isolation. [b] Only isolated product was decomposition of iodo-serine. [c] Recovered SM.

Table 3.1. Screening for the Negishi cross coupling of 1-bromo-1,3-cyclohexadiene and iodo-serine.

prepared by heating the vinyl bromide **3.10** in neat DBU. At the reaction temperature of 50 °C, 1-bromo-1,3-cyclohexadiene **3.11** can be distilled directly into a 0 °C trap. With this molecule in hand, the Negishi cross coupling with iodo-serine[6] was screened for the production of 4,5-dihydro-L-phenylalanine **3.13** (Table 3.1). Boc-N aminoacrylate formation was the main byproduct. Under the reaction conditions, this acrylate polymerized rapidly so it was difficult to determine actual conversions for its formation. Entries 4 and 6 produced the best original yields (with $P(o\text{-tol})_3$ and X-Phos respectively) with Zn dust as the vinyl bromide activator. TMEDA was used as an additive to stabilize the *in-situ* zincate to reduce the amount of elimination to the Boc-N aminoacrylate; however, as seen in entries (10-12), TMEDA was relatively ineffective at improving the conversion for the reaction. Interestingly, changing the Zn source to $ZnCl_2$ (entry 8) resulted in recovered starting material; whereas, changing the Zn source to Zn/Cu couple (entry 9) increased the yield of the reaction by almost 10% to give an overall modest yield of 53%. It is unclear why the Zn/Cu couple is more effective as an activator than Zn dust. With 4,5-dihydro-L-phenylalanine **3.13**, a study on regio-selective epoxidations was undertaken to provide access to the needed racemic epoxide **3.1**. Epoxidation of 4,5-dihydro-L-phenylalanine **3.13** under basic conditions employing *m*-CPBA solely produced Boc-N-L-phenylalanine-OMe (Figure 3.2). This full oxidation to phenylalanine was temperature independent. Presumably this oxidation occurs through the epoxidation of the more substituted olefin. Elimination of the epoxide to produce the 1-cycloexadienol would undergo aromatic dehydration to produce the Boc-N-L-phenylalanine-OMe. It is unclear if the Boc-N carbamate is uninvolved in this rearomatization. The epoxidation was difficult to monitor beyond crude ^1H NMR spectra, which is how the formation of the trisubstituted **3.15** was detected. The life time of this

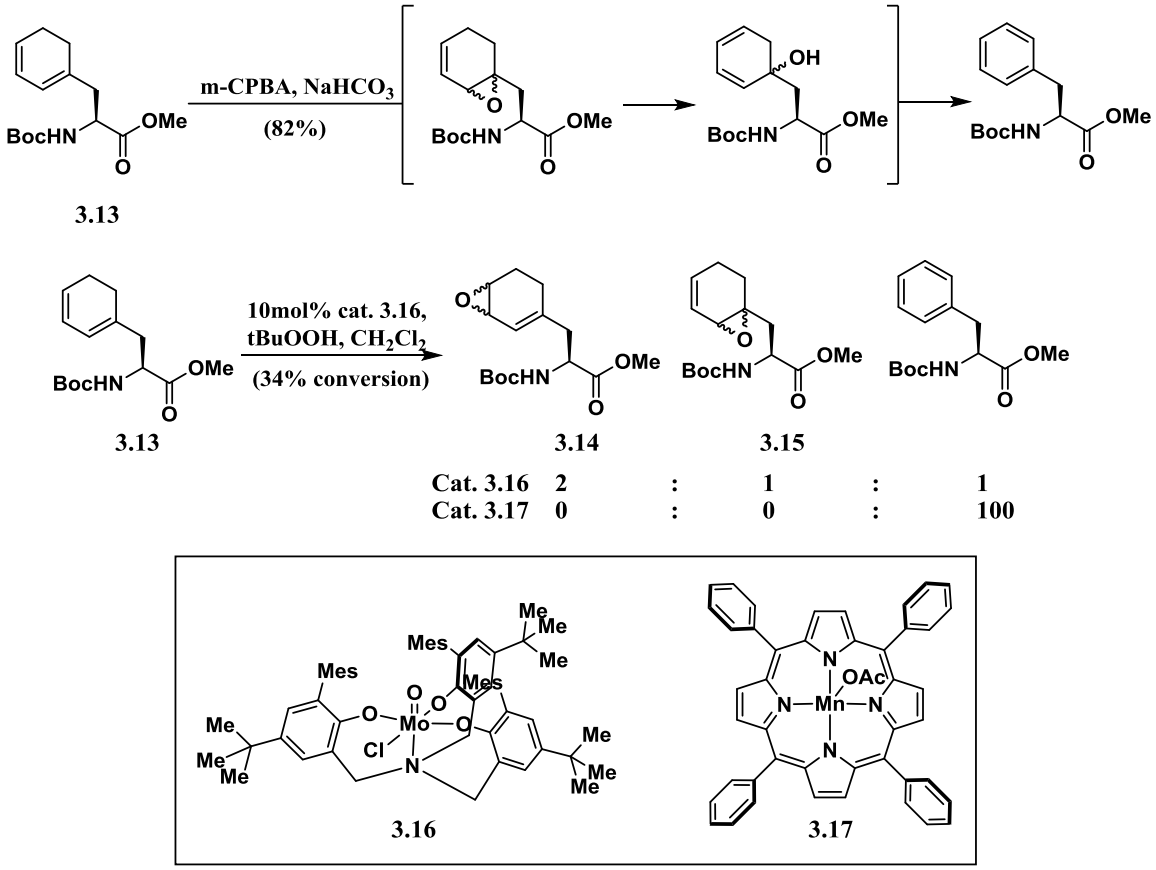

Figure 3.2. Regio-selective epoxidation studies on 4,5-dihydro-L-phenylalanine

epoxide was short lived in solution and attempts to purify (HPLC or bench top chromatography) resulted in a more expedient oxidation to the Boc-N-L-phenylalanine-OMe. The inability to purify the epoxidation reaction would prove to be an insurmountable problem; separation of the regio-isomers was necessary and instability of the allylic oxide was problematic. Shi[7] and Jacobsen[8] epoxidation reactions were all attempted but all led to high impurity profiles where an unclear product distribution was created. In light of the work done by Suslick,[9] described in detail in Chapter 2, porphyrin catalyst **3.17** was investigated for its ability to regio-selectively forge epoxides. However, using catalyst **3.17** with NaOCl resulted in direct oxidation of 4,5-dihydro-L-phenylalanine to Boc-N-L-phenylalanine-OMe. By crude ^{1}H NMR, the most success in the regio-selective epoxidation came in the use of Mo catalyst **3.16** that had been previously synthesized for the efforts in the chemoselective macrocyclic ligand projects documented in

Chapter 2. The disadvantage to using this catalyst, is the reaction conditions consisted of heating the mixture to 50 °C, over a 24-36 hour period, in which a total conversion of 34% was measured. Nevertheless, the catalyst had shown indications of providing access to the unexpected epoxide **3.14**. Once again the stability of the vinyl epoxide mixture was problematic and all attempts at purification of the mixture resulted in only isolated Boc-N-L-phenylalanine-OMe. The regio-selective epoxidation of the 4,5-dihydro-L-phenylalanine residue **3.13** had become far more challenging than first anticipated due to the instability of the vinyl epoxide products toward autoxidation to Boc-N-phenylalanine-OMe and the ineffectiveness of the catalyst technology at our disposal.

In a parallel screening of the regio-selective epoxidation, we were also searching for regio-resolution (AORR) conditions with phenolic based nucleophiles and mimics of the C4-substituted allylic oxide represented by racemic epoxide **3.1**. We suspected that methyl ester substitution at the C3 position partially attributed to the efficiency of the regio-resolution of phenolic nucleophiles show in Figure 3.1. It was suspected that removing the methyl ester from the C3 position or altering the substitution pattern away from the allylic oxide substrates generally show in Figure 3.1, would greatly affect the previously defined reaction conditions. The screening began with commercial cyclohexen-oxide, removing the substitution from the C3 position. The Tsuji-Trost reaction of cylcohexen-oxide with $Pd(PPh_3)_4$ and malonate nucleophiles is documented.[10] This reaction provides solely the *syn*-(1,4) product without producing any *syn*-(1,2) product. The experiment run in (equation 1) (Figure 3.3) provides proof as only the *syn*-(1,4) aryl ether **3.18** was isolated with no *syn*-(1,2) aryl ether **3.19**.

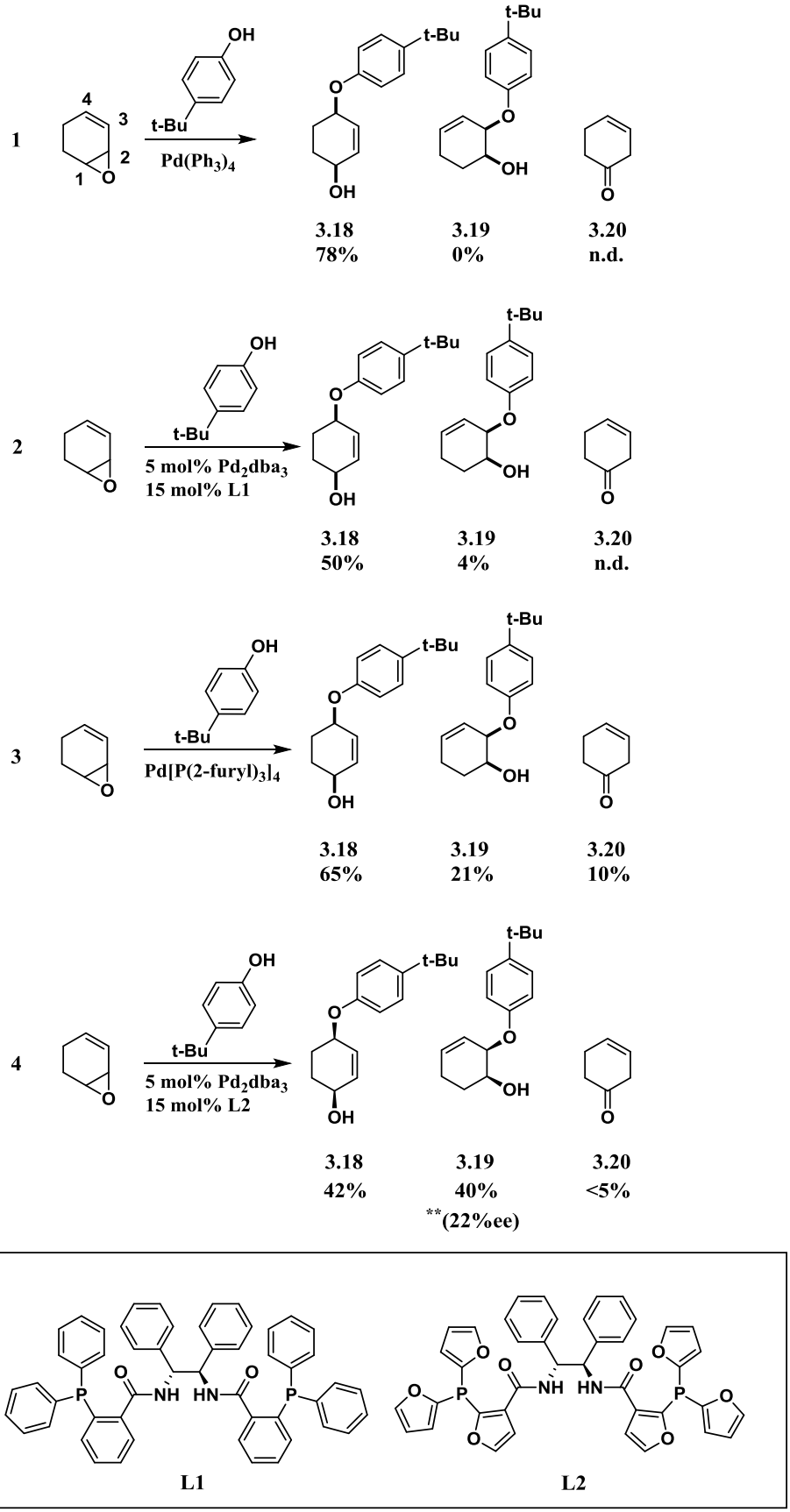

Figure 3.3. AORR studies on cyclohexen-oxide.

No detectable amounts of the β-hydride eliminated product **3.20** were observed. This is not surprising as the AORR developed in our group is an outlier as access to the *syn*-(1,2) product is uncommon. In fact, the only known examples provide precedence that the nucleophile bind to the alcohol through a Lewis acid or other covalently bound intermediate so the *syn*-(1,2) product is specifically delivered.[11] Performing the same Pd catalyzed allylation with the AORR conditions studied by our group provided *syn*-(1,4) aryl ether **3.18** in a 50% yield; however, only provided *syn*-(1,2) aryl ether **3.19** in a 4% yield, where neither aryl ether was enantioenriched (equation 2). This result helps bolster the results from (equation 1) and indicates that the methyl ester on C3 played a significant role. However, an interesting trend arose from the screening of Pd allylation reactions in the discovery that the phosphine ligand could dictate the ratios of *syn*-(1,2) and *syn*-(1,4)(equation 3). We found that using the tri(2-furyl) phosphine ligand complex, instead of the triphenyl phosphine ligand complex, provided a product profile of the *syn*-(1,4) addition **3.18** in a 65% yield while also affording the *syn*-(1,2) addition **3.19** in a 21% yield. Of the phosphine ligands screened, tri(2-furyl) phosphine gave the best yields of the *syn*-(1,2) **3.19**, and the only other ligand to give access to this pathway was triphenyl phosphite yields below 5%. It is unclear why tri(2-furyl) phosphine provides access to the *syn*-(1,2) pathway. Nevertheless, the tri(2-furyl) phosphine ligand derivative (**L2**) was synthesized (Scheme 3.3), and provided a promising result in a regio-resolution (AORR) of cyclohexen-oxide to produce *syn*-(1,4) aryl ether **3.18** and *syn*-(1,2) aryl ether **3.19** in 42% and 40%, respectively, where the *syn*-(1,2) product was enantioenriched albeit in a very modest 22% ee (equation 4). This provided us with the initial results needed to approach the more complex allylic oxides with the substitution switched from the C3 to the C4 position (Figure 3.4).

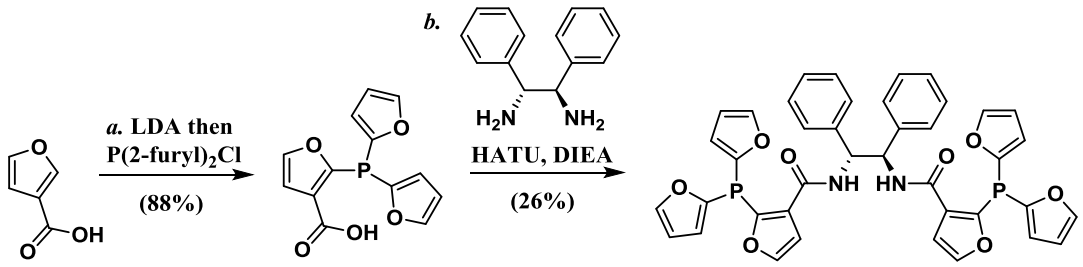

Reagents: (a) n-BuLi, DIA, THF, 0 °C, 30 min then 3-furoic acid, -78 °C, 60 min then P(2-furyl)$_2$Cl, -78 °C for 60 min; (b) HATU, DIEA, (R,R)-1,2-diphenylethylenediamine, THF.

Scheme 3.3. Synthesis of tri(2-furyl) phosphine derived (R,R)-DPEN ligand.

TBS-protected vinyl epoxide **3.21** (along with the unprotected and O-acetate protected allylic oxide) could be prepared as a racemate through a seven step synthesis using known methods.[12] As an initial test, Pd (*R,R*)-DPEN mediated allylation of 4-*tert*-butylphenol gave a mix of the *syn*-(1,4) aryl ether **3.22** in a 61% yield and β-hydride elimination product **3.24** in a 39% yield (equation 5). This result is on par with the reactions outlined in Figure 3.3, but also in line with trends observed and recorded in the literature.[13] On simple substrates, sterically hindered nucleophiles such as phenol, tend to give the more branched products in a Pd allylation reaction. Consistent with (equation 3), the tri(2-furyl) phosphine Pd complex facilitated access to the *syn*-(1,2) aryl ether **3.23** in 37% yield and the *syn*-(1,4) aryl ether **3.22** in 15% yield (equation 6). Unfortunately, the formation of the β-hydride elimination product **3.24** was the major isolated product. Interestingly, the tri(2-furyl) phosphine ligand derivative (**L2**) did not facilitate a regio-resolution like in equation 4 (equation 7). In fact, the (R,R)-tri(2-furyl) phosphine-DPEN ligand impeded access to the *syn*-(1,2) aryl ether **3.23**. A solvent screen established that toluene used in place of THF did produce the *syn*-(1,2) aryl ether **3.23**; however, it was produced in low yields, providing a relatively higher conversion to β-hydride elimination product **3.24**, and was not enantioenriched. Reactivity trends considering vinyl epoxide **3.21** were independent of the

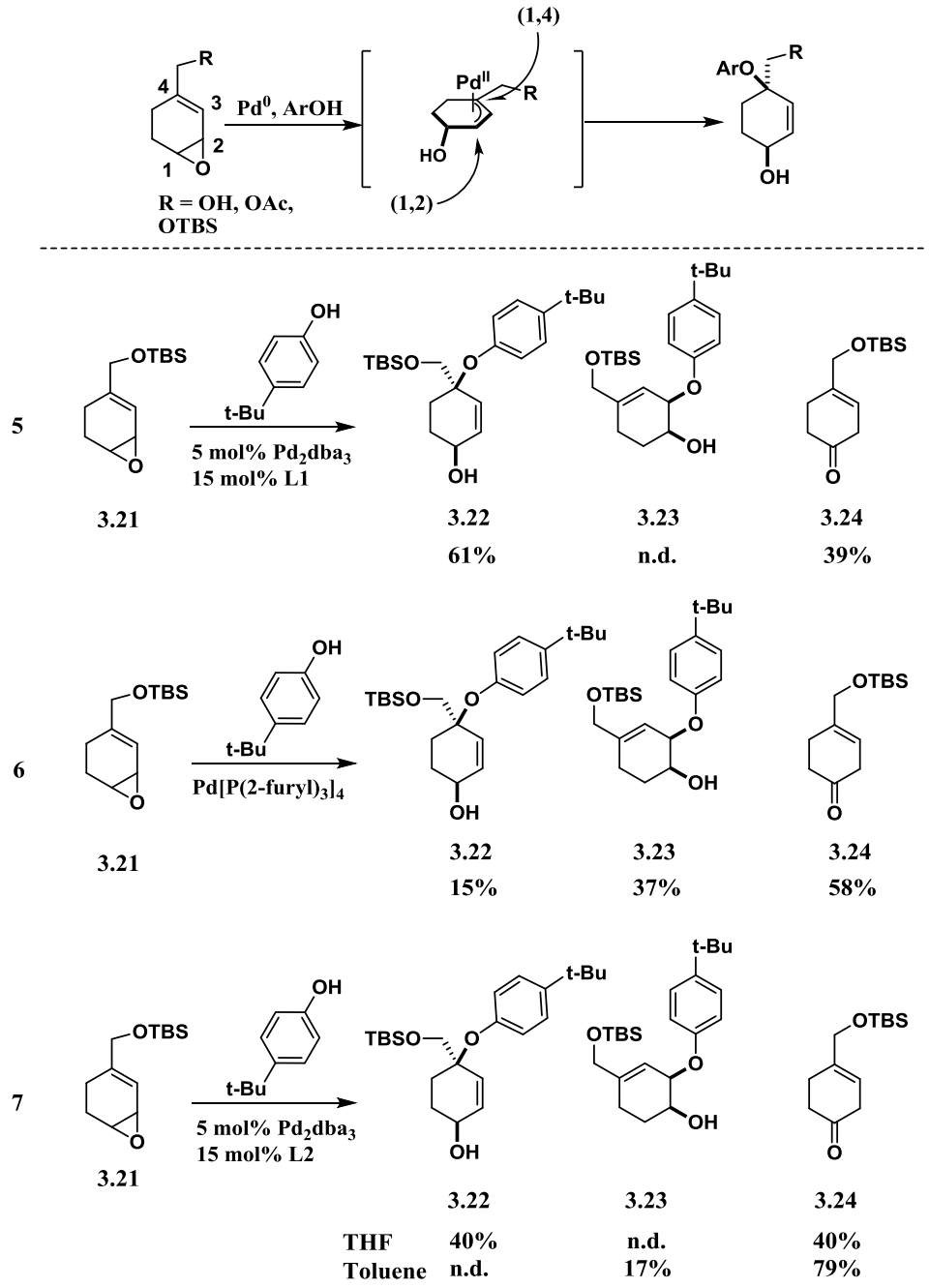

Figure 3.4. AORR studies on C4-substituted cyclohexen-oxide.

identity of allylic alcohol protecting group. The propensity for Pd allylation of the C4 substituted cyclohexen-oxide to produce the *syn*-(1,4) aryl ether was problematic. Ligand screens were not effective in overturning this bias. Considering these challenges and the problematic regio-selective epoxidation of the 4,5-dihydro-L-phenylalanine residue **3.13**, we set out to change the original retrosynthetic analysis for the rubiyunnanin A synthesis.

3.2 First generation asymmetric synthesis of the benzofuran in rubiyunnanin A

Considering the results of the regio-selective epoxidation and the indication that a regio-resolution (AORR) of racemic epoxide **3.1** and tyrosine residue **3.2** may not be possible, we turned to a system in which the C4 substitution on cyclohexen-oxide would outright inhibit the formation of any *syn*-(1,4) aryl ether. This would prevent the ability to induce a regio-resolution; however, under our current studies it appears the methyl ester C3 substitution may have been more pertinent to the mechanism of action than previously believed.

This new approach to gain sole access to the *syn*-(1,2) aryl ether moiety began with 4-bromo allylic oxide **3.25** (equation 8, Figure 3.5). However, in the screening of this reaction, it was found the presence of the bromide deactivated the allylic oxide to the formation of a π -allyl species. In all cases there was complete recovery of starting material regardless of the catalyst system. 4-Cyano allylic oxide **3.29** did not suffer the same deactivation as 4-bromo allylic oxide **3.25** (equation 9). Unfortunately, it was found this substrate converts exclusively to the β-hydride elimination product **3.32**. In all cases there was never any isolation of *syn*-(1,4) or *syn*-(1,2) aryl ethers **3.30** or **3.31**, respectively. The results for the π -allyl formation of 4-methylcarboxylate allylic oxide **3.33** were promising (equation 10). In all cases, no *syn*-(1,4) aryl ether **3.34** was isolated. Not surprisingly, considering previously discussed results, all catalyst systems except for that of the tri(2-furyl) phosphine Pd complex gave exclusively β-hydride elimination product **3.36**. Tri(2-furyl) phosphine Pd complex gave *syn*-(1,2) aryl ether **3.35** in a 21% yield with the remaining mass balance attributed to a 71% isolated yield of the β-hydride elimination product **3.36**. The immediate concern was access to enantiopure allylic oxide **3.33**; stereoselective access to similar allylic oxides via direct epoxidation is not known.

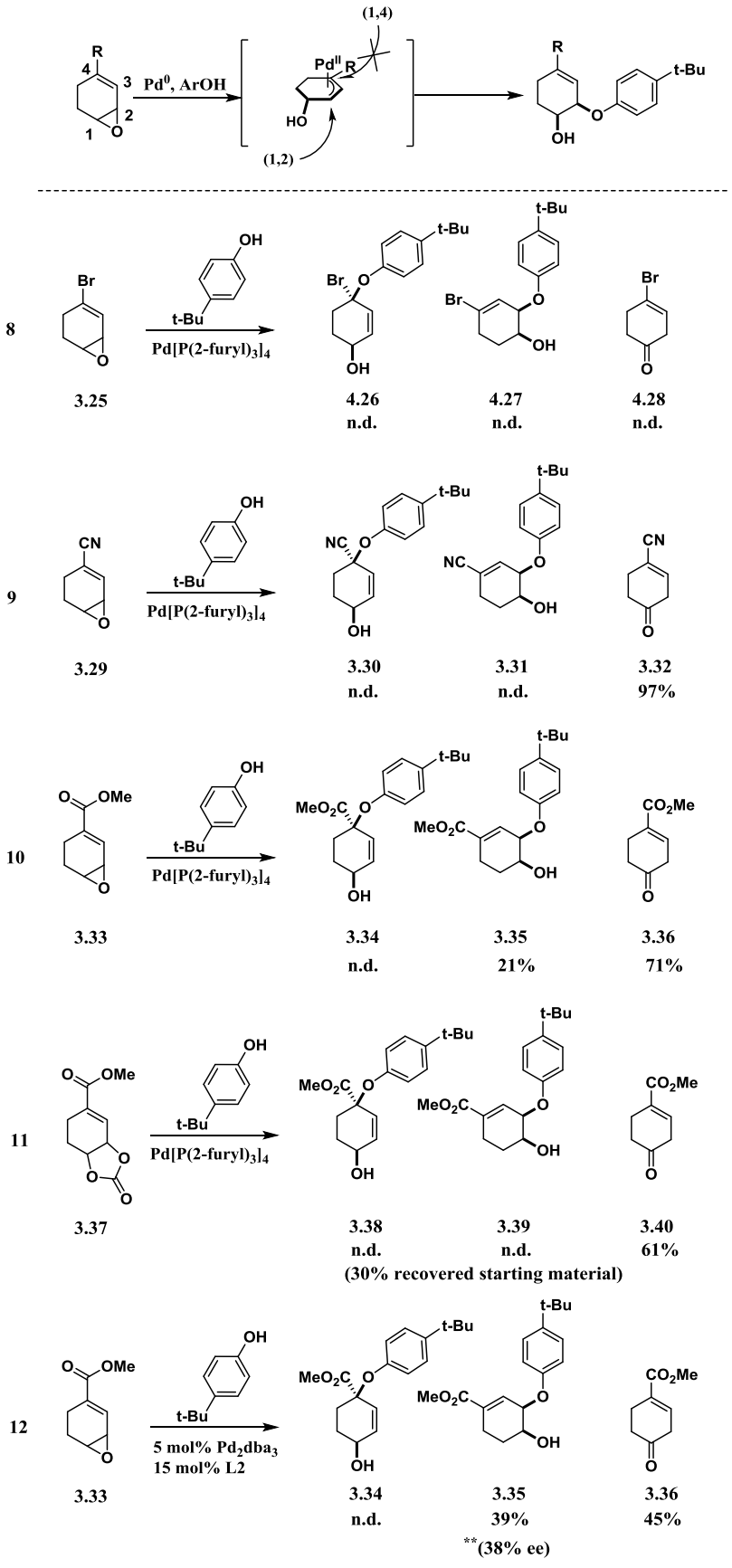

Figure 3.5. Allylic oxide studies on with C4 position blocked.

It is well documented in the literature that this type of cyclohexen-oxide could not efficiently be provided via enantioselective epoxidation by the Jacobsen and Shi groups.[14] An enantioselective dihydroxylation was a more attractive option but the cyclic carbonate **3.37** was not a good substrate for the Pd allylation as the closely related allylic oxide (equation 11). This reaction only produced the β-hydride elimination product **3.40** and 30% recovered starting material, which is not surprising under prolonged reaction conditions considering the Pd π -allyl species will form reversibly by ring opening of the cyclic carbonate. Surprisingly, the aforementioned regio-resolution conditions using the tri(2-furyl) phosphine **L2** Pd complex provided a resolution of the racemic epoxide **3.33** (equation 12). The regio-divergent resolution produced the *syn*-(1,2) aryl ether **3.35** in a 39% yield with a 38% ee. Presumably the other enantiomer of the epoxide was converted to the 45% isolated β-hydride elimination product **3.36**. Through exhaustive screening a 69:31 e.r. was established to be the optimized selectivity. Tri(2-furyl) phosphine **L2** Pd complex has provided interesting insight into ligand control of the Tsuji-Trost reactions' regio-selectivity; however, it is not imparting high levels of stereoselectivity on the substrates in study. Part of the issue could be the lack of substitution on the tri(2-furyl) phosphine (Figure 3.6). The (R,R)-DPEN ligand **L1** has been shown by our group to facilitate the regio-resolution

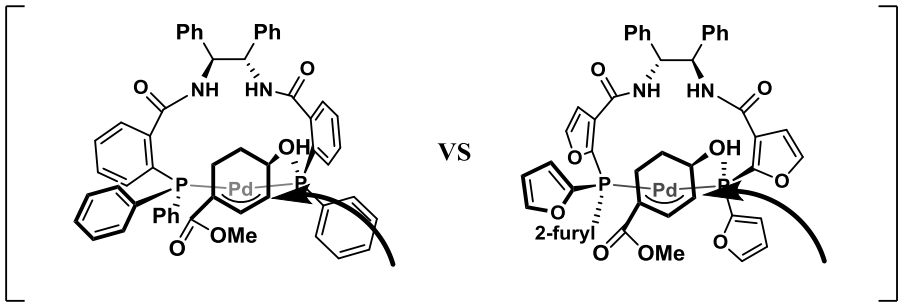

Figure 3.6. Steric difference between the **L1** and **L2** ligands.

(AORR) with high stereoselectivity. It's possible that size increase of the phenyl substituents

relative to the furyl provides enhanced ligand control over the π-allyl species. Members of our group have begun syntheses of the tri(2-benzofuryl) phosphine ligand equivalent and other 4,5-substituted tri(2-furyl) phosphine ligands with little to no success. The ligand syntheses are difficult due to the propensity for the electron rich phosphine to oxidize over a multi-step synthesis. Changing one of the furyl groups out for a functionalized phenyl ring completely destroys the ligands ability to access the *syn*-(1,2) aryl ether moiety.

With the promising initial results shown in Figure 3.5 (equation 10), we devised a new retrosynthetic breakdown towards the synthesis of rubiyunnanin A (Figure 3.7). Unfortunately, without the success of the regio-resolution (AORR), it would no longer be possible to access rubiyunnanin B through one divergent total synthesis; rubiyunnanin A became the focal point. The new efforts towards the total synthesis of rubiyunnanin A would involve the asymmetric

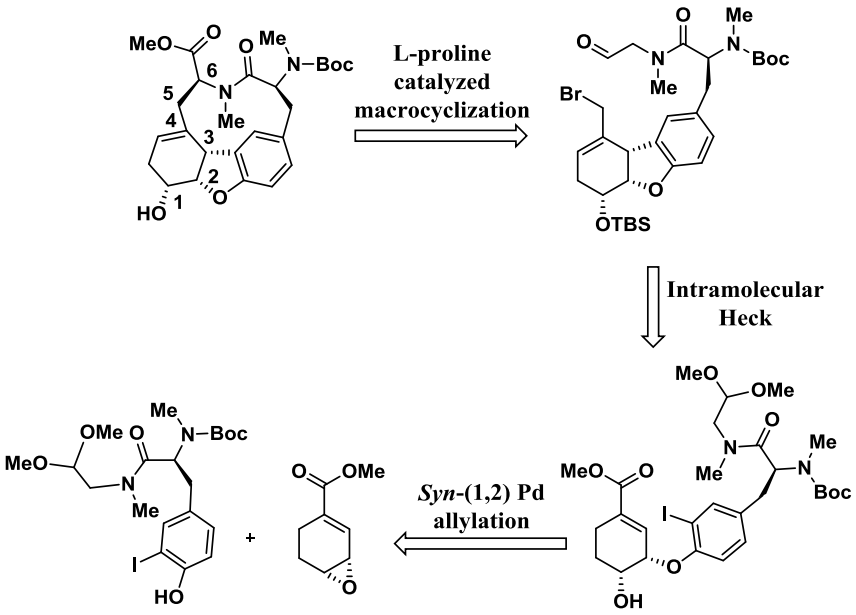

Figure 3.7. Second generation retrosynthesis for rubiyunnanin A.

synthesis of the benzofuran linkage first with the assistance of the C4 blocked-allylic oxide Pd allylation of a tyrosine residue. An intramolecular Heck reaction would complete the synthesis

of the all *syn*-stereoarray (C1, C2 and C3) of the benzofuran linkage. In this version of the synthesis, the macrocyclization would be conducted by the mediation of an L-proline catalyzed alkylation to form the C5-C6 bond, that was originally synthesized by a Negishi cross coupling. In order for this approach to work, an asymmetric synthesis was needed for allylic oxide **3.33** (Scheme 3.4). This was accomplished by converting commercially available crotonaldehyde to

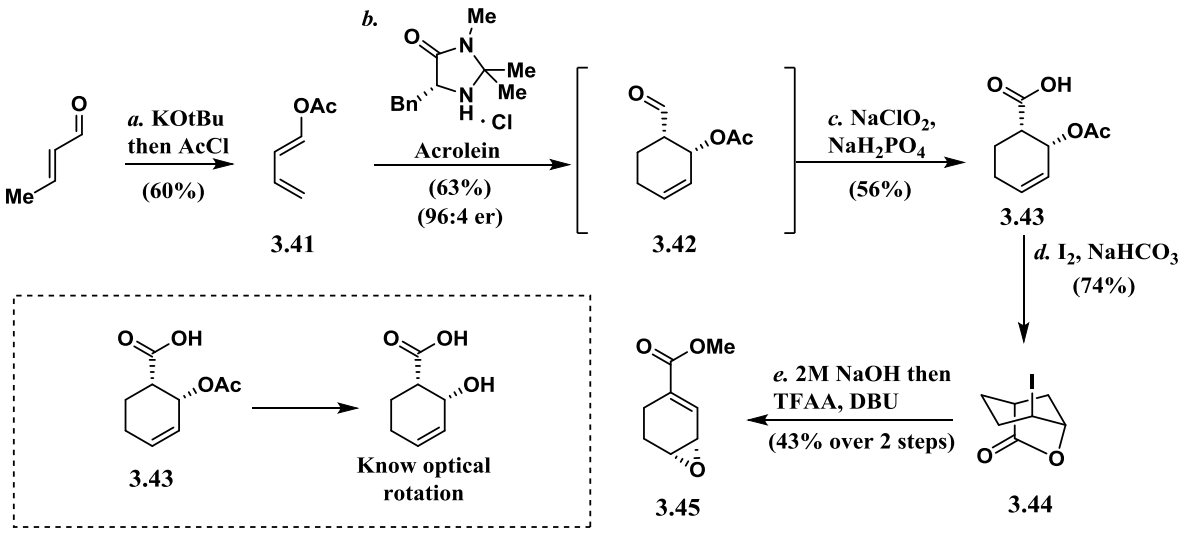

Reagents: (a) KOtBu, AcCl, THF, -78 - 23 °C; (b) 10 mol% (5R)-2,2,3-Trimethyl-5-phenylmethyl-4-imidazolidinone monohydrochloride, acrolein, TFE, 0 °C; (c) $NaClO_2$, NaH_2PO_4, 2-methyl-2-butene, t-BuOH:H_2O; (d) I_2, KI, $NaHCO_3$ (aq), CH_2Cl_2; (e) 2M NaOH, THF, MeOH then TFAA, DBU, CH_2Cl_2.

Scheme 3.4. Synthesis of enantiopure allylic oxide **3.45** through an asymmetric Diels-Alder.

the (E)-diene **3.41** by deprotonation with KOtBu and acylation. The key step in this synthesis was the asymmetric Diels-Alder catalyzed by a phenylalanine derived imidazoline catalyst. This transformation occurred in a relatively high 63% yield with a 96:4 e.r. in the presence of excess acrolein. Key to this reactions success the 2,2,2-trifluorethanol solvent and the reaction performed at a concentrated of 1 M in respect to the (E)-diene **3.41**. The major disadvantage to this asymmetric Diels-Alder was the scalability. The reaction could not be achieved on a larger scale than 1-2 grams in respect to the (E)-diene **3.41**. On large scale, the acrolein needed to be

added dropwise over a 24 hour period by syringe pump to reduce the loss in e.r. and byproducts associated with acrolein reacting with itself. Aldehyde **3.42** could be isolated by column chromatography with losses in yield; for efficiency, the reaction was filtered through a plug of silica gel and carried directly into a Pinnick oxidation. The oxidation gave acid **3.43** in only modest yields of 56%. It is unclear as to why the isolated yield is so poor for this reaction. Treatment with I_2 in a biphasic mixture of CH_2Cl_2 and aqueous $NaHCO_3$ furnished iodolactone **3.44** in 74% yield. Hydrolysis of iodolactone **3.44** gave the crude β-alcohol, which could be directly converted to the desired allylic oxide **3.45** through an elimination-dehydration with TFAA and DBU. Allylic oxide **3.45** was confirmed to be the (*R,R*)-epoxide through literature comparison to the deprotected acid **3.43**.[15] With the asymmetric allylic oxide synthesis in hand, we began the forward synthesis of rubiyunnanin A (Scheme 3.5). L-tyrosine could be converted to Boc-NMe-L-I-Tyrosine-OH **3.46** through a three step sequence that involved a one pot NI_3 mediated iodination[16] followed directly by a Boc-N protection. Treatment with formaldehyde gave an oxazolidinone intermediate that subsequently underwent a reductive opening with Et_3SiH to furnish the Boc-NMe-L-I-Tyrosine-OH **3.46** over steps in a 61% yield. Amide coupling via isobutyl chloroformate mediated mixed anhydride formation followed by quenching with N-methylaminoacetaldehyde dimethyl acetal gave tyrosine **3.47** in a modest 42% yield. Pd_2dba_3 and P(2-furyl)$_3$ catalyzed *syn*-(1,2) addition of tyrosine **3.47** to enantiopure allylic oxide **3.45** provided aryl ether **3.48** in a 34% yield. There was a 60% recovery of the starting material tyrosine residue **3.47** as the major product was a result of the β-hydride elimination pathway. Direct attempts to proceed with an intramolecular Heck reaction were problematic. The Heck reaction required the secondary alcohol at C1 to be protected. Without protection, the Heck reaction produced a high impurity profile indicating full aromatization of the benzofuran.

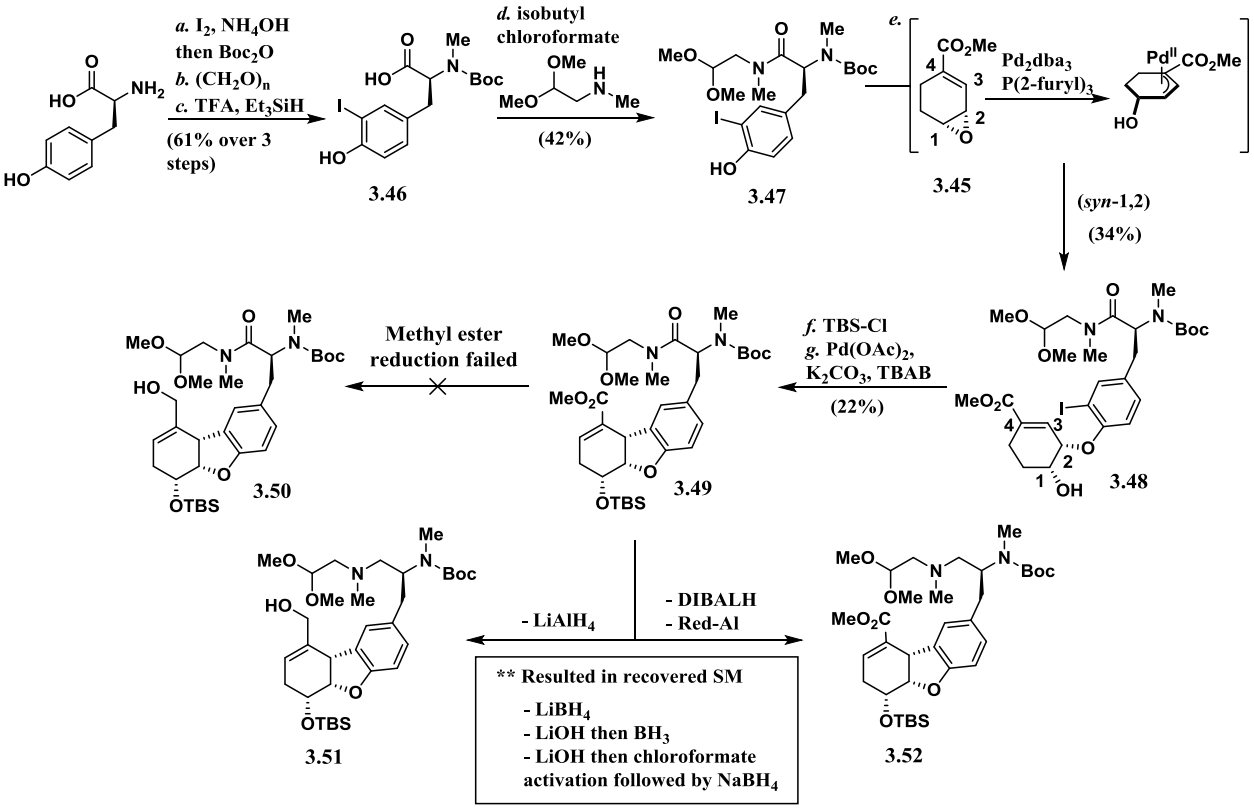

Reagents: (a) I_2, NH_4OH, EtOH:H_2O, 0 °C, then Boc_2O, 1M NaOH, dioxane:H_2O, 0 °C; (b) $(CH_2O)_n$, TsOH, DMF:Toluene, 120 °C; (c) TFA, Et_3SiH then Boc_2O, 2M NaOH, dioxane:H_2O; (d) isobutyl chloroformate, NMM, THF then methylaminoacetaldehyde dimethyl acetal, 0 °C; (e) 5 mol% Pd_2dba_3, 25 mol% P(2-furyl)$_3$, THF; (f) TBS-Cl, Pyridine, DMAP, CH_2Cl_2; (g) 10 mol% $Pd(OAc)_2$, K_2CO_3, TBAB, DMF, 60 °C.

Scheme 3.5. Forward synthesis of rubiyunnanin A using second generation retrosynthesis.

After TBS protection of the alcohol, "Jeffery's ligandless" conditions[17] proved to give the highest conversion for the Heck reaction using $Pd(OAc)_2$, K_2CO_3 and TBAB (found to be crucial for conversion of the reaction). This two-step sequence gave benzofuran **3.49**, albeit in a low yield of 22%. With benzofuran **3.49**, a reduction of the unsaturated methyl ester was needed; however, this reduction became more problematic than anticipated as the desired allylic alcohol **3.50** could not be accessed through this route. DIBAL-H and Red-Al mediated reductions did not reduce the unsaturated methyl ester but in fact selectively reduced the amide to provide alkyl amine **3.52**. DIBAL-H facilitated these amide reductions with increased temperatures. At room temperature, or the more common conditions at -78 °C, full recovery of the starting material was

possible. $LiAlH_4$, maybe not surprisingly, caused a global reduction to the unwanted allylic alcohol **3.51**. $LiBH_4$ resulted in a complete recovery of starting material. The methyl ester of benzofuran **3.49** could be hydrolyzed to the unsaturated carboxylic acid with LiOH. However, typical acid reduction conditions including BH_3 and "activated ester" reductions mediated by quenching mixed anhydrides with $NaBH_4$ all resulted in complete recovery of the carboxylic acid starting material. In some cases, there were small amounts of (α, β)-unsaturation detected. It was unclear as to why this unsaturated methyl ester reduction proved problematic. This synthetic effort had two problems that needed to be overcome; 1) the Pd allylation and Heck reaction sequence needed to be improved for material throughput purposes and 2) there needed to be an alternative plan for the resisted reduction of the unsaturated methyl ester at the C4 position.

4.3 Second generation asymmetric synthesis of the benzofuran in rubiyunnanin A

There were two problems associated with the benzofuran synthesis. The β-hydride elimination for the Pd allylation of the allylic oxide was the major product pathway and the Heck reaction was producing significant amounts of methylparaben, presumably through a reverse Pd allylation reaction that cleaves the C-O bond of the aryl ether. As seen in Scheme 3.6, the desired

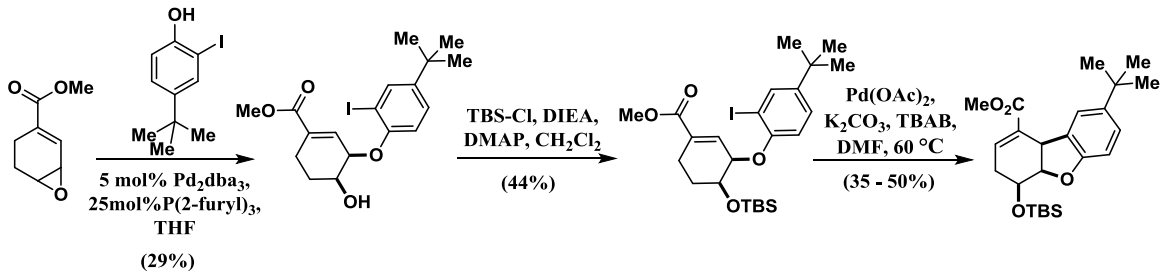

Scheme 3.6. Benzofuran synthesis derived from 2-iodo-4-*tert*-butylphenol.

benzofuran derived from 2-iodo-4-*tert*-butylphenol could be achieved over a three step sequence with an overall 6% yield, representative of the problems just discussed in relation to the forward synthesis shown in Scheme 3.7. Extensive studies were performed on the *syn*-(1,2) Pd allylation reaction (Table 3.2). As evident by entries (1-10), solvent effects are quite pronounced. Except for THF (entry 5), MeCN (entry 8) and 1,4-dioxane (entry 9), all other solvents essentially gave complete conversions to the β-hydride elimination product **3.36**. The β-hydride elimination

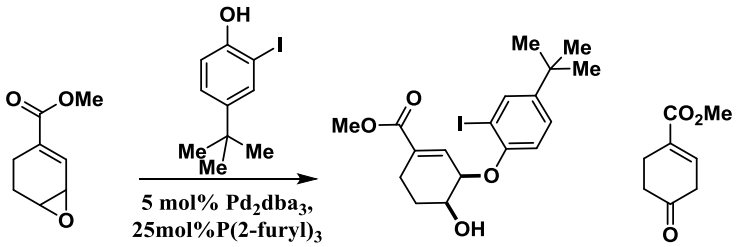

3.33 **3.53** **3.36**

A **B**

Entry	Solvent	Additive	Product Ratio (A:B)[a]
1	CH_2Cl_2	-	0:100
2	1,2-DCE	-	0:100
3	Toluene	-	02:98
4	C_6H_6	-	0:100
5	THF	-	23:77
6	Et_2O	-	0:100
7	DMF	-	0:100
8	MeCN	-	21:79
9	1,4-Dioxane	-	64:36
10	DMSO	-	0:100
11	THF	CSA	0:100
12	THF	Me_3SnOAc	29:71
13	THF	DIEA	0:100
14	THF	$AgCO_3$	31:69
15	THF	K_3PO_4	35:65
16	1,4-Dioxane	CSA	0:100
17	1,4-Dioxane	Me_3SnOAc	65:35
18	1,4-Dioxane	DIEA	0:100
19	1,4-Dioxane	$AgCO_3$	72:28
20	1,4-Dioxane	K_3PO_4	79:21

[a] Product ratios were measured by integration of crude ^1H NMR spectra.

Table 3.2. Solvent and additive effects on *syn*-(1,2) Pd allylation.

in the Tsuji-Trost reaction has previously been reported as a problem.[18] In these contexts, the Pd π -allyl species is stabilized by the presence of acids or Lewis acids, slowing the β-hydride elimination pathway. Continuing the screening with THF and 1,4-dioxane specifically, CSA as an additive promoted the β-hydride elimination pathway producing none of the desired *syn*-(1,2) allylation product **3.53** (entries 11 and 16). Hunig's base had the same effect as that of CSA, completely promoting the β-hydride elimination pathway (entries 13 and 18). Trimethyltin acetate has previously been used by the Trost group to slow the β-hydride elimination pathway.[18] As seen in entries 12 and 17, the effect trimethyltin acetate had on the reaction product distribution was negligible. Interestingly, $AgCO_3$ and K_3PO_4 had a much greater effect on the reaction product distribution (entries 14, 15, 19 and 20). $AgCO_3$ and K_3PO_4 reduced β-hydride elimination as Trost observed with trimethyltin acetate. Although there is no precedence for using these salts as additives in the Tsuji-Trost reaction, we believed the presence of an ion capable of chelating to the C1 alcohol could have a positive effect on slowing down the β-hydride elimination pathway. These salts were also screened because they potentially open up the possibility to facilitate a Heck reaction in a one-pot/tandem sequence. Although the Tsuji-Trost reaction and subsequent Heck reaction have been used as a sequence in total synthesis of molecules like morphine and galantamine,[19] it has never been demonstrated to be a one-pot sequence to our knowledge. Not only did K_3PO_4 help facilitate the formation of the *syn*-(1,2) aryl ether **3.53**, we were pleased to discover that it also facilitated the Heck reaction when the temperature was increased to 90 °C in an overall tandem sequence of 73% yield (scheme 3.7). TBS protection yielded the desired benzofuran derived from 2-Iodo-4-*tert*-butylphenol in a two-step overall sequence with a 44% yield as compared to the three-step overall sequence with a 6% overall yield.

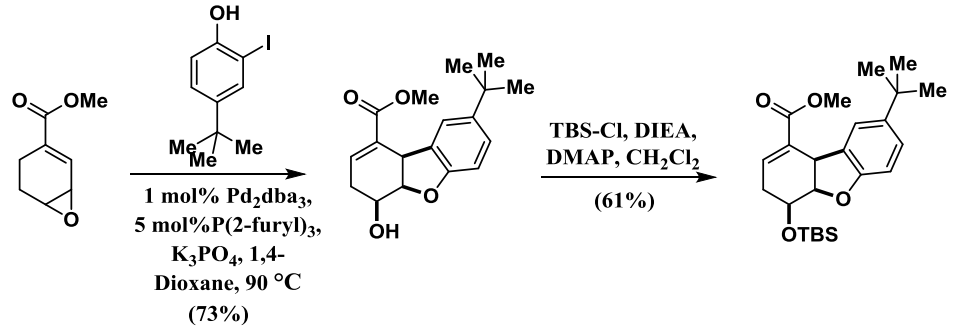

Scheme 3.7. Optimized one-pot Pd allylation/Heck reaction.

With this optimized one-pot Pd allylation/Heck reaction, we sought to expand it toward the forward synthesis of rubiyunnanin A (Scheme 3.8). Tyrosine oxazolidinone **3.54** could be synthesized through the same sequence mentioned previously in this chapter. The one-pot Pd allylation/Heck reaction of tyrosine oxazolidinone **3.54** and allylic oxide **3.45** furnished benzofuran **3.55** consistently with a 50-67% yield. This provided a far more expedient route to

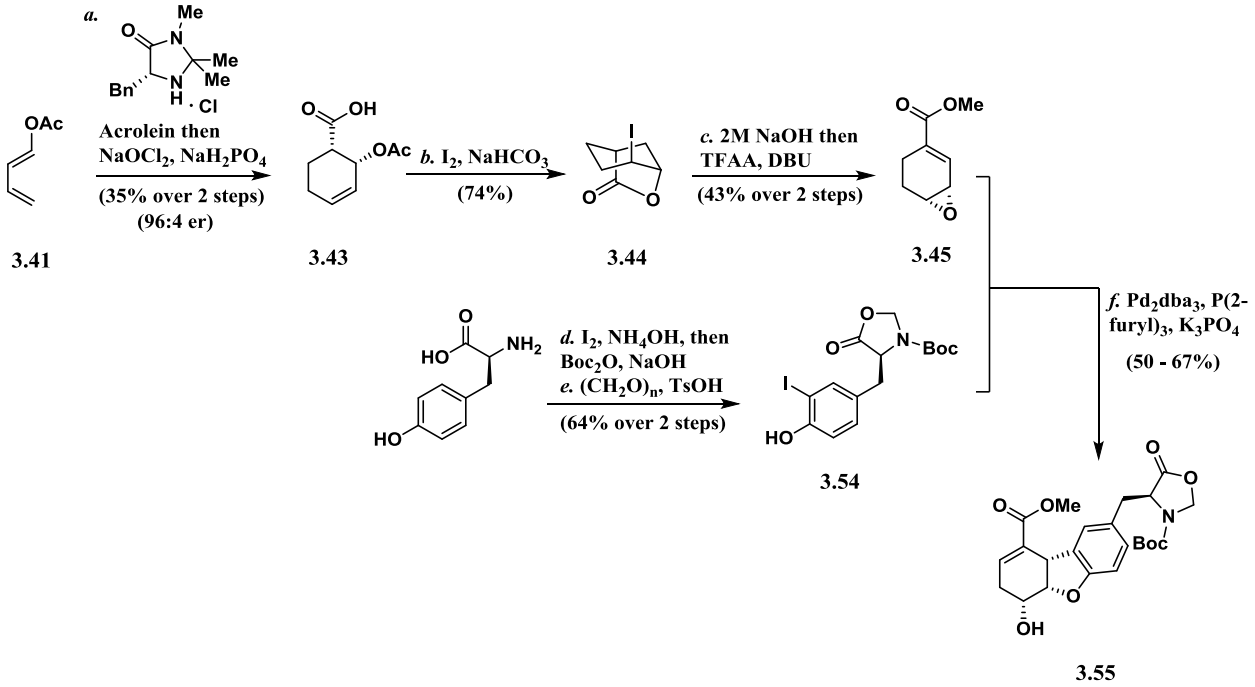

Scheme 3.8. One-pot Pd allylation/Heck reaction using enantiopure epoxide **3.45**.

the enantiopure benzofuran core of rubiyunnanin A then previously reported in Scheme 3.5. Subsequent MOM protection and hydrolysis with LiOH could give access to either bis

carboxylic acid **3.56** or mono-carboxylic acid **3.57** depending equivalency of LiOH used (Scheme 3.9). In results similar to the first generation of the asymmetric benzofuran, mono-acid **3.57** did not undergo reduction of the unsaturated methyl ester. Attempts at using DIBAL-H, Red-Al, $LiBH_4$, $NaBH_4$ or activated forms of $NaBH_4$ all resulted in recovered starting material. Not surprisingly, most attempts a chemoselective reduction by BH_3 or "activated esters" led to the sole isolation of primary alcohol **3.58**. However, in an intriguing transformation it was found that CDI activation followed by $NaBH_4$ reduction completely reversed the chemoselectivity of

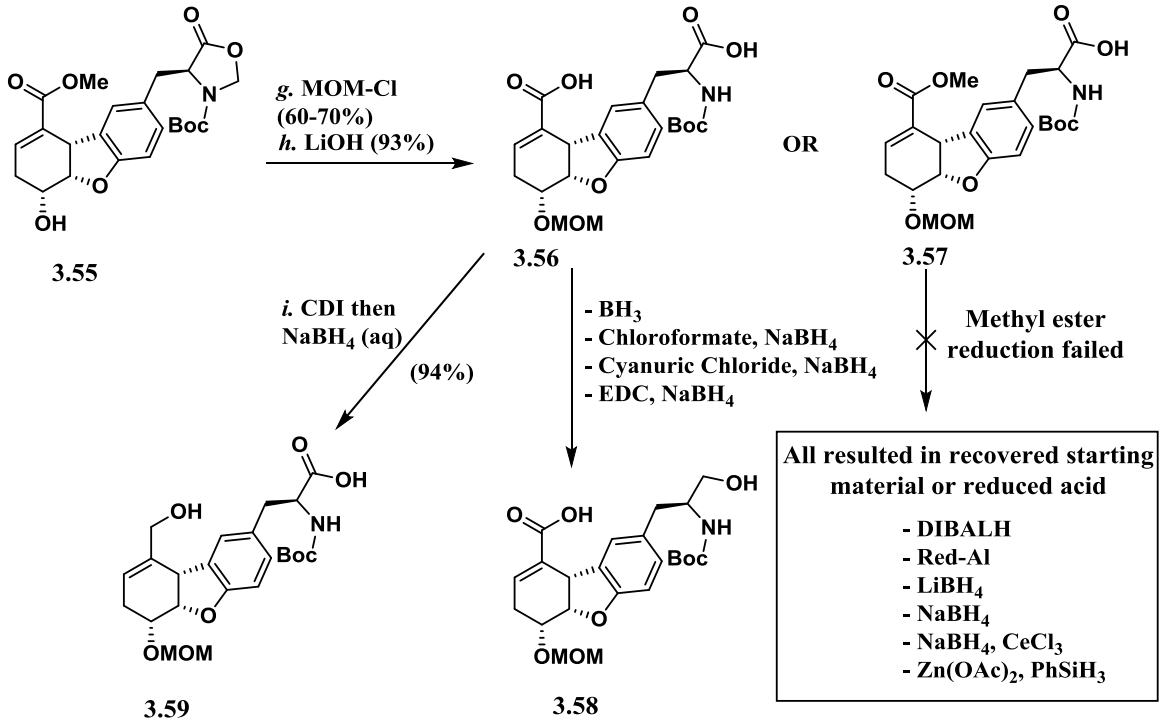

Scheme 3.9. Chemoselective acid reduction by CDI activation.

the reduction giving the desired allylic alcohol **3.59** in 94% yield. There was no detection of alcohol **3.58** in this reaction. Studying the CDI activation reaction led to some interesting discoveries about the mechanism of action (Figure 3.8). Upon reaction of bis carboxylic acid

3.56 with 2.0 equivalents of CDI, a presumed mixed anhydride intermediate **3.56-A** is formed. In a typical CDI activation, the mixed anhydride would undergo nucleophilic attack by the previously released equivalent of imidazole, to evolve CO_2 gas and form an "activated" acyl imidazole species. Indeed when running this CDI activation reaction, the creation of CO_2 gas is observed. However, under extremely inert and dry conditions intermediate **3.56-A** converts to the cyclic anhydride intermediate **3.56-B**. This species is observable by ^{1}H NMR and MS analysis of the crude reaction mixture (SI-154). Upon the addition of H_2O to the reaction mixture, this anhydride quickly degrades under the basic conditions to mono-carboxylic acid **3.56-C**. Addition of solid $NaBH_4$ to the THF (aq) solution results in the formation of the desired allylic alcohol **3.59** by reduction of the "activated" acyl imidazole, leaving the remaining carboxylic acid untouched. This chemoselective reduction result and the previously discussed advances to the one-pot Pd allylation/Heck reaction solved the two problems that previously plagued the second generation retrosynthesis used for the total synthesis of rubiyunnanin A.

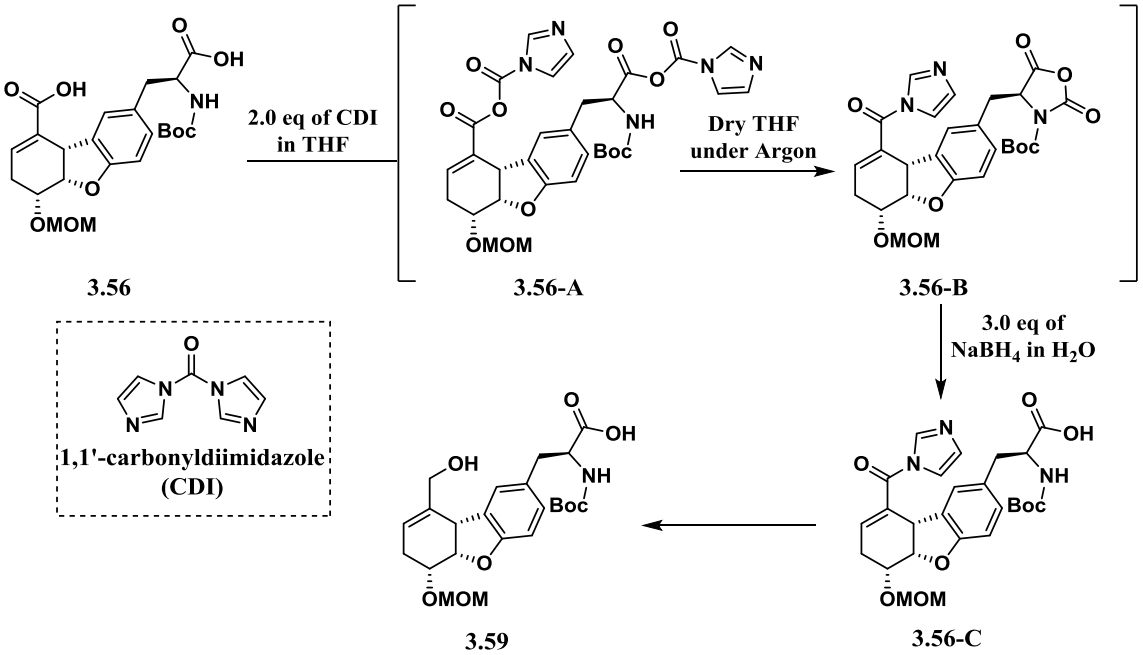

Figure 3.8. Mechanism of the CDI activated chemoselective acid reduction.

In optimizing the utility of the anhydride intermediate **3.56-B**, H_2O was not the only nucleophile that could be used (Scheme 3.10). Both N-methylaminoacetaldehyde dimethyl acetal and N-methyl-dimethylaminomalonate could provide an *in-situ* amide coupling instead of an aqueous decomposition of intermediate **3.56-B**, but also still allow for the reduction of the remaining acyl imidazole. This provided access to a tandem amide coupling/acid reduction that provided amides **3.60** and **3.61** in relatively good yields of 77% and 44%, respectively. This provided us direct access to the previously desired derivative of the allylic alcohol **3.50**.

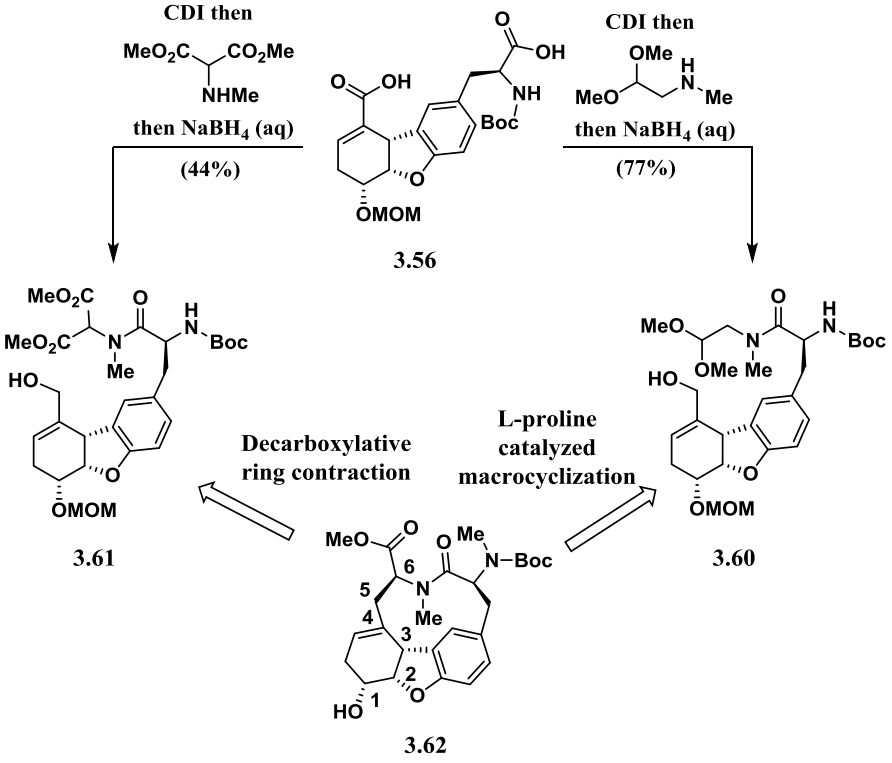

Scheme 3.10. Tandem amide coupling/acid reduction mediated by CDI activation.

From this point we could continue our push on the forward synthesis of rubiyunnanin A by the aforementioned macrocyclic C5-C6 bond formation of the left-hand amino acid to produce the desired core of rubiyunnanin A **3.62**. We could carry out our originally designed L-proline

catalyzed macrocyclization from allylic alcohol **3.60**; however, we also had an idea for a decarboxylative ring contraction to form the same C5-C6 bond. The attempts to form this C5-C6 bond are documented in Figure 3.9. Allylic alcohol **3.60** could be converted to the allyl bromide by treatment with Br_2 and PPh_3, and the dimethyl acetal could be deprotected with 1M HCl, but under acidic conditions the aldehyde produced immediately cycled to give cyclic enamine **3.63** (equation 13). This cyclization could be avoided by N-methylation of the Boc-N group; however, attempts at methylation led to unknown decompositions of the molecule. To avoid this acidic cyclization, ethanolamine could be used as a nucleophile in the CDI activated tandem amide coupling/acid reduction to give bis-alcohol **3.64**. DMP oxidation of the alcohols could provide a possible L-proline catalyzed macrocyclic aldol but the bis-aldehyde produced was not stable and the oxidation provided a highly populated decomposition profile (equation 14). We then turned to a possible decarboxylative ring contraction as the pathway to forge the C5-C6 bond (equation 15). Macrocyclic peptide **3.65** could undergo a Pd catalyzed decarboxylation providing a π -allyl species that would be susceptible to attack by the glycine derived enolate that was produced by the formation of the π -allyl species. This transformation would give direct access to mono-N-Me core of rubiyunnanin A **3.66**. Macrocycle **3.65** could be synthesized by subjection of allylic alcohol **3.61** to TsOH albeit in low yields (equation 16). This cyclization had to be accomplished under acidic conditions. Attempts to hydrolyze the N-Me aminomalonate led to racemization of the tyrosine residue. Unfortunately, with screening of Pd sources, the desired cyclization was not detected. The reactions produced complex impurity profiles. <1 mg test reactions mad it difficult to determine the impurity pathways. LC/MS analysis indicated decarboxylation occurred but with no C5-C6 macrocyclization. Direct alkylation or Pd allylation of the N-Methyl aminomalonate was unsuccessful (equation 17).

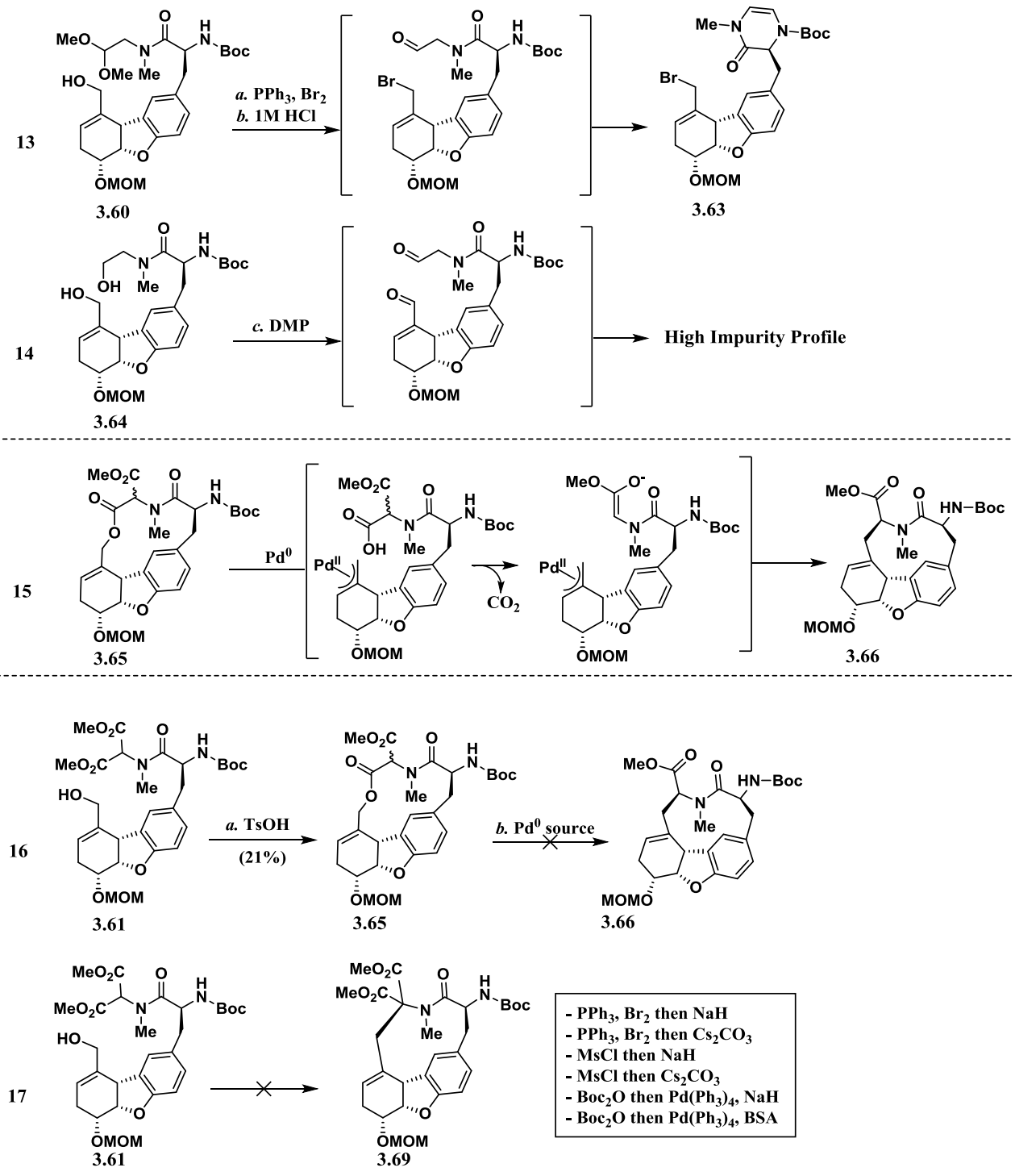

Figure 3.9. Attempts at macrocyclization to forge C5-C6 bond.

3.4 Third generation synthesis of rubiyunnanin A

With no proof that the C5-C6 bond could be formed through a macrocyclization event, we turned our attention to forging the cycle through a macrolactamization; arguably the most obvious of the retrosynthetic approaches. This method was avoided originally due to the historical evidence that iso-dityrosine based natural products do not undergo facile macrolactamization because of ring strain; outlined in the Chapter 1 review. The forward synthesis using this approach is represented in Scheme 3.11. The synthesis through allylic alcohol **3.59** has already been thoroughly discussed in this Chapter (Schemes 3.8-3.9). The strategy in this synthesis was to install the amino acid racemically (formation of the C5-C6 bond) and then use macrolactamization technology to furnish the core structure of rubiyunnanin A **3.72**. Installation of nitroacetate seemed favorable as the nitro could cleanly reduce to give dipeptide intermediate **3.71**. Initial efforts to displace an allylic bromide with ethyl nitroacetate as a nucleophile were unfruitful so we turned to the use of a Pd catalyzed allylation reaction. Allylic alcohol **3.59** could easily be acylated using Ac_2O in the presence of the free carboxylic acid. The results for the screening of this Pd catalyzed allylation can be observed in Table 3.3. Although there is precedence in the literature for the use of ethyl nitroacetate as a nucleophile in Tsuji-Trost chemistry,[20] we encountered some challenges that have not been reported for this type of reaction. $Pd(PPh_3)_4$ provided the desired product **3.70** but only in a 20% yield (entry 1). In this initial test, there was an abnormal amount of triphenylphosphine oxide detected. Upon mixing ethyl nitroacetate and $Pd(PPh_3)_4$ in THF, there was a color change in solution and triphenylphosphine oxide was being produced under diligent air free techniques. However, no literature has reported the oxidation of phosphine via nitroacetate derivatives to our knowledge. To bolster this theory, a stoichiometric excess of triphenylphosphine (entry 4) was

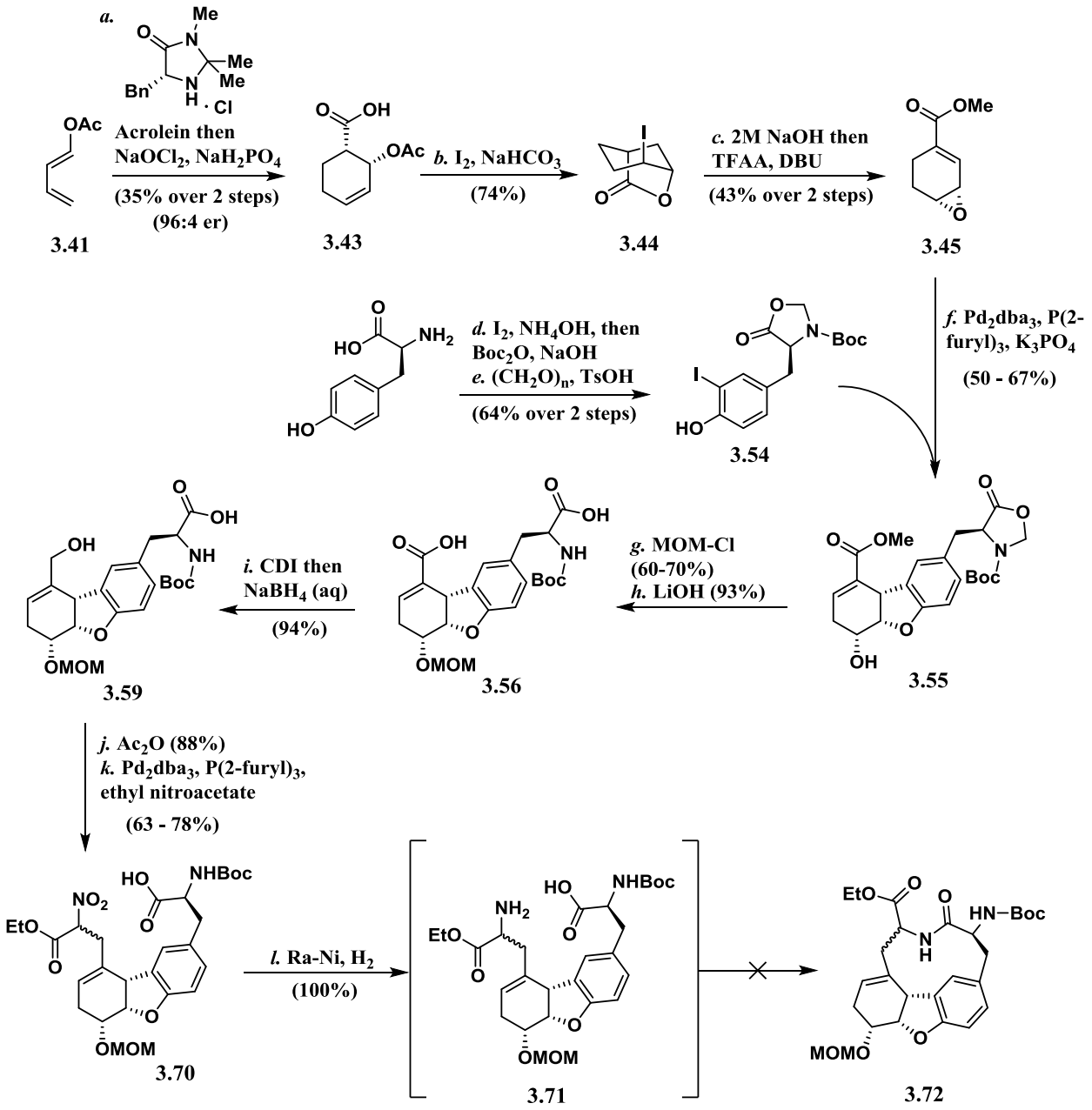

Reagents: (a) 10 mol% (5R)-2,2,3-Trimethyl-5-phenylmethyl-4-imidazolidinone monohydrochloride, acrolein, TFE, 0 °C then $NaClO_2$, NaH_2PO_4, 2-methyl-2-butene, t-BuOH:H_2O; (b) I_2, KI, $NaHCO_3$ (aq), CH_2Cl_2; (c) 2M NaOH, THF, MeOH then TFAA, DBU, CH_2Cl_2; (d) I_2, NH_4OH, EtOH:H_2O, 0 °C, then Boc_2O, 1M NaOH, Dioxane:H_2O, 0 °C; (e) $(CH_2O)_n$, TsOH, DMF:Toluene, 120 °C; (f) 1 mol% Pd_2dba_3, 5 mol% P(2-furyl)$_3$, K_3PO_4, 1,4-dioxane, 90 °C; (g) MOM-Cl, DIEA, DMAP, CH_2Cl_2, 0 - 23 °C; (h) LiOH, THF, H_2O, 0 - 23 °C; (i) CDI, THF, 50 °C then H_2O, 23 °C then $NaBH_4$; (j) Ac_2O, Et_3N, DMAP, CH_2Cl_2, 0 - 23 °C; (k) 5 mol% Pd_2dba_3, 25 mol% P(2-furyl)$_3$, DIEA, ethyl nitroacetate, 50 °C; (l) Raney-Ni, H_2, MeOH.

Scheme 3.11. Forward synthesis utilizing macrolactamization technology.

employed and desired product **3.70** was produced in an increase of nearly 30% compared to that of entry 1. However, there were still extensive amounts of triphenylphosphine oxide detected in

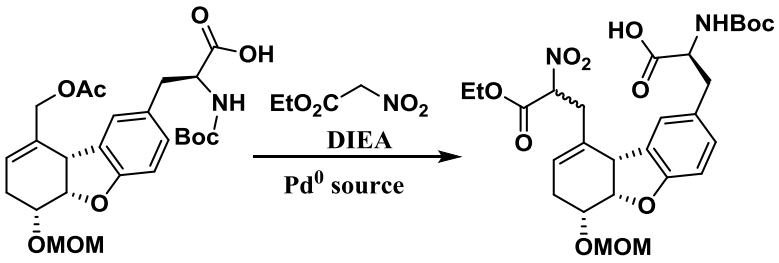

Entry	Catalyst[a]	Additive	Product Yield[b]
1	$Pd(PPh_3)_4$	-	20%
2	Pd_2dba_3, dppf	-	0%
3	Pd_2dba_3, dppe	-	0%
4	$Pd(PPh_3)_4$	PPh_3[c]	49%
5	Pd_2dba_3, P(2-furyl)$_3$	-	40%
6	Pd_2dba_3, P(t-Bu)$_3$	-	71%
7	Pd_2dba_3, P(2-furyl)$_3$	-	78%[d]

[a] 10 mol% Pd catalyst was used. [b] Yields determined by column chromatagraphy isolation. [c] PPh_3 was used in excess from 2.0 - 3.0 equivalents. [d] Used 2.0 equivalents of ethyl nitroacetate.

Table 3.3. Screening of ethyl nitroacetate Pd catalyzed allylation.

the reaction mixture. We proposed that if indeed the phosphine was being oxidized by the ethyl nitroacetate substrate, a counter-intuitive increase in choice, selective for electron rich phosphine ligands would indeed slow that oxidation process down. Dppf and dppe ligands produced none of the desired product **3.70** (entries 2 and 3). However, using more electron rich tri(2-furyl) phosphine gave a 40% yield without any additives (entry 5). Tri(tert-butyl) phosphine gave an increase to a 71% yield (entry 6). The trend observed in entry 5 and 6, seems to indicate that increasing to an electron rich ligand indeed favored the Pd allylation step over oxidation of the phosphine ligand. At the time, due to stock and expenses, we did not have access to quantities of the tri(tert-butyl) Pd complex so simply increasing the amount of ethyl nitroacetate to 2.0

equivalents while using the tri(2-furyl) Pd complex increased the yield of the reaction to 78% (entry 7). Nitroacetate **3.70** could be accessed in high yields in a 1:1 diastereomeric mixture. It is interesting to note that the optimal conditions for reaction success are one where the carboxylic acid is left unprotected. Protection of the carboxylic acid as the methyl ester results in significantly less conversion in the Pd allylation reaction of ethyl nitroacetate. The overall conversion was diminished and a [3+2] cycloaddition side-reaction between ethyl nitroacetate and the olefin was detected. Employing the free carboxylic acid not only increased conversion, but resulted in detection of the desired nitroacetate **3.70** exclusively. Raney-Ni could be used to selectively hydrogenate the nitro group down to the primary amine without affecting the olefin in the benzofuran ring system (Scheme 3.11). The intermediate **3.71** could be isolated just by filtration and concentration out of the methanol reaction solvent. Unfortunately, exhaustive screening of the macrolactamization with available peptide coupling agents did not afford the desired rubiyunnanin A core **3.72**. These results, although unfortunate, are not surprising considering the challenge this type of macrocyclization has presented in other iso-dityrosine natural product syntheses. Dimerization of intermediate **3.71** was observed in reactions diluted between [0.5 – 0.08] M; however, the results of these reactions are mostly recovered starting material. Reactions diluted between [0.08 – 0.005] M result in nothing other than starting material recovery. Other approaches have been taken by "activating" the carboxylic acid **3.70** with N-hydroxy succinimide and pentafluorophenol prior to the Raney-Ni mediated hydrogenation. These reactions independent of concentration always produce a white insoluble precipitate. MALDI analysis of the solids seems to indicate a possible oligomerization of the molecule. The most alarming approach was the activation of the carboxylic acid **3.70** as the acid chloride, which was also unfruitful in the macrolactamization. If the acid chloride activation

does not facilitate closure to form this key amide bond, it is unclear if the strain of this closure is surmountable.

4.5 Future work

More screening needs to be examined for the macrolactamization to fully eliminate this current route to rubiyunnanin A. An extensive investigation of the tri(2-furyl) phosphine (R,R)-DPEN derivative ligand **L2** is required. Perhaps an investigation into new bidentate phosphine ligand technology could still be fruitful considering the first generation efforts towards the synthesis of rubiyunnanin A and B. We could not use ligand control with current technology to facilitate a useable regio-resolution (AORR), but perhaps further functionalized furans could provide the access needed.

In a general sense, it may be necessary to reconsider the retrosynthesis of rubiyunnanin A altogether. Historical insight into iso-dityrosine natural products lends to the fact that most of the macrocyclization events were driven by the aryl ether formation after synthesis of the dipeptide. An investigation into new methods for asymmetric benzofuran synthesis may be warranted. It is also a possibility that this strained cyclization will require the 18-membered cyclic peptide be intact before formation of the iso-dityrosine unit.

REFERENCES

[1] (a) Moschitto, M. J.; Vaccarello, D. N.; Lewis, C. A. *Angew. Chem. Int. Ed.* **2015**, *54*, 2142-2145. (b) Vaccarello, D. N.; Moschitto, M. J.; Lewis, C. A. *J. Org. Chem.* **2015**, *80*, 5252-5259.

[2] Trost, B. M.; Xie, J.; Sieber, J. D. *J. Am. Chem. Soc.* **2011**, *133*, 20611-20622.

[3] Sutter, M.; Lafon, R.; Raoul, Y.; Métay, E.; Lemaire, M. *Eur. J. Org. Chem.* **2013**, *2013*, 5902-5916.

[4] Skolaut, A.; Retey, J. *Arch. Biochem. Biophys.* **2001**, *393*, 187-191.

[5] Spaggiari, A.; Vaccari, D.; Davoli, P.; Torre, G.; Prati, F. *J. Org. Chem.* **2007**, *72*, 2216-2219.

[6] Trost, B. M.; Rudd, M. T. *Org. Lett.* **2003**, *5*, 4599-4602.

[7] Burke, C. P.; Shi, Y. *Angew. Chem. Int. Ed.* **2006**, *45*, 4475-4478.

[8] (a) Chang, S.; Lee, N. H.; Jacobsen, E. N. *J. Org. Chem.* **1993**, *58*, 6939-6941. (b) De, S. R.; Kumar, G.; Jat, J. L.; Birudaraju, S.; Lu, B.; Manne, R.; Puli, N.; Adebesin, A. M.; Falck, J. R. *J. Org. Chem.* **2014**, *79*, 10323-10333.

[9] Suslick, K. S.; Cook, B. R. *J. Chem. Soc., Chem. Commun.* **1987**, 200-202.

[10] Trost, B. M.; Molander, G. A. *J. Am. Chem. Soc.* **1981**, *103*, 5969-5972.

[11] (a) Trost, B. M.; Tenaglia, A. *Tetrahedron Lett.* **1988**, *29*, 2931-2934. (b) Trost, B. M.; Sudhakar, A. R. *J. Am. Chem. Soc.* **1987**, *109*, 3792-3794.

[12] (a) Moriarty, R. M.; Enache, L. A.; Zhao, L.; Gilardi, R.; Mattson, M. V.; Prakash, O. *J. Med. Chem.* **1998**, *41*, 468-477. (b) Delany, J. J.; Berchtold, G. A. *J. Org. Chem.* **1988**, *53*, 3262-3265.

[13] Trost, B. M.; Van Vranken, D. L. *Chem. Rev.* **1996**, *96*, 395-422.

[14] (a) Chang, S.; Heid, R. M.; Jacobsen, E. N. *Tetrahedron Lett.* **1994**, *35*, 669-672. (b) Hentemann, M. F.; Fuchs, P. L. *Tetrahedron Lett.* **1997**, *38*, 5615-5618.

[15] Mayer, S. C.; Pfizenmayer, A. J.; Joullié, M. M. *J. Org. Chem.* **1996**, *61*, 1655-1664.

[16] Cochrane, J. R.; White, J. M.; Wille, U.; Hutton, C. A. *Org. Lett.* **2012**, *14*, 2402-2405.

[17] (a) Carrow, B. P.; Hartwig, J. F. *J. Am. Chem. Soc.* **2010**, *132*, 79-81. (b) Jeffery, T. *J. Chem. Soc., Chem. Commun.* **1984**, 1287-1289. (c) Heck, R. F.; Nolley, J. P. *J. Org. Chem.* **1972**, *37*, 2320-2322.

[18] Trost, B. M.; Chupak, L. S.; Lübbers, T. *J. Am. Chem. Soc.* **1998**, *120*, 1732-1740.

[19] (a) Uchida, K.; Yokoshima, S.; Kan, T.; Fukuyama, T. *Org. Lett.* **2006**, *8*, 5311-5313. (b) Marco-Contelles, J.; do Carmo Carreiras, M.; Rodriguez, C.; Villarroya, M.; Garcia, A. G. *Chem. Rev.* **2006**, *106*, 116-133.

[20] (a) Kammerer, C.; Prestat, G.; Gaillard, T.; Madec, D.; Poli, G. *Org. Lett.* **2008**, *10*, 405-408. (b) Fu, Y.; Etienne, M. A.; Hammer, R. P. *J. Org. Chem.* **2003**, *68*, 9854-9857. (c) Khan, P. M.; Wu, R.; Bisht, K. S. *Tetrahedron* **2007**, *63*, 1116-1126. (d) Genet, J. P.; Ferround, D. *Tetrahedron Lett.* **1984**, *25*, 3579-3582. (e) Brakta, M.; Lhoste, P.; Sinou, D. *J. Org. Chem.* **1989**, *54*, 1890-1896. (f) Trost, B. M.; Thaisrivongs, D. A.; Hansmann, M. M. *Angew. Chem. Int. Ed.* **2012**, *51*, 11522-11526. (g) Krishnamoorthy, P.; Sivappa, R.; Du, H.; Lovely, C. J. *Tetrahedron* **2006**, *62*, 10555-10566. (h) Trost, B. M.; Surivet, J.-P. *Angew. Chem. Int. Ed.* **2000**, *39*, 3122-3124.

Chapter 4: Supplemental Information

4.1 Experimental Procedures

General Procedures. Where appropriate, reactions were carried out under an inert atmosphere of argon or nitrogen with dry solvents, using anhydrous conditions unless otherwise stated. Dry toluene, dichloromethane (CH_2Cl_2), N,N-dimethylformamide (DMF), diethyl ether (Et_2O) and triethylamine (Et_3N), were obtained by passing the previously degassed solvents through activated alumina columns. Tetrahydrofuran (THF) was distilled from the blue solutions of sodium benzophenone ketal before use or could also be obtained by passing through an activated alumina column. Anhydrous 1,4-dioxane was purchased as the highest commercial quality and used without any further degassing/drying purification. Trifluoroacetic acid (TFA) was distilled before use. Tripotassium phosphate (K_3PO_4) was oven-dried (dehydrated) before use. Bis(dibenzylideneacetone)palladium(0) (Pd_2dba_3) and tri(2-furyl)phosphine were specifically purchased commercially from Strem Chemicals. All other reagents were purchased at the highest commercial quality and used without further purification, unless otherwise stated. Yields refer to chromatographically and spectroscopically (^{1}H-NMR) homogeneous material. Flash column chromatography was performed using Silicycle Silica Gel 60 Å (40-53 μm). Analytical thin-layer chromatography (TLC) was performed using Merck Silica Gel 60 Å F-254 precoated plates (0.25 mm thickness). Reverse phase analytical thin-layer chromatography (RTLC) was performed using Merck Silica Gel 60 Å RP-18 WF_{254} precoated plates (0.25 mm thickness). Preparatory HPLC (P-HPLC) was performed on a Waters DeltaPrep chromatograph equipped with a single wavelength detector using either an Xterra Prep RP8 (5μm, 7.6 x 100 mm) or Atlantis Prep T3 (10 μm, 19 x 150 mm) column. Proton NMR spectra were recorded on either a Varian 400, Varian 500 or Varian 600 MHz spectrometer. Proton chemical shifts are reported in

ppm (δ) relative to residual undeuterated solvent. Data is reported as follows: chemical shift (multiplicity [singlet (s), broad singlet (bs), doublet (d), triplet (t), quartet (q) and multiplet (m)], coupling constants [Hz], integration). Carbon NMR spectra were recorded on a Varian 500 (125 MHz) spectrometer with proton decoupling. Carbon chemical shifts are reported in ppm (δ) relative to deuterated chloroform (δ 77.16). NMR data was collected at 25 °C. Infrared spectra were obtained on a ThermoNicolet iS10 FT-IR spectrometer. Melting points were obtained on a Mel-Temp melting point apparatus and are uncorrected. Analytical normal phase HPLC was performed on a Hewlett-Packard 1050 Series chromatograph equipped with a single wavelength detector (230 nm) using a Chiralpak AD-RH column (5 μm, 4.6 x 150 mm, 20 °C). Low-resolution mass spectra (LRMS) were recorded on an Agilent LC/MSD 1100 TOF mass spectrometer by electrospray (ES) or atmospheric-pressure chemical ionization (ACPI) time of flight experiment. High-resolution mass spectra were obtained on an Agilent 6890N Network GC System with a JEOL JMS-GCmate II Mass Spectrometer (magnetic sector) using electron impact experiments or on an Exactive Plus Orbitrap Mass Spectrometer with a DART SVP ion source from Ion Sense. The method of ionization is given in parentheses. Optical rotations were recorded on a Perkin-Elmer 241 polarimeter at the sodium D line (path length 1 dm, corrected to 20.0 °C).

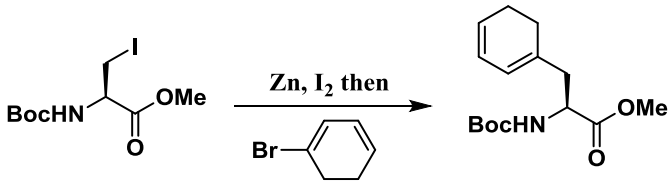

3.12 **3.11** **3.13**

Zinc dust (45 mg, 0.688 mmol, 2.2 eq.) was suspended in dry DMF (1.25 mL) under an Ar atmosphere. I_2 (8 mg, 0.031 mmol, 0.10 eq.) was added in one portion and the resulting mixture was stirred at 23 °C. Upon dissipation of the I_2 color, Boc-N-L-I-Ser-OMe **3.12** (205 mg, 0.623 mmol, 2.0 eq.) dissolved in dry DMF (700 uL) was added and the reaction was heated to 40 °C for 1 hr at which time zincate formation was complete (monitored by TLC). Degassed solution of $Pd_2(dba)_3$ (14 mg, 0.015 mmol, 0.05 eq.), P(o-tol)$_3$ (14 mg, 0.046 mmol, 0.15 eq.) and 1-bromo-1,3-cyclohexandiene **3.11** (50 mg, 0.314 mmol, 1.0 eq.) in dry DMF (700 uL) was added dropwise over 5 min. The reaction was heated at 60 °C for 2 hr until full consumption of the 1-bromo-1,3-cyclohexadiene **3.11** was detected by TLC. The reaction was quenched with 1M HCl (1mL), extracted with EtOAc (x2), dried over Na_2SO_4 and concentrated under reduced pressure. Flash chromatography (1:9 EtOAc:hexanes (v:v)) afforded Boc-L-dihydrophenylalanine-OMe **3.13** (47 mg, 0.167 mmol, 53%) as a yellow oil. [R_f = 0.66 (2:3 EtOAc:hexanes (v:v))]

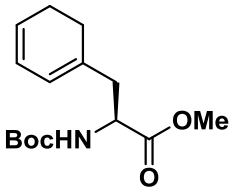

^{1}H NMR ($CDCl_3$, 600 MHz) δ 5.83 (ddq, *J* = 9.4, 5.1, 1.8 Hz, 1H), 5.71 (dt, *J* = 9.4, 4.0 Hz, 1H), 5.67 (d, *J* = 5.1 Hz, 1H), 4.93 (d, *J* = 7.7 Hz, 1H), 4.41 (m, 1H), 3.71 (s, 3H), 2.54 (dd, *J* = 13.8, 5.8 Hz, 1H), 2.39 (dd, *J* = 13.8, 7.9 Hz, 1H), 2.14 - 2.07 (m, 4H), 1.41 (s, 9H); **^{13}C NMR** ($CDCl_3$, 125 MHz) δ 173.1, 155.3, 133.6, 125.3, 124.2, 122.7, 80.0, 52.3, 52.1, 40.7, 28.4, 25.8, 22.8; **LRMS** (ESI^+) *m/z* Calc'd for $C_{10}H_{16}NO_2$ $(M+H)^+$ 182.1181, found 181.90. Due to abandoning the synthetic route, no optical rotation, IR or HRMS data was obtained.

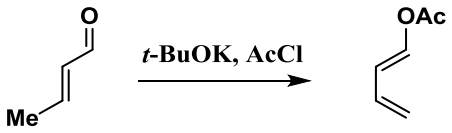

3.41

Solid KOtBu (14.8 g, 0.132 mol, 1.1 eq.) was suspended/dissolved in dry THF (360 mL) under an Ar atmosphere and the solution was cooled to -78 °C. Crotonaldehyde (9.96 mL, 0.12 mol, 1.0 eq.) was added dropwise over a 10 minute period and upon complete addition the reaction was allowed to stir for another 30 minutes at -78 °C. At this time acetyl chloride (9.4 mL, 0.132 mol, 1.1 eq.) was added dropwise over a 10 minute period of time. The reaction was allowed to stir for 60 minutes at -78 °C at which time the reaction was warmed to 23 °C. The reaction was diluted with Et_2O, washed with sat'd $NaHCO_3$ (x2), washed with brine (x4), dried over Na_2SO_4 and concentrated under reduced pressure. Flash chromatography (30% Et_2O:hexanes (v:v)) gave 8.04 g (0.072 mol, 60%) of (E)-OAc diene **3.41** as a yellow oil. [R_f = 0.55 (1:4 Et_2O:hexanes (v:v))] **^{1}H NMR** ($CDCl_3$, 400 MHz) δ 7.39 (dd, *J* = 12.4, 0.7 Hz, 1H), 6.27 (dddd, *J* = 16.9, 11.0, 10.2, 0.5 Hz, 1H), 6.03 (ddt, *J* = 12.3, 11.0, 0.7 Hz, 1H), 5.21 (ddt, *J* = 16.9, 1.6, 0.7 Hz, 1H), 5.09 (ddt, *J* = 10.2, 1.4, 0.6 Hz, 1H), 2.14 (s, 3H). Data matches previously reported data for this molecule.[1]

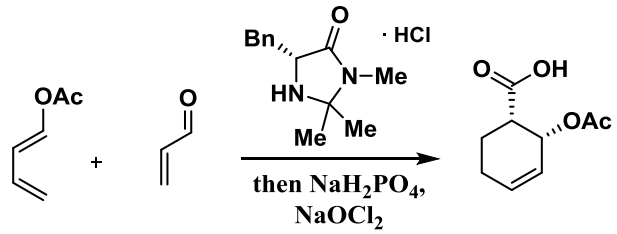

3.41 **3.43**

(5R)-2,2,3-Trimethyl-5-phenylmethyl-4-imidazolidinone monohydrochloride (450 mg, 1.76 mmol, 0.1 eq.) was dissolved in an 18:1 solvent mixture of TFE:H_2O (19 mL, (v:v)) under an Ar

atmosphere. The solution was cooled to 0 °C. Acrolein (3.6 mL, 53.8 mmol, 3.0 eq.) was added, the reaction was stirred for 5 minutes and then (E)-OAc diene **3.41** (2 g, 17.8 mmol, 1.0 eq.) was added. The reaction was stirred at 0 °C for 18-24 hours. The reaction was concentrated under reduced pressure and diluted with Et_2O. The solution was washed with 1M HCl (x2), washed with brine (x1), dried over Na_2SO_4 and reduced under pressure to give a red oil. The crude red oil was run thru a plug of silica gel (20% Et_2O:hexanes (v:v)) to afforded cyclic aldehyde **3.42** (1.25 g, 7.43 mmol, 42%) as a clear oil. [R_f = 0.17 (1:3 Et_2O:hexanes (v:v)] The material could be carried into the next reaction without further purification. An analytical sample of aldehyde **3.42** could be achieved by flash chromatography (30% Et_2O:hexanes (v:v)). **^{1}H NMR** ($CDCl_3$, 400 MHz) δ 9.75 (s, 1H), 6.04 (m, 1H), 5.90 (ddt, *J* = 10.0, 4.4, 1.9 Hz, 1H), 4.67 (t, *J* = 4.4 Hz, 1H), 2.63 (ddd, *J* = 11.2, 4.1, 3.5 Hz, 1H), 2.25 (br dd, *J* = 18.5, 4.8 Hz, 1H) 2.10 – 1.96 (m, 2H), 2.02 (s, 3H), 1.87 (m, 1H). There was no detection of the exo product and the data matches previously reported data for the racemic molecule.[2]

Cyclohexen-al **3.42** (1.25 g, 7.43 mmol, 1.0 eq.) was dissolved in t-BuOH (24.5 mL) and to this mixture was added 2-methyl-2-butene (15.7 mL, 0.148 mol, 20.0 eq.) under an Ar atmosphere. The solution was cooled to 0 °C. A solution of NaH_2PO_4 (4.45 g, 37.1 mmol, 5.0 eq.) and $NaOCl_2$ (2.69 g, 29.7 mmol, 4.0 eq.) in H_2O (10.5 mL) was added dropwise over a 5 minute period of time. Upon complete addition of this solution, the reaction was allowed to warm to 23 °C and it was stirred at this temperature for 3 hr at which time the reaction had been deemed completed by TLC analysis. The reaction was concentrated under reduced pressure, diluted with Et_2O, washed with H_2O (x1), and extracted with 1M $NaHCO_3$ (x3). The aqueous solution was acidified to pH of 2-3 with 12 M HCl, extracted with CH_2Cl_2 (x3), washed with brine (x1) and

dried over Na_2SO_4. Concentration under reduced pressure afforded cyclohexenoic acid **3.43** (761 mg, 4.13 mmol, 56%) as a thick, clear oil. [R_f = 0.32 (2:3 EtOAc:hexanes (v:v))] The material could be carried into the next reaction without further purification. An analytical sample of cyclohexenoic acid **3.43** could be achieved by flash chromatography (1:1:0.06 EtOAc:hexanes:AcOH (v:v:v)).

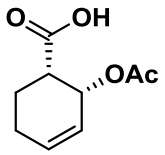

[α] $^{20.0}_{D}$ -216.9 ° (*c* 0.92, $CHCl_3$); **^{1}H NMR** ($CDCl_3$, 600 MHz) δ 11.22 (bs, 1H), 6.02 (ddd, *J* = 9.9, 5.2, 2.6 Hz, 1H), 5.91 (dddd, *J* = 9.9, 5.3, 2.7, 1.4 Hz, 1H), 5.53 (ddt, *J* = 5.2, 3.8, 1.4 Hz, 1H), 2.72 (dt, *J* = 12.9, 3.5 Hz, 1H), 2.26 (dtt, *J* = 18.4, 5.3, 1.8 Hz, 1H), 2.15 – 2.01 (m, 2H), 2.00 (s, 3H), 1.88 (tdd, *J* = 12.9, 11.6, 5.6 Hz, 1H); **^{13}C NMR** ($CDCl_3$, 125 MHz) δ 178.0, 170.5, 133.6, 123.8, 66.3, 43.4, 24.9, 21.1, 18.9; **IR** (film, cm^{-1}) 3037 (br), 2969, 1739, 1718, 1430, 1372, 1234, 1011, 964, 906; **HRMS** ($DART^+$) *m/z* Calc'd for $C_9H_{12}O_4$ $((M-C_2H_5O_2)+H)^+$ 125.0603, found 125.05973.

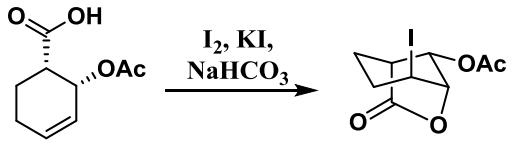

3.43 **3.44**

To a biphasic mixture of aqueous $NaHCO_3$ (38 mL of 0.5 M solution in H_2O, 19 mmol, 6.5 eq.) and CH_2Cl_2 (25 mL) was added solid cyclohexenoic acid **3.43** (545 mg, 2.9 mmol, 1.0 eq.). This solution was stirred extremely vigorously as to fully mix the two layers. Iodine (3.75 g, 14.7 mmol, 5.0 eq.) and KI (1.98 g, 23.5 mmol, 8.0 eq.) were dissolved in H_2O (25 mL) and added dropwise to the biphasic solution over 20 minutes. Upon completion of the addition, the reaction

was vigorously stirred at 23 °C for 20 hours. The reaction was quenched by the addition of an aqueous $Na_2S_2O_3$ solution, extracted with CH_2Cl_2 (x2), washed with saturated $NaHCO_3$ (x2), washed with brine (x1), dried over Na_2SO_4 and concentrated under reduced pressure. The concentration furnished lactone **3.44** (663 mg, 2.14 mmol, 70%) as an off-white solid that was carried into the next reaction without any further purification. [R_f = 0.28 (1:3 EtOAc:hexanes (v:v))]

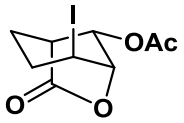

$[\alpha]_D^{20.0}$ -48.3 ° (*c* 1.00, $CHCl_3$); **M.p.** 106-108 °C; **^{1}H NMR** ($CDCl_3$, 500 MHz) δ 5.73 (s, 1H), 4.78 (dd, *J* = 4.6, 1.5 Hz, 1H), 4.53 (ddt, *J* = 5.9, 4.4, 1.3 Hz, 1H), 2.80 (dt, *J* = 4.7, 1.7 Hz, 1H), 2.37 – 2.29 (m, 1H), 2.11 (s, 3H), 2.10 – 1.96 (m, 3H); ^{13}C NMR ($CDCl_3$, 125 MHz) δ 175.3, 170.0, 82.7, 78.0, 44.5, 28.4, 22.6, 21.0, 20.9; **IR** (film, cm^{-1}) 3012, 2964, 2933, 2871, 1775, 1744, 1446, 1362, 1224, 1162, 1131, 1060, 1032, 956, 898; **HRMS** (DART$^+$) *m/z* Calc'd for $C_9H_{11}IO_4$ $(M+H)^+$ 310.9780, found 310.9765.

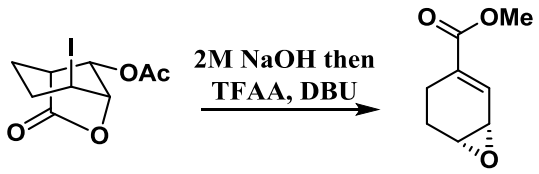

3.44 **3.45**

Iodolactone **3.44** (784 mg, 2.52 mmol, 1.0 eq.) was dissolved in the minimal amount of THF for complete solubility and then diluted with HPLC grade MeOH (25 mL). 2M NaOH (1.39 mL, 2.78 mmol, 1.1 eq.) was added. The reaction was stirred for 2 hr when the reaction was deemed complete by TLC analysis. The reaction was concentrated under reduced pressure and diluted with H_2O. The aqueous mixture was extracted with EtOAc (x3), washed with brine (x1), dried

under Na_2SO_4 and concentrated under reduced pressure to give 195 mg (1.13 mmol, ~45%) of a yellow/brown solid that was taken directly crude into the next reaction.

Yellow/brown solid intermediate [presuming 195 mg (1.13 mmol, 1.0 eq.)] was dissolved in CH_2Cl_2 (11 mL) under an Ar atmosphere and cooled to 0 °C. DBU (423 uL, 2.83 mmol, 2.5 eq.) was added followed by the dropwise addition of TFAA (175 uL, 1.24 mmol, 1.1 eq.). The reaction was stirred at 0 °C for 50 minutes at which point the reaction was allowed to warm to 23 °C. The reaction progress was monitored by TLC analysis. The reaction was concentrated under reduced pressure and diluted with a small amount of Et_2O. This solution was filtered thru a plug of silica gel and the silica gel was washed with Et_2O (x1). Combined Et_2O was filtered thru Celite and concentrated under reduced pressure to afford allylic oxide **3.45** (126 mg, 0.82 mmol, 72%) as a clear, fragrant oil. [R_f = 0.37 (1:3 EtOAc:hexanes (v:v))]

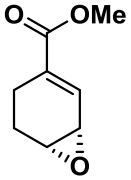

[α] $^{20.0}_{D}$ -183.0 ° (*c* 1.00, $CHCl_3$); **^{1}H NMR** ($CDCl_3$, 500 MHz) δ 7.08 (dd, *J* = 4.3, 3.1 Hz, 1H), 3.74 (s, 3H), 3.59 (m, 1H), 3.38 (t, *J* = 4.3 Hz, 1H), 2.56 (ddt, *J* = 17.1, 6.3, 1.5 Hz, 1H), 2.33 (dddd, *J* = 14.6, 7.7, 2.6, 1.4 Hz, 1H), 2.06 (dddd, *J* = 17.1, 12.6, 7.7, 3.1 Hz, 1H), 1.60 (dddd, *J* = 14.6, 12.6, 6.3, 1.0 Hz, 1H); ^{13}C NMR ($CDCl_3$, 125 MHz) δ 166.7, 134.3, 133.7, 55.7, 52.1, 46.5, 21.1, 19.5; **IR** (film, cm^{-1}) 2969, 2952, 2850, 1716, 1437, 1300, 1266, 1091, 1058, 1028, 913, 743; **HRMS** ($DART^+$) *m/z* Calc'd for $C_8H_{10}O_3$ $(M+H)^+$ 155.0708, found 155.0703; **HPLC** 94:6 e.r., Chiral HPLC eluting at 1.0 mL/min with 99% hexanes/isopropanol. Retention times: RT= 10.4 min, 11.9 min.

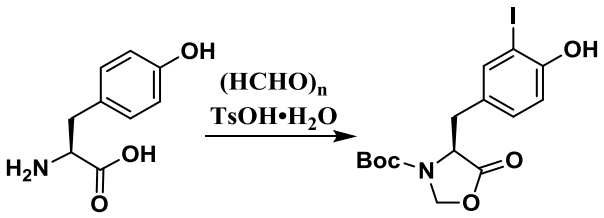

3.54

** ***Extreme caution should be taken when following the below procedure. The reaction in-situ produces N_3I which is an extremely sensitive touch explosive <u>when dry</u>. The tip of the addition flask or the surface of other glassware may collect this solid during the I_2 addition as it reacts with gaseous NH_3. Sat'd $Na_2S_2O_3$ (aq) should be used to quench any solids forming.***

L-tyrosine (12 g, 66.2 mmol, 1.0 eq.) was dissolved in NH_4OH (aq) (700 mL) and cooled to 0 °C. Solid I_2 (16.8 g, 66.2 mmol, 1.0 eq.) was dissolved in EtOH (150 mL) and was added dropwise via an addition funnel over 1 hr. After the addition, the reaction was allowed to stir at 23 °C for an additional 2 hr at which time the reaction was fully concentrated, under reduced pressure, down to a wet, beige colored slurry. This slurry was dissolved/suspended in H_2O (200 mL) and 4M NaOH (200 mL, 0.80 mol, ~12.0 eq.) was added. To this solution was added a solution of Boc_2O (44.8 g, 0.20 mol, 3.1 eq.) in 1,4-dioxane (200 mL). The reaction was stirred for 10 hr until deemed complete by LC/MS analysis. The reaction solution was washed with Et_2O (x3) and acidified to pH of 3 with 12 M HCl. The aqueous solution was extracted with EtOAc (x3), washed with sat'd $Na_2S_2O_3$ (x2), washes with brine (x2), dried over Na_2SO_4 and concentrated under reduced pressure to afford Boc-N-L-I-tyrosine-OH (23.6 g, 57.7 mmol, 87%) as a white amorphous solid. This procedure is a derivation of a known prep and within, Boc-N-L-I-tyrosine-OH is fully characterized.[3] The material was taken forward without any further characterization.

Boc-N-L-I-tyrosine-OH (20.46 g, 50.0 mmol, 1.0 eq.) was dissolved in the minimal amount of DMF for complete solubility and then was diluted with toluene (950 mL). Solid paraformaldehyde (7.49 g) was added followed by $TsOH \cdot H_2O$ (942 mg, 4.95 mmol, 0.1 eq.) and the reaction was heated to reflux at 120 °C for 3 hr. The reaction solution was diluted with EtOAc and sat'd $NaHCO_3$ (aq). The aqueous layer was extracted with EtOAc (x2), combined EtOAc was washed with brine (x3), dried over Na_2SO_4 and concentrated under reduced pressure. Flash chromatography (3:2 EtOAc:hexanes (v:v)) afforded oxazolidinone **3.54** (18.8 g, 44.8 mmol, 90%) as a white amorphous solid. [R_f = 0.56 (1:1 EtOAc:hexanes (v:v))]

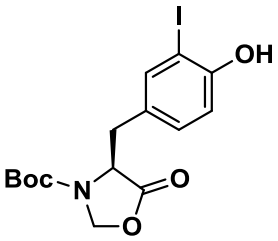

^{1}H NMR ($CDCl_3$, 500 MHz) δ 7.45 (d, *J* = 2.1 Hz, 1H), 7.03 (dd, *J* = 8.3, 2.1 Hz, 1H), 6.89 (d, *J* = 8.2 Hz, 1H), 5.52 (s, 1H), 5.40 - 5.10 (m, 2H), 4.40 (m, 2H), 3.45 - 3.02 (m, 2H), 1.52 (s, 9H); **^{13}C NMR** ($CDCl_3$, 125 MHz) δ 172.3, 154.6, 139.5, 131.4, 130.9, 128.9, 115.3, 85.6, 82.4, 78.2, 56.4, 34.4, 28.4; **IR** (film, cm^{-1}) 3368, 2978, 2931, 1799, 1704, 1415, 1369, 1262, 1136, 1505, 970; **HRMS** ($DART^+$) *m/z* Calc'd for $C_{15}H_{18}INO_5$ $((M-C_5H_8O_2)+H)^+$ 319.9784, found 319.9744.

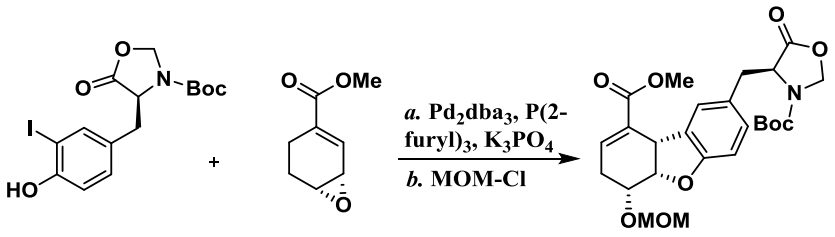

3.54 **3.45** **3.55**

Pd_2dba_3 (6.2 mg, 6.77 umol, .01 eq.) and P(2-furyl)$_3$ (7.9 mg, 34.0 umol, 0.05 eq.) were stirred in degassed 1,4-dioxane (350 uL) for 10 minutes until a yellow color had persisted. The solution

was then added to an already prepared solution of oxazolidinone **3.54** (285 mg, 0.68 mmol, 1.0 eq.) and allylic oxide **3.45** (126 mg, 0.82 mmol, 1.2 eq.) in degassed 1,4-dioxane (3.15 mL) under an Ar atmosphere. The reaction was stirred for 10 minutes at which time K_3PO_4 (433 mg, 2.03 mmol, 3.0 eq.) was added and the reaction was heated to 90 °C until deemed complete by either TLC or LC/MS analysis (typically reaction times varied between 10-12 hr). Renewal of catalyst (1 mol% pd_2dba_3/5 mol% P(2-furyl)$_3$) was done as needed if reaction progression had stalled by TLC or LC/MS analysis. Upon completion, the reaction was filtered and concentrated under reduced pressure. Flash chromatography (45:55 EtOAc:hexanes to 3:2 EtOAc:hexanes (v:v)) afforded benzofuran **3.55** (190 mg, 0.426 mmol, 63%) as an off-white foam that was slightly contaminated with P(2-furyl)$_3$ and P(2-furyl)$_3$ oxide. [R_f = 0.27 (1:1 EtOAc:hexanes (v:v))] **^{1}H NMR** ($CDCl_3$, 600 MHz) δ 7.17 (d, *J* = 2.0 Hz, 1H), 6.93 - 6.90 (m, 2H), 6.72 (d, *J* = 8.1 Hz, 1H), 5.36 - 5.10 (br m, 1H), 5.05 (dd, *J* = 7.9, 2.9 Hz, 1H), 4.49 - 4.29 (m, 3H), 4.03 (m, 1H), 3.81 (s, 3H), 3.20 - 3.00 (br m, 2H), 2.49 (m, 2H), 1.51 (s, 9H).

Crude benzofuran **3.55** (190 mg, 0.426 mmol, 1.0 eq.) was dissolved in CH_2Cl_2 (3 mL) under an Ar atmosphere and cooled to 0 °C. DMAP (5.13 mg, 0.042 mmol, 0.01 eq.), DIEA (520 uL, 2.98 mmol, 7.0 eq.) and MOM-Cl (160 uL, 2.10 mmol, 5.0 eq.) was added in that order. The reaction was allowed to warm to 23 °C. The reaction was stirred for 2 hr and then DIEA (297 uL, 1.70 mmol, 4.0 eq.) and MOM-Cl (96 uL, 1.26 mmol, 3.0 eq.) were added. The reaction continued to stir for 10 hr when the reaction was deemed complete by TLC. The reaction was quenched with H_2O, washed with 1M HCl (x2), washed with brine (x1), dried over Na_2SO_4 and concentrated under reduced pressure. Flash chromatography (2:3 EtOAc:hexanes (v:v)) afforded

MOM protected benzofuran **3.55** (127 mg, 0.259 mmol, 61%) as an off-white amorphous foam. [R_f = 0.48 (1:1 EtOAc:hexanes (v:v))]

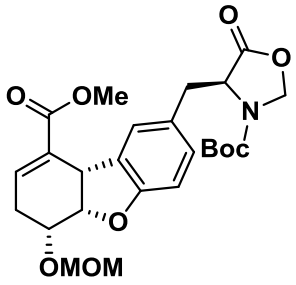

$[\alpha]_D^{20.0}$ +120.0 ° (*c* 1.00, $CHCl_3$); **^{1}H NMR** ($CDCl_3$, 600 MHz) δ 7.18 (d, *J* = 2.1 Hz, 1H), 6.92 - 6.89 (m, 2H), 6.77 (d, *J* = 8.6 Hz, 1H), 5.37 - 5.13 (br m, 1H) 5.09 (ddd, *J* = 7.6, 2.8, 1.6 Hz, 1H), 4.80 (s, 2H), 4.43 - 4.35 (m, 3H), 4.01 (ddd, *J* = 10.9, 5.2, 2.8 Hz, 1H), 3.80 (s, 3H), 3.44 (s, 3H), 3.20 - 3.0 (br m, 2H), 2.63 (ddt, *J* = 17.4, 10.9, 2.5 Hz, 1H), 2.50 (dddt, *J* = 17.4, 7.5, 5.1, 1.3 Hz, 1H), 1.51 (s, 9H); **^{13}C NMR** ($CDCl_3$, 500 MHz) δ 175.3, 158.7, 155.7, 135.9, 130.1, 129.6, 128.4, 128.1, 126.5, 122.0, 121.7, 110.6, 110.3, 95.4, 83.2, 81.8, 80.5, 72.8, 73.0, 63.9, 56.6, 55.6, 54.7, 43.6, 42.7, 38.3, 37.6, 37.1, 29.8, 28.4, 25.4; **IR** (film, cm^{-1}) 2974, 2950, 2929, 1799, 1709, 1487, 1394, 1254, 1053, 1024; **HRMS** (ESI^+) *m/z* Calc'd for $C_{19}H_{20}NO_6$ $(M+H)^+$ 358.1291, found 358.1281.

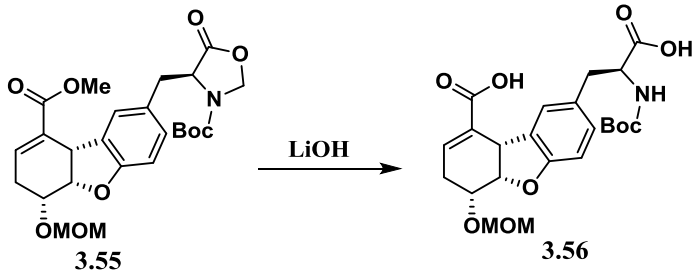

MOM-protected benzofuran **3.55** (62.5 mg, 0.128 mmol, 1.0 eq.) was dissolved in THF (1 mL) and cooled to 0 °C. $LiOH \cdot H_2O$ (0.643 mmol, 5.0 eq.) dissolved in H_2O (300 uL) was added in one portion to the reaction solution and stirred at 0 °C for 1hr. The reaction was warmed to 23 °C and stirred until deemed complete by LC/MS analysis. The reaction solution was diluted

with H_2O, washed with EtOAc (x2), acidified to pH of 3 with 12 M HCl, and extracted with EtOAc (x3). The combined EtOAc was dried over Na_2SO_4 and concentrated under reduced pressure to afford bis-carboxylic acid **3.56** (55 mg, 0.119 mmol, 93%) as a white amorphous gel. This material was used without further purification. [LC/MS eluting at 0.7 mL/min with gradient 10% MeCN:H_2O to 99% MeCN:H_2O over 6 min. Retention times: RT = 2.45 min.]

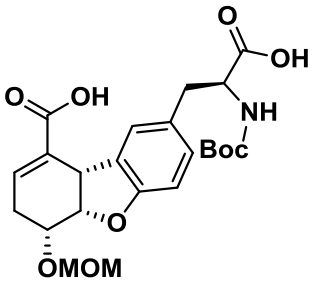

$[\alpha]_D^{20.0}$ +33.7 ° (*c* 1.00, $CHCl_3$); **^{1}H NMR** ($CDCl_3$, 600 MHz) δ 10.04 (br, 2H), 7.33 (m, 1H), 7.06 - 6.92 (m, 2H), 6.80 (dd, *J* = 10.9, 8.4 Hz, 1H), 5.11 (d, *J* = 7.3 Hz, 1H), 5.07 (br m, 1H), 4.83 (s, 2H), 4.56 (q, *J* = 7.1 Hz, 0.6 H), 4.41 (br d, *J* = 7.3 Hz, 1H), 4.29 (br m, 0.4 H), 4.03 (ddd, *J* = 10.9, 6.1, 2.6 Hz, 1H), 3.45 (s, 3H), 3.08 (m, 1H), 3.02 - 2.93 (m, 1H), 2.65 (br m, 1H), 2.53 (br dt, *J* = 17.4, 5.9 Hz, 1H), 1.35 (m, 9H); **^{13}C NMR** ($CDCl_3$, 100 MHz) δ 176.9, 176.4, 170.0, 169.7, 158.4, 158.3, 157.0, 155.6, 139.1, 138.6, 130.3, 130.1, 129.8, 129.4, 129.3, 129.0, 128.3, 127.5, 126.9, 110.1, 110.0, 95.5, 81.6, 82.1, 80.4, 72.6, 56.7, 55.6, 54.6, 42.5, 38.4, 37.3, 28.2, 28.0, 26.0; **IR** (film, cm^{-1}) 2977 (br), 2934 (br), 2606, 1700 (br), 1654, 1489, 1395, 1243, 1163, 1054, 1017, 911, 732; **HRMS** (ESI^+) *m/z* Calc'd for $C_{18}H_{22}NO_7$ $(M+H)^+$ 364.1396, found 364.1386.

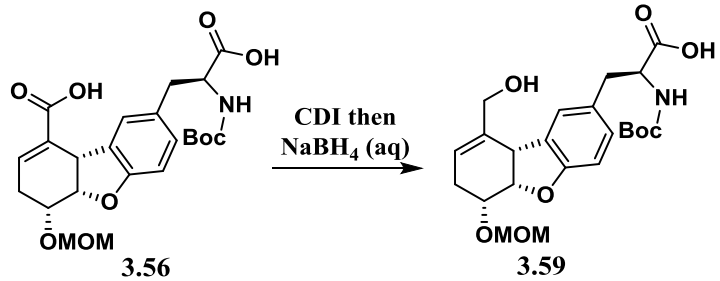

3.56 **3.59**

Bis-carboxylic acid **3.56** (52.3 mg, 0.113 mmol, 1.0 eq.) was dissolved in dry THF (600 uL) under an Ar atmosphere. 1,1'-carbonyldiimidazole (CDI) (55mg, 0.339 mmol, 3.0 eq.) was added in one portion and was gently heated to 50 °C for 1 hr. The reaction was cooled to 23 °C whereupon H_2O (60 uL, 10% original reaction volume) was added and the reaction was stirred for an additional 3 hr. At this time, solid $NaBH_4$ (12.8 mg, 0.338 mmol, 3.0 eq.) was added to the aqueous THF solution. The reaction was stirred at 23 °C until deemed complete by LC/MS analysis, at which time the reaction was quenched with 1M NaOH (60 uL). The reaction solution was acidified to pH 3 with 3M HCl, extracted with EtOAc (x3), washed with brine (x1) and dried over Na_2SO_4. The resulting solution was concentrated under reduced pressure to afford allylic alcohol **3.59** (47.7 mg, 0.106, 94%) as an off-white foam, which was used without further purification. Analytically pure sample could be obtained by flash chromatography (1:9 MeOH:CH_2Cl_2 (v:v)). [R_f = 0.16 (1:9 MeOH:CH_2Cl_2 (v:v))]

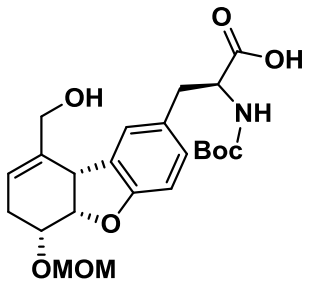

$[\alpha]_D^{20.0}$ +74.0 ° (*c* 1.00, $CHCl_3$); **^{1}H NMR** ($CDCl_3$, 600 MHz); δ 7.17 (br s, 1H), 7.03 - 6.91 (m, 1H), 6.80 (br d, *J* = 7.8 Hz, 1H), 5.63 (m, 1H), 5.18 - 5.08 (br m, 1H), 5.03 (br d, *J* = 6.1 Hz, 1H), 4.81 (m, 2H), 4.57 (m, 0.7 H), 4.35 (m, 0.3 H), 4.24 - 3.97 (br m, 4H), 3.44 (s, 3H), 3.07 (m, 1H), 3.00 (m, 1H), 2.43 (m, 1H), 2.34 (dt, *J* = 14.7, 5.3 Hz, 1H), 1.37 (s, 9H); **^{13}C NMR** ($CDCl_3$, 100 MHz) δ 175.4, 158.7, 155.7, 135.8, 130.14, 129.6, 128.1, 125.9, 122.0, 110.3, 95.4, 83.21, 80.5, 73.0, 72.8, 63.9, 56.6, 55.6, 54.6, 43.6, 37.6, 28.4, 25.4; **IR** (film, cm^{-1}) 3433, 3349, 2977 (br), 2930 (br), 2604, 1698, 1488, 1392, 1367, 1241, 1213, 1164, 1108, 1055, 1019, 911; **HRMS** (ESI$^-$) *m/z* Calc'd for $C_{23}H_{30}NO_8$ $(M-H)^-$ 448.1971, found 448.1976.

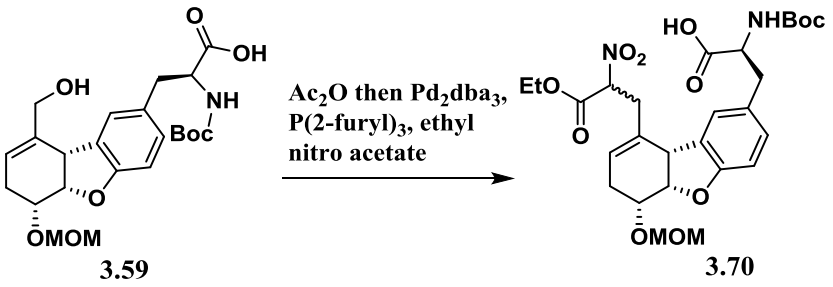

3.59 **3.70**

Allylic alcohol **3.59** (60.7 mg, 0.135 mmol, 1.0 eq.) was dissolved in dry CH_2Cl_2 (1.7 mL) under an Ar atmosphere. Et_3N (57 uL, 0.408 mmol, 3.0 eq.) was added followed by the addition of Ac_2O (38 uL, 0.402 mmol, 3.0 eq.). The reaction was stirred for 1 hr at which point Et_3N (57 uL, 0.408 mmol, 3.0 eq.) and Ac_2O (38 uL, 0.402 mmol, 3.0 eq.) were added. The reaction was stirred for an additional 2 hr and quenched with 1M HCl. The mixture was extracted with EtOAc (x3), washed with brine (x1) and dried over Na_2SO_4. The solution was concentrated under reduced pressure to afford crude OAc-allylic alcohol **3.59** (58 mg, 0.119 mmol, ~88%) as a yellow amorphous gel that was carried to the next reaction without any further purification.

Crude OAc-allylic alcohol **3.59** (58 mg, 0.119, 1.0 eq.), ethyl nitroacetate (42 uL, 0.353 mmol, 3.0 eq.), and DIEA (86 uL, 0.493 mmol, 4.1 eq.) were dissolved in degassed CH_2Cl_2 (1.2 mL) under an Ar atmosphere. Pd_2dba_3 (10.8 mg, 0.012 mmol, 0.10 eq.) and $P(2\text{-furyl})_3$ (13.7 mg, 0.059 mmol, 0.50 eq.) were stirred in degassed CH_2Cl_2 (200 uL) under an Ar atmosphere for 10 min at which time this solution was added to previously prepared solution containing OAc-allylic alcohol **3.59**. The reaction was heated at 50 °C for 9 hr when deemed complete by LC/MS analysis. Flash chromatography (2:3:0.03 EtOAc:hexanes:AcOH (v:v:v) to 3:2:0.03 EtOAc:hexanes:AcOH (v:v:v)) afforded nitroacetate **3.70** (52 mg, 0.093 mmol, 78%) as a yellow foam. The material was isolated as mixture of two diastereomers and at least two rotameric

species. Crude analysis of the ^{1}H NMR is shown below. [R_f = 0.20 (1:1:0.01 EtOAc:hexanes (v:v:v))]

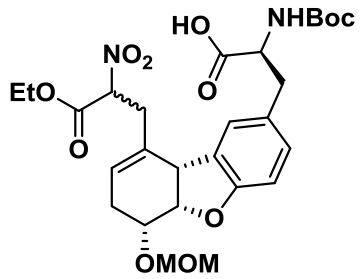

^{1}H NMR ($CDCl_3$, 600 MHz); δ 7.20 -6.77 (m, 3H), 5.54 – 5.25 (m, 2H), 5.00 (m, 1H), 4.80 (s, 2H), 4.66 – 4.45 (br m, 0.7H), 4.34 (m, 2H), 3.99 (m, 0.4H), 3.77 (m, 1H), 3.08 (m, 1H), 2.88 (m, 1H), 2.35 (m, 1H), 2.28 (m, 1H), 1.47 – 1.27 (m, 12H); **LRMS** (ESI) *m/z* Calc'd for $C_{10}H_{16}NO_2$ $(M-H)^-$ 563.2241, found 563.20. No optical rotation, 13C, IR or HRMS was collected because the molecule was isolated as a mixture of diastereomers and rotamers. COSY is available in the SI for this molecule.

REFERENCES

[1] Neier, R.; Soldermann, N.; Velker, J.; Neels, A.; Stoeckli-Evans, H. *Synthesis.* **2007**, *2007*, 2379-2387.

[2] Imagawa, H.; Saijo, H.; Yamaguchi, H.; Maekawa, K.; Kurisaki, T.; Yamamoto, H.; Nishizawa, M.; Oda, M.; Kabura, M.; Nagahama, M.; Sakurai, J.; Kubo, M.; Nakai, M.; Makino, K.; Ogata, M.; Takahashi, H.; Fukuyama, Y. *Bioorg. Med. Chem. Lett.* **2012**, *22*, 2089-2093.

[3] Cochrane, J. R.; White, J. M.; Wille, U.; Hutton, C. A. *Org. Lett.* **2012**, *14*, 2402-2405.

4.2 Spectra and supplemental information

^{1}H NMR ($CDCl_3$, 600 MHz) – 3.13

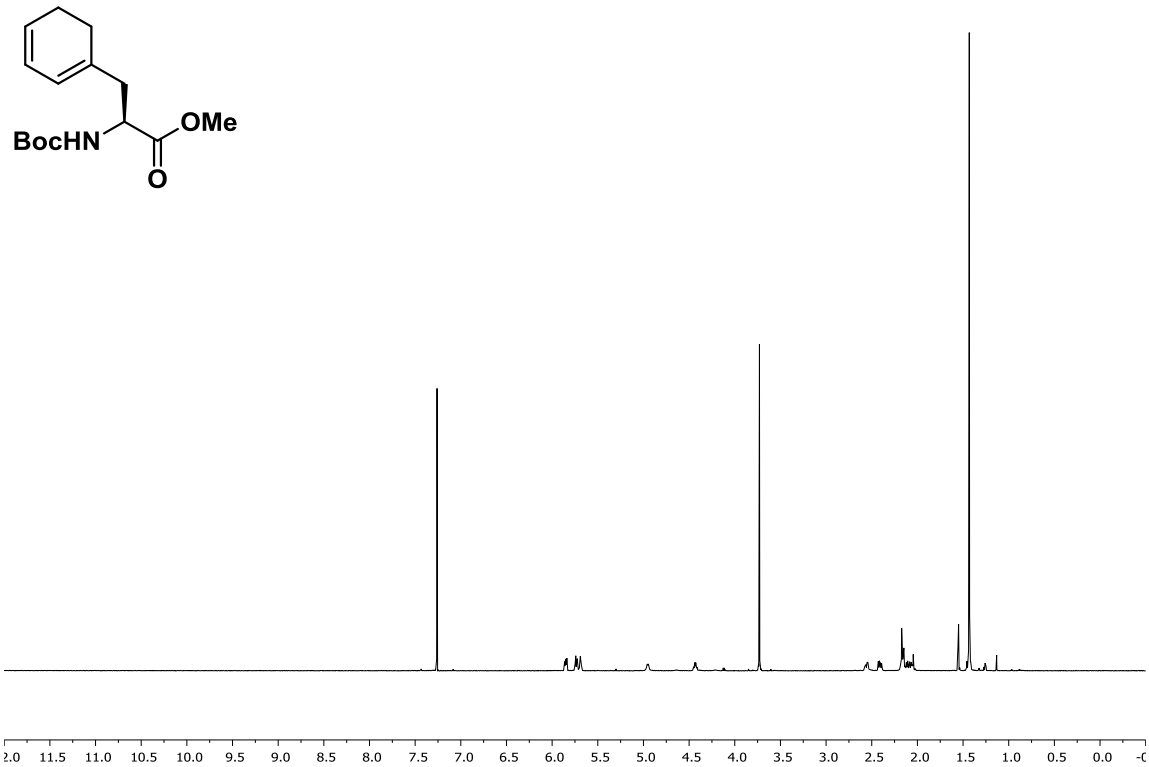

^{13}C NMR ($CDCl_3$, 125 MHz) – 3.13

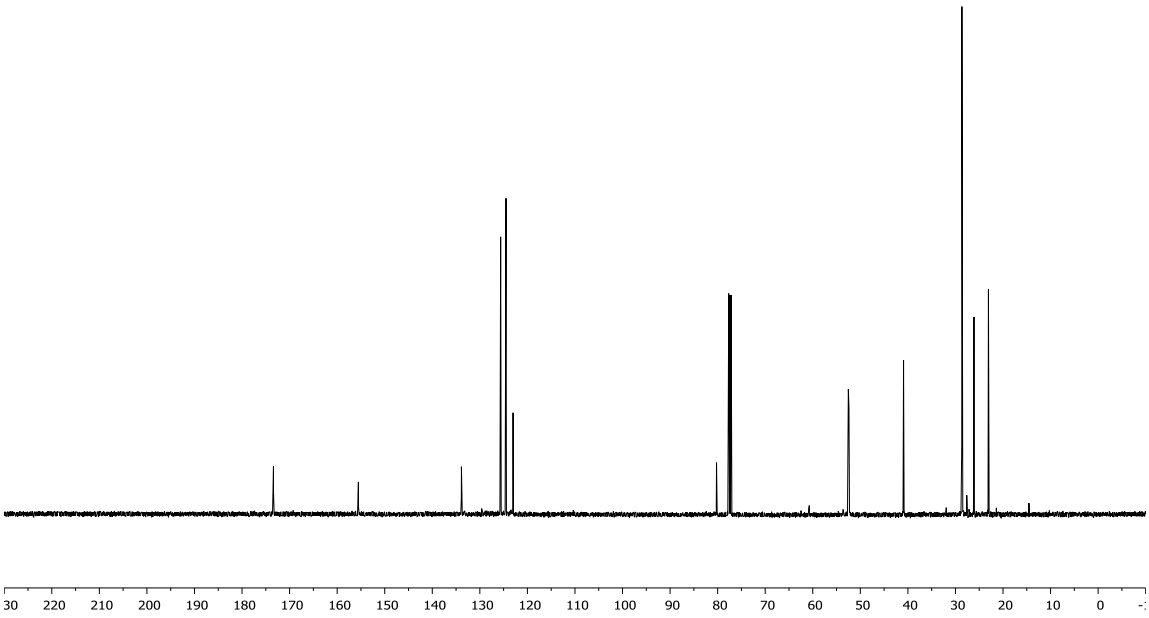

REFERENCE ^{1}H NMR ($CDCl_3$, 400 MHz) – 3.41

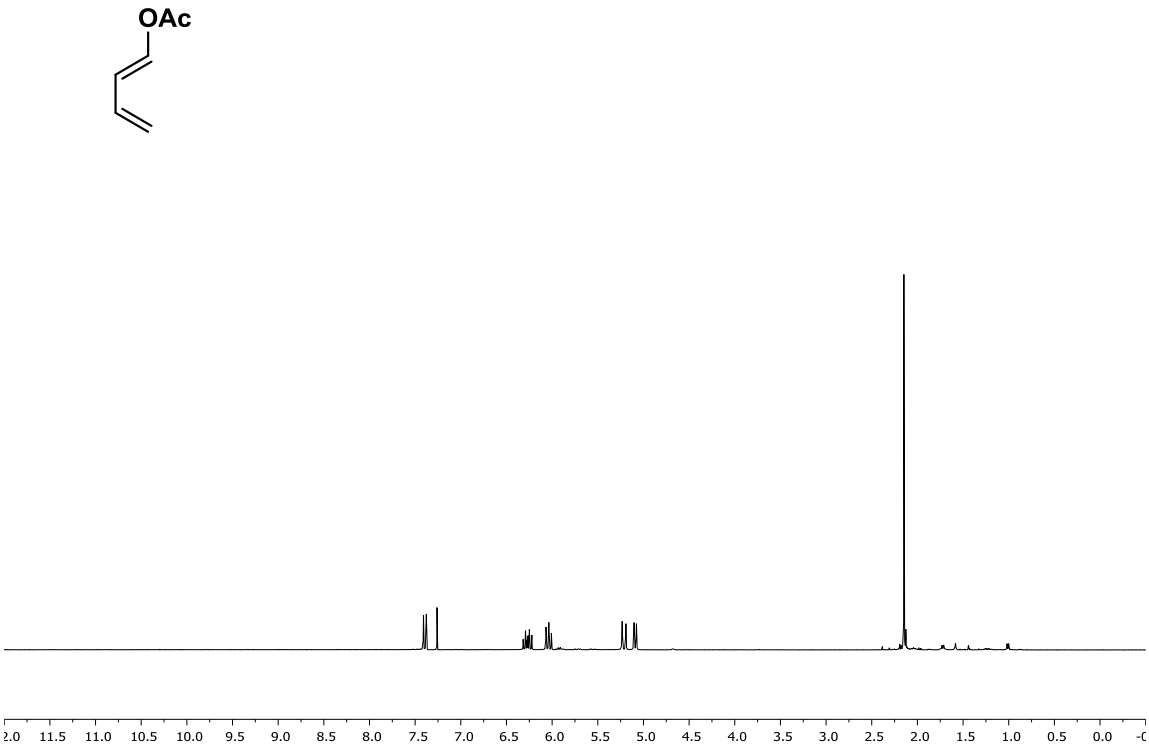

^{1}H NMR ($CDCl_3$, 400 MHz) – at 23 °C – 3.54

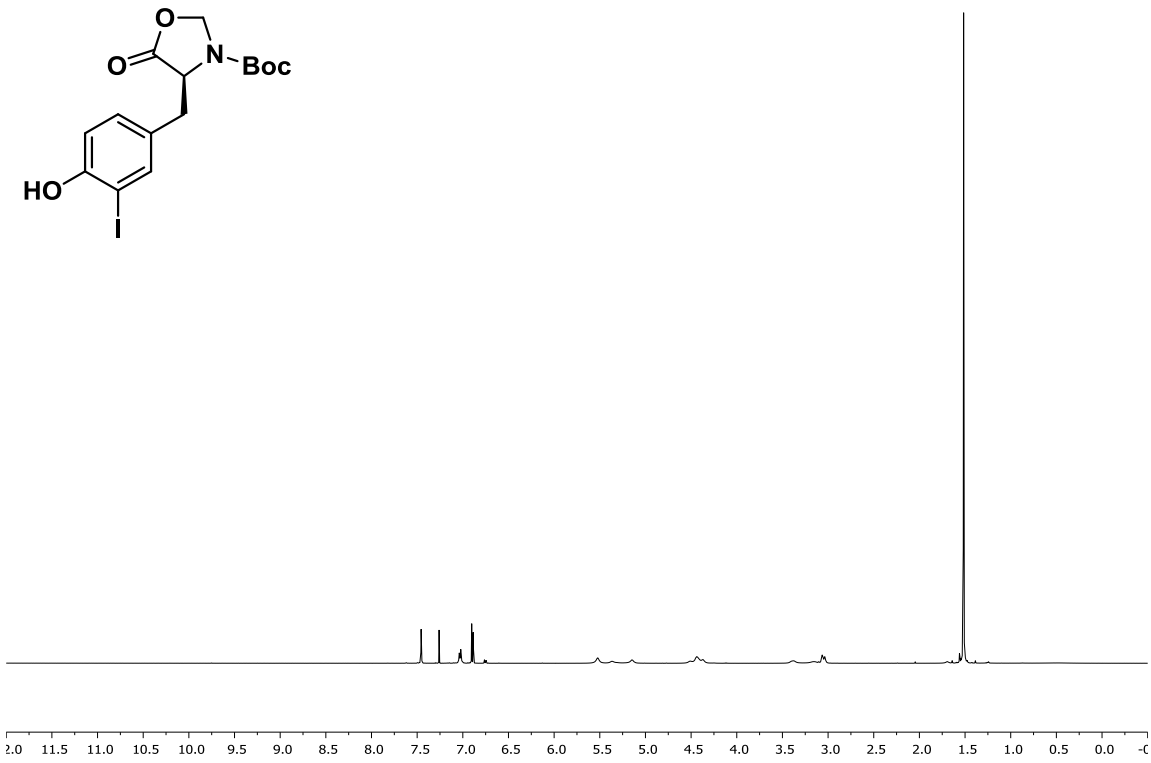

^{13}C NMR ($CDCl_3$, 125 MHz) – at 23 °C – 3.54

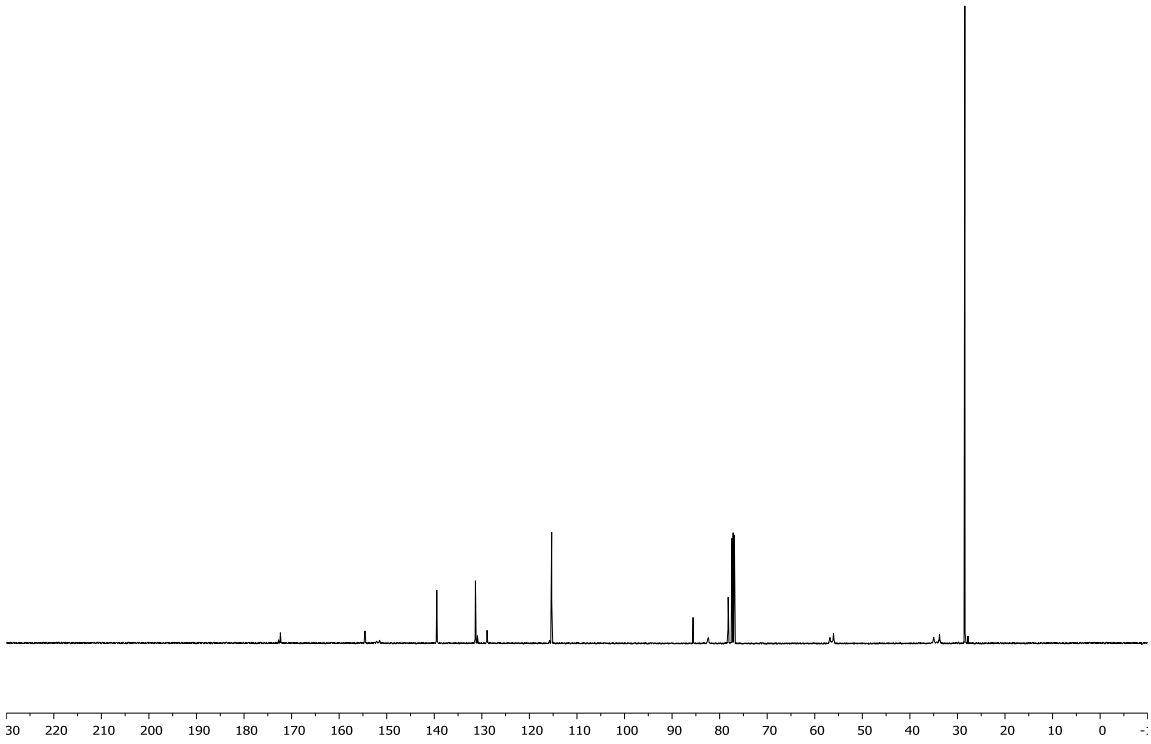

^{1}H NMR ($CDCl_3$, 500 MHz) – 3.43

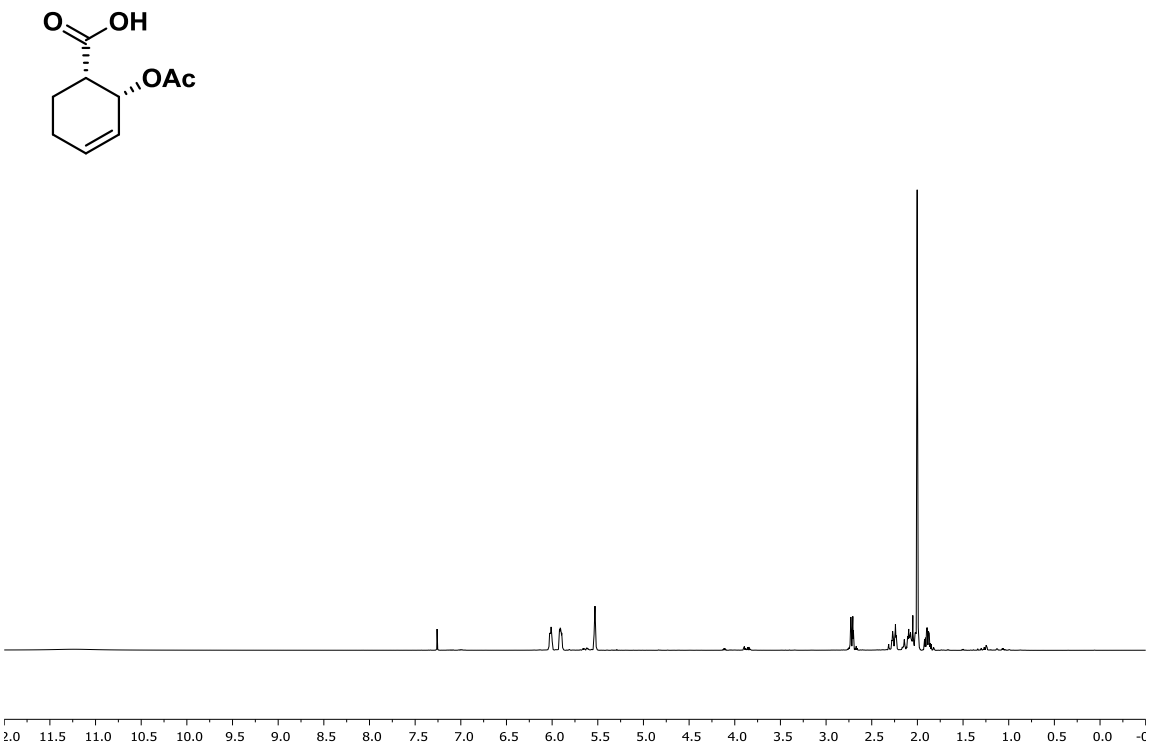

^{13}C NMR ($CDCl_3$, 125 MHz) – 3.43

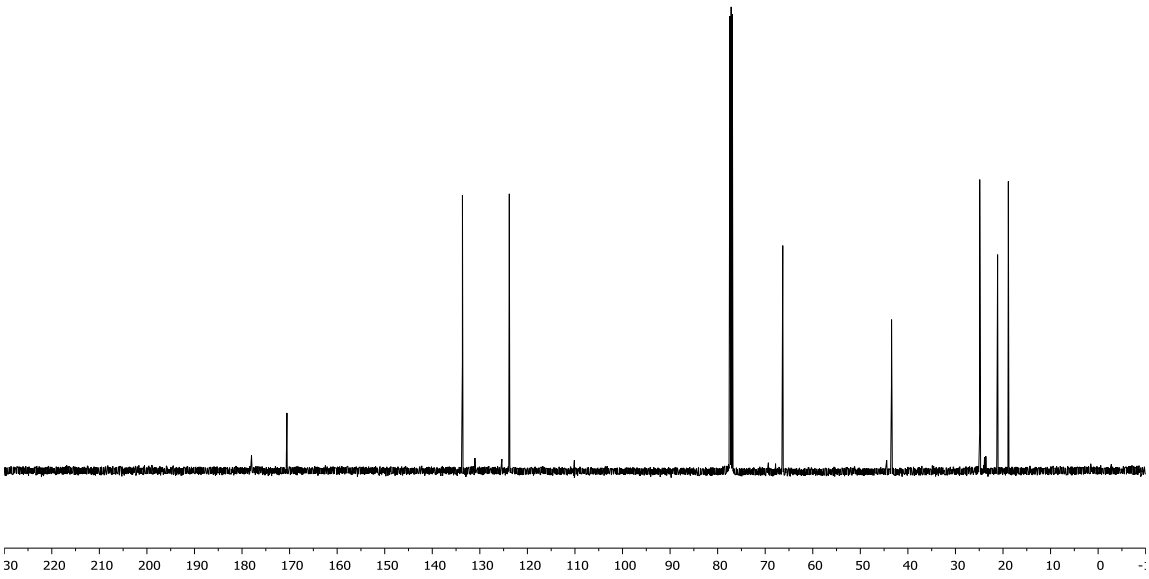

^{1}H NMR ($CDCl_3$, 500 MHz) – 3.44

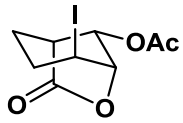

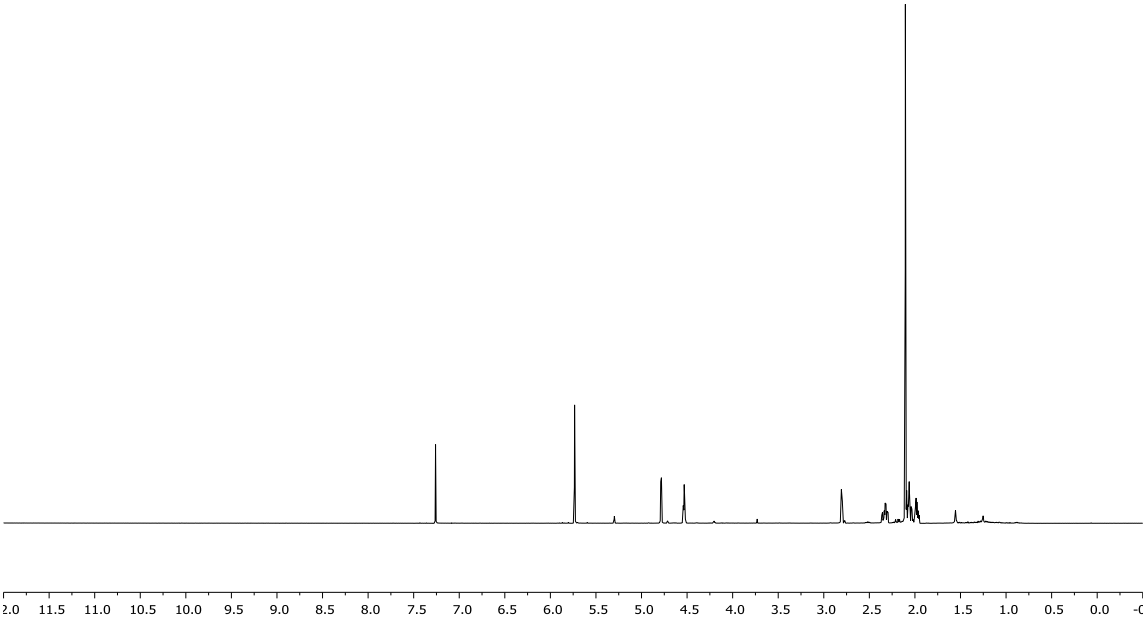

^{13}C NMR ($CDCl_3$, 125 MHz) – 3.44

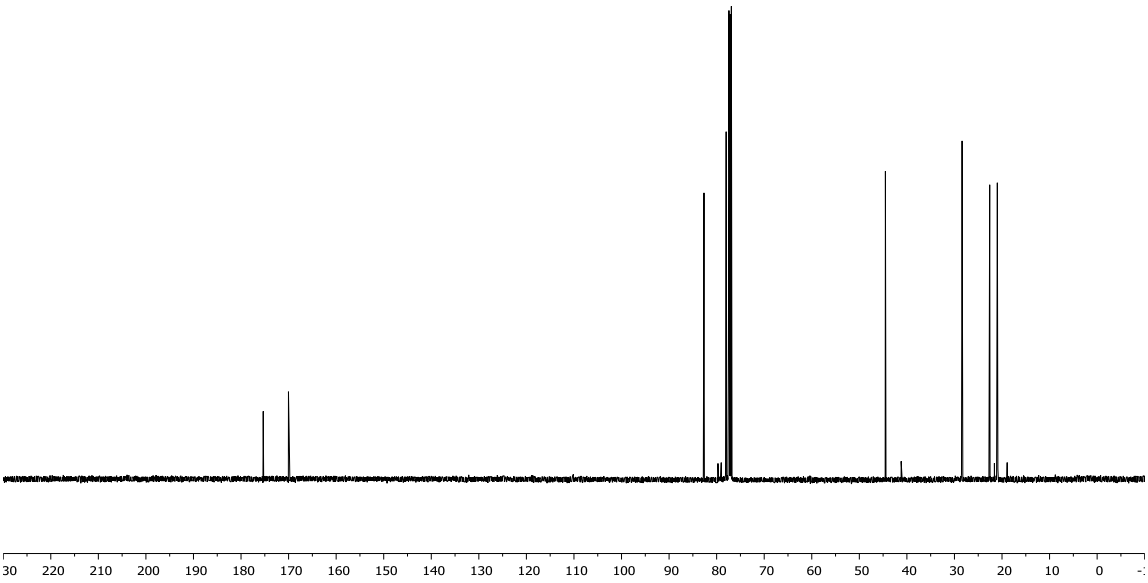

^{1}H NMR ($CDCl_3$, 500 MHz) – 3.45

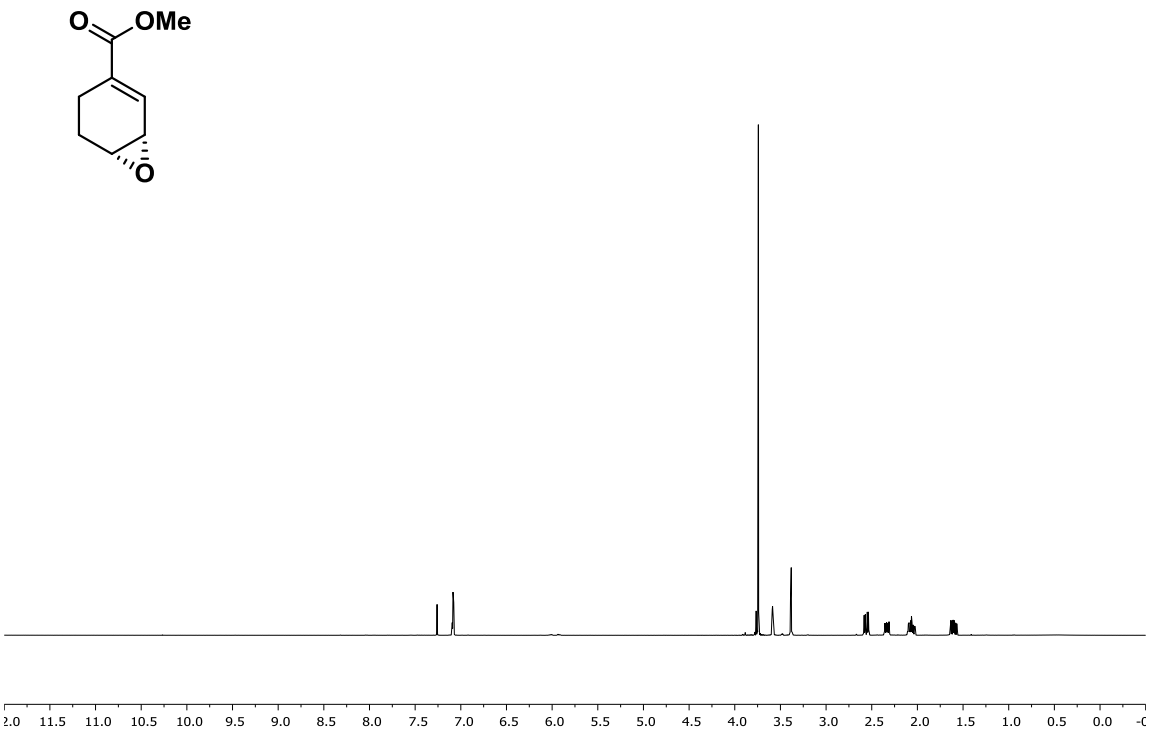

^{13}C NMR ($CDCl_3$, 125 MHz) – 3.45

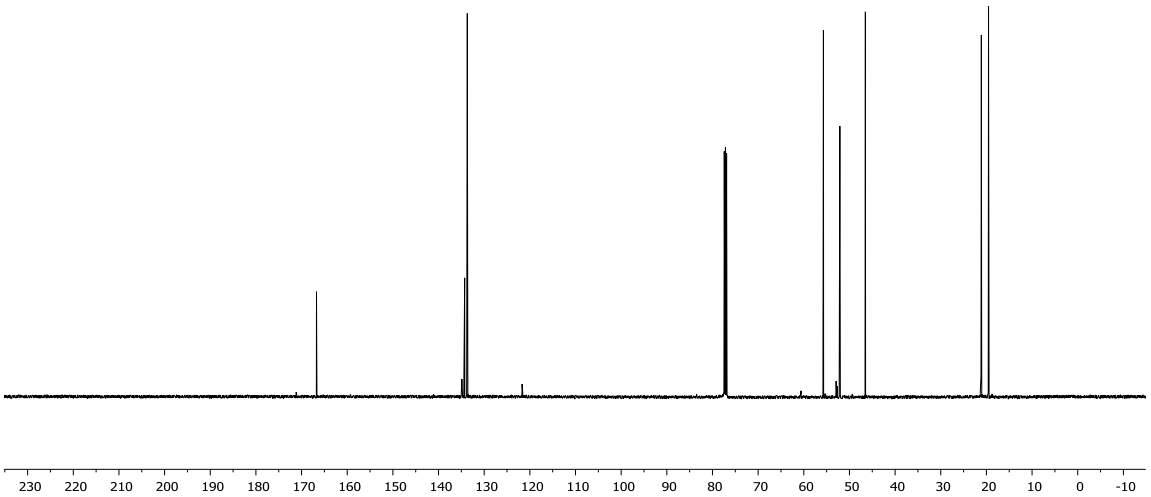

CRUDE ^{1}H NMR ($CDCl_3$, 600 MHz) – 3.55 (Contaminants of tri(2-furyl) phosphine And tri(2-furyl) phosphine oxide)

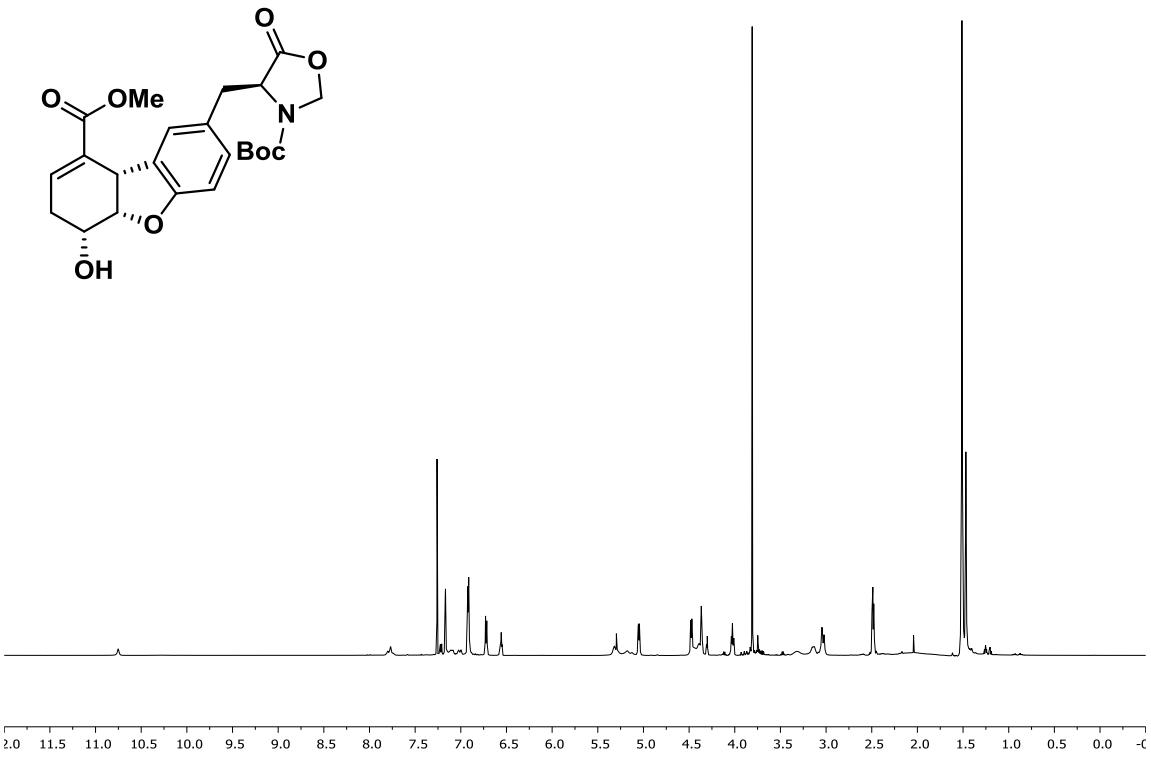

^{1}H NMR ($CDCl_3$, 600 MHz) – 3.55

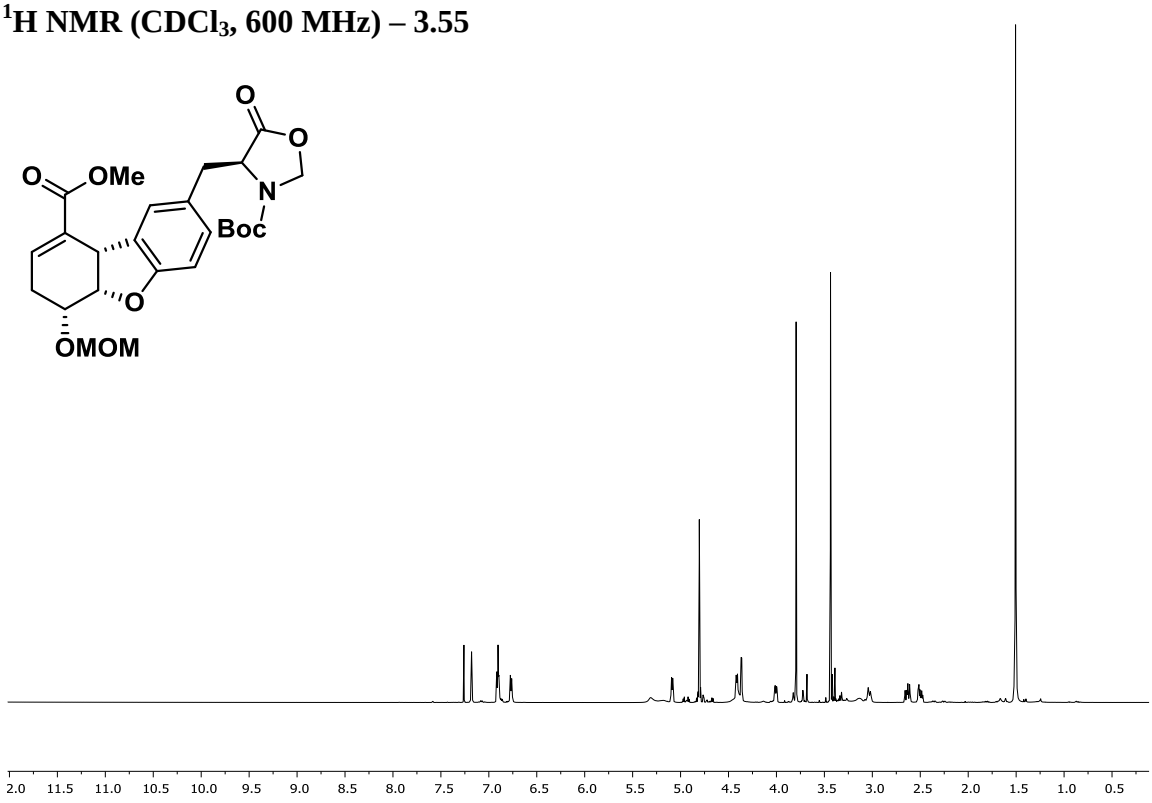

^{13}C NMR ($CDCl_3$, 500 MHz) – 3.55

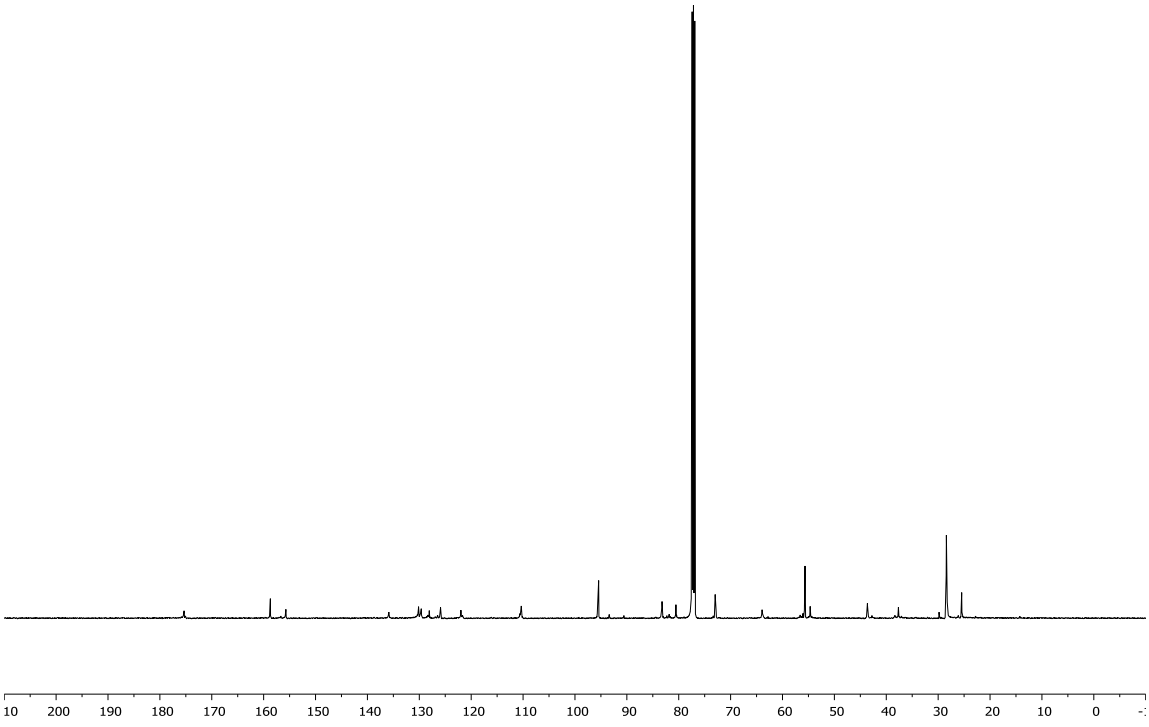

^{1}H NMR - COSY ($CDCl_3$, 600 MHz) – 3.55

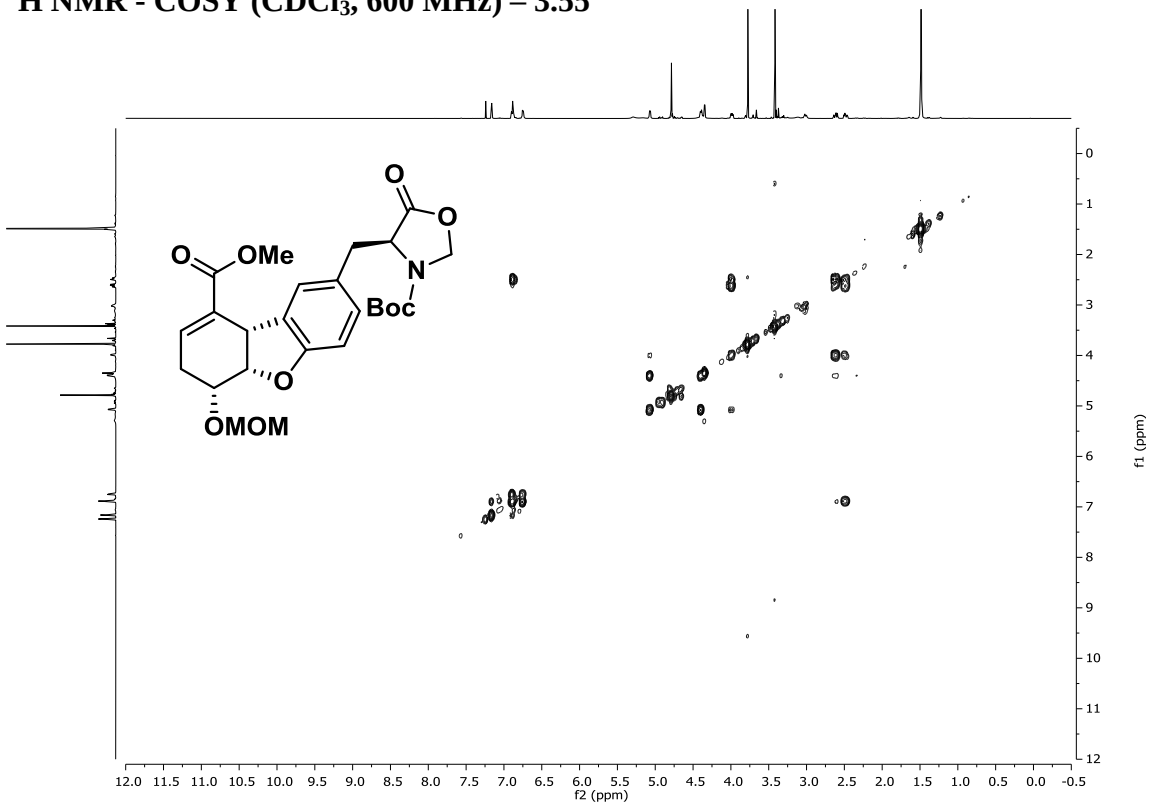

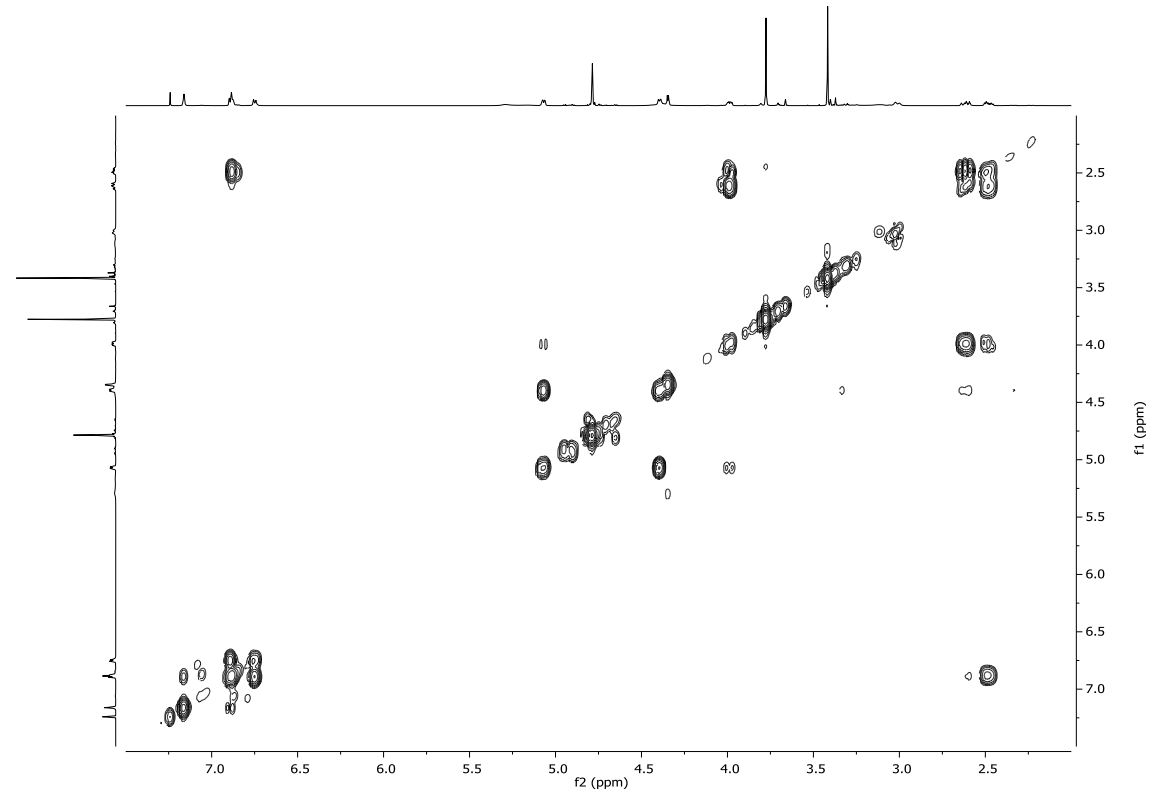

^{1}H NMR - COSY ($CDCl_3$, 500 MHz) – 3.55

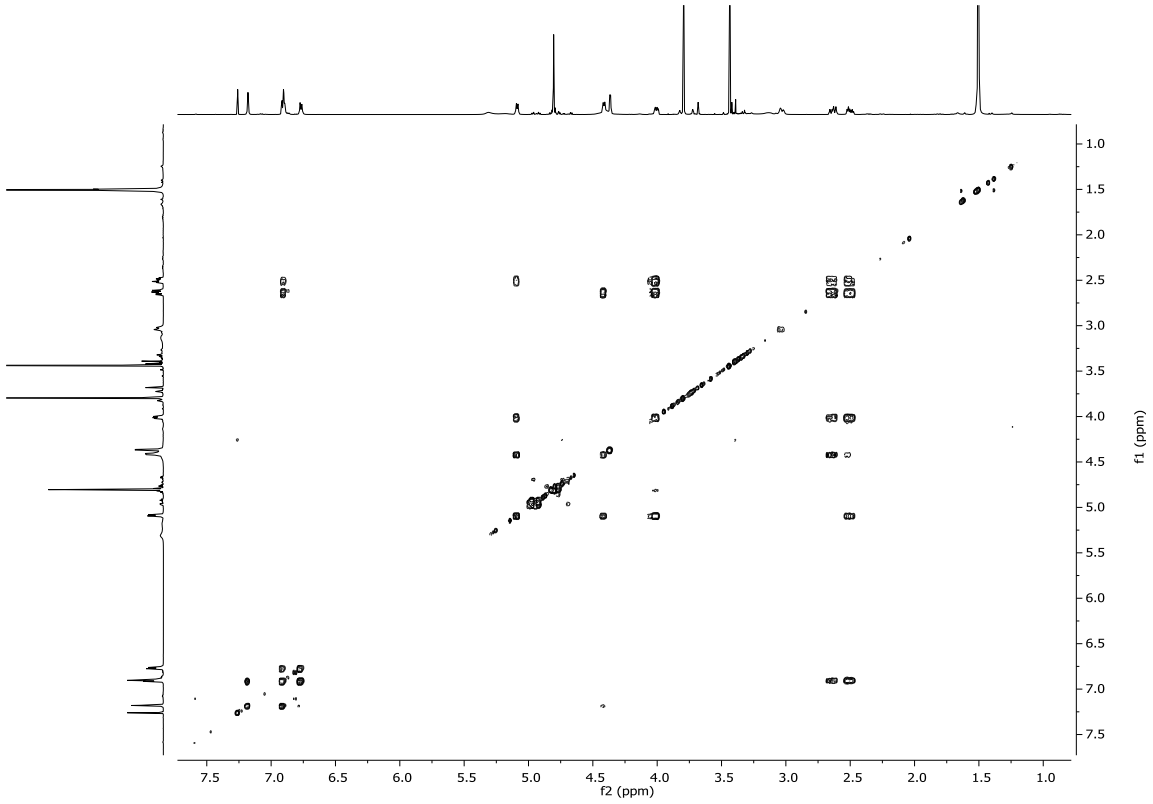

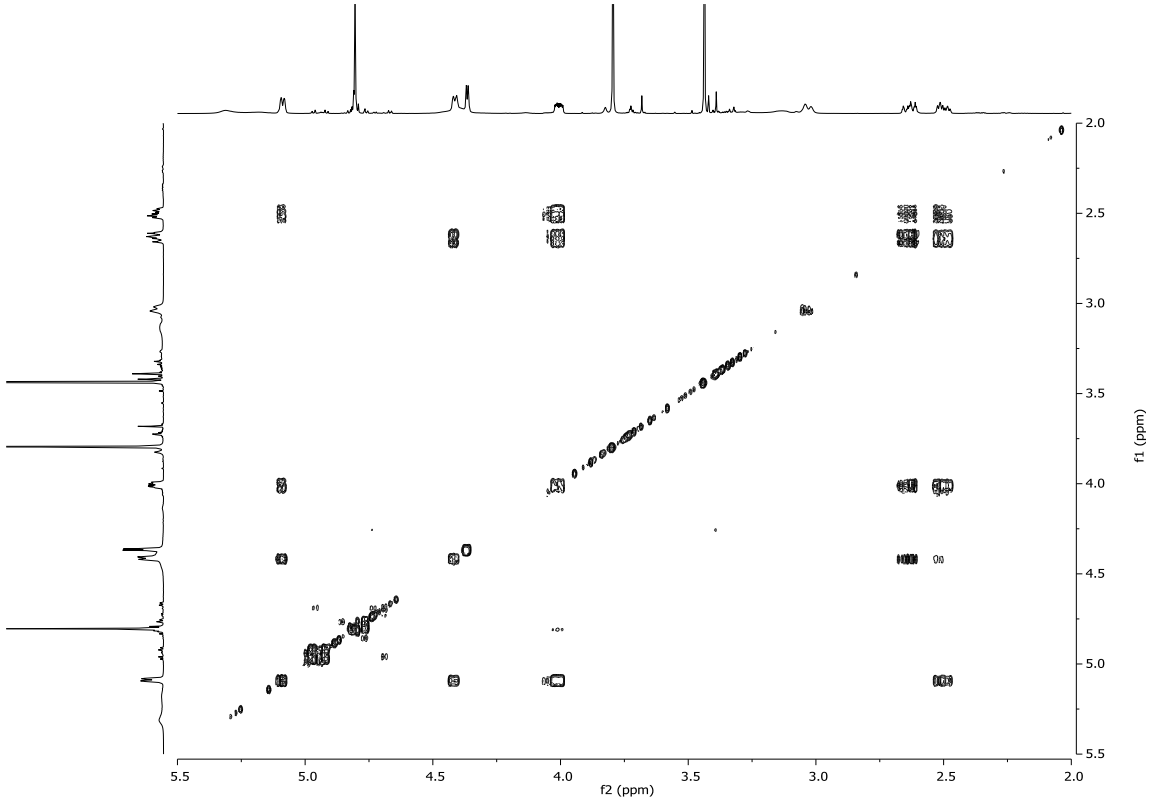

^{1}H NMR - NOESY ($CDCl_3$, 500 MHz) – 3.55

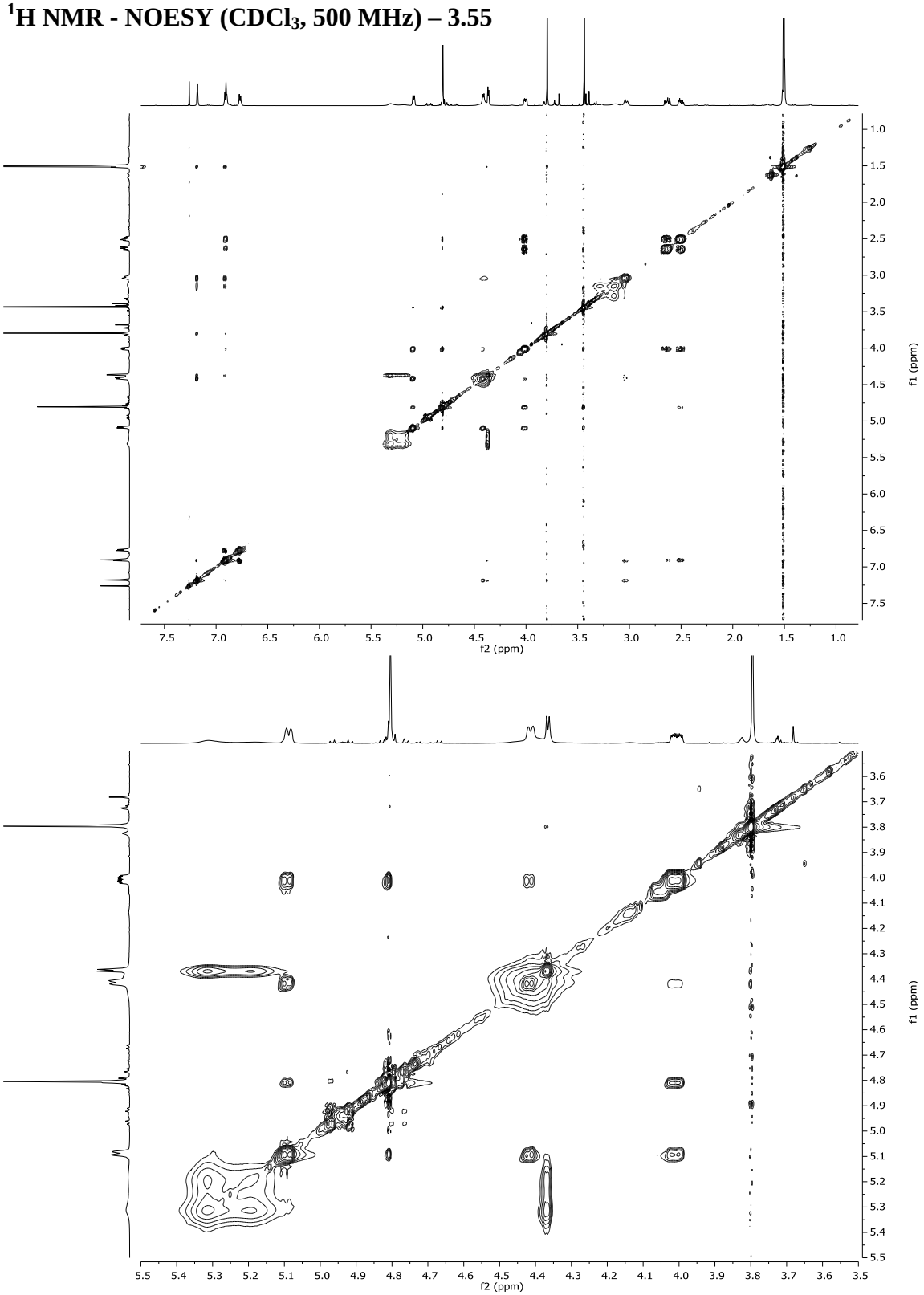

^{1}H NMR - HSQC ($CDCl_3$, 500 MHz) – 3.55

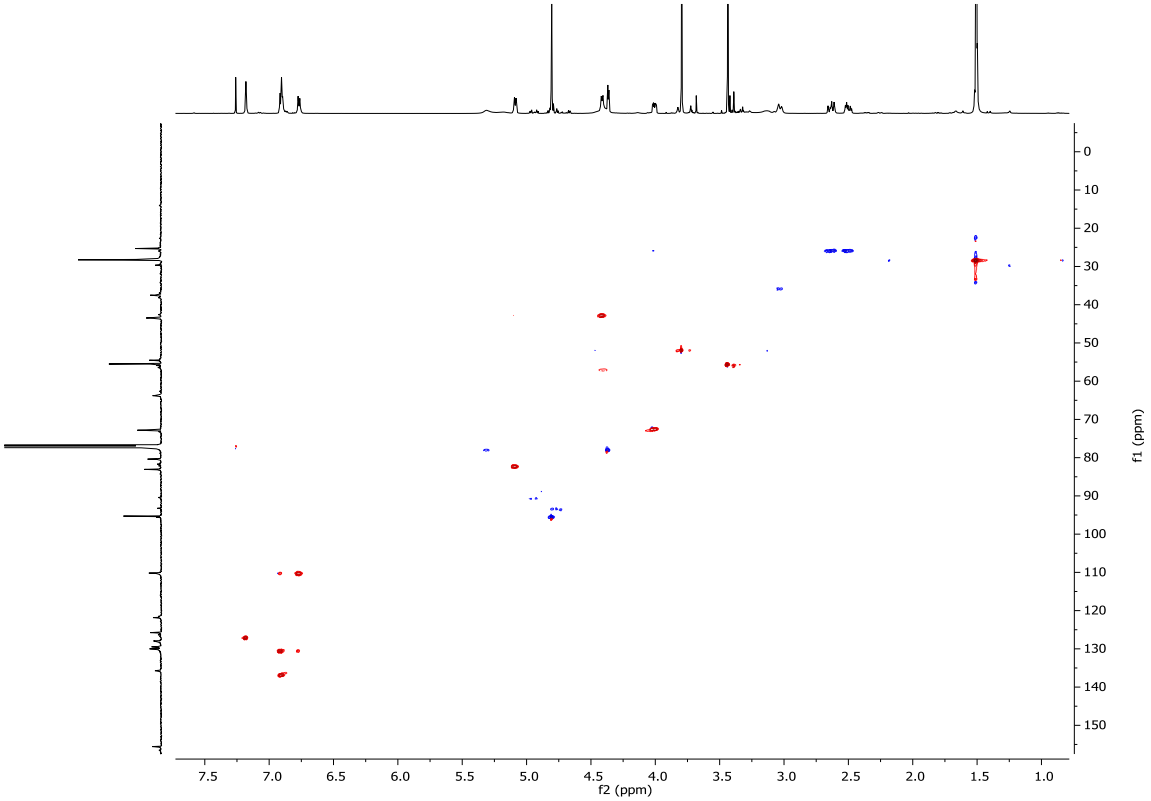

^{1}H NMR - HMBC ($CDCl_3$, 500 MHz) – 3.55

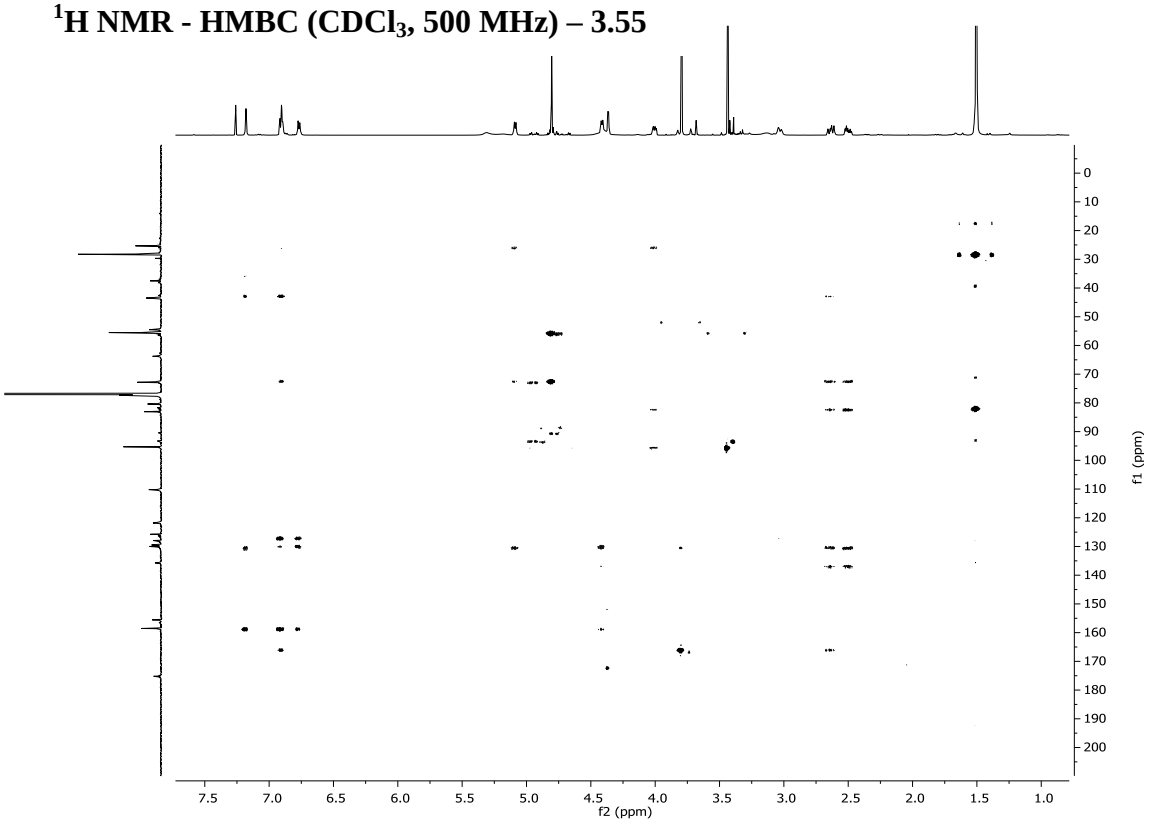

^{1}H NMR ($CDCl_3$, 600 MHz) – 3.56

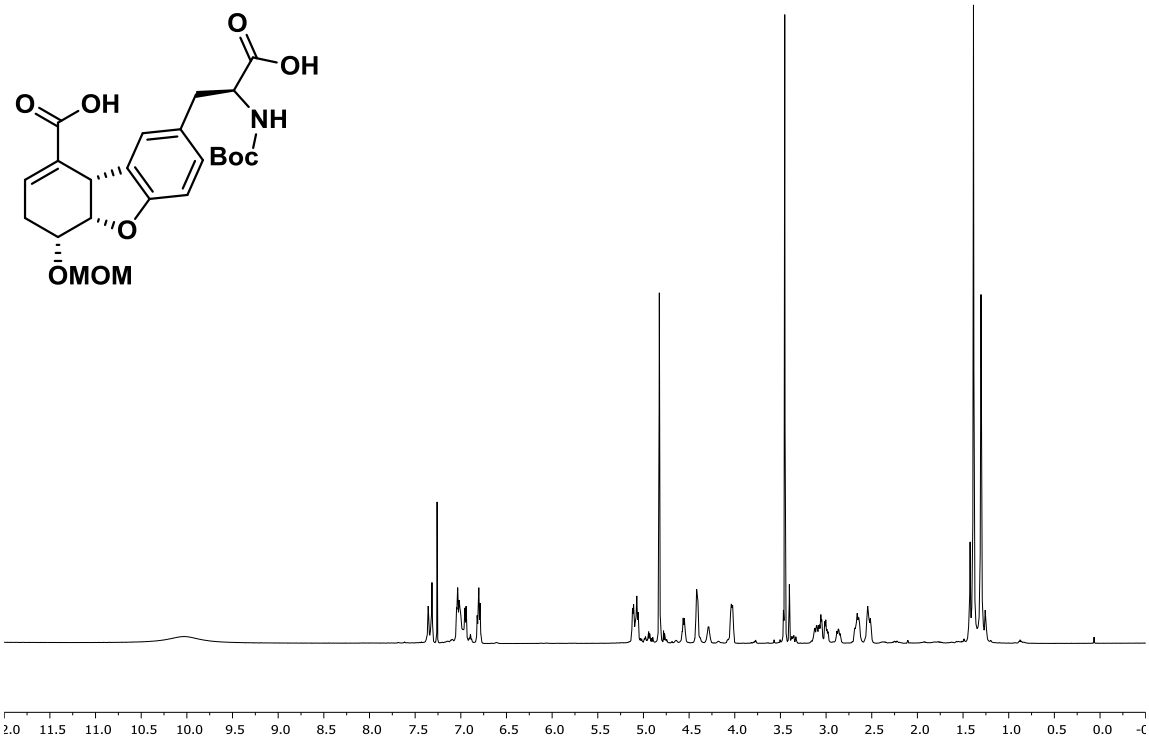

^{13}C NMR ($CDCl_3$, 100 MHz) – 3.56

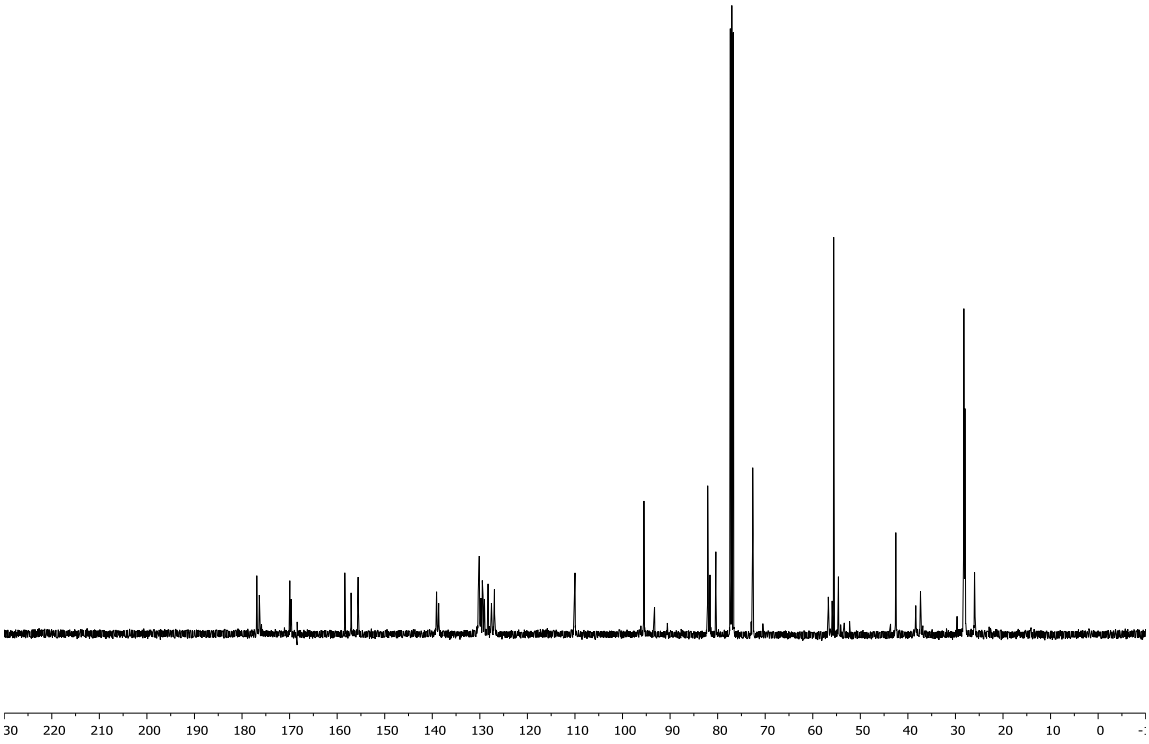

^{1}H NMR ($CDCl_3$, 600 MHz) – 3.59

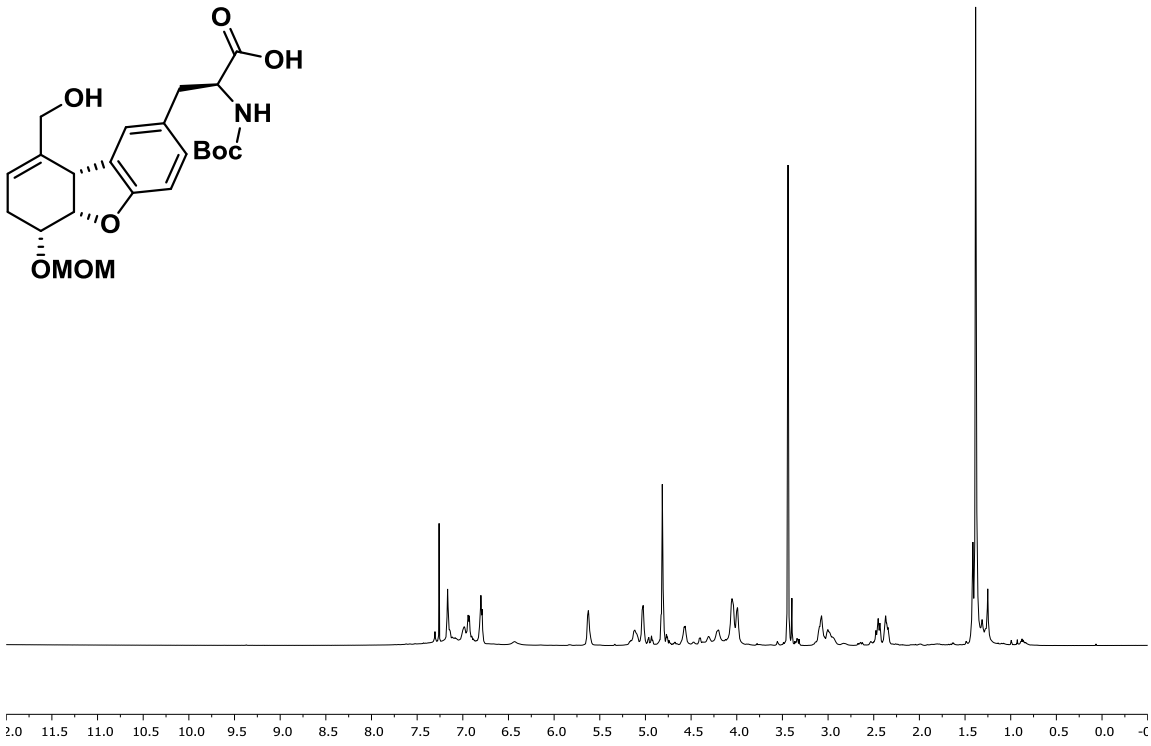

^{13}C NMR ($CDCl_3$, 100 MHz) – 3.59

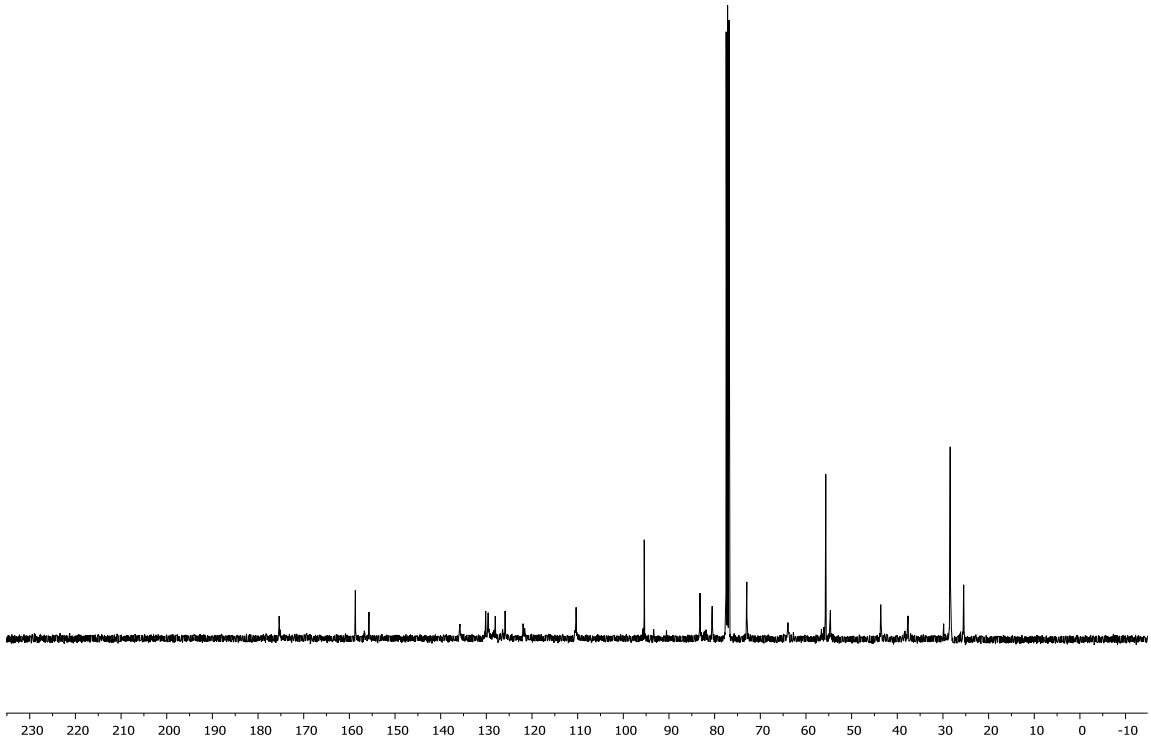

LC/MS ANALYSIS – 3.56 to 3.59 CONVERSION (LRMS)

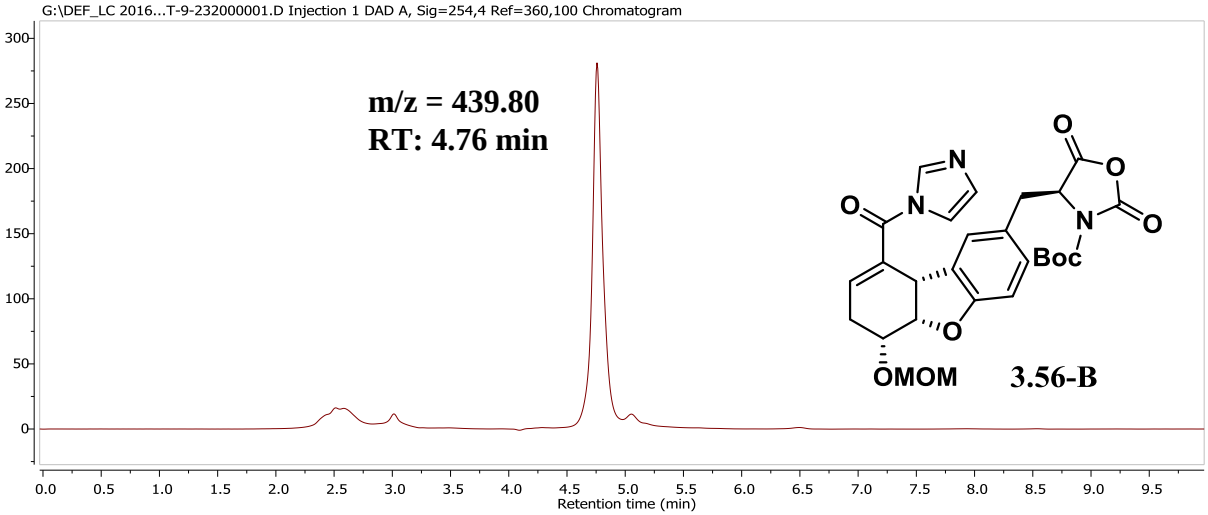

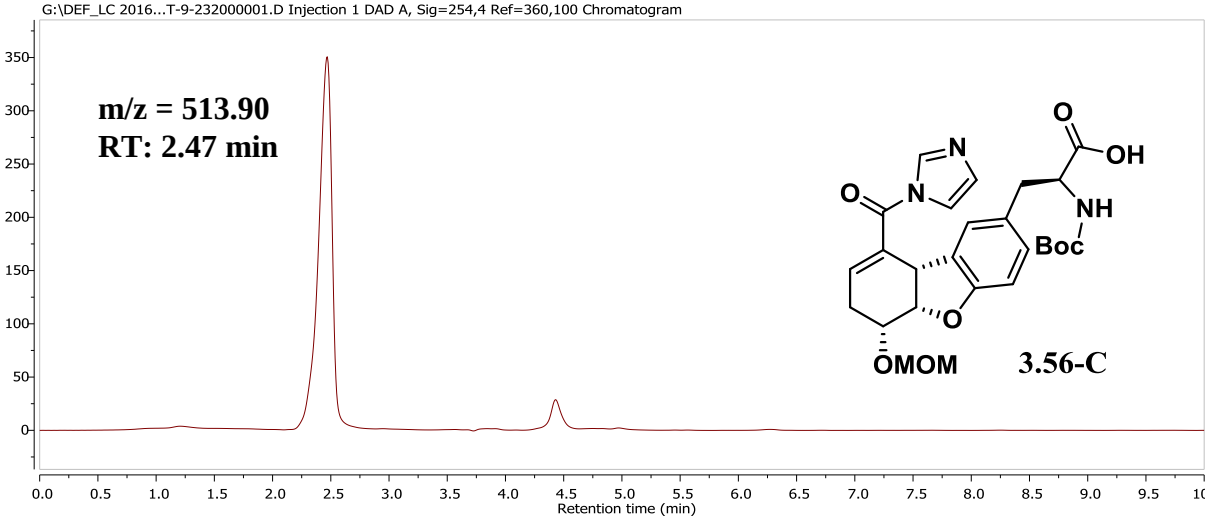

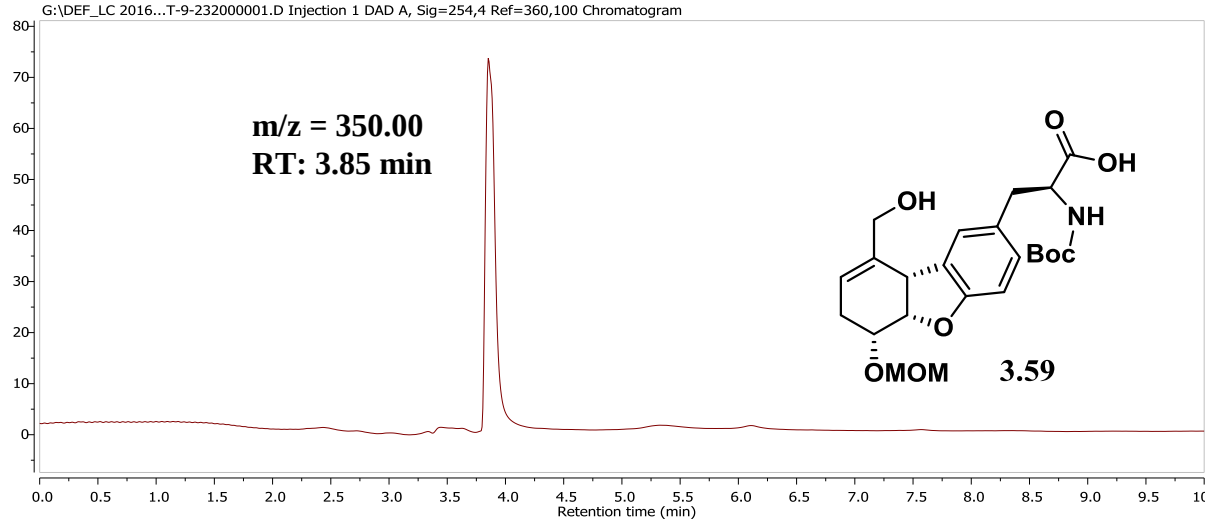

CRUDE - ^{1}H NMR ($CDCl_3$, 600 MHz) – 3.70

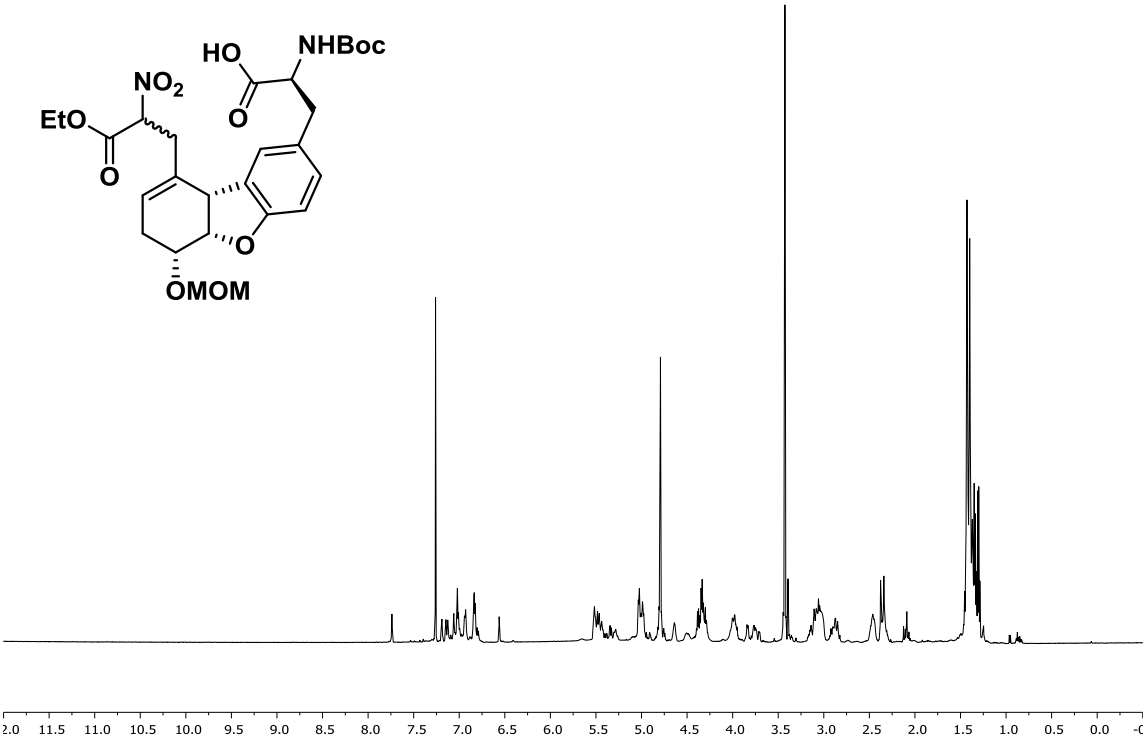

CRUDE - ^{1}H NMR - COSY ($CDCl_3$, 600 MHz) – 3.70

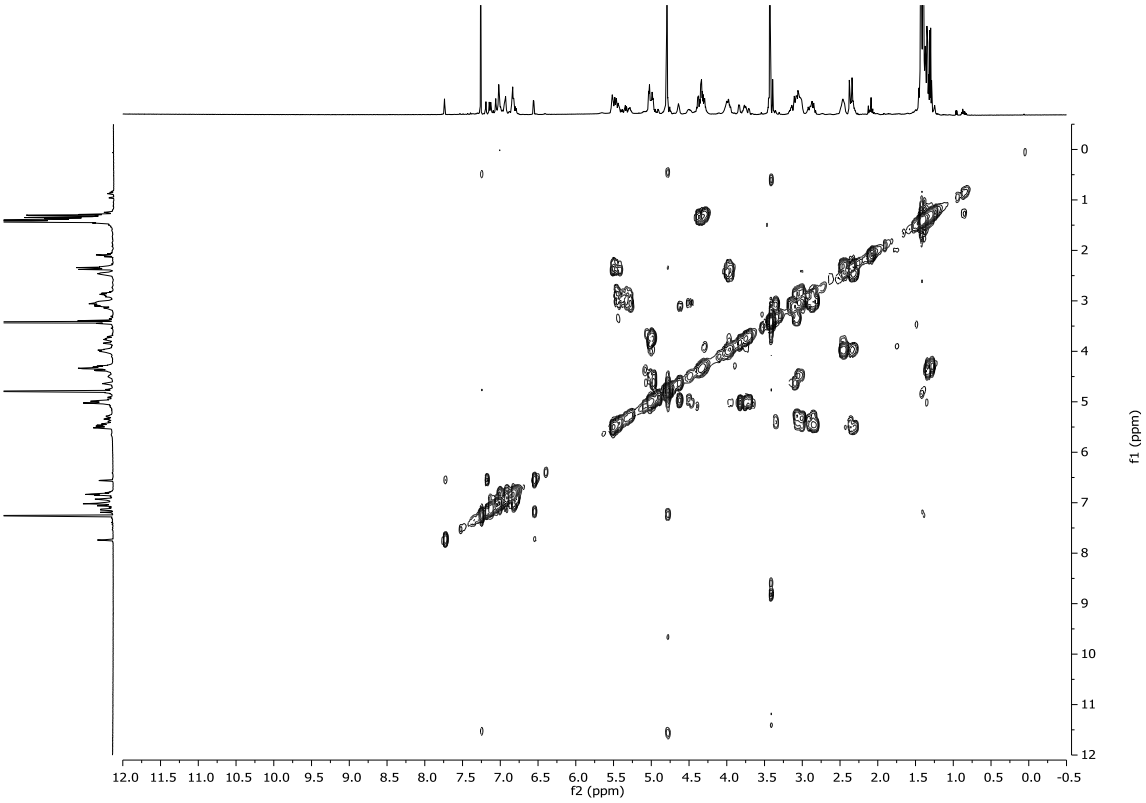

CRUDE - ^{1}H NMR - COSY ($CDCl_3$, 600 MHz) – 3.70 - EXPANDED